Ghrelin beeinflusst die pankreatische β-Zelle durch Modulation von K_{ATP}-Kanälen über den cAMP/PKA Signalweg

Dissertation

der Mathematisch-Naturwissenschaftlichen Fakultät

der Eberhard Karls Universität Tübingen

zur Erlangung des Grades eines

Doktors der Naturwissenschaften

(Dr. rer. nat.)

vorgelegt von

Julia Marion Kaiser

aus Malsch

Tübingen 2019

Gedruckt mit Genehmigung der Mathematisch-Naturwissenschaftlichen Fakultät der Eberhard Karls Universität Tübingen.

Tag der mündlichen Qualifikation:	20.11.2019
Dekan:	Prof. Dr. Wolfgang Rosenstiel
1. Berichterstatter:	Prof. Dr. Gisela Drews
2. Berichterstatter:	Prof. Dr. Susanne Ullric

Inhaltsverzeichnis

Abkürzungsverzeichnis

$[Ca^{2+}]_c$	cytosolische Ca^{2+}-Konzentration
$[cAMP]_c$	cytosolische cAMP-Konzentration
a.u.	arbitary units, Fluoreszenzeinheiten
Abb.	Abbildung
ABC	ATP binding cassette
AC	Adenylylcylcase
ADP	Adenosindiphosphat
AG	Acylghrelin, acyliertes Ghrelin
AgRP	agouti-related peptide
AMP	Adenosinmonophosphat
AMPK	AMP-aktivierte Proteinkinase
ANP	atriales natriuretisches Peptid
AS	Aminosäure
ATP	Adenosintriphosphat
BMI	body mass index
BRET	bioluminescence resonance energy transfer, Biolumineszenz-Resonanzenergietransfer
cAMP	cyclisches Adenosinmonophosphat
cGMP	cyclisches Guanosinmonophosphat
CART	cocaine and amphetamine regulated transcript
CDC	chenodeoxycholic acid, Chenodesoxycholsäure
DAG	Desacylghrelin, deacyliertes Ghrelin
db-cAMP	dibutyryl-cAMP
DIO	diet-induced obesity
DRD2-R	Dopaminrezeptor D2
ECL	extrazellulärer Loop

Epac	exchange protein directly activated by cAMP
$Epac2^{-/-}$	Epac2-knockout
ER	endoplasmatisches Retikulum
FCCP	Carbonylcyanid-4-(trifluoromethoxy)phenylhydrazon, entkoppelt die Atmungskette
FFA-R	free fatty acid receptor, Fettsäurerezeptor
FFS	freie Fettsäuren
Fig.	figure
FRET	Förster-Resonanzenergietransfer
FXR	farnesoid X receptor
$FXR^{-/-}$	FXR-knockout
GDP	Guanosindiphosphat
GTP	Guanosintriphosphat
GHRL	humanes Ghrelin Gen
GHS-R1a	growth hormone secretagogue receptor 1a
GHS-R1b	growth hormone secretagogue receptor 1b
GLUT2	Glucosetransporter Typ 2
GLTx	Gluco-Lipotoxizität
GOAT	ghrelin O-acyl transferase, Ghrelin O-Acyltransferase
GPCR	G-Protein coupled receptor, G-Protein gekoppelter Rezeptor
GDP	Guanosindiphosphat
GSIS	Glucose-stimulierte Insulinsekretion
GTP	Guanosintriphosphat
HEC	hyperinsulinemic-euglycemic clamp
HEK239	human embryonic kidney cells
HOMA	index homeostasis model assessment index
IL	Interleukin
IP_3	Inositol-1,4,5-triphosphat
IPGTT	intraperitonaler Glucosetoleranztest

K_{ATP}- Kanal	ATP-sensitiver K^+-Kanal
K_{ATP}-Strom	ATP-abhängiger K^+-Strom
K_{Ca}-Kanal	Ca^{2+}-abhängiger K^+-Kanal
MBOAT	membrane-bound O-acyl transferase
NEUROD1	neurogenic differentiation 1
NGN3	Neurogenin 3
NICC	neonatal islet-like cell cluster
Nkx2.2	Nk2 homeobox
NPY	Neuropeptid Y
OLA	oleanolic acid
Pax4/Pax6	paired box protein Pax4/Pax6
PC	Proprotein-Convertase
PDE	Phosphodiesterase
PDX-1	pancreas/duodenum homeobox protein 1
PI3K	Phosphoinositid-3-Kinase
PIP_2	Phosphatidylinositol-4,5-bisphosphat
PKA	Proteinkinase A
PKG	Proteinkinase G
PLC	Phospholipase C
POMC	Proopiomelanocortin
ROS	reactive oxygen species, reaktive Sauerstoffspezies
SCT-R	Sekretinrezeptor
SNARE	ethylmaleimide-sensitive factor attachment protein receptor
SNAP	synaptosomal protein of 25 kDa
SSC	stimulus-secretion coupling
SSK	Stimulus-Sekretions-Kopplung
SST	Somatostatin
SST-R	somatostatin receptor, Somatostatinrezeptor

STZ	Streptozotocin
SUR1	sulfonylurea receptor 1, Sulfonylharnstoff Rezeptor 1
SUR1 $^{-/-}$	SUR1-knockout
TM	transmembranäre Domäne
TNF_{α}	Tumornekrosefaktor α
Tolb	Tolbutamid, K_{ATP}-Kanal Antagonist
TRP	transient receptor potential channels
V_m	Membranpotential
VTA	Area tegmentalis ventralis
WT	Wildtyp
ZDF	Zucker diabetic fatty
ZNS	Zentrales Nervensystem
$\Delta\psi$	mitochondriales Membranpotential

Zusammenfassung

Ghrelin (Acylghrelin, AG) ist insbesondere bekannt durch seine hungerinduzierende Wirkung, die es über Bindung an seinen Rezeptor, den growth hormone secretagogue receptor 1a (GHS-R1a), im Nucleus arcuatus ausübt. Aufgrund dieser zentralen Wirkung und des Nachweises, dass AG neben der Magenschleimhaut ebenfalls in den ε-Zellen des Pankreas gebildet sowie sekretiert wird und die Insulinsekretion hemmt, bietet AG einen spannenden Therapieansatz und stellt eine interessante Verbindung zwischen Erkrankungen wie Adipositas und Diabetes mellitus Typ 2 her.

Desacylghrelin (DAG), der Metabolit von AG, bei dem die acylierte Fettsäure abgebaut ist, ist an mehreren biologischen Prozessen beteiligt, die vor allem in Verbindung mit AG stehen. Von Bedeutung sind insbesondere die antagonisierenden Eigenschaften von DAG in Bezug auf die von AG vermittelnden Wirkungen und das Verhältnis von DAG zu AG, welche ebenfalls in dieser Arbeit thematisiert werden. Es wird gezeigt, dass die beobachteten Effekte von AG auf die Stimulus-Sekretions-Kopplung (SSK) in Anwesenheit von DAG und AG im Verhältnis 2:1 in Bezug auf die cytosolische Ca^{2+} - Konzentration ($[Ca^{2+}]_c$), das Membranpotential und die Glucose-induzierte Insulinsekretion (GSIS) nicht mehr vorhanden sind.

Die hier vorliegende Arbeit untersucht durch Verwendung des glucolipotoxischen (GLTx) Modells, in dem β-Zellen und Langerhans-Inseln mittels Inkubation hoher Glucose- und Palmitatkonzentration einem Überernährungszustand ausgesetzt werden, den Einfluss von AG, DAG und beider Peptide auf die durch GLTx-ausgelösten Schäden auf die Glucose-induzierten Oszillationen der $[Ca^{2+}]_c$ und GSIS. Dabei wird gezeigt, dass die alleinige Inkubation von DAG im GLTx-Modell keinen Effekt auf die Glucose-induzierten Oszillationen der $[Ca^{2+}]_c$-Konzentration und GSIS hatte. Die Coinkubation von DAG und AG im Verhältnis 2:1 konnte zwar nicht die durch GLTx-ausgelösten Schäden auf die Insulinsekretion verhindern, jedoch jene auf die Glucose-induzierten Oszillationen der $[Ca^{2+}]_c$-Konzentration und verdeutlicht damit abermals die Bedeutung des Verhältnisses von DAG zu AG.

Die präsentierten Ergebnisse verdeutlichen außerdem, dass die konstitutive Aktivität des GHS-R1a mittels inversem Agonisten neben der Verwendung eines GHS-R1a Antagonisten berücksichtigt werden muss, um eine vollständige Hemmung des AG-Effekts in murinen Langerhans-Inseln und daraus isolierten β-Zellen zu erreichen.

Mehrere Studien haben nachgewiesen, dass AG die Insulinsekretion des Pankreas inhibiert und sich negativ auf die Insulinsensitivität und die Glucosehomöostase auswirkt. Dieser Effekt wird im Rahmen dieser Arbeit in murinen β-Zellen sowie Langerhans-Inseln, in der Zelllinie MIN6 und in aus jungen Ferkeln isolierten neonatal islet-like cell clusters (NICCs) gezeigt.
Wie diese Wirkung von AG auf die pankreatische β-Zelle zustande kommt und damit einhergehend die Expression des GHS-R1a in β- oder δ-Zellen, wurde in den letzten Jahren mehrfach und stellenweise kontrovers diskutiert. Es besteht Uneinigkeit darüber, ob AG seine Effekte durch parakrinen Einfluss auf die β-Zelle oder über die Stimulation der Somatostatin- (SST-) Sekretion aus δ-Zellen erzielt, wodurch schlussendlich SST parakrin die $[Ca^{2+}]_c$ erniedrigt und nachfolgend die Insulinsekretion der β-Zellen hemmt.

Die vorliegende Arbeit belegt, dass die Wirkung von AG auf die β-Zelle nicht von SST imitiert wird und sich der Wirkmechanismus von SST und AG in murinen β-Zellen unterscheidet. SST wirkt im Gegensatz zu AG nicht über die Modulation von K_{ATP}-Kanälen, was in dieser Arbeit mit Experimenten in isolierten β-Zellen aus SUR1-knock-out ($SUR^{-/-}$) Mäusen belegt wird, welche keinen K_{ATP}-Kanal exprimieren. In Verbindung mit den Ergebnissen aus der GSIS Messreihe mit der β-Zelllinie MIN6 betrachtet, vermittelt folglich nicht SST allein die Effekte von AG auf die β-Zelle. Es wird jedoch ebenfalls gezeigt, dass Somatostatinrezeptoren (SST-R) neben dem GHS-R1a an dem Einfluss von AG auf das Pankreas beteiligt sind.

Der Wirkmechanismus von AG wird im Rahmen dieser Arbeit mittels Patch-Clamp Experimenten in der inside/out und Perforated-Patch Konfiguration sowie GSIS

unter Verwendung eines cAMP-Analogons und eines Phosphodiesterase- (PDE-) Inhibitors dahingehend spezifiziert, dass AG indirekt den K_{ATP}-Kanal über den cAMP/PKA Signalweg durch Hemmung der Adenylylcyclase (AC) moduliert, wodurch die Inhibition der Insulinsekretion erklärt werden kann.

Summary

Ghrelin (acyl-ghrelin, AG) is well-known for its hunger-inducing effects, which it establishes by binding to its receptor, the growth hormone secretagogue receptor 1a (GHSR1a), in the arcuate nucleus. Aside from the stomach, AG is also localized in ε-cells in the pancreas and inhibits insulin secretion of β-cells. Regarding these facts, AG is an interesting therapeutical approach and link between diseases such as obesity and diabetes type 2.

Desacylghrelin (DAG) is the metabolite of AG, that lacks the acylated fatty acid. It is involved in multiple biological processes, which are, among other things, also connected to AG. Especially the antagonizing attributes of DAG are of great importance regarding the mediated effects of AG and the DAG:AG ratio, which will be a subject of this thesis. It is shown that the observed effects of AG on the cytosolic Ca^{2+} concentration ($[Ca^{2+}]_c$), the membrane potential and the GSIS are absent in the presence of a DAG to AG ratio of 2:1.

Glucolipotoxicity (GLTx) provides a model, in which pancreatic β-cells and islets are exposed to high concentrations of glucose and palmitat to recreate fuel excess and therefore the deterioration of β-cell function. This thesis used the model to investigate the influence of DAG, AG and both peptides on this condition. It is shown that DAG alone could not protect the GLTx-induced disturbances of Ca^{2+} dynamics in contrast to coincubation of a DAG to AG ratio of 2:1. Neither DAG alone nor the aforementioned ratio could avert the GLTx-induced impairment of GSIS. This underlines the importance of the DAG to AG ratio.

The presented results illustrate that the constitutive activity of GHSR1a is an important feature of this receptor, which has to be considered to achieve a complete inhibition of the AG-mediated effects on pancreatic β-cells and islets.

As several studies have shown AG inhibits insulin secretion and has a negative impact on both insulin sensitivity as well as glucose homeostasis. This effect will be

showcased in murine β-cells, with the MIN6 cell-line as well as in neonatal islet-like cell clusters of piglets, as part of this thesis.

The exact mechanism of how AG influences the pancreatic β-cells and islets is still a topic of sometimes controversial debate. There is conflicting data regarding the expression of GHSR1a in β- or δ-cells and how AG mediates its effect. On one hand, it is postulated that AG directly affects the β-cell function through binding on GSHR1a expressed in β-cells, while others claim that AG affects β-cells by inducing paracrine the somatostatin (SST) secretion from the GHSR1a expressed in δ-cells. SST acts on β-cells and decreases $[Ca^{2+}]_{c,}$ subsequently inhibiting the insulin secretion instead of AG.

This thesis shows that the impact of AG on the pancreatic β-cells cannot be imitated by SST; their mechanisms differ in their effect on murine β-cells. SST (in contrast to AG) does not modulate K_{ATP} channels, which is shown by experiments in β-cells isolated from SUR1-KO mice. Combined with the result that AG decreased GSIS in MIN6, it is plausible that SST alone does not mediate the effect of AG on β-cells. It is also shown that somatostatin receptors (SSTRs) are involved in the mode of action of AG together with its own receptor, the GHSR1a.

This thesis specifies the signaling pathway of AG with patch-clamp experiments in the inside/out and perforated-patch configuration as well as GSIS by using a cAMP analogue and a PDE inhibitor. AG indirectly interacts with K_{ATP} channels by interfering with the amplifying cAMP/PKA pathway through the inhibition of adenylylcyclase (AC) and therefore decreases insulin secretion.

Liste der Publikationen der Dissertation

Die vorliegende Arbeit ist eine kumulative Dissertation.
In den folgenden wissenschaftlichen Arbeiten sind einige der Forschungsergebnisse bereits veröffentlicht:

a) Akzeptierte Publikationen

S. Undank, J. Kaiser, J. Sikimic, M. Düfer, P. Krippeit-Drews, G. Drews (2017).
Atrial Natriuretic Peptide Affects Stimulus-Secretion Coupling of Pancreatic β-Cells. Diabetes 66(11):2840-2848

Diese Veröffentlichung befindet sich unter der Kennzeichnung **M-ANP** in dieser Arbeit.

C. Bauer, J. Kaiser, J. Sikimic, P. Krippeit-Drews, M. Düfer, G. Drews (2018).
ATP mediates a negative autocrine signal on stimulus-secretion coupling in mouse pancreatic β-cells. Endocrine: 1-14

Diese Veröffentlichung befindet sich unter der Kennzeichnung **M-ATP** in dieser Arbeit.

J. Maczewsky, J. Kaiser, A. Gresch, F. Gerst, M. Düfer, P. Krippeit-Drews, G. Drews (2018).
TGR5 Activation Promotes Stimulus-Secretion Coupling of Pancreatic β-Cells via a PKA-Dependent Pathway. Diabetes 68(2):324-336

Diese Veröffentlichung befindet sich unter der Kennzeichnung **M-TGR5** in dieser Arbeit.

b) Manuskripte, welche noch nicht veröffentlicht wurden

J. Kaiser, P. Krippeit-Drews, G. Drews

Ghrelin Influences β-cell Function by Interference with K_{ATP} Channels.

Diese Veröffentlichung befindet sich unter der Kennzeichnung **M-AG** in dieser Arbeit.

c) Manuskripte, welche eingereicht wurden

T. Hoffmeister, J. Kaiser, G. Drews, M. Düfer

Interactions between Atorvastatin and the Farnesoid X Receptor Impair Insulinotropic Effects of Bile Acids and Modulate Diabetogenic Risk.

Diese Veröffentlichung befindet sich unter der Kennzeichnung **M-FXR** in dieser Arbeit.

Beschreibung der Bedeutung der Eigenanteile

S. Undank, J. Kaiser, J. Sikimic, M. Düfer, P. Krippeit-Drews, G. Drews (2017).

Atrial Natriuretic Peptide Affects Stimulus-Secretion Coupling of Pancreatic β-Cells. Diabetes 66(11):2840-2848

Die Arbeit wurde unter der Leitung von Gisela Drews durchgeführt. Alle nachfolgend nicht näher beschriebenen Messreihen und Auswertungen wurden von Sabrina Undank durchgeführt. Die Messung und die Auswertung der Frequenz der Aktionspotentiale in der Perforated-Patch Konfiguration mit ANP in β-Zellen aus $SUR1^{-/-}$ Mäusen erfolgte durch Jelena Sikimic und mich. Die Messungen in der cell-attached Konfiguration in Gegenwart von ANP und des PKA-Inhibitors myr-PKI wurden von Jelena Sikimic durchgeführt und ausgewertet.

Zur vervollständigenden Evaluierung der Involvierung des cGMP/PKG und cAMP/PKA Signalwegs bei der Wirkung von ANP erhob ich die Ergebnisse der Insulinsekretion mit ANP, dem PKG-Inhibitor Rp-8 sowie dem PKA-Inhibitor myr-PKI. Die Messungen der GSIS in Gegenwart von ANP und GLP-1 wurden von mir durchgeführt sowie ausgewertet und zeigten, dass ANP die durch GLP-1 vermittelten Effekte potenziert. Diese Messreihe wiederholte ich in Langerhans-Inseln von $SUR^{-/-}$-Mäusen, in denen dieser Effekt nicht mehr zu beobachten war und die Abhängigkeit dieser Potenzierung in Verbindung mit K_{ATP}-Kanälen brachte.

Das Manuskript wurde von Gisela Drews verfasst. An Bearbeitungen und Erweiterungen des Manuskripts waren Jelena Sikimic und ich ebenfalls beteiligt. Peter Krippeit-Drews und Martina Düfer wirkten bei der wissenschaftlichen Diskussion sowie der Korrektur des Manuskriptes mit.

C. Bauer, J. Kaiser, J. Sikimic, P. Krippeit-Drews, M. Düfer, G. Drews (2018).

ATP mediates a negative autocrine signal on stimulus-secretion coupling in mouse pancreatic β-cells. Endocrine: 1-14

Die Arbeit entstand unter der Leitung von Gisela Drews. Alle nachfolgend nicht näher beschriebenen Messreihen und Auswertungen wurden von Cita Bauer durchgeführt. Die Erfassung der $[Ca^{2+}]_c$ unter der Zugabe des $P2X_1$-Antagonisten Suramin und ATP wurden von Cita Bauer und mir durchgeführt sowie ausgewertet. Die GSIS Experimente mit Vorinkubation von ATP wurden von mir vorgenommen und konnten beweisen, dass die Kapsel, die die murinen Langerhans-Inseln umgibt, die Penetration und damit Wirkung von ATP in geringeren Konzentrationen auf die GSIS beeinflusst. Um diese These weiter zu stützen, wurden von Jelena Sikimic und mir Messungen der $[Ca^{2+}]_c$ mit Langerhans-Inseln in Anwesenheit von ATP in verschiedenen Konzentrationen durchgeführt. Die Perforated-Patch Messreihe mit dem $P2X_1$-Antagonisten NF-279 bearbeitete und wertete ich zusammen mit Jelena Sikimic aus, um den Einfluss von $P2X_1$ Kanälen zu spezifizieren.
Das Manuskript wurde von Gisela Drews verfasst. An der Überarbeitung und Ergänzung des Manuskriptes waren Jelena Sikimic und ich beteiligt und trugen dadurch zur Vervollständigung und Ausbau der Studie bei. Peter Krippeit-Drews und Martina Düfer wirkten bei der wissenschaftlichen Diskussion sowie der Korrektur des Manuskriptes mit.

J. Maczewsky, J. Kaiser, A. Gresch, F. Gerst, M. Düfer, P. Krippeit-Drews, G. Drews (2018).

TGR5 Activation Promotes Stimulus-Secretion Coupling of Pancreatic β-Cells via a PKA-Dependent Pathway. Diabetes 68(2):324-336

Die Arbeit entstand unter der Leitung von Gisela Drews. Alle nachfolgend nicht näher beschriebenen Messreihen und Auswertungen wurden von Jonas Maczewsky durchgeführt. Die MIN6-Zelllinie wurde von Martina Düfer aus Münster

zur Verfügung gestellt. Der Einfluss von OLA auf die intrazelluläre cAMP Konzentration wurde von Anne Gresch aus dem Arbeitskreis von Martina Düfer erfasst und ausgewertet. Die Auswertung der maximalen $[Ca^{2+}]_c$ unter OLA 10 mM erfolgte durch mich.

Zur Aufklärung der Dosis-Wirkungsbeziehung von OLA führte ich die GSIS Messreihe mit OLA in verschiedenen Konzentrationen durch und wertete diese aus. Ich war verantwortlich für die Messungen in der Perforated-Patch Konfiguration zur Erfassung des Einflusses von OLA auf das Membranpotential und die Frequenz der Aktionspotentiale. Außerdem verifizierte ich den PKA-abhängigen Wirkmechanismus von OLA mittels Messungen des Membranpotentials in der Perforated-Patch Konfiguration in Gegenwart von OLA und des PKA-Inhibitors KT5720. Die Ergebnisse der $[Ca^{2+}]_c$ Messungen in aus humanen Langerhans-Inseln isolierten β-Zellen wurden von Jonas Maczewsky und Jelena Sikimic erhoben. Das humane Material wurde von Felicia Gerst bereitgestellt.

Das Manuskript wurde von Jonas Maczewsky mit Beteiligung von Gisela Drews geschrieben. An der Überarbeitung und Ergänzung des Manuskriptes war ich beteiligt und konnte dadurch zu Vervollständigung und Ausbau der Studie beitragen. Peter Krippeit-Drews und Martina Düfer wirkten bei der wissenschaftlichen Diskussion sowie der Korrektur des Manuskriptes mit.

b) Noch nicht eingereichtes Manuskript

J. Kaiser, P. Krippeit-Drews, G. Drews

Ghrelin Influences β-cell Function by Interference with K_{ATP} Channels. Paper in preparation

Die Arbeit wurde unter der Leitung von Gisela Drews durchgeführt. Das Versuchsdesign wurde von Gisela Drews, Peter Krippeit-Drews und mir erstellt. Alle Experimente wurden von mir durchgeführt und ausgewertet. In dieser Arbeit verwendete ich mehrere Messmethoden und murine Genotypen zur Evaluierung

der Wirkung von AG und DAG auf verschiedene Abschnitte der SSK, wie die Bestimmung der $[Ca^{2+}]_c$, der GSIS, des Membranpotentials, K_{ATP}-Kanalstrom sowie -Kanalaktivität. Der Fokus dieses Manuskriptes liegt dabei auf der Antagonisierung der Wirkung von AG, der Bedeutung von DAG und insbesondere auf der Fragestellung, über welchen Signalweg AG die β-Zellfunktion beeinflusst. Zudem wurde die in der Literatur kontrovers diskutierte Rolle von SST und SST-Rs ermittelt. Das Manuskript wurde von mir in Zusammenarbeit mit Gisela Drews verfasst. Peter Krippeit-Drews wirkte bei der wissenschaftlichen Diskussion sowie der Korrektur des Manuskriptes mit.

c) Eingereichtes Manuskript

T. Hoffmeister, J. Kaiser, G. Drews, M. Düfer

Interactions between Atorvastatin and the Farnesoid X Receptor Impair Insulinotropic Effects of Bile Acids and Modulate Diabetogenic Risk. Submitted paper

Die Arbeit entstand unter der Leitung von Martina Düfer aus Münster. Die Ergebnisse wurden von Theresa Hoffmeister erhoben. Die Präparation der $FXR^{-/-}$ Mäuse und die Isolation der Langerhans-Inseln wurden von mir durchgeführt und die Langerhans-Inseln anschließend Theresa Hoffmeister in Münster zur Verfügung gestellt. Dadurch konnte gezeigt werden, dass FXR in Abhängigkeit mit der Interaktion mit CDC das Ausmaß der durch Atorvastatin ausgelösten Schädigung beeinflusst. Das Manuskript wurde von Theresa Hoffmeister in Zusammenarbeit von Martina Düfer geschrieben. Ich war an der Korrektur und Bearbeitung des Manuskripts beteiligt. Gisela Drews wirkte bei der wissenschaftlichen Diskussion sowie der Korrektur des Manuskriptes mit.

1 Einleitung

Der Diabetes mellitus Typ 2 ist ein konstantes Wohlstandsproblem in den Ländern der sogenannten ersten Welt, trotz immenser Präventionsmaßnahmen und intensiver Forschung. Mit dem steigenden Konsum und Reichtum Asiens sind Stoffwechselerkrankungen wie Diabetes mellitus Typ 2 heutzutage sogar noch weiter verbreitet und damit ein brisantes Thema, das nach wie vor einen konstanten Fokus der pharmazeutischen/medizinischen Entwicklung und Forschung erfordert. Die beim Diabetes mellitus Typ 2 bestehende Insulinresistenz und Glucoseintoleranz sind neben Bluthochdruck und Dyslipidämie Bestandteil des metabolischen Syndroms (Grundy 2006), das verheerende Auswirkungen auf die Gesundheit und Lebenserwartung der Betroffenen hat.
Mit der Entdeckung von Ghrelin (Kojima et al. 1999) eröffnete sich die Möglichkeit, eine Substanz für die Therapie des Diabetes mellitus Typ 2 zu evaluieren, die sowohl Einfluss auf die Nahrungsaufnahme als auch auf das Pankreas und die Glucosehomöostase ausübt und damit ein Bindeglied zwischen Ernährung und Diabetes mellitus Typ 2 sein könnte. Für die Entwicklung neuer Therapiemöglichkeiten ist es unerlässlich, die Wirkung und den Signalweg einer Substanz zu verstehen. Die vorliegende Arbeit hat sich zum Ziel gesetzt dazu beizutragen, die Effekte, die Ghrelin in der β-Zelle und dem Pankreas hervorruft, nachzuvollziehen und Aufklärung in Bezug auf den Wirkmechanismus zu leisten.

1.1 Die Bildung von Ghrelin

Ghrelin (Acylghrelin, AG) ist ein strukturell aus 28 Aminosäuren (AS) bestehendes Peptidhormon, welches am Ser3 eine Octanoylgruppe acyliert hat. GHRL, das humane Ghrelin Gen, ist auf dem Chromosom 3p25-26 lokalisiert (Kojima and Kangawa 2005). AG wird aus dem 117 AS bestehenden Vorläufermolekül Präproghrelin gebildet. Das Präprogrehlin setzt sich aus einem Signalpeptid (23 AS), einer AG Sequenz (28 AS) und einem C-terminalen Peptid (66 AS) zusammen. Präproghrelin wird cotranslational zu Proghrelin, einem 94 AS Peptid, gespalten und in das Lumen des endoplasmatischen Retikulums (ER) freigesetzt.

Die anschließende Veresterung zu Acylproghrelin mit einer Octansäure des Ser3 des aus 28 AS bestehenden AG erfolgt im ER durch die Ghrelin O-Acyltransferase (GOAT), die zu der Familie der membranständigen O-Acyltransferasen (MBOAT) gehört (Taylor et al. 2013). Im ER bindet die GOAT n-Octanoyl-CoA an Proghrelin, welches anschließend in den Golgi-Apparat transportiert wird (Gutierrez et al. 2008, Yang et al. 2008, Taylor et al. 2012). GOAT mRNA ist besonders im Magen stark exprimiert, konnte aber auch im Pankreas und vielen anderen Geweben wie Ileum, Jejunum und Niere nachgewiesen werden (Sakata et al. 2009, Lim et al. 2011). Schlussendlich erfolgt die Abspaltung des C-Terminus des Acylproghrelins durch die Prohormon Convertase 1/3 (PC1/3) (Zhu et al. 2006), was zur Sekretion des acylierten Ghrelins (AG) führt (Abb. 1). Ein weiteres Produkt, welches aus dem Präproghrelin entsteht, ist das 23 Aminosäure lange amidierte Peptid Obestatin (Zhang et al. 2005).

Die Acylierung von Ghrelin kann auch mit anderen Fettsäuren als Octansäure erfolgen. Das acylierte Substrat ist abhängig von der dietätischen Verfügbarkeit von Fettsäuren (Nishi et al. 2005, Kirchner et al. 2009). Die Octanoylgruppe ist jedoch die vorherrschende Form und weist zudem die höchste am AG-Rezeptor induzierte Aktivität auf (Hosoda et al. 2003). Die Octanoylgruppe bzw. Fettsäuregruppe am Ser3 wird hauptsächlich für die physiologischen Effekte von AG verantwortlich gemacht, welche die Regulation der Nahrungsaufnahme, sowie den Einfluss auf Adipositas und Insulinsekretion umfassen (Bednarek et al. 2000, Bender et al. 2019).

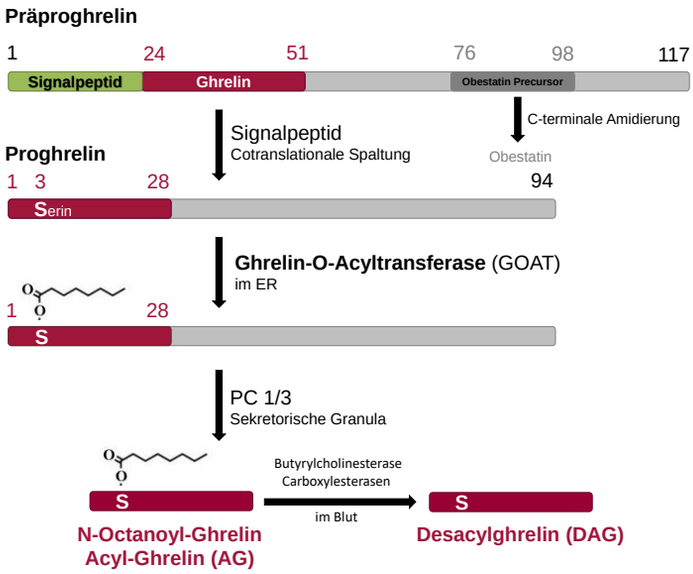

Abb. 1 Die Prozessierung und Bildung der Präproghrelinprodukte AG, DAG und Obestatin.

1.2 Der Rezeptor von AG

AG ist der Ligand des growth hormone secretagogue receptor 1a (GHS-R1a), bei dem es sich um einen Rhodopsin-ähnlichen G-Protein gekoppelten Rezeptor handelt, der aus 366 AS besteht (Howard et al. 1996, Kojima et al. 1999). GHS-R1a mRNA liegt fast ausschließlich in Bereichen des ZNS vor; darunter fallen die Nuclei des Hypothalamus und andere Areale des Gehirns, wie die Substantia nigra, die Raphekerne und die Area tegmentalis ventralis (VTA). Die Expression des GHS-R1a im Pankreas ist im Vergleich zum Gehirn von Menschen und Ratten wesentlich geringer ausgeprägt (Guan et al. 1997).

Man unterscheidet hauptsächlich zwei Varianten des GHS-R: GHS-R1a, der aus sieben transmembranären Domänen (TM1-TM7) besteht und GHS-R1b, der eine gespleißte Variante des GHS-R1a darstellt, nur fünf transmembranäre Domänen (TM1-TM5) besitzt und sich aus 289 AS zusammensetzt (Howard et al. 1996). Sowohl der GHS-R1a als auch der GHS-R1b werden von einem Gen codiert, welches beim Menschen auf dem Chromosom 3q26.31 lokalisiert ist (Howard et al. 1996, Liu et al. 2011). Der GHS-R1b wurde zunächst als nicht-funktioneller Rezeptor angesehen. Inzwischen wurde nachgewiesen, dass der GHS-R1b indirekt und direkt die Expression und die Signalwege des GHS-R1a beeinflusst.

Das liegt darin begründet, dass der GHS-R1b mit dem GHS-R1a im ER heterodimerisieren kann und damit verhindert, dass der GHS-R1a das ER verlässt und an die Plasmamembran gelangt (Leung et al. 2007, Chow et al. 2012). Es wird vermutet, dass dieser Effekt jedoch nur zum Tragen kommt, wenn eine unphysiologisch hohe Menge des GHS-R1b zur Verfügung steht (Navarro et al. 2016). Zudem konnte in Lipid Discs nachgewiesen werden, dass die Heterodimerisierung der beiden Rezeptoren zu einer Konformationsänderung des GHS-R1a führt, was im Resultat eine Verminderung der Aktivierung des G-Proteins und die Rekrutierung von Arrestin 2 bei Bindung von AG an das Heteromer zur Folge hat (Mary et al. 2013). Diese Rekrutierung von Arrestin 2 führt zur Downregulation der durch Ligandbindung induzierten Signaltransduktion von G-Protein gekoppelten Rezeptoren und dient der Desensitisierung.

Sowohl mit dem GHS-R1b als auch mit anderen G-Protein gekoppelten Rezeptoren kann der GHS-R1a Heteromere bilden. Beispielsweise können in Neuronen des Hypothalamus in Abwesenheit von AG der Dopaminrezeptor D2 (DRD2-R) und der GHS-R1a miteinander heteromerisieren und die Signalkopplung des DRD2-R verändern (Kern et al. 2012). Dimerisation von GHS-R1a mit 5-HT_{2C} verringert den GHS-R1a vermittelten Ca^{2+}-Influx, der normalerweise durch die Bindung eines Agonisten am GHS-R1a ausgelöst wird (Schellekens et al. 2013). Park und Kollegen legen dar, dass sie im Pankreas Heteromere des GHS-R1a mit dem Somatostatinrezeptor 5 (SST-R5) vorgefunden haben, die je nach Verhältnis von AG zu Somatostatin (SST) die kanonische Signalkopplung des GHS-R1a ($G_{\alpha q/11}$) oder die des SST-R5 ($G_{\alpha i}$) transduzieren (Park et al. 2012).

Eine hervorzuhebende Eigenschaft des GHS-R1a ist seine hohe konstitutive Aktivität (Holst et al. 2004). Diese ist für mehrere G-Protein gekoppelte Rezeptoren bekannt (Arvanitakis et al. 1998, Seifert and Wenzel-Seifert 2002, Smit et al. 2007), ist jedoch beim GHS-R1a besonders stark ausgeprägt. Nach dem Preassembly Model bilden metabotrope Rezeptoren und das GTP-bindende Protein (G-Protein) selbst in Abwesenheit eines Agonisten einen Komplex (Nobles et al. 2005, Gales et al. 2006, Qin et al. 2011). Die erste aktive Form (GHS-R1a:G_q Komplex) ist eine Anordnung, die für den Rezeptor-katalysierten Guanosindiphosphat- (GDP-) zu Guanosintriphosphat- (GTP-) Austausch verantwortlich ist. Der zweite GHS-R1a:G_q Komplex unterscheidet sich von der eben erwähnten Form durch eine

davon abweichende Struktur und zeigt keine Aktivierung des G-Proteins und daher auch keine GDP- zu-GTP-Umwandlung. In Abwesenheit von AG und Anwesenheit von G_q kann der GHS-R1a die aktive Konformation einnehmen, die für die konstitutive Aktivität verantwortlich ist (Abb. 2A, 2B) (Damian et al. 2015). Dadurch können der $G_{\alpha q/11}$ - PLC Signalweg und damit einhergehende Kaskaden aktiv sein, selbst wenn AG als Ligand nicht vorhanden ist (Damian et al. 2012, Damian et al. 2015, M'Kadmi et al. 2015). Dabei entspricht die PLC-Aktivität und die damit vermittelte IP_3-Akkumulation ungefähr 50% der Aktivität, die der Rezeptor beim Vorhandensein von AG als Ligand aufweist. Sobald AG bindet, wird die aktive Form des Rezeptors konsolidiert. Durch Verwendung eines inversen Agonisten wird eine zusätzliche inaktive Konformation stabilisiert und somit die konstitutive Aktivität herabgesetzt. Die Bindung von AG an den Rezeptor wird dabei nicht beeinflusst. Das Ausmaß dieser Eigenschaft wird deutlich bei einer natürlich auftretenden Genmutation im zweiten extrazellulären Loop (ECL2) (Ala204Glu), bei der die konstitutive Aktivität des GHS-R1a durch die Mutation ausgeschaltet ist. Sie geht mit einer kleineren Statur bei Menschen einher, obwohl die Bindung von AG dadurch nicht beeinflusst wird (Pantel et al. 2006).

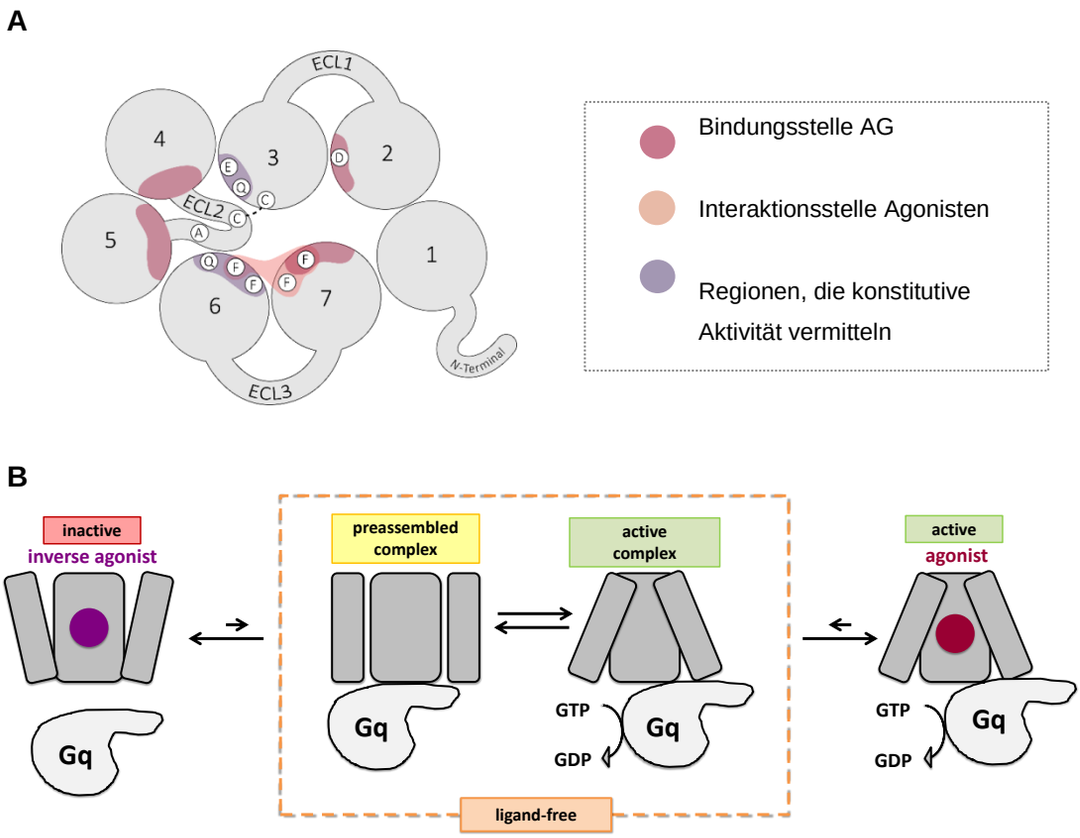

Abb. 2 Aufbau und Interaktionsstellen des GHS-R1a. Modell zur Darstellung der Interaktionen von GHS-R1a mit G_q.

A Modifiziert nach (Callaghan and Furness 2014) und erstellt von Celina Wijesekera. Dargestellt sind die transmembranären Domänen 1-7, die extrazellulären Loops 1-3 (ECL) sowie für die beschriebenen Bindungsstellen wichtige Aminosäuren. **B** Modifiziert nach (Damian et al. 2015). In Abwesenheit eines Liganden ist der aktive Komplex verantwortlich für die konstitutive Aktivität des Rezeptors. Die Bindung eines Agonisten stabilisiert den aktiven Komplex. Durch Bindung eines inversen Agonisten wird die inaktive Konformation des GHS-R1a unterstützt, wodurch der Rezeptor nicht mehr mit G_q interagieren kann.

1.3 Die Regulation der Ausschüttung von AG aus dem Magen

Die Plasmakonzentration an AG steigt während der Nahrungskarenz bzw. in Nüchternphasen und sinkt rapide nach Nahrungsaufnahme (Ariyasu et al. 2001, Cummings et al. 2001, Toshinai et al. 2001, Tschöp et al. 2001a, Shiiya et al. 2002). Die Abnahme der AG-Plasmakonzentration ist abhängig von den oral eingenommenen Nährstoffen; die Dehnung des Magens beeinflusst diese nicht (Tschöp et al. 2000, Callahan et al. 2004). Die Präsenz von Chymus im Magen hat

keinen Einfluss auf die Sekretion von AG, was darauf zurückzuführen ist, dass die AG-produzierenden Zellen keinen Kontakt mit dem Lumen haben (closed-type cells) (Date et al. 2000a, Sakata et al. 2002, Mizutani et al. 2009). Die Sekretion von AG wird stattdessen durch basolaterale Stimuli beeinflusst. Die Plasmaghrelinkonzentration sinkt, sobald die Nährstoffe den Dünndarm erreicht haben (Williams et al. 2003). Die Ausschüttung von AG aus den Belegzellen bzw. den X/A-like cells im Magenfundus wird durch mehrere transmembranäre G-Protein-gekoppelte Rezeptoren reguliert (Engelstoft et al. 2013a). Zu den stimulierenden Rezeptoren gehören beispielsweise der β_1-Adrenorezeptor (Zhao et al. 2010, Gagnon and Anini 2012) und der Sekretinrezeptor SCT-R (Engelstoft et al. 2013a), zu den inhibierenden die Fettsäurerezeptoren FFA-R2 (GP-R43) und FFA-R4 (GP-R120) (Lu et al. 2012, Gong et al. 2014) sowie SST-R1-3, die durch Freisetzung von SST aus den benachbarten Somatostatin-haltigen Zellen in der Magenschleimhaut aktiviert werden und anschließend die AG-Ausschüttung hemmen (de la Cour et al. 2007, Engelstoft et al. 2013b).

1.4 Die zentralen Wirkungen von AG

AG ist zum einem für die Ausschüttung von Wachstumshormonen aus den Zellen des Hypophysenvorderlappens verantwortlich (Shuto et al. 2002). Zum anderen ist AG das bisher einzig bekannte peripher gebildete Peptidhormon, welches die Nahrungsaufnahme fördert (Date et al. 2000b, Cowley et al. 2003, Cummings and Overduin 2007). Dabei ist der Magen das Organ, welches die höchsten Konzentrationen an AG aufweist und hauptsächlich für die Menge an zirkulierendem AG im Blutkreislauf verantwortlich ist. AG wird nicht in den Magen, sondern direkt in das Blutgefäßsystem sekretiert. Über mehrere Wege kann es anschließend seine zentrale orexigene Wirkung ausüben: AG erreicht vom Magen aus über den Blutkreislauf das Gehirn entweder durch einen nicht von der Blut-Hirn-Schranke geschützten Bereich, direkt über ein Transportsystem, welches das Überschreiten der Blut-Hirn-Schranke ermöglicht, oder indirekt über den Nervus Vagus (Angelidis et al. 2010). Die im Nucleus arcuatus lokalisierten Neurone, die Neuropeptid Y (NPY) und Agouti-related peptide (AgRP) sekretieren, exprimieren in hohem Maße den GHS-R1a, während die Proopiomelanocortin-haltigen (POMC)

Neurone zu einem wesentlich geringeren Anteil den GHS-R1a aufweisen (Willesen et al. 1999). Aus dem Vorläuferprotein POMC werden α-, β- und γ-Melanocortin-stimulierende Peptidhormone (MSH) sowie Adrenocorticotropin (ACTH) gebildet. Durch die Bindung von α-MSH an den Melancortin-4-Rezeptor 4 (MC4R) wird die Nahrungsaufnahme gehemmt (Millington 2007). Nach Bindung von AG an den $G_{\alpha q}$-gekoppelten GHS-R1a werden durch die Phospholipase C (PLC) induzierte Freisetzung von Ca^{2+} aus dem ER über die Calmodulin-abhängige Proteinkinase Kinasen aktiviert. Diese Kinasen regen die Adenosinmonophosphat-aktivierte Proteinkinase (AMPK) an (Hawley et al. 2005, Anderson et al. 2008). Die AMPK inhibiert physiologisch Adenosintriphosphat- (ATP-) konsumierende Prozesse und forciert ATP-produzierende Mechanismen wie die Fettsäureoxidation und die Glucoseaufnahme. Über diese Signalkaskade wird schlussendlich die Transkription der orexigenen Neuropeptide NPY und AgRP induziert. Gleichzeitig sind anorexigene Signalwege der POMC-Neurone verringert (Cowley et al. 2003, Cabral et al. 2015).

1.5 Expression von AG im Pankreas

Neben dem Magen wurde AG auch in anderen Organen und Geweben gefunden, wie Gehirn, Ventrikel, Lunge, Dünndarm und Pankreas (Gnanapavan et al. 2002). Im Pankreas wurde AG in geringem Ausmaß mit Glucagon in den α-Zellen kolokalisiert und darüber hinaus in einer distinkten Zellgruppe, den ε-Zellen, nachgewiesen (Date et al. 2000a, Wierup et al. 2002, Heller et al. 2005). Neurogenin 3 (NGN3) und pancreas/duodenum homeobox protein 1 (PDX1) sind nicht nur für die Entwicklung der pankreatischen endokrinen Zellen unabdingbar, sondern erwiesenermaßen ebenso für die Entwicklung von ε-Zellen aus endokrinen Vorläuferzellen (Heller et al. 2005). Wichtige Transkriptionsfaktoren sind Nk2 homeobox (Nkx2.2), paired box protein 4 sowie paired box protein 6 (Pax4, Pax6), wobei durch Deletion bzw. Inhibierung der genannten Transkriptionsfaktoren die Differenzierung zu ε-Zellen begünstigt und diejenige zu β-Zellen beeinträchtigt wird (Wang et al. 2008, Swisa et al. 2017). Von Bedeutung bei der Differenzierung zu ε-Zellen ist zusätzlich die Beteiligung des Transkriptionsfaktors NeuroD1, welcher durch Nkx2.2 reguliert wird (Chao et al.

2007, Mastracci et al. 2013). Nkx2.2 spielt bei der Maturierung der ε-Zellen eine wichtige Rolle, indem es an den AG-Promoter bindet und diesen aktiviert (Hill et al. 2010) (Abb. 3).

Eine Kolokalisation von AG mit Glucagon tritt nur kurzzeitig perinatal in Ratten auf. Beim adulten Pankreas ist AG allein in den ε-Zellen vertreten (Wierup et al. 2004). Während der Gravidität sind die Konzentrationen an AG im fetalen Pankreas von Mensch und Ratte insbesondere im Vergleich zum Magen stark erhöht. Neonatal bzw. postnatal kehrt sich dieser Umstand ins Gegenteil um (Rindi et al. 2002, Chanoine and Wong 2004, D'Amour et al. 2006). Grund hierfür ist vermutlich die Bedeutung von AG für die pränatale pankreatische Entwicklung und sein parakriner Einfluss auf die Hormonsekretion im Pankreas (Wierup et al. 2004). Auszuschließen ist dabei auch nicht, dass im Pankreas produziertes AG als Rezeptorligand in Bezug auf seine Wachstumshormon-freisetzende Wirkung im Fötus fungiert bzw. generell die intrauterine Entwicklung des Fötus unterstützt (Shimon et al. 1998, Cortelazzi et al. 2003).

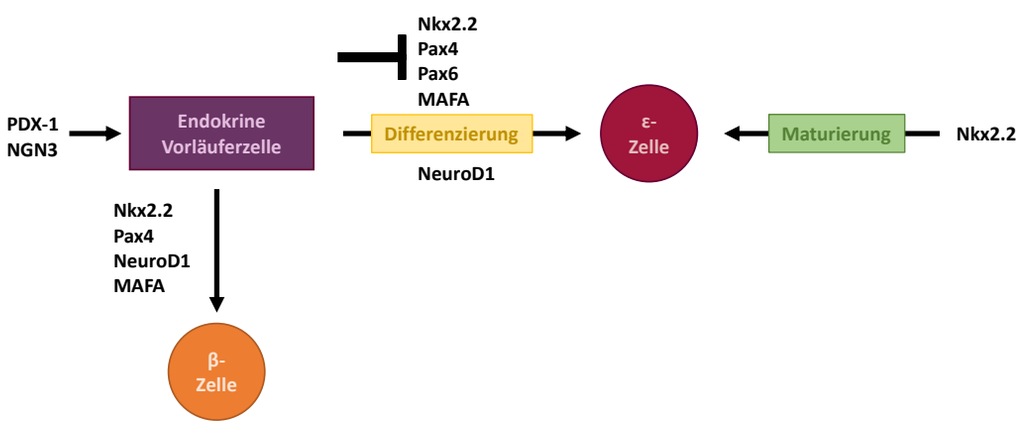

Abb. 3 Differenzierung der ε-Zellen aus NGN3 und PDX-1 stimulierten endokrinen Vorläuferzellen
Modifiziert nach (Sakata et al. 2019).

1.6 Desacylghrelin

Desacylghrelin (DAG) ist der Metabolit von AG und entsteht beim Abbau der acylierten Octansäure. Dabei wird die Octanoylgruppe von AG am Ser3 mittels Butyrylcholinesterase und Carboxylesterasen deacyliert (De Vriese et al. 2004, Schopfer et al. 2015). Die Konzentration an im humanen Blutkreislauf zirkulierendem AG beträgt etwa 10-20 fmol/ml, diejenige von AG und DAG

zusammen erreicht zwischen 100-150 fmol/ml (Kojima and Kangawa 2005). DAG macht 67% im Magen und 90% im Blut der Gesamt-Ghrelin-Immunreaktivität in Ratten aus (Hosoda et al. 2000). DAG liegt im Magenfundus und Antrum kolokalisiert mit AG in den sogenannten closed-type round cells vor. Ohne AG, dafür jedoch mit SST kolokalisiert, findet sich DAG in den sogenannten open-type cells. Im Gegensatz zu AG ist die Ausschüttung von DAG pH-abhängig, denn eine pH Erniedrigung von pH 4 auf pH 2 erhöht die DAG-Sekretion in Rattenmägen (Mizutani et al. 2009).

DAG wurde längere Zeit als ein inertes Degradationsprodukt von AG angesehen; sein Bindungsvermögen an den GHS-R1a und die Existenz eines eigenen Rezeptors für DAG werden bis heute diskutiert. Es wurde einerseits nachgewiesen, dass DAG *in vitro* als Agonist an den GHS-R1a in Aequorin-exprimierenden CHO-K1-Zellen mit einem EC_{50} zwischen 1,6 und 2 µM bindet, jedoch nach Gauna *et al.* nicht AG am GHS-R1a antagonisieren kann (Gauna et al. 2007). Ähnliche Ergebnisse wurden bei *in vitro* Experimenten mit HEK-239-Zellen und *in vivo* mit C57BL/6 Mäusen von Heppner und Kollegen erbracht, welche sich insbesondere mit der Fragestellung auseinandersetzten, ob DAG zentral wirksam ist (Heppner et al. 2014). Ihre Daten zeigen, dass DAG die PLC-Signalkaskade in HEK-239-Zellen analog zu den von Gauna *et al.* verwendeten CHO-K1-Zellen aktiviert, wenngleich der IP_3-Umsatz unter AG im Vergleich zu DAG höher ausfiel. Damit einhergehend imitierte DAG die zentralen Wirkungen von AG bei intracerebroventrikulärer Injektion in den Seitenventrikel bei Mäusen, auch in Bezug auf orexigene Effekte und Gewichtszunahme. Diametral dazu stehen die Ergebnisse einer anderen Studie aus dem Jahr 2005, in der DAG ebenfalls intracerebroventrikulär in den dritten Ventrikel und i.p. in Mäuse des ddy Stamms injiziert wurde. DAG wirkte hier jedoch anorexigen, was sich in einer reduzierten Nahrungsaufnahme und einer erhöhten Genexpression von cocaine-and-amphetamine-regulated-transcript (CART) äußerte (Asakawa et al. 2005). Da die jeweiligen Konzentrationen an DAG in beiden Studien in einem vergleichbaren nanomolaren Bereich lagen, begründet sich die Ergebnisdiskrepanz eventuell durch die verwendeten, unterschiedlichen Mausstämme.

Hinweise auf nicht durch GHS-R1a vermittelte Effekte wurden in einer weiteren Studie von Gauna und Kollegen deutlich. In primären Hepatozyten, isoliert aus

sechs Monate alten Schweinen, beobachteten sie, dass AG (100 nM) die Glucoseproduktion (output) erhöhte, während DAG in derselben Konzentration jene senkte und die Kombination aus DAG und AG die AG-vermittelten Effekte verhindern konnte. Dabei war es ihnen nicht möglich, den GHS-R1a oder den GHS-R1b in den Hepatozyten in nennenswertem Ausmaß nachzuweisen, was die Vermutung nahelegt, dass es einen weiteren Rezeptor(sub)typ geben könnte, an den AG und eventuell DAG binden (Gauna et al. 2005). In derselben Studie zeigen Gauna *et al.*, dass DAG die durch AG erfolgte Stimulation der $[Ca^{2+}]_c$ in GHS-R1a- und Aequorin-exprimierenden Zellen nicht antagonisierte. Zusätzlich konnten sie keinen kompetitiven Antagonismus nachweisen, weshalb sie eine Bindung von DAG an GHS-R1a ausschließen.

Eine Studie zur Aufklärung der Struktur des GHS-R1a wies nach, dass der Ser3-Rest mit der acylierten Octanoylgruppe eng mit dem Rezeptor verbunden ist (Bender et al. 2019). Das lässt wiederum die potente Bindung von DAG an den GHS-R1a unwahrscheinlich erscheinen bzw. würde sie, wie Gauna und Kollegen postulieren, tatsächlich nur in sehr hohen Konzentrationen möglich machen. Es konnte außerdem nachgewiesen werden, dass DAG in NPY-haltigen Neuronen die von peripher applizierten AG ausgelösten Signalkaskaden abschwächt (Inhoff et al. 2008, Fernandez et al. 2016).

Die beschriebenen Ergebnisse verdeutlichen, dass DAG kein biologisch inaktiver Metabolit von AG ist. Die durch AG ausgelösten Effekte konnten in Anwesenheit von DAG in mehreren Modellen verhindert werden, wobei nicht gesichert ist, ob dies auf einen Antagonismus am GHS-R1a zurückzuführen ist oder ein bisher unbekannter Rezeptor involviert ist.

1.6.1 Die physiologische Bedeutung von AG und DAG in Bezug auf Glucosehomöostase, Insulinresistenz und Adipositas

In mehreren Studien konnte nachgewiesen werden, dass AG in Menschen, Mäusen und Ratten die Insulinsekretion senkt und die Glucosetoleranz negativ beeinflusst bzw. Hyperglykämien bewirkt (Broglio et al. 2001, Egido et al. 2002, Reimer et al. 2003, Dezaki et al. 2004). Daher ist die physiologische Wirkung von

AG im Pankreas ein interessanter und potenzieller Ansatz für Therapien des Diabetes mellitus Typ 2.

Aufgrund der orexigenen Wirkung von AG wurde zunächst vermutet, dass mit steigendem Körpergewicht die im Blutkreislauf zirkulierende Konzentration an AG zunimmt und sich somit in adipösen Personen im Vergleich zu normalgewichtigen unterscheidet. Nachweislich verhält es sich jedoch so, dass diese in adipösen Menschen unverändert ist, wohingegen die Konzentration an DAG erniedrigt und somit das AG zu DAG Verhältnis erhöht ist. Aufgrund dieser Daten kam die Vermutung auf, dass Übergewicht bzw. ein hoher Body Mass Index (BMI) einen relativen DAG Mangel zur Folge hat und diese Faktoren miteinander korrelieren (Barazzoni et al. 2007, Longo et al. 2008, Pacifico et al. 2009b). Andererseits konnte gezeigt werden, dass in übergewichtigen Patienten die Nüchtern-Plasmakonzentration an AG durch Gewichtsabnahme wieder zunimmt (Hansen et al. 2002). Bei dieser Studie wurde jedoch kein Vergleich mit einer normalgewichtigen Kontrollgruppe durchgeführt. In anorektischen Patienten wurden höhere AG Konzentrationen vorgefunden als in Normal- und Übergewichtigen (Otto et al. 2001, Rigamonti et al. 2002, Tanaka et al. 2003).

Die Bedeutung des DAG zu AG Verhältnisses wird auch bei Methoden zur Erfassung des Ausmaßes einer Insulinresistenz deutlich. Beim hyperinsulinemic-euglycemic clamp (HEC) können durch Insulininfusionen und Konstanthalten der Glucosekonzentration Rückschlüsse auf die Fähigkeit des Gewebes gezogen werden, Glucose aufzunehmen und somit auf das Bestehen einer Insulinresistenz. DAG konnte in übergewichtigen und an Diabetes mellitus Typ 2 erkrankten Patienten die Glykämie verbessern, was mit einer herabgesetzten basalen und postprandialen AG-Konzentration im Plasma korrelierte (Ozcan et al. 2014). Übereinstimmende, aber auch gegensätzliche Ergebnisse verzeichneten Rodríguez und Kollegen in übergewichtigen Probanden und solchen, die einen durch Übergewicht ausgelösten Diabetes mellitus Typ 2 aufwiesen (Rodriguez et al. 2009). Die Konzentration an im Blutkreislauf befindlichen AG war bei ihnen allerdings nicht unverändert, sondern erhöht sowie, analog zu anderen Studienresultaten, jene von DAG erniedrigt. Diese Beobachtungen, insbesondere die erhöhte AG Konzentration, korrelierten positiv mit BMI, Taillenumfang, Insulin und dem homeostasis model assessment (HOMA) Index als repräsentativem

Parameter für eine erhöhte Insulinresistenz. Zusätzlich führten sowohl AG als auch DAG zu einer Lipidakkumulation in viszeralen Adipozyten. Zusammengenommen erklärt diese Publikation die Adipositas als eine durch erhöhte Konzentration an AG ausgelöste Hyperphagie.

Alle Studien haben gemeinsam, dass sie einen Zusammenhang zwischen den Änderungen der im Blutkreislauf befindlichen AG und DAG Konzentrationen, dem metabolischen Syndrom und einer eingeschränkten Insulinsensitivität feststellten. Dadurch wird deutlich, dass das AG zu DAG Verhältnis eine nicht zu vernachlässigende Rolle bei Erkrankungen wie Adipositas und insulinresistentem Diabetes einnimmt.

1.7 SST und sein Einfluss auf die Glucosehomöostase

Bereits kurze Zeit nach der Entdeckung von SST im Jahre 1973 (Brazeau et al. 1973) wurde konstatiert, dass SST nicht nur im Hypothalamus, sondern ebenso in Magen, Pankreas und vielen anderen Geweben exprimiert ist (Patel and Reichlin 1978). SST spielt eine wichtige Rolle im endokrinen Pankreas und wirkt auf die Glucosehomöostase ein, indem es Einfluss auf die Insulin- und Glucagonausschüttung hat. Aus Pro-SST, bestehend aus 92 AS, entstehen primär zwei aktive Produkte, SST1-14 und SST1-28, wovon Ersteres v.a. in Hypothalamusneuronen, D-Zellen des Magens und δ-Zellen des Pankreas vorhanden ist, während Letzteres in D-Zellen des Darmepithels vorliegt (Patel 1999). Die Initiierung der SST-Ausschüttung erfolgt ähnlich zu der von Insulin: Die Generierung von ATP über den Glucosemetabolismus schließt K_{ATP}-Kanäle und führt zur Depolarisation des Membranpotentials (Rorsman and Huising 2018). Die Erhöhung der intrazellulären Ca^{2+}-Konzentration über R-Typ Ca^{2+}-Kanäle und die nachfolgend über Ryanodin-Rezeptoren-induzierte Ca^{2+}-induzierte Ca^{2+}-Freisetzung stellt den Trigger für die Sekretion von SST aus den δ-Zellen dar (Zhang et al. 2007). SST inhibiert die Insulinsekretion, indem es aus δ-Zellen sekretiert parakrin an Somatostatinrezeptoren (SST-R) in den β-Zellen bindet, von denen es fünf Subtypen gibt (Bruno et al. 1992, Yamada et al. 1992, Yamada et al. 1993). Über den $G_{\alpha i/o}$-gekoppelten Signalweg hemmt SST die Aktivität der Adenylylcyclase (AC) und erniedrigt die Freisetzung von Insulin aus β-Zellen

(Alberti et al. 1973, Hsu et al. 1991, Patel et al. 1994). Im Gegensatz zu β-Zellen machen δ-Zellen nur einen geringen Anteil der endokrinen Zellmasse des Pankreas aus (Brissova et al. 2005).

SST-Rs können sowohl als Monomere als auch als Homomere vorliegen (Rocheville et al. 2000, Grant and Kumar 2010) und sind ebenso wie der GHS-R1a dazu befähigt, mit anderen G-Protein gekoppelten Rezeptoren zu heteromerisieren, wie u.a. der SST-R5 mit dem β_1-Adrenozeptor (Somvanshi et al. 2011) sowie SST-R1 und SST-R5 mit dem epidermalen Wachstumsfaktorrezeptor (EGF-R) (Watt et al. 2009).

Durch die Erforschung des Wirkmechanismus von AG durch die Arbeitsgruppen von Park, Adriaenssens und DiGruccio (Park et al. 2012, Adriaenssens et al. 2016, DiGruccio et al. 2016), deren Theorien den Einfluss von SST und SST-Rs in Bezug auf die AG-Wirkung postulieren, rückten SST und SST-Rs ins Zentrum der Aufmerksamkeit. Darauf wird insbesondere im Abschnitt 3.5 in „Ergebnis und Diskussion“ eingegangen.

2 Zielsetzung

Die Bedeutung von AG und DAG für die Glucosehomöostase, Insulinausschüttung und -resistenz wurde in mehreren Arbeiten nachgewiesen (Review von Yanagi et al. 2018). Der Konsens zeigt, dass aus dem Magen ausgeschüttetes AG über AgrP- und NPY-haltige Neurone orexigene Wirkung hat (Kojima et al. 1999, Date et al. 2000b, Cowley et al. 2003, Cummings and Overduin 2007) und im Pankreas aus den ε-Zellen (Date et al. 2000a, Wierup et al. 2004, Heller et al. 2005, Wierup et al. 2014) freigesetztes AG die Insulinausschüttung *in vitro* und in *vivo* hemmt (Broglio et al. 2001, Egido et al. 2002, Reimer et al. 2003, Dezaki et al. 2004). Diese Einigkeit in der Literatur über die zentralen Effekte von AG und seine Wirkung auf pankreatische β-Zellen ist jedoch nicht übertragbar auf die Aufklärung des Wirkmechanismus. Dabei sind insbesondere die drei differenzierten und stellenweise diametral unterschiedlichen Ergebnisse der Arbeitsgruppen Dezaki, Park sowie Adriaenssens und DiGruccio zu nennen (Dezaki et al. 2011, Park et al. 2012, Adriaenssens et al. 2016, DiGruccio et al. 2016), welche im Verlauf der nachfolgenden Abschnitte näher behandelt werden.

Diese Arbeit hat sich einerseits zum Ziel gesetzt, zur Aufklärung des Wirkmechanismus von AG in pankreatischen β-Zellen und Langerhans-Inseln beizutragen und andererseits zu eruieren, wie die Effekte von AG inhibiert und antagonisiert werden können.

Der Einfluss von DAG und die Bedeutung des Verhältnisses von AG zu DAG werden in dieser Arbeit ebenfalls thematisiert, um Rückschlüsse auf die Bedeutung dieses Verhältnisses auf die pankreatische β-Zelle zu ziehen. Dies geschieht u.a. unter Verwendung eines *in vitro* Modells, welches darauf abzielt, Nährstoff-induzierten Zellstress auszulösen.

Generell wurden verschiedene Abschnitte der Stimulus-Sekretions-Kopplung (SSK) in Bezug auf die $[Ca^{2+}]_c$ und das mitochondriale Membranpotential mittels fluoreszenzmikroskopischer Methoden sowie die Glucose-induzierte Insulinsekretion (GSIS) im Steady-State untersucht. Dabei kamen elektrophysiologische Messmethoden zur Anwendung, um den Einfluss von AG auf das Membranpotential und K_{ATP}-Kanalaktivität sowie K_{ATP}-Strom zu analysieren. Die Experimente hatten die Intention, den Einfluss von SST und SST-Rs zu eruieren und die konstitutive Aktivität des GHS-R1a zu berücksichtigen sowie die widersprüchlichen Ergebnisse der bereits veröffentlichten Studien zu diesem Thema zu validieren.

3 Ergebnisse und Diskussion

3.1 Inhibition der SSK durch AG in WT Mäusen und MIN6-Zellen

Um die Effekte von AG in murinen β-Zellclustern und Langerhans-Inseln zu untersuchen, wurden verschiedene Abschnitte der SSK näher betrachtet. Die Insulinausschüttung erfolgt nach der durch den Glucosemetabolismus verursachten Verschiebung des cytosolischen ADP/ATP Verhältnisses zu Gunsten von ATP, was zur Schließung der K_{ATP}-Kanäle führt (Ashcroft et al. 1984, Dunne and Petersen 1986, Detimary et al. 1998). Durch die Abnahme der K^+-Leitfähigkeit aufgrund der geschlossenen K_{ATP}-Kanäle überwiegt ein bislang unbekannter Strom, der die Depolarisation der Zellmembran (Henquin 1978, Rorsman and Trube 1985, Smith et al. 1990a, Drews et al. 2010, Rorsman and Ashcroft 2018) und Öffnung von spannungsabhängigen L-Typ Ca^{2+}-Kanälen zur Folge hat, wodurch der anschließende Ca^{2+}-Einstrom schlussendlich die Exozytose von Insulin aus den Vesikeln triggert (Rorsman and Renstrom 2003). Zur Evaluierung der Effekte von AG wurden neben den Langerhans-Inseln auch aus Langerhans-Inseln vereinzelte β-Zellcluster aus WT Mäusen verwendet. Letztere fanden Anwendung bei der Bestimmung der cytosolischen Ca^{2+}-Konzentration ($[Ca^{2+}]_c$) nach Inkubation mit dem Fluoreszenzfarbstoff Fura-2AM. Dabei wurde ersichtlich, dass AG (10 nM) zur Erniedrigung der $[Ca^{2+}]_c$ führte (M-AG: Fig. 1A,1B). In der Konzentration 0,5 nM hatte AG keinen Effekt mehr auf die unter G10 induzierten Oszillationen der $[Ca^{2+}]_c$ in β-Zellcluster von WT Mäusen (Messungen aus 23 β-Zellclustern, Serie mit n = 3 Mäusen beendet, Daten nicht abgebildet).

Bei der Bestimmung des Membranpotentials (V_m) in der Perforated-Patch Konfiguration wird das Polyen-Antimykotikum Amphotericin B zur Porenbildung in der Membran eingesetzt (Rae et al. 1991), wodurch Zugang zum Cytosol ohne Zellruptur geschaffen wird und die zelltypischen Signalwege aktiv bleiben. In dieser Konfiguration wurden in Gegenwart von AG die unter stimulatorischen Glucosekonzentrationen typischerweise auftretenden Aktionspotentiale verringert und außerdem die Membran hyperpolarisiert (M-AG: Fig. 1C,1D).

Kohärent zu diesen Ergebnissen konnte während einstündiger Inkubation in der Steady-State Methode AG die GSIS inhibieren, und zwar in Anwesenheit von 8 mM Glucose (G8) tendenziell sowie in G10 signifikant (M-AG: Fig. 1E). Unter der

substimulatorischen Glucosekonzentration G3 und der Schwellenglucosekonzentration G6 hatte AG keinen Effekt. Nachweislich konnte diese Wirkung auch in der murinen Insulinom-β-Zelllinie MIN6 (Ishihara et al. 1993) beobachtet werden, wodurch auf eine β-zellspezifische Wirkung von AG geschlossen werden kann (Abb. 4A).

Die dargestellten Ergebnisse unterstützen und bestätigen größtenteils die Resultate anderer Studien. Dezaki und Kollegen konnten bei Messungen der $[Ca^{2+}]_c$ in aus Ratten isolierten β-Zellen mit AG (10 nM) unter G8,3 ebenfalls eine Erniedrigung der $[Ca^{2+}]_c$ feststellen (Dezaki et al. 2004). Die erniedrigte Insulinsekretion wurde von ihnen sowohl bei i.p. Injektion von AG in männlichen ddy Mäusen als auch in isolierten Langerhans-Inseln aus Ratten unter G8,3 verzeichnet. Im perfundierten Rattenpankreas wurde sowohl von ihnen, als auch von Egido und Kollegen eine herabgesetzte Insulinsekretion mit AG (10 nM) unter stimulatorischen Glucosekonzentrationen beobachtet (Egido et al. 2002). Bei Messungen des Membranpotentials in der Perforated-Patch Konfiguration wurde von Dezakis Arbeitsgruppe lediglich eine leichte Erniedrigung der Amplitude der APs in β-Zellen von Ratten erfasst, jedoch keine Hyperpolarisation (Dezaki et al. 2007).

3.1.1 Der Effekt von AG in neonatal islet-like cell clusters (NICCs)

NICCs, die aus Pankreata wenige Tage alter Ferkel gewonnen werden (Korbutt 2009), bieten eine neue Möglichkeit der Beschaffung von primärem Zellmaterial für die Forschung. Die Genetik des Schweins ist hinsichtlich Parametern wie der Organentwicklung und (Patho)Physiologie dem Menschen ähnlicher als die von Nagetieren (Lunney 2007, Swindle et al. 2012, Wolf et al. 2014). Sowohl das exokrine und endokrine Pankreas, als auch das pankreatische Ductussystem, kommen dem des Menschen sehr nahe. Dies erlaubt eine gute Übertragbarkeit von Ergebnissen auf den Menschen (Murakami et al. 1997). Die Verteilung der β-Zellen im endokrinen Pankreas und die Morphologie der Inseln von Mensch und Schwein sind außerdem kongruenter als die von Mensch und Maus (Steiner et al. 2010, Hoang et al. 2014). Bei Menschen und Schweinen liegen die einzelnen Zelltypen verteilt und trilaminar in epithelialen Schichten organisiert vor, wodurch

mehr Interaktionen zwischen den unterschiedlichen endokrinen Zelltypen stattfinden (Bosco et al. 2010). Im Gegensatz dazu zeigen murine Langerhans-Inseln einen sogenannten Kern (Core) an β-Zellen, während sich die α-Zellen eher am Rand befinden (Samols et al. 1988, Hoang et al. 2014). Neben den Aspekten, die für die Verwendung von Zellmaterial aus dem Schwein sprechen, sind die erhöhten Tierhaltungskosten der Aufzucht vom Ferkel bis zum erwachsenen Tier, die Wirtschaftlichkeit sowie die längere Dauer, bis zum Erreichen der Adoleszenz, zu beachten. Darüber hinaus sind die Langerhans-Inseln des adulten Schweines schwer in Kultur zu halten, da sie *in vitro* recht fragil sind (Binette et al. 2001). Aufgrund der zuvor genannten Faktoren wird die Nutzung von NICCs erforscht. Direkt nach der Präparation des Jungtieres existieren noch keine Cluster von Langerhans-Inseln. Am Tag der Isolation bestehen die NICCs zu etwa 35% aus differenzierten pankreatischen endokrinen Zellen und zu ungefähr 57% aus primären epithelialen Zellen/Ductuszellen und Inselvorläuferzellen (persönliche Mitteilung von Dr. Elisabeth Kemter). Durch mehrtägige *in vitro* Kultivierung erfolgt die Maturierung der NICCs, was sich in einer Erhöhung des Anteils an differenzierten endokrinen Zellen und einer Erniedrigung des Anteils an Inselpräkursorzellen äußert (Hassouna et al. 2018). Entsprechend entwickelt sich daraus die Fähigkeit der NICCs, auf Glucosestimulus physiologisch mit der Sekretion von Insulin zu reagieren.

Die verwendeten Isolate wurden vom Genzentrum der Ludwig-Maximilians-Universität (LMU) München (Deutschland) zur Verfügung gestellt. Um die ausreichende Maturierung und physiologische Reaktion auf stimulatorische Glucosekonzentrationen zu gewährleisten wurden die entsprechenden Isolate der NICCs vor Verwendung in der GSIS für 13-15 (Isolat 1 und 2) bzw. 10, 17 und 18 Tage (Isolat 3) im Kulturmedium gehalten, dessen Zusammensetzung an die Empfehlungen von Dr. Elisabeth Kemter vom Genzentrum sowie an Ellis und Kollegen (Ellis et al. 2016) angelehnt war. Bei Isolat 1 handelte es sich um die Präparation eines 16 Tage, bei Isolat 2 und 3 eines 8 Tage alten Ferkels. Die Daten der drei Isolate sind im Diagramm Abb. 4B zusammengefasst. Die GSIS (Steady-State) der NICCs wurde methodisch an die der murinen Langerhans-Inseln angelegt, jedoch war u.a. die Inkubationszeit im Wasserbad bei 37°C von 1

h auf 1,5 h erhöht worden, um im Radioimmunassay (RIA) innerhalb der Eichkurve besser erfassbare Werte zu erhalten.
Bei jedem innerhalb der Versuchsreihen verwendeten Isolat konnte eine gute Stimulation der Insulinsekretion von G3 auf G15 beobachtet werden (Abb. 4B). Im Vergleich zum Glucosestimulationsindex G15/G3 bei murinem oder humanem Material ist dieser bei NICCs jedoch wesentlich kleiner. Dieser liegt bei NICCs etwa zwischen 1,5 und 8 (G15/G3), während bei den hier dargestellten Messungen mit murinen Langerhans-Inseln der Glucosestimulationsindex G10/G3 zwischen 30 und 50 lag. Das ist unter anderem durch das Alter der Zellen begründet. Während bei Messungen mit murinem Material etwa 4-12 Monate alte Mäuse verwendet wurden, handelte es sich bei den NICCs, wie oben erwähnt, um neonatale Isolate, welche zwar nachträglich in Kultur maturierten, aber trotzdem noch fernab der Adoleszenz waren. Analog zu den GSIS Experimenten mit murinen Langerhans-Inseln senkte AG die Insulinsekretion in NICCs, ebenso DAG (20 nM). Der Grund, weshalb DAG in NICCs die Insulinsekretion senkte, kann nicht auf eine konkrete Ursache valide reduziert werden. Eine potenzielle Theorie wäre, dass DAG in NICCs mit einer höheren Affinität an den GHS-R1a bindet, sofern die Effekte in NICCs ebenfalls über diesen Rezeptor vermittelt werden. Über die Expression des GHS-R1a in Schweinepankreata, sowie *in vitro* maturierten NICCs, ist bisher nichts bekannt, daher sind weitergehende Hypothesen an dieser Stelle nicht möglich.

Zusammenfassend ist festzuhalten, dass AG in einer Konzentration von 10 nM einen negativen Einfluss auf die wichtigsten Abschnitte der SSK in murinen β-Zellen und Langerhans-Inseln hat. Dasselbe gilt für die Insulinsekretion in der β-Zelllinie MIN6 sowie in NICCs unter stimulatorischen Glucosekonzentrationen.

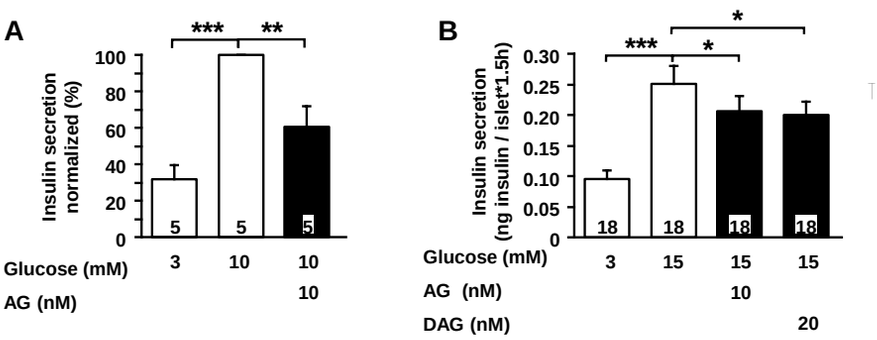

Abb. 4 AG erniedrigt die GSIS in MIN6-Zellen und neonatal islet-like cell clusters (NICCs)

A) AG erniedrigt die GSIS in MIN6-Zellen unter G10. **B)** AG und DAG erniedrigen die Glucose-stimulierte Insulinsekretion in NICCs. Die Durchführung der Experimente erfolgte bei Isolat 1 und 2 nach Kultivierung und Maturierung für 13-15 Tage, wobei an Kulturtag 13, 14 und 15 jeweils zwei Insulinsekretionen durchgeführt wurden. Mit Isolat 3 wurde analog an den Kulturtagen 10, 17 und 18 verfahren. Dargestellt sind zusammengefasst die Ergebnisse der drei Isolate mit jeweils n = 6 Insulinsekretionen.
Die Angabe n steht für die Anzahl der durchgeführten Messungen mit MIN6-Zellen bei Passage 32 und 34 und NICCs aus drei Isolationen. * $p \leq 0,05$; ** $p \leq 0,01$; *** $p \leq 0,001$

3.2 Die Bedeutung von DAG und das Verhältnis DAG zu AG

Wie bereits in Abschnitt 1.6 erwähnt, handelt es sich bei DAG um das Degradationsprodukt von AG, welches ursprünglich für metabolisch unwirksam gehalten wurde. Im Verlauf der weiteren Forschung fand man heraus, dass DAG in der Lage ist, die Effekte von AG zu antagonisieren oder eigenständige Effekte hervorzurufen (Review von Delhanty et al. 2014). Bei Messungen der $[Ca^{2+}]_c$ konnte in Gegenwart von DAG die durch AG induzierte $[Ca^{2+}]_c$ Erniedrigung verhindert werden (Abb. 5A, 5B). DAG allein steigerte die $[Ca^{2+}]_c$. In der Perforated-Patch Konfiguration hatte DAG keinen Einfluss auf das Membranpotential, und AG in Kombination mit DAG führte nicht mehr zu einer Hyperpolarisation (Abb. 5C, 5D). Trotz der Erhöhung der $[Ca^{2+}]_c$ beeinflusste DAG in den Konzentrationen 10 und 20 nM die GSIS nicht signifikant (Abb. 5E), antagonisierte jedoch erneut die Erniedrigung der Insulinsekretion durch AG (Abb. 5F).

Ob die Wirkung von AG durch DAG verhindert wird, weil Letzteres ebenfalls an den GHS-R1a bindet, ist nicht gesichert. Der von Gauna *et al*. und Heppner *et al.*

postulierte Agonismus von DAG am GHS-R1a (Gauna et al. 2007, Heppner et al. 2014) ist hier nicht zwingend die Ursache für die Befunde, da bei den Experimenten von Gauna und Kollegen DAG in weit höheren Konzentrationen eingesetzt worden ist und bei Heppner und Kollegen sich die Ergebnisse ausschließlich auf das ZNS konzentrieren. Zusätzlich ist die Vergleichbarkeit dadurch eingeschränkt, dass von Gauna *et al.* CHO-K1-Zellen und Heppner *et al.* HEK-293-Zellen verwendet wurden, während hier primäres, murines Zellmaterial aus C57BL/6 Mäusen Anwendung fand. Die Möglichkeit, dass DAG über einen bis dato unbekannten Rezeptor die Wirkung von AG antagonisiert, ist allerdings nicht auszuschließen.

Das Potential von DAG, die Wirkungen von AG zu inhibieren und sich positiv auf die Glucosehomöostase und Insulinresistenz auszuwirken (Broglio et al. 2004b, Gauna et al. 2004), führte zu ersten therapeutischen Ansätzen. Daraus resultierte die Entwicklung von AZP-531, einem DAG 6-13 Analogon, welches durch Cyclisierung eine verbesserte Stabilität und Bioverfügbarkeit aufweist, da der Abbau durch Peptidasen verzögert wird (Julien et al. 2012). Im Jahr 2016 wurde AZP-531 bereits in einer Phase II-Studie bei Hyperphagie in Folge des Prader-Willi Syndroms und in einer Phase Ib-Studie zu Diabetes mellitus Typ 2 eingesetzt. AZP-531 war insgesamt gut verträglich, jedoch fielen die ersten Studienergebnisse mit kleiner Teilnehmeranzahl eher mäßig aus. Probanden, welche eine beeinträchtigte Glucosetoleranz aufwiesen, profitierten dabei am ehesten von der AZP-531 Gabe in Form von erniedrigter Blutglucosekonzentration und reduziertem Körpergewicht (Allas et al. 2016).

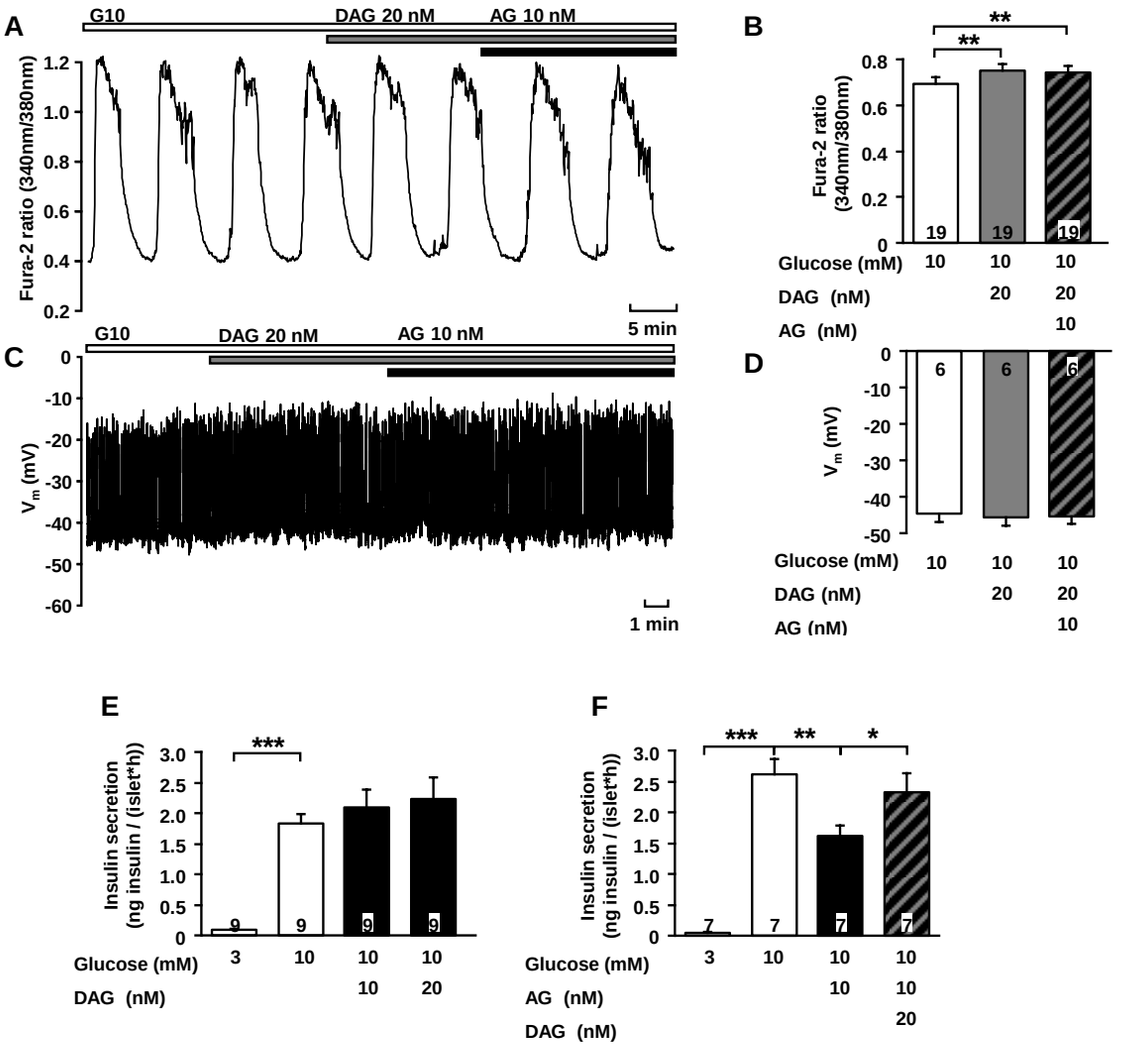

Abb. 5 DAG verhindert die Effekte von AG in β-Zellen und Langerhans-Inseln von WT Mäusen

A) Repräsentative Messung des Effekts von DAG und AG auf Glucose-induzierte Oszillationen der $[Ca^{2+}]_c$ unter G10. **B)** DAG erhöht die $[Ca^{2+}]_c$. In Anwesenheit von DAG hat AG keinen Effekt mehr auf die $[Ca^{2+}]_c$. **C)** Repräsentative Messung des Effekts von DAG und AG auf das Membranpotential in der Perforated-Patch Konfiguration unter G10. **D)** DAG hat keinen Einfluss auf das Membranpotential. In Anwesenheit von DAG tritt unter AG keine Veränderung des Membranpotentials auf. **E)** DAG steigert in den Konzentrationen von 10 und 20 nM lediglich tendenziell die GSIS. **F)** In Anwesenheit von DAG hat AG keinen Effekt mehr auf die GSIS. Die Angabe n steht für die Anzahl der durchgeführten Messungen mit Langerhans-Inseln oder β-Zellclustern aus mindestens 3 WT Mauspräparationen. * $p \leq 0,05$; ** $p \leq 0,01$; *** $p \leq 0,001$

3.2.1 AG und DAG im glucolipotoxischen Modell

Das glucolipotoxische Modell (GLTx) vereint die Folgen des langfristigen Einflusses von Hyperglykämie (Glucotoxizität) und Hyperlipidämie (Lipotoxizität) (Unger and Grundy 1985, Zhou and Grill 1995, Ritz-Laser et al. 1999, Poitout and Robertson 2008). Es dient als Modell, um im vorliegenden Fall *in vitro* murine β-Zellen und Langerhans-Inseln einem Überernährungszustand auszusetzen, zu schädigen und über Nährstoffe Zellstress zu induzieren, der demjenigen von an Diabetes mellitus Typ 2 und/oder Adipositas erkrankten Patienten nahekommt. Die Folgen sind der Verlust der β-Zellfunktion und damit einhergehend eine Reduktion des Insulingehaltes sowie eine Verschlechterung der Insulinsekretion (Poitout et al. 2006). Der dadurch ausgelöste Zellstress ist dabei einerseits durch die Generierung von reaktiven Sauerstoffspezien (ROS) zu erklären, die durch den gesteigerten Glucosemetabolismus entstehen (Robertson et al. 2004, Robertson et al. 2007), und andererseits durch Interaktion mit der Exozytose und Insulinverfügbarkeit sowie ATP-Depletion (Barroso Oquendo et al. 2018). Die Involvierung von ROS bei GLTx ist jedoch inzwischen in Bezug auf die einzeln vermittelten Effekte von Lipo-, also auch von Glucotoxizität in Frage gestellt worden (Martens et al. 2005, Lacraz et al. 2009, Barroso Oquendo et al. 2018). Die Prozesse, durch welche das GLTx *in vitro* Modell exakt Diabetes mellitus Typ 2 imitiert, sind noch nicht vollständig geklärt.

Um Glucotoxizität zu erzeugen, verwendet man in der mehrtägigen Inkubation hohe Glucosekonzentrationen. Lipotoxizität wird durch die Inkubation mit gesättigten Fettsäuren wie Palmitat ausgelöst, wodurch u.a. die Insulingenexpression herabgesetzt wird (Lameloise et al. 2001, Kelpe et al. 2003, Olofsson et al. 2007a, Poitout et al. 2010). Im hier angewendeten GLTx-Modell wurden die β-Zellcluster oder Langerhans-Inseln für 72 h in RPMI1640 Medium bei 37°C inkubiert, welches 30 mM Glucose, 1 mM Palmitat (GLT_{G30P1}) und entsprechend AG, DAG oder beides enthielt. Mit dieser Methode sollte analysiert werden, welchen Einfluss die beiden Peptide allein und kombiniert auf dieses *in vitro* GLTx-Modell ausüben. Dabei sollte zum einen untersucht werden, ob AG die *in vitro* erzeugten Folgen von überhöhtem Nährstoffangebot in Bezug auf die Glucose-induzierten Oszillationen der $[Ca^{2+}]_c$ und Insulinsekretion beeinflusst. Zum

anderen dienten die Experimente der Eruierung, ob DAG und die Kombination aus AG und DAG die durch GLT_{G30P1}-ausgelösten Schäden reduzieren können.

Die experimentell in Bezug auf $[Ca^{2+}]_c$ betrachteten β-Zellcluster wurden in zwei Gruppen unterteilt: Solche, die Glucose-induzierte Oszillationen der $[Ca^{2+}]_c$ in G15 zeigten („positive cells“) und jene, die durch die Behandlung so geschädigt waren, dass sie keine Oszillationen der $[Ca^{2+}]_c$ mehr aufwiesen. Die Inkubation in GLT_{G30P1} Medium senkte erwartungsgemäß die Anzahl der oszillatorisch aktiven β-Zellcluster im Vergleich zur Kontrolle (Abb. 6A). Die Inkubation mit AG hatte dabei keinen Einfluss (Abb. 6A). Der Zusatz von DAG zu AG in GLT_{G30P1} Medium konnte die oszillatorische Aktivität der β-Zellcluster bewahren (Abb. 6B). Die Inkubation mit ausschließlich DAG (20 nM) erhöhte den Prozentsatz an oszillatorisch aktiven β-Zellclustern nicht signifikant (Messungen aus 79 β-Zellclustern, Serie mit n = 4 Mäusen, Daten nicht abgebildet). Das Versuchsschema wurde für die GSIS übernommen. Unter GLT_{G30P1} Bedingungen war die Stimulation der Insulinsekretion von G3 auf G15 erwartungsgemäß nicht mehr vorhanden (Abb. 6C). Weder die Inkubation von AG allein noch kombiniert mit DAG bewirkte eine Veränderung (Abb. 6C).

Die Ergebnisse zeigen, dass AG in diesem GLTx-Modell keinen Einfluss auf die oszillatorische Aktivität der $[Ca^{2+}]_c$ von β-Zellclustern oder Insulinsekretion hat. Dies bedeutet nicht zwangsläufig, dass AG nicht zu einer weiteren Verschlechterung des metabolischen Zustandes führen könnte. Durch die Inkubation mit GLT_{G30P1} Medium waren die β-Zellen und Langerhans-Inseln jedoch bereits stark geschädigt, wodurch ein eventuell negativer Einfluss von AG nicht mehr detektierbar war. Die Verwendung von geringeren Konzentrationen an Palmitat oder Glucose würde eine Möglichkeit darstellen, dies genauer zu untersuchen. Da die Plasmaghrelinkonzentration in adipösen Personen jedoch nachweislich unverändert ist (Barazzoni et al. 2007, Longo et al. 2008, Pacifico et al. 2009a), ist es zusammen mit den hier präsentierten Ergebnissen unwahrscheinlich, dass AG allein eine zentrale Rolle in der Entwicklung der Adipositas und des Diabetes mellitus Typ 2 spielt. Zu beachten ist insbesondere das Verhältnis von DAG zu AG, welches in dem genannten Personenkreis erniedrigt ist und zu einer beeinträchtigten Insulinsensitivität beiträgt (Rodriguez et al. 2009, Blijdorp et al. 2013, Ozcan et al. 2014). Im hier verwendeten GLTx-Modell

konnte belegt werden, dass das höhere DAG zu AG Verhältnis, welches physiologisch annähernd dem von gesunden, normalgewichtigen Personen entspricht, zumindest die Glucose-induzierten Oszillationen der $[Ca^{2+}]_c$ erhalten kann, während DAG alleine keine signifikanten Veränderungen verursachte. Die Kombination aus DAG und AG konnte jedoch nicht die durch GLTx-verursachten Folgen auf die GSIS verhindern. Die Resultate bestätigen die Ergebnisse, dass ein Schutzeffekt gegen ROS auf die Ca^{2+}-Homöostase nicht zwangsläufig dazu führt, dass die GSIS ebenfalls geschützt ist (Barroso Oquendo et al. 2018). Die Auswirkung des Nährstoff-induzierten Zellstresses betrifft nicht nur die ersten Abschnitte der SSK, sondern auch die Bereitstellung von ATP und (u.a.) infolgedessen die Exozytose z.B. in Bezug auf die Fusion der Vesikel mit der Zellmembran sowie die damit einhergehende Freisetzung von Insulin aus den Granula oder die Insulinverfügbarkeit (Nagamatsu et al. 1999, Tsuboi et al. 2006, Dubois et al. 2007, Olofsson et al. 2007b). Folglich bietet ein höheres DAG zu AG Verhältnis keinen vollständigen Schutz gegen GLTx-verursachte Schäden, kann aber zumindest einen Teilabschnitt der SSK bewahren.

Granata und Kollegen konnten in ihren Studien die Beweise erbringen, dass AG und DAG über den cAMP/PKA Signalweg die Apoptose von β-Zellen verringern konnte, die durch Serummangel oder Cytokine (IFN-γ, TNF-α und IL1β) induziert wurde (Granata et al. 2007). DAG und Fragmente aus diesem Peptid förderten u.a. das β-Zellüberleben in Streptozotocin (STZ) behandelten Ratten (Granata et al. 2012). Die Behandlung mit STZ führt zum Untergang von β-Zellen im Pankreas und dient somit vorwiegend als Modell für Diabetes mellitus Typ 1 oder einen akut insulinpflichtigen Diabetes. Ebenso verhält es sich mit der Verwendung von Cytokinen, welche die entzündlichen Prozesse und den nachfolgenden Untergang von β-Zellen während der Entwicklung des Diabetes mellitus Typ 1 imitieren. Das hier verwendete GLT_x Modell dient, wie oben erwähnt, zur Betrachtung eines an den Diabetes mellitus Typ 2 angelehnten *in vitro* Modells, dessen Pathogenese sich grundlegend von denen des Diabetes mellitus Typ 1 unterscheidet, weshalb die Ergebnisse der oben genannten Arbeitsgruppen auf dieses Modell nicht übertragbar sind.

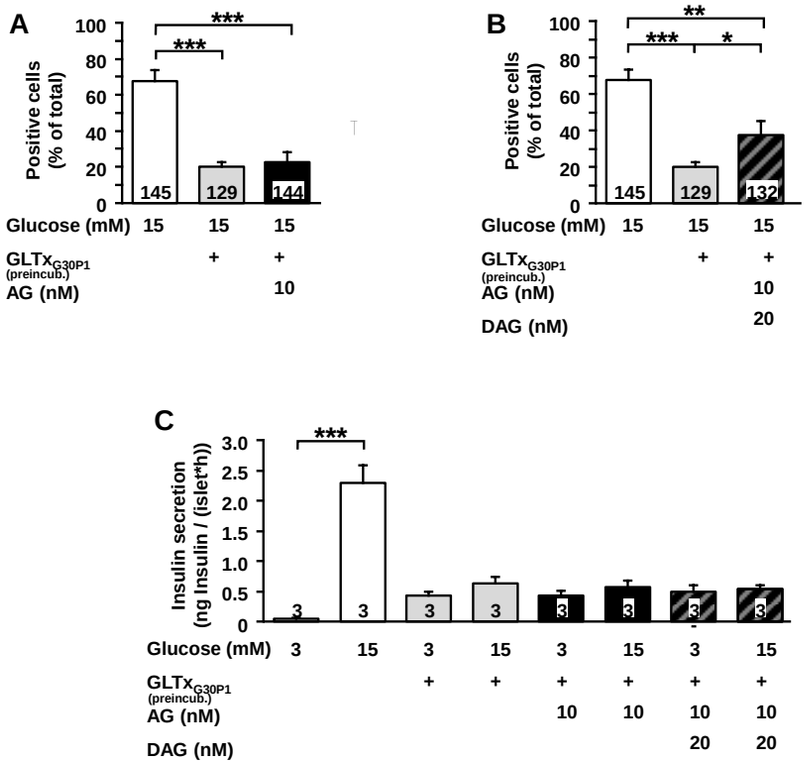

Abb. 6 Die Coinkubation von DAG und AG schützt Glucose-induzierte Oszillationen der $[Ca^{2+}]_c$ unter glucolipotoxischen (GLT_{G30P1}) Bedingungen, hat jedoch keinen Einfluss auf die GSIS.

A) Die 72-stündige Inkubation von β-Zellclustern in GLT_{G30P1} Medium senkt signifikant die Anzahl der β-Zellcluster, welche auf G15 mit Glucose-induzierten Oszillationen von $[Ca^{2+}]_c$ reagieren. Der Zusatz von AG verändert nicht die Anzahl bzw. den Prozentsatz an β-Zellen, bei denen Glucose-induzierte Oszillationen von $[Ca^{2+}]_c$ auftreten. **B)** Die 72-stündige Inkubation von β-Zellclustern in GLT_{G30P1} Medium senkt signifikant die Anzahl der β-Zellcluster, welche auf G15 mit Glucose-induzierten Oszillationen von $[Ca^{2+}]_c$ reagieren. Der Zusatz von DAG zu AG erhöht die Anzahl bzw. den Prozentsatz an β-Zellen, bei denen Glucose-induzierte Oszillationen von $[Ca^{2+}]_c$ beobachtet werden. **C)** Durch die Inkubation mit GLT_{G30P1} Medium für 72 h ist die Stimulation der Insulinsekretion von G3 auf G15 merklich verringert, sodass unter G15 keine zu G3 signifikante Steigerung der GSIS mehr erfolgt. Die gleichzeitige Inkubation mit AG oder DAG und AG unter GLT_{G30P1}-Bedingungen hat keinen Einfluss auf die Stimulation der Insulinsekretion von G3 auf G15. Die Angabe n steht für die Anzahl der durchgeführten Messungen mit Langerhans-Inseln oder β-Zellclustern aus mindestens 3 WT Mauspräparationen. * $p \leq 0,05$; ** $p \leq 0,01$; *** $p \leq 0,001$

3.3 Die Antagonisierung des AG-Effekts

In mehreren Studien wurde bisher beobachtet, dass die Verwendung eines GHS-R1a Antagonisten ausreichend ist, um die durch AG vermittelten Effekte zu nivellieren (Asakawa et al. 2003, Dezaki et al. 2004, Dezaki et al. 2007).

In den nachfolgend präsentierten Ergebnissen erwies sich die erfolgreiche Antagonisierung der AG-Wirkung jedoch als komplexer. Bei der Erfassung der $[Ca^{2+}]_c$ in β-Zellen von WT Mäusen erhöhte der peptidische Antagonist des GHS-R1a, [D-Lys^3]-GHRP-6, die $[Ca^{2+}]_c$. Bei Zugabe von AG zu [D-Lys^3]-GHRP-6 konnte die Beobachtung gemacht werden, dass [D-Lys^3]-GHRP-6 nicht in allen Messungen die $[Ca^{2+}]_c$-erniedrigende Wirkung von AG antagonisierte, obwohl sich rein statistisch gesehen eine Aufhebung des AG-Effektes ergibt, wenn man alle Experimente miteinbezieht (Abb. 7A, 7B). Die Annahme, dass ein GHS-R1a Antagonist möglicherweise nicht ausreichend ist, um die inhibierenden Effekte von AG auf die SSK zu unterbinden, wurde insbesondere in Messungen des Membranpotentials in der Perforated-Patch Konfiguration in β-Zellclustern von WT Mäusen deutlich. Nur in 50% der durchgeführten Messungen konnte durch [D-Lys^3]-GHRP-6 die Hyperpolarisation und Abnahme der AP-Frequenz verhindert werden (Abb. 7C). Die Statistik ergibt, dass AG auch in Anwesenheit von [D-Lys^3]-GHRP-6 weiterhin signifikant das Membranpotential hyperpolarisierte (Abb. 7D). Auch eine Erhöhung der Konzentration von [D-Lys^3]-GHRP-6 auf 2 µM konnte den AG-Effekt nicht inhibieren (Serie nur mit einer Maus durchgeführt).

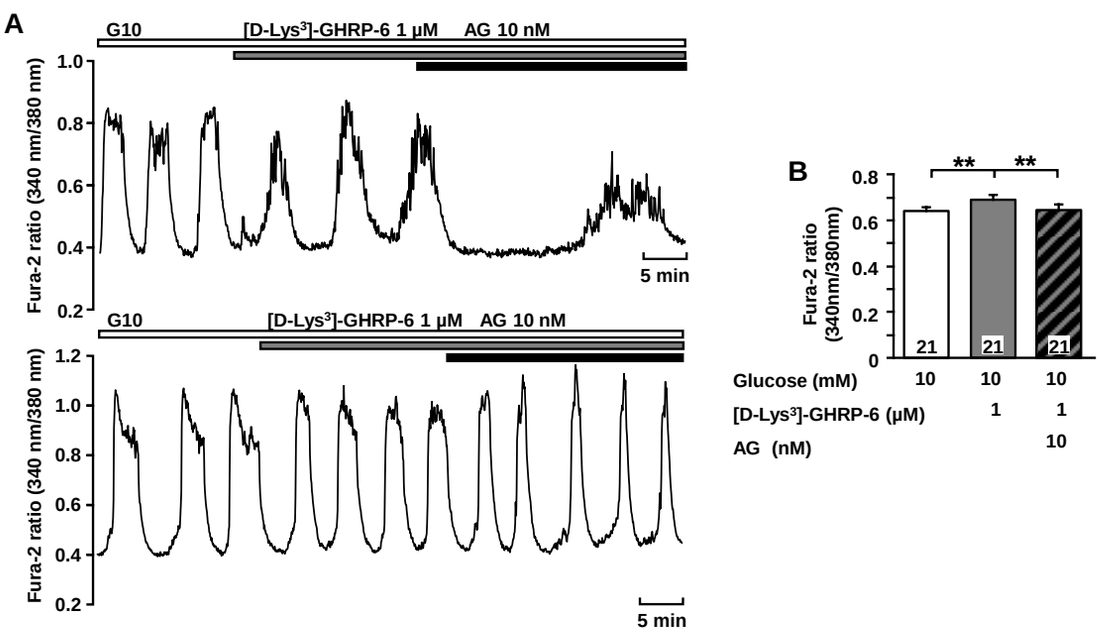

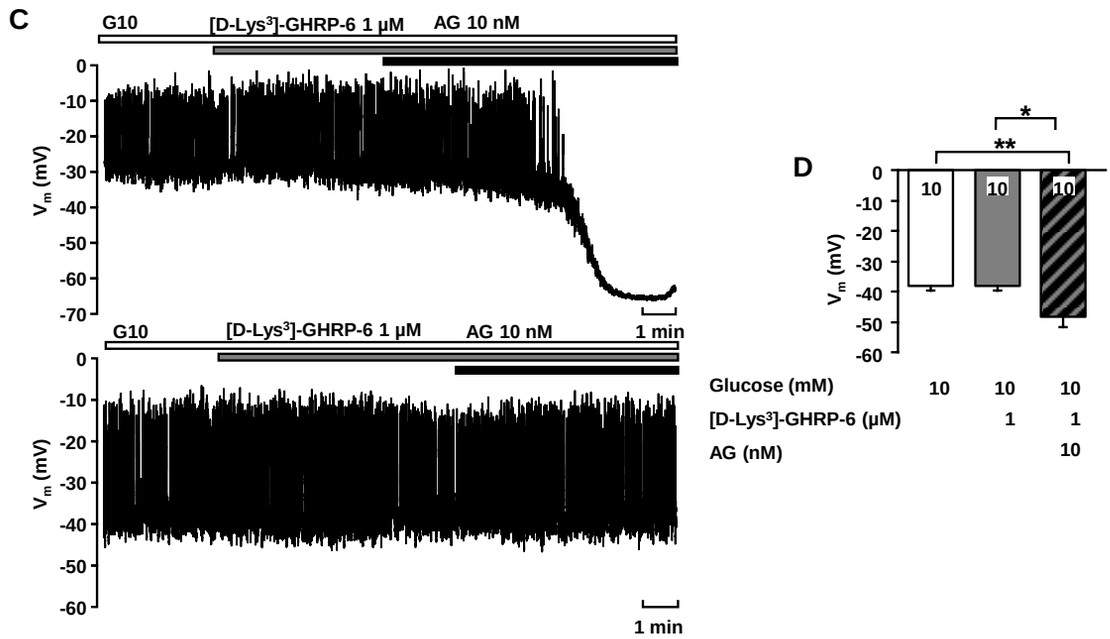

Abb. 7 Die Wirkung von AG kann nicht ausreichend mit dem peptidischen GHS-R1a-Antagonisten [D-Lys3]-GHRP-6 inhibiert werden.

A) Repräsentative Messungen des Effekts von [D-Lys3]-GHRP-6 und AG auf Glucose-induzierte Oszillationen der $[Ca^{2+}]_c$. Die obere Abb. verdeutlicht, dass AG auch in Anwesenheit von [D-Lys^3]-GHRP-6 die $[Ca^{2+}]_c$ senkt. Die untere Abb. zeigt, dass die Zugabe von AG zu [D-Lys^3]-GHRP-6 keine Veränderung der $[Ca^{2+}]_c$ verursacht. **B)** [D-Lys3]-GHRP-6 erhöht die $[Ca^{2+}]_c$. Die Kombination aus [D-Lys3]-GHRP-6 und AG hat keinen Effekt auf die $[Ca^{2+}]_c$. $[Ca^{2+}]_c$ kehrt unter [D-Lys3]-GHRP-6 und AG auf den Kontrollwert (G10) zurück. **C)** Die obere Abb. zeigt eine repräsentative Messung, bei der in Anwesenheit des peptidischen GHS-R1a Antagonisten [D-Lys3]-GHRP-6 unter AG weiterhin eine Hyperpolarisation des Membranpotentials und Erniedrigung der Aktionspotentialfrequenz auftritt (5 von 10 Messungen). Bei der unteren Abb. zeigt die repräsentative Messung, dass AG keinen Einfluss auf das Membranpotential in Gegenwart von [D-Lys3]-GHRP-6 hat. **D)** [D-Lys3]-GHRP-6 allein hat keinen Einfluss auf das Membranpotential. AG hyperpolarisiert in Anwesenheit von [D-Lys3]-GHRP-6 das Membranpotential. * $p \leq 0{,}05$; ** $p \leq 0{,}01$

Um auszuschließen, dass diese Beobachtung auf die Verwendung eines peptidischen Antagonisten zurückzuführen war, wurde die Messreihe mit dem nicht-peptidischen GHS-R1a Antagonisten YIL781 (Esler et al. 2007) wiederholt. Hierbei konnten analoge Beobachtungen gemacht und dieselben Schlüsse gezogen werden wie bei der Messreihe mit [D-Lys^3]-GHRP-6 (Abb. 8A, 8B).

Bei ausschließlicher Gabe des GHS-R1a Antagonisten [D-Lys^3]-GHRP-6 konnten Dezaki et al. in ihren Studien die Effekte von AG (10 nM) auf die $[Ca^{2+}]_c$ in β-Zellen von Ratten inhibieren. Dies belegten sie ebenfalls mit Messungen der Blutglucosekonzentration nach i.p. Gabe von AG in männlichen ddy Mäusen

(Dezaki et al. 2004). Unter Umständen sind die Messmethoden von Dezaki *et al.* nicht sensibel genug, um eine eventuell unzureichende Inhibition von AG aufzuzeigen, worauf die hier durchgeführten Patch-Clamp Experimente hindeuten, welche nachweisen, dass allein die Präsenz eines Antagonisten des GHS-R1a nicht zuverlässig die Effekte von AG auf das Membranpotential verhindern konnte (Abb. 7C, 7D, 8A, 8B).

Die Messergebnisse des Membranpotentials in Gegenwart eines GHS-R1a-Antagonisten zeigen, dass entweder die Wirkung von AG nicht ausschließlich durch den GHS-R1a vermittelt wird, oder die konstitutive Aktivität des GHS-R1a berücksichtigt werden muss. Zur Validierung wurde der Einfluss des inversen Agonisten K-(D1-NaI)-FwLL-NH_2 (M'Kadmi et al. 2015) in Kombination mit AG in Bezug auf das Membranpotential untersucht. In 4 von 6 Messungen konnte die Anwesenheit des inversen Agonisten die Effekte von AG verhindern (Abb. 8C, 8D). Statistisch war eine Hyperpolarisation durch AG im Vergleich zur Kontrolle nicht mehr sicherbar, jedoch war weiterhin eine Tendenz erkennbar.

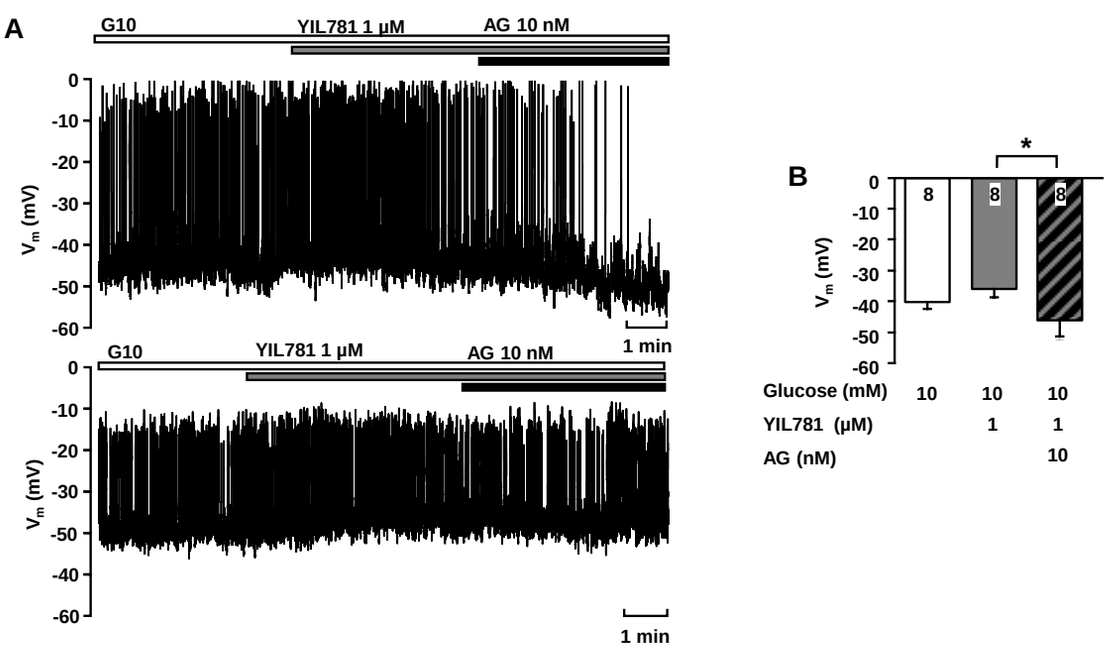

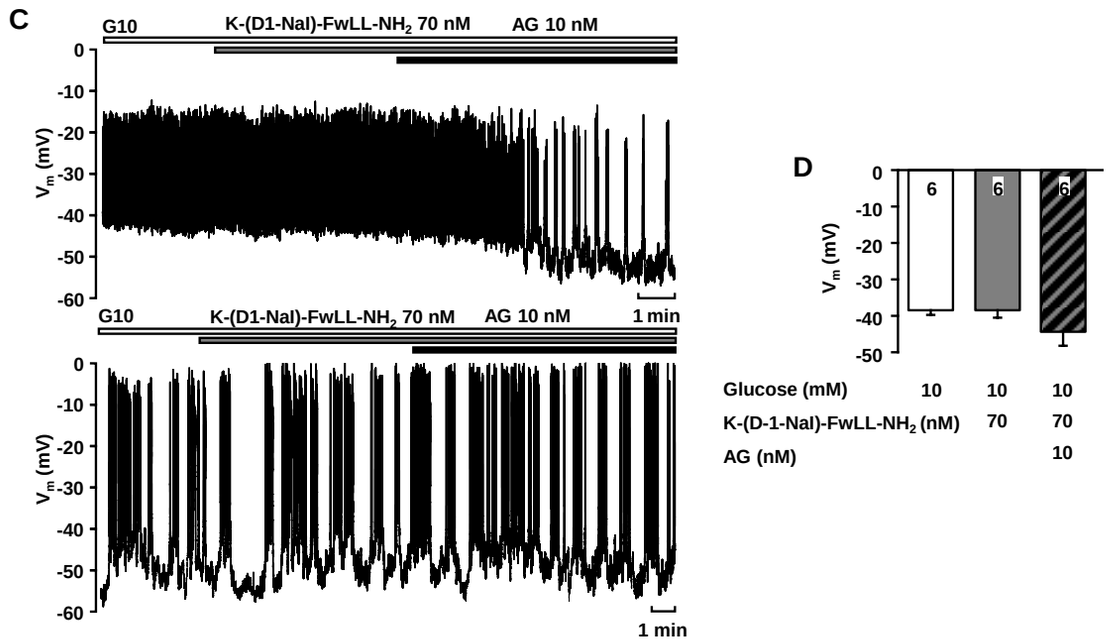

Abb. 8 Die Wirkung von AG kann nicht vollständig mit dem nicht-peptidischen GHS-R1a-Antagonisten YIL781 oder mit dem inversen Agonisten K-(D1-Nal)-FwLL-NH2 inhibiert werden.

A) Die obere Abb. zeigt eine repräsentative Messung, bei der der nicht-peptidische GHS-R1a Antagonist YIL781 das Membranpotential leicht depolarisiert, aber die Zugabe von AG dennoch das Membranpotential hyperpolarisiert und die Aktionspotentialfrequenz erniedrigt (4 von 8 Messungen). Die untere Abb. zeigt eine repräsentative Messung, in der AG in Gegenwart von YIL781 keinen Einfluss auf das Membranpotential hat. **B)** YIL781 hat keinen Einfluss auf das Membranpotential. AG hyperpolarisiert in Anwesenheit von YIL781 tendenziell das Membranpotential. **C)** Die obere Abb. zeigt eine Messung, bei der der inverse Agonist des GHS-R1a K-(D1-Nal)-FwLL-NH_2 keinen Effekt auf das Membranpotential hat, aber die Zugabe von AG das Membranpotential hyperpolarisiert und die Aktionspotentialfrequenz senkt (2 von 6 Messungen). Die untere Abb. ist eine repräsentative Messung, bei der AG in Anwesenheit von K-(D1-Nal)-FwLL-NH_2 keinen Effekt auf das Membranpotential hat. **D)** K-(D1-Nal)-FwLL-NH_2 hat keinen Effekt auf das Membranpotential. AG hyperpolarisiert in Anwesenheit von K-(D1-Nal)-FwLL-NH_2 das Membranpotential tendenziell, aber nicht signifikant. * $p \leq 0,05$

Die hyperpolarisierende und AP-Frequenz-erniedrigende Wirkung von AG wurde nur zuverlässig in der Kombination des GHS-R1a Antagonisten [D-Lys^3]-GHRP-6 und des inversen Agonisten K-(D1-Nal)-FwLL-NH_2 inhibiert (Abb. 9A, 9B). Diese Beobachtungen konnten von $[Ca^{2+}]_c$ und Patch-Clamp Messungen mit den β-Zellclustern auf GSIS-Bestimmungen mit Langerhans-Inseln übertragen werden (Abb. 9C-E). Gleichzeitig bilden diese Resultate die strukturaufklärenden Studien ab, die aufzeigen, dass die Anwendung eines inversen Agonisten die inaktive

Konformation des GHS-R1a stabilisiert, aber nicht die Bindung von AG verhindert, wodurch die durch AG induzierten Signalkaskaden trotzdem aktiv sind (Damian et al. 2012, Callaghan and Furness 2014). Im Umkehrschluss beeinflusst die alleinige Anwendung eines GHS-R1a Antagonisten nicht die konstitutive Aktivität des Rezeptors. Damit wird eine erfolgreiche Inhibierung der Wirkung von AG nur erreicht, wenn sowohl ein Antagonist als auch ein inverser Agonist verwendet werden, wie diese Messungen zeigen.

Der Ansatz, GHS-R1a Antagonisten bei T2DM und Adipositas als zukünftige Therapieoptionen in Betracht zu ziehen, brachte in der Forschung unterschiedliche Ergebnisse. Die Anwendung des nicht-peptidischen GHS-R1a Antagonisten YIL781 zeigte dabei vielversprechende Resultate (Esler et al. 2007). In insulinresistenten, diet-induced obesity (DIO) Ratten senkte YIL781 die Blutglucosekonzentration und steigerte im i.p. Glucosetoleranztest (IPGTT) die Insulinsekretion, ohne dabei die Nüchternblutglucose zu beeinflussen. Neben YIL781 fand in dieser Studie auch YIL870 Verwendung, welches sich strukturell von YIL781 durch eine geringere, polare Oberfläche und reduzierte molekulare Flexibilität unterscheidet. Beide wiesen ähnliche orale Plasmakonzentrationen auf, jedoch war die ZNS-Gängigkeit aufgrund der veränderten Struktur von YIL780 höher und damit auch der erzielte Gewichtsverlust im Vergleich zu YIL781. Daraus schließen Esler und Kollegen, dass trotz der geringeren AG-Konzentration in übergewichtigen Menschen und Mäusen, die Therapie mit einem GHS-R1a Antagonisten von Vorteil bei T2DM und Adipositas sein könnte.
Zu einem anderen Ergebnis kamen Mosa und Kollegen, die sich in ihrer Studie mit dem peptidischen GHS-R1a Antagonisten [D-Lys^3]-GHRP-6 auseinandersetzten (Mosa et al. 2017). Deren Bewertung zur Einsetzbarkeit von [D-Lys^3]-GHRP-6 in der Therapie fiel negativ aus, jedoch führten sie ihre Experimente mit normalgewichtigen, diabetischen MKR Mäusen durch. Eine Langzeittherapie mit [D-Lys^3]-GHRP-6 konnte zwar die Körperfettmasse verringern, erhöhte jedoch die Nahrungsaufnahme durch die reduzierte POMC Genexpression, wodurch anorexigene Signalwege herunterreguliert sind. Zusätzlich verschlechterte [D-Lys^3]-GHRP-6 die Glucose- und Insulintoleranz und senkte die Insulinausschüttung, was nach Mosa und Kollegen auf eine direkte Inhibition der

Insulinsekretion zurückzuführen war. Inwieweit die Ergebnisse dieser beiden Studien sich ergänzen oder ausschließen ist zu diskutieren. Bei MKR Mäusen handelt es sich um Tiere, die den dominant negativen IGF-1 Rezeptor im Skelettmuskel exprimieren, der wiederum mit dem endogenen IGF-1 Rezeptor und Insulinrezeptoren interagiert, wodurch in Leber und Fettgewebe eine Insulinresistenz entsteht. Andererseits konnten i.p. und i.c.v. Injektionen von [D-Lys^3]-GHRP-6 in normalgewichtigen und übergewichtigen ob/ob Mäusen die Nahrungsaufnahme verringern und bei Letzteren die Gewichtszunahme, Blutglucosekonzentration und Konzentration der FFS reduzieren (Asakawa et al. 2003). Insbesondere ist die Beobachtung von Asakawa und Kollegen hervorzuheben, der zufolge neben der Blutglucose- auch die Seruminsulinkonzentration und Konzentration der FFS reduziert waren. Dies deutet somit auf eine Verbesserung der Insulinresistenz hin.
Die Anwendung eines inversen Agonisten erzielte ähnlich aussichtsreiche Ergebnisse: Die Inhibierung der konstitutiven Aktivität des GHS-R1a führte bei Zucker diabetes fatty (ZDF) Ratten, die im jungen Alter sowohl adipös, als auch insulinresistent werden, zu einer verbesserten Glucosetoleranz, reduzierter Nahrungsaufnahme sowie reduziertem viszeralem Fettgewebe ohne dabei jedoch zu einer nennenswerten Gewichtsreduktion zu führen (Abegg et al. 2017).

Ähnlich wie bei Diabetes mellitus Typ 2, bei dem sich im späteren Krankheitsverlauf eine Insulinresistenz entwickelt, wird vermutet, dass bei Adipositas eine gewisse Resistenz gegenüber AG entstehen kann. Den Nachweis hierfür erbringt eine Studie von Briggs und Kollegen an DIO Mäusen, die aufzeigt, dass NPY- und AgRP-haltige Neurone nicht mehr auf AG-Stimuli reagierten (Briggs et al. 2010). Diese Resistenz schützt möglicherweise vor weiterer Gewichtszunahme, da die periphere Gabe von AG in übergewichtigen Mäusen die Nahrungsaufnahme nicht mehr stimulierte. Dieser Zustand war reversibel bei Gewichtsabnahme (Perreault et al. 2004). Die Tatsache, dass die Konzentration an AG in anorektischen Patienten erhöht und in adipösen wiederum erniedrigt ist (Tschöp et al. 2001b), deutet darauf hin, dass AG eher die physiologische Aufgabe hat, den Körper vor dem Verhungern zu schützen, als Übergewicht zu fördern, indem AG als afferentes Signal fungiert, welches das ZNS über die dietätische

Verfügbarkeit von Nährstoffen informiert und wodurch eine Anpassung des Metabolismus an den Energieverbrauch erfolgen kann (Tschöp et al. 2000, Tschöp et al. 2001a).

Insgesamt zeigen die hier dargestellten Ergebnisse und die Resultate anderer Studien, dass die Antagonisierung von AG durchaus wünschenswerte Auswirkungen auf metabolische Erkrankungen, einschließlich Diabetes mellitus Typ 2 hat.

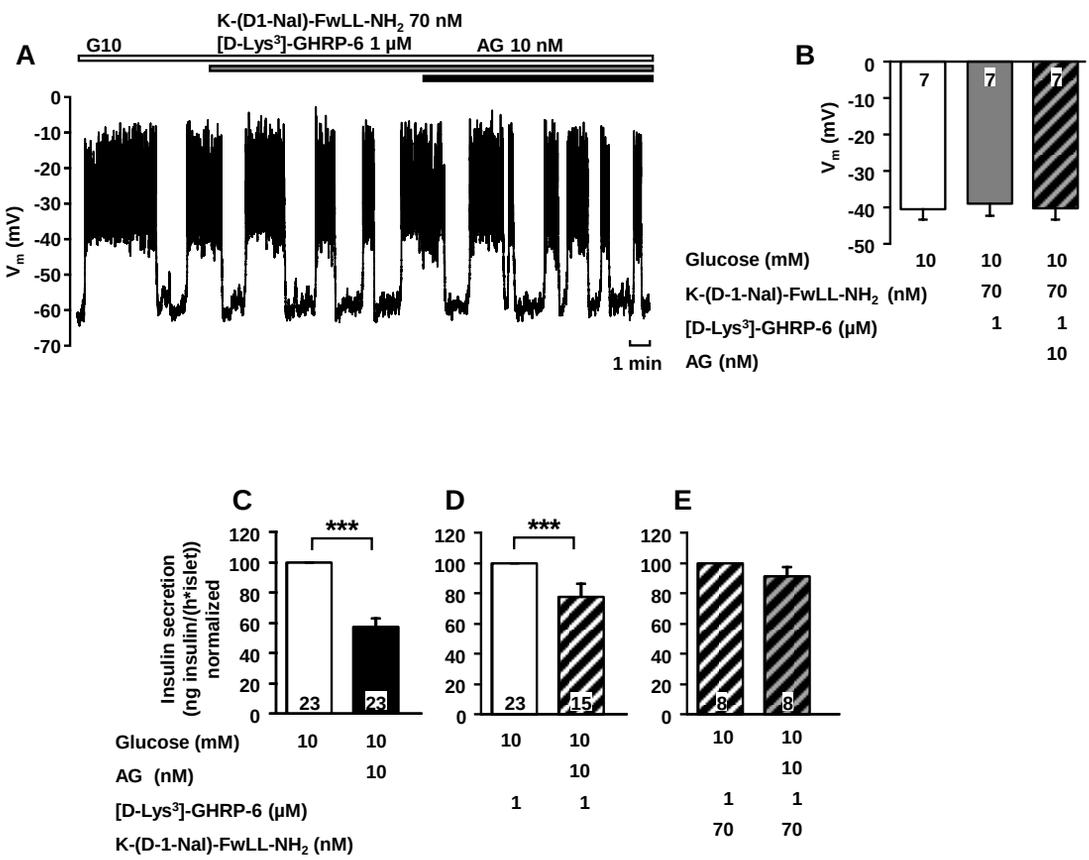

Abb. 9 Die Wirkung von AG kann nur in Anwesenheit von einem Antagonisten und inversen Agonisten des GHS-R1a inhibiert werden.

A) Repräsentative Messung des Effekts von K-(D1-Nal)-FwLL-NH_2 und [D-Lys3]-GHRP-6, sowie K-(D1-Nal)-FwLL-NH_2, [D-Lys3]-GHRP-6 und AG auf das Membranpotential. **B)** AG hat keinen Einfluss auf das Membranpotential in Gegenwart von K-(D1-Nal)-FwLL-NH_2 und [D-Lys3]-GHRP-6. **C)** AG erniedrigt die GSIS unter G10. **D)** In der Anwesenheit des GHS-R1a Antagonisten [D-Lys3]-GHRP-6 und AG ist die Erniedrigung

der GSIS im Vergleich zu Abb. 7K verringert, aber weiterhin signifikant. **E)** In der Gegenwart von K-(D1-Nal)-FwLL-NH_2 und [D-Lys3]-GHRP-6 1 hat AG keinen Einfluss auf die GSIS.
Die Angabe n steht für die Anzahl der durchgeführten Messungen mit Langerhans-Inseln oder β-Zellclustern aus mindestens 3 WT Mauspräparationen. *** $p \leq 0{,}001$

3.4 Die Effekte von AG auf β-Zellcluster und Langerhans-Inseln aus SUR1$^{-/-}$ Mäusen

Der K_{ATP}-Kanal gehört zu den einwärts gleichrichtenden K^+-Kanälen und ist ein Heterooctamer, welches sich aus zwei Untereinheiten (UE) zusammensetzt: vier porenbildendenen Kir6.2 UE und vier regulatorischen SUR1 Einheiten (Clement et al. 1997, Aguilar-Bryan and Bryan 1999). Die SUR1-UE, welche vom ABCC8 Gen codiert wird, gehört zu den ABC Proteinen und besitzt u.a. zwei cytosolische Nukleotid-bindende Domänen (NBD), an die MgADP bzw. ATP binden. Im SUR1-knockout (SUR1$^{-/-}$) Mausmodell ist das ABCC8 Gen deletiert (Seghers et al. 2000). Der K_{ATP}-Kanal wird vom ER an die Plasmamembran transportiert, wenn er im ER korrekt aus den beiden UE zusammengesetzt wurde (Zerangue et al. 1999). Folglich verfügen SUR1$^{-/-}$ Mäuse über keine K_{ATP}-Kanäle. Obwohl der K_{ATP}-Kanal eine zentrale Rolle in der SSK einnimmt, reagieren SUR$^{-/-}$ Mäuse auf Glucosestimuli mit der Sekretion von Insulin, wenngleich sich Unterschiede abzeichnen: Bei basalen Glucosekonzentrationen weisen SUR$^{-/-}$ Mäuse eine erhöhte und bei stimulatorischen Glucosekonzentrationen eine erniedrigte Insulinsekretion im Vergleich zu WT Mäusen auf (Shiota et al. 2002, Nenquin et al. 2004, Haspel et al. 2005). Außerdem ist die erste der beiden Phasen der GSIS, welche sich durch einen schnellen und transienten Anstieg der Insulinsekretion auszeichnet, bei SUR$^{-/-}$ Mäusen nicht vorhanden.
Die im WT beobachtete inhibierende Wirkung von AG auf die SSK war in β-Zellen und Langerhans-Inseln von SUR1$^{-/-}$ Mäusen nicht mehr vorhanden (M-AG Fig. 4A-4E). In Bezug auf das Membranpotential wurde in Gegenwart von AG (10 nM) eine leichte, aber signifikante Depolarisation des V_m erfasst. In aus SUR$^{-/-}$ isolierten β-Zellclustern steigerte DAG (20 nM) analog zum WT die $[Ca^{2+}]_c$ unter G10. Die Zugabe von AG (10 nM) zu DAG (20 nM) bewirkte keine Veränderung der $[Ca^{2+}]_c$ oder der GSIS (Messungen aus 12 β-Zellclustern aus n = 3 Mäusen und n = 6 Sekretionen aus mindestens 3 Mäusen, Daten nicht abgebildet). DAG (20 nM)

hatte keinen Einfluss auf die GSIS in isolierten Langerhans-Inseln aus $SUR^{-/-}$ Mäusen (n = 6 Sekretionen aus mindestens 3 Mäusen, Daten nicht abgebildet). Diese Ergebnisse zeigen, dass der Effekt von AG durch den K_{ATP}-Kanal vermittelt wird, während der K_{ATP}-Kanal bei der Wirkung von DAG nur eine untergeordnete Rolle zu spielen scheint.

3.4.1 AG interagiert indirekt mit K_{ATP}-Kanälen

Durch den Glucosemetabolismus stellt das Mitochondrium mittels Redoxreaktionen ATP zur Verfügung, welches zum Schließen der K_{ATP}-Kanäle führt und ein Schlüsselelement in der SSK ist (Krippeit-Drews et al. 2000). Ein möglicher Angriffspunkt für AG wäre somit die ATP-Produktion in der Atmungskette im Mitochondrium. Zur Untersuchung dieser Möglichkeit wurde das mitochondriale Membranpotential ($\Delta\psi$) mit dem Fluoreszenzfarbstoff Rhodamin123 erfasst. Unter Kontrollbedingungen ist erwartungsgemäß unter G0,5 die Depolarisation und unter G10 die Hyperpolarisation des $\Delta\psi$ zu beobachten, wobei AG keinen Einfluss auf $\Delta\psi$ unter G10 ausübte (Abb. 10A, 10B). Dadurch ist unwahrscheinlich, dass AG über die mitochondriale ATP-Produktion den K_{ATP}-Kanal beeinflusst.

Der exzidierte Patch in der inside/out Konfiguration dient dazu, Einzelkanalströme zu analysieren. Mittels der inside/out Patch Konfiguration wurde untersucht, ob AG direkt mit dem K_{ATP}-Kanal interagieren kann, ohne dass das Cytosol mit physiologischen Signaltransduktionsketten und second messenger Molekülen vorhanden ist. In Gegenwart von ATP im Konzentrationsbereich zwischen 0,1 und 1 mM schließen die K_{ATP}-Kanäle, wodurch die mittlere Stromdichte signifikant sinkt (Abb. 10C, 10D). Bei Zugabe von AG zu ATP nahm die mittlere Stromdichte tendenziell, jedoch nicht signifikant zu. Eine Öffnung von K_{ATP}-Kanälen war in der Anwesenheit von ATP und AG nicht zu beobachten (Abb 10C, 10D). Bei Messungen des Stroms in der Perforated-Patch Konfiguration bleibt der Zellmetabolismus intakt, wodurch second messenger Signalwege weiterhin funktionsfähig sind. Dabei wird das Membranpotential auf -70 mV „geklemmt“, um die Aktivität von spannungsabhängigen L-Typ Ca^{2+}-Kanälen auszuschließen. Da der K_{ATP}-Kanal spannungsunabhängig ist, kann unter diesen Bedingungen folglich v.a. der K_{ATP}-Strom (Garrino et al. 1989) erfasst sowie untersucht werden, ob AG

über diesen Weg den K_{ATP}-Kanal aktiviert. AG erhöht signifikant den K_{ATP}-Strom in der Gegenwart von G6 (Abb. 10E, 10F). Der Einfluss von AG auf den Strom scheint nicht nur von der Öffnung von K_{ATP}-Kanälen herzurühren, was die Ergebnisse mit Tolbutamid, einem K_{ATP}-Kanal Inhibitor, wiedergeben (Abb. 10G, 10H). In Gegenwart von Tolbutamid und AG bleibt weiterhin ein Reststrom vorhanden, der nicht auf den K_{ATP}-Kanal zurückzuführen ist. AG verändert nicht das Umkehrpotential, wie durchgeführte Spannungssprünge von -50 bis -100 mV zeigen (Messungen aus 4 β-Zellclustern, Serie mit n = 1 Maus, Daten nicht abgebildet). Um zu untersuchen, ob unspezifische K^+-Kanäle an den Effekten von AG beteiligt sind, wurde die Messserie in Gegenwart von Tolbutamid und Tetraethylammoniumchlorid (TEA) wiederholt, einem unspezifischen K^+-Kanal Inhibitor, welcher u.a. verzögert gleichrichtende K_v Ströme (delayed rectifier K_v currents) blockiert. TEA konnte den erzeugten Strom unter AG weiter herabsetzen, aber der Strom kehrte erst nach längerer Zugabe auf Kontrollniveau zurück (Abb. 10I, 10J). Diese Beobachtungen lassen darauf schließen, dass die Wirkung von AG nicht ausschließlich auf die Öffnung von K_{ATP}-Kanälen zurückzuführen ist, sondern ebenfalls unspezifische K^+-Kanäle involviert sind. Der Einfluss von verzögert gleichrichtenden K_v-Kanälen, welche an der Repolarisation der β-Zellmembran beteiligt sind (Velasco and Petersen 1987), ist jedoch eher unwahrscheinlich, da diese während des Ruhemembranpotentials nicht aktiv sind und die Messungen bei einer Haltespannung von -70 mV durchgeführt worden waren (Henquin 1990, Smith et al. 1990b). Einen nicht zu vernachlässigenden Beitrag zur Repolarisation von β-Zellen haben außerdem Ca^{2+}-abhängige K^+-Kanäle (K_{Ca}-Kanäle), zu denen die large-conductance BK-Kanäle, die intermediate-conductance SK4-Kanäle und die small-conductance SK1-3-Kanäle zählen. BK-Kanäle öffnen durch Ca^{2+}-Stimulus und sorgen für einen Ausstrom von K^+. Ihre Ca^{2+}-Sensitivität ist abhängig vom Membranpotential, d.h., dass sie sensitiver bei Depolarisation reagieren, womit eine Beteiligung von BK-Kanälen an dieser Stelle unwahrscheinlich ist. SK4-Kanäle hingegen sind zwar ebenfalls Ca^{2+}-abhängig, jedoch weitgehend spannungsunabhängig (Jensen et al. 1998, Vogalis et al. 1998), wodurch sie eventuell an der Wirkung von AG beteiligt sein könnten. Um den Einfluss von AG auf SK4-Kanäle zu untersuchen könnte man die K_{ATP}-Strom-Messreihe in Anwesenheit des SK4-Kanal-Inhibitors Tram 34 wiederholen.

Ein weiterer, möglicher Angriffspunkt von AG wäre die Inhibition von transient receptor potential channels (TRP-Kanäle), welche in TRPV, TRPM und TRPC differenziert werden. TRP-Kanäle sind nicht-selektive, Ca^{2+}-durchlässige Kationenkanäle, die zum depolarisierenden Strom in β-Zellen beitragen (Jacobson and Philipson 2007, Philippaert and Vennekens 2018). Kurashina *et al.* finden in ihrer Studie mittels Perforated-Patch Messungen in WT und $TRMP2^{-/-}$ Mäusen heraus, dass AG über Erniedrigung der cAMP-Konzentration TRPM2-Kanäle inhibiert, und erklären u.a. damit den negativen Einfluss von AG auf die SSK (Kurashina et al. 2015).

Die Arbeitsgruppen von Dezaki und Kurashina sind neben den hier präsentierten elektrophysiologischen Messreihen die einzigen, die Patch-Clamp Experimente mit AG durchgeführt haben. Sie zeigten, dass AG in der Perforated Whole-Cell Konfiguration die Amplitude von K_V-Kanalströmen erhöhte und dieser Effekt durch den PKA-Aktivator 6-Phe-cAMP verhindert wurde (Dezaki et al. 2011).

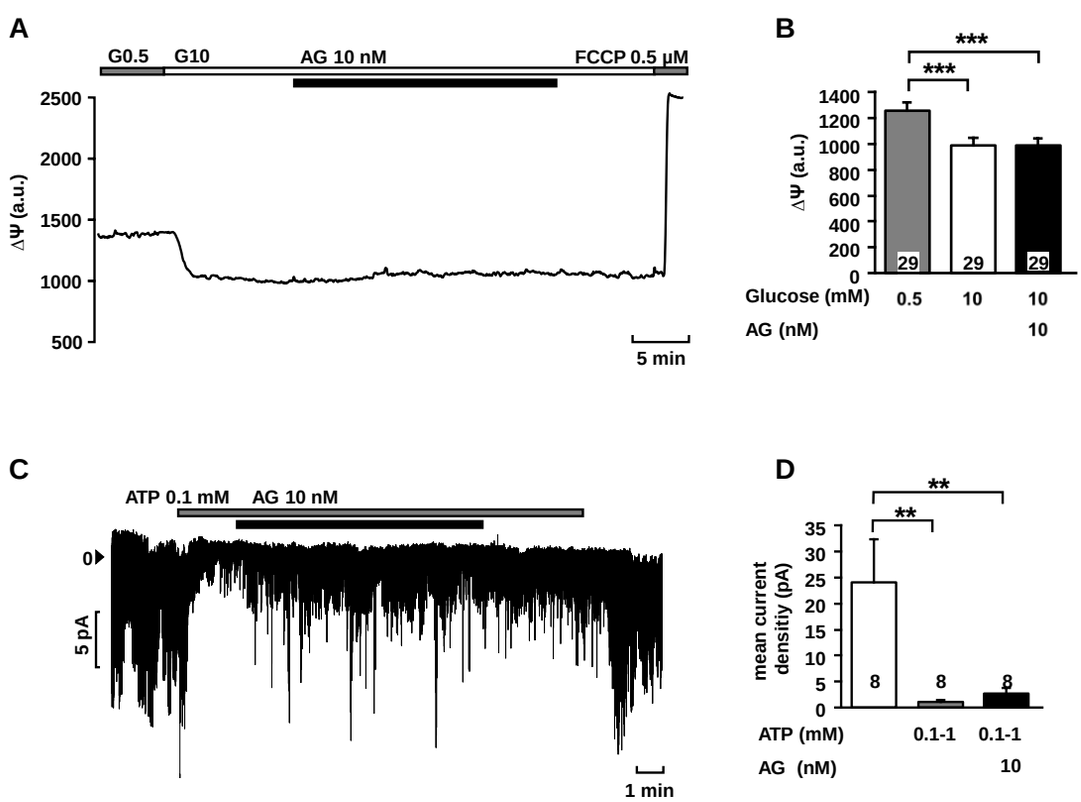

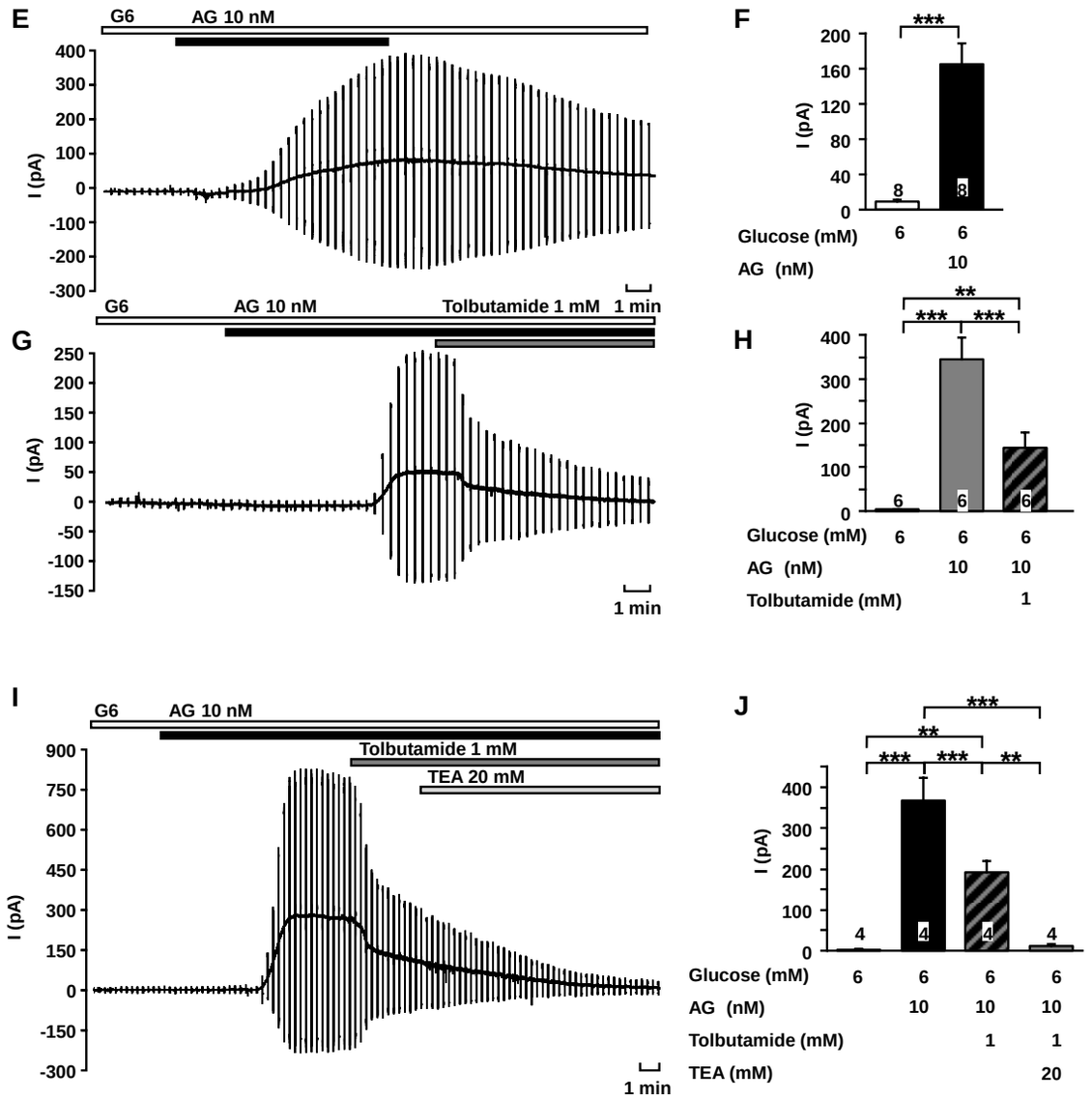

Abb. 10 AG interagiert indirekt mit K_{ATP}-Kanälen

A) Repräsentative Messung des Effekts von AG unter G10 auf ∆ψ in β-Zellclustern. FCCP entkoppelt die Atmungskette und führt zur vollständigen Depolarisation des ∆ψ. **B)** AG hat keinen Effekt auf ∆ψ. **C)** Repräsentative Messung der Wirkung von ATP und AG auf die mittlere Stromdichte in der inside/out Patch Konfiguration. **D)** Unter ATP schließen K_{ATP}-Kanäle und die mittlere Stromdichte sinkt. Die Zugabe von AG hat keinen Einfluss auf die mittlere Stromdichte. **E)** Repräsentative Messung des Effekts von AG auf K_{ATP}-Strom unter G6 in der Perforated-Patch Konfiguration. **F)** AG erhöht den K_{ATP}-Strom. **G)** Repräsentative Messung des Effekts von AG in Gegenwart von Tolbutamid auf den K_{ATP}-Strom unter G6 in der Perforated-Patch Konfiguration. **H)** In Anwesenheit von Tolbutamid ist unter AG weiterhin ein Reststrom vorhanden. **I)** Repräsentative Messung des Effekts von AG bei Zugabe von Tolbutamid und TEA auf den K_{ATP}-Strom unter G6 in der Perforated-Patch Konfiguration. **J)** Der Zusatz von Tolbutamid und TEA senkt den durch AG ausgelösten K_{ATP}-Strom auf Kontrollniveau (G6).

Die Angabe n steht für die Anzahl der durchgeführten Messungen mit β-Zellclustern aus mindestens 3 WT Mauspräparationen. ** $p \leq 0{,}01$; *** $p \leq 0{,}001$

3.5 Die Interaktion von AG und SST und der Einfluss von SST-Rezeptoren

Die langjährig etablierte Theorie von Dezaki und Kollegen war, dass AG seine Wirkung in der β-Zelle über den darin exprimierten GHS-R1a ausübt. Der $G_{\alpha i}$-gekoppelte GHS-R1a führt nach der Bindung von AG über die Erniedrigung von cAMP und dadurch herabgesetzter PKA-Aktivität zu der Öffnung von K_v-Kanälen und damit einhergehend zur Hemmung der SSK und Erniedrigung der Insulinsekretion (Dezaki et al. 2011). Später spezifizierten sie ihren postulierten Signalweg dahingehend, dass der GHS-R1a die beschriebene Signalkaskade über eine Kopplung mit TRPM2 bewirkt (Kurashina et al. 2015). Im Jahr 2012 beschrieben Park und Kollegen eine neue Hypothese: Da der GSH-R1a kanonisch in anderen Geweben $G_{\alpha q}$-gekoppelt ist, bedeutet das im Umkehrschluss, dass AG auf die pankreatische β-Zelle über den PLC-Signalweg eine steigernde Wirkung auf die GSIS haben müsste. Um dieses Paradoxon aufzulösen zeigten die Autoren mittels Förster-Resonanzenergietransfer (FRET) und Biolumineszenz-Resonanzenergietransfer (BRET), dass der in der Ratteninsulinomzelllinie INS-1J exprimierte $G_{\alpha i}$-gekoppelte SST-R5 und $G_{\alpha q}$-gekoppelte GHS-R1a miteinander heteromerisieren. Ihren Daten zufolge erniedrigt AG genaugenommen die cAMP-Akkumulation dann, wenn das relative Verhältnis von AG zu SST hoch ist (in Nüchternphasen), während ein niedriges AG zu SST Verhältnis das aus GHS-R1a und SST-R5 zusammengesetzte Heteromer dissoziiert und die $G_{\alpha q}$-gekoppelte, PLC-typische Mobilisierung von $[Ca^{2+}]_c$ steigert (Park et al. 2012).

Zwei weitere Arbeitsgruppen veröffentlichten im Jahr 2016 unabhängig voneinander übereinstimmende Ergebnisse. Sie konnten durch Erstellung eines transkriptomischen Profils den GHS-R1a in murinen β-Zellen nicht nachweisen, dafür jedoch in murinen δ-Zellen (Adriaenssens et al. 2016, DiGruccio et al. 2016). Ihre Theorie besagt, dass aufgrund der kanonischen $G_{\alpha q}$-Kopplung des GHS-R1a die Bindung von AG die PLC aktiviert und die bereits durch Glucose initiierte SST-Sekretion steigert. SST bindet anschließend an SST-R3 Rezeptoren in der β-Zelle und setzt über $G_{\alpha i}$-Kopplung die cAMP-Konzentration durch Hemmung der AC herab, wodurch die Insulinsekretion erniedrigt wird. Zusätzlich wiesen die Arbeitsgruppen von Adriaenssens und DiGruccio im perfundierten Mauspankreas nach, dass AG (100 nM) die Glucose-induzierte SST-Sekretion erhöhte. Folglich

argumentieren sie in ihren Veröffentlichungen, dass schlussendlich nicht AG an der β-Zelle die GSIS senkt, sondern die beobachteten Effekte auf SST zurückzuführen sind.

Zur Evaluierung der beschriebenen Theorien und der möglichen Interaktion von AG und SST wurde u.a. die $[Ca^{2+}]_c$ bestimmt. Für die nachfolgenden Messreihen wurde SST1-14 verwendet, welches die dominant vorkommende Form im Pankreas darstellt (Noe 1981, Patel 1999). Eingesetzt wurde SST1-14 in der Konzentration von 2 nM, um die Glucose-induzierten Oszillationen der $[Ca^{2+}]_c$ in der Anwesenheit von SST1-14 moderat und zumindest nicht in jedem erfassten β-Zellcluster vollständig zu hemmen. Bei dieser Messreihe konnten zwei Effekte beobachtet werden, wobei einer davon häufiger auftrat. Zum einen konnte unter SST1-14 eine vollständige oder moderate Hemmung der Glucose-induzierten Oszillationen der $[Ca^{2+}]_c$ erfasst werden, welche unter AG wieder auftraten (Abb. 11A, 11B). Zum anderen trat gelegentlich unter der Zugabe von AG zu SST1-14 eine synergistische Hemmung der Glucose-induzierten Oszillationen von $[Ca^{2+}]_c$ auf (Abb. 11C, 11D). Diese Ergebnisse machen deutlich, dass es in β-Zellclustern zwischen AG und SST1-14 zu verschiedenen Interaktionen kommt. Der Versuchsansatz wurde angepasst und für die GSIS in Langerhans-Inseln aus WT Mäusen übernommen wobei zusätzlich die Konzentration von 10 nM SST1-14 untersucht wurde. Die Ergebnisse konnten die Beobachtungen aus den $[Ca^{2+}]_c$-Messungen statistisch nicht bestätigen (Abb. 12E). Die Begründung hierfür liegt vermutlich in der Methode bzw. Verwendung von Langerhans-Inseln, wodurch Einzeleffekte jeder Substanz und synergistische Effekte beider Substanzen an den einzelnen Zelltypen des Pankreas schlechter zu differenzieren sind.

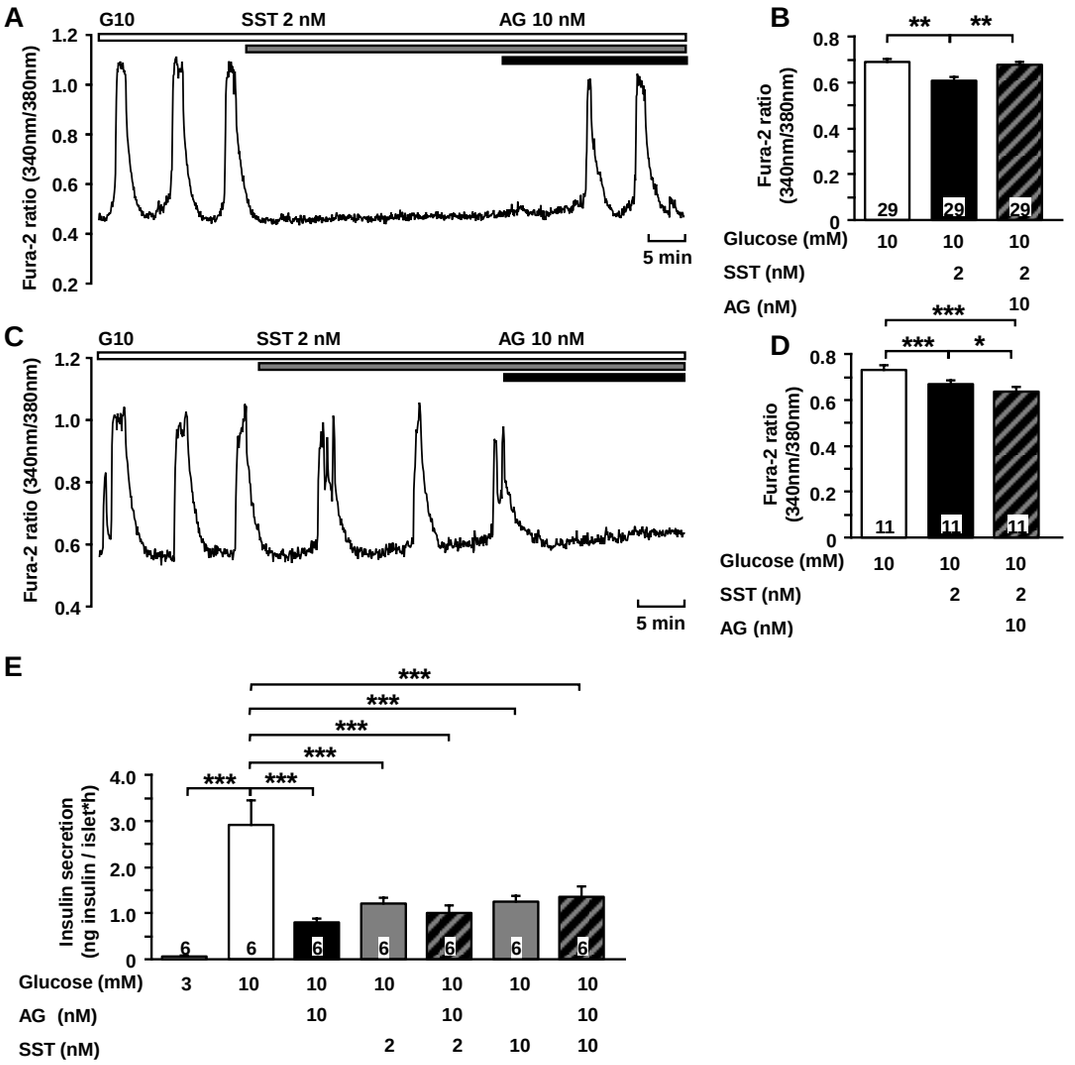

Abb. 11 Der Einfluss von SST und AG auf β-Zellen und Langerhans-inseln

A) Repräsentative Messung des Effekts von SST und AG auf die Glucose-stimulierten Oszillationen der $[Ca^{2+}]_c$. Auch bei vollständiger Hemmung der Glucose-stimulierten Oszillationen der $[Ca^{2+}]_c$ treten unter AG Oszillationen der $[Ca^{2+}]_c$ auf. **B)** SST senkt die $[Ca^{2+}]_c$. In der Anwesenheit von SST und AG steigt die $[Ca^{2+}]_c$ auf Kontrollniveau (G10). **C)** Repräsentative Messung des Effekts von SST und AG auf die Glucose-stimulierten Oszillationen der $[Ca^{2+}]_c$. Bei moderater Hemmung der $[Ca^{2+}]_c$ unter SST erfolgt unter AG eine synergistische Hemmung der Glucose-stimulierten Oszillationen der $[Ca^{2+}]_c$. **D)** SST senkt die $[Ca^{2+}]_c$ und in Anwesenheit von AG wird die $[Ca^{2+}]_c$ weiter erniedrigt. **E)** AG und SST in den Konzentrationen 2 und 10 nM senken die GSIS. Die Kombination aus AG und SST erniedrigt ebenfalls die GSIS im Vergleich zu G10. * $p \leq 0{,}05$; ** $p \leq 0{,}01$; *** $p \leq 0{,}001$

Zur weiteren Untersuchung, ob SST-Rs an der Wirkung von AG im Pankreas beteiligt ist, wurde eine GSIS-Reihe mit dem unspezifischen SST-R-Antagonisten Cyclosomatostatin (CSS) durchgeführt (Abb. 12A). CSS zeigte in beiden verwendeten Konzentrationen die Tendenz, die Insulinsekretion zu erniedrigen, hatte aber keinen signifikanten Einfluss auf die GSIS (Abb. 12A). AG und CSS (1 µM) reduzierte die GSIS (Abb. 12A). Die hier beobachtete tendenziell negative Wirkung von CSS auf die GSIS steht diametral zu einer anderen Studie, in der CSS unter G6,6 die GSIS in isolierten Langerhans-Inseln aus Ratten signifikant erhöhte (Kaczmarek et al. 2009). Die Anwendung des spezifischen SST-R2 Antagonisten H6056, der in der eingesetzten Konzentration von 1 µM jedoch auch die Subtypen 1-5 hemmt, brachte interpretierbare Resultate: In der Gegenwart von H6056 konnte keine AG-Wirkung mehr auf die GSIS in murinen Langerhans-Inseln nachgewiesen werden (Abb. 12B). Die Diskrepanz der erfassten Effekte der SST-R-Antagonisten CSS und H6056 kann ihre Begründung in einem autokrinen Feedbackmechanismus haben, der von SST auf δ-Zellen beschrieben wird. Pankreatische, murine δ-Zellen exprimieren ebenfalls SST-Rs, genauer genommen SST-R1 und SST-R3 (Adriaenssens et al. 2016, DiGruccio et al. 2016, Rorsman and Huising 2018). Durch die Bindung eines Antagonisten an diese SST-R-Subtypen in δ-Zellen kann die SST-Ausschüttung erhöht werden (Adriaenssens et al. 2016, Orgaard and Holst 2017). Da es sich bei CSS um einen unspezifischen SST-R-Antagonisten handelt, ist diese Interaktion wahrscheinlicher, als bei H6056 und erklärt eventuell dadurch die beobachteten Unterschiede.

Der SST-R-Antagonist H6056 1 µM wurde auch von Adriaenssens und Kollegen in Kombination mit dem SST-R5 Antagonisten H5884 1 µM verwendet und zeigte dasselbe Ergebnis (Adriaenssens et al. 2016). Daraus lässt sich ableiten, dass SST-Rs bei dem Einfluss von AG auf die β-Zellen und Langerhans-Inseln eine nicht zu vernachlässigende Bedeutung hat, erklärt aber nicht, ob dabei parakrin aus den δ-Zellen ausgeschüttetes SST eine Rolle spielt. Würde der Effekt von AG über SST aus den δ-Zellen vermittelt werden, dürfte SST, genau wie AG, in β-Zellen von $SUR1^{-/-}$ Mäusen keine Wirkung mehr haben. Bei der Erfassung der $[Ca^{2+}]_c$ stellte sich unter dem Einfluss von SST1-14 aber heraus, dass SST1-14 in den ersten 5 min der etwa 20-minütigen Zugabe transient die Glucose-induzierten Oszillationen der $[Ca^{2+}]_c$ unter G10 hemmt. In den nachfolgenden 15 min der

Zugabe bewirkte SST1-14 eine anhaltende, wenngleich etwas schwächere, Abnahme der $[Ca^{2+}]_c$ in β-Zellen von $SUR1^{-/-}$ Mäusen (Abb. 12C, untere Messung). Bei β-Zellclustern, welche ein Plateau der $[Ca^{2+}]_c$ aufwiesen, unterbrach die Zugabe von SST1-14 die Plateauphase und führte stellenweise zu einer weiterführenden oszillatorischen Aktivität der $[Ca^{2+}]_c$ (Abb. 12C, obere Messung). Dies widerspricht den Ergebnissen von AG auf die $[Ca^{2+}]_c$ im $SUR1^{-/-}$ (M-AG Fig. 4A, 4B). Die Beobachtung, dass die Wirkung von SST an β-Zellen nicht durch den K_{ATP}-Kanal vermittelt wird, wurde in zwei anderen Studien ebenfalls nachgewiesen. Bei Messungen des Membranpotentials hemmte SST (10-30 nM) in G6 das Auftreten von Aktionspotentialen und führte zu einer Hyperpolarisation in humanen β-Zellen. Diese Effekte waren in Gegenwart des K_{ATP}-Kanal Blockers Tolbutamid (200 µM) ebenfalls präsent (Kailey et al. 2012). Analoge Beobachtungen konnten bei Patch-Clamp Messungen in der cell-attached Konfiguration in Gegenwart von G15, SST (0,1 µM) und Tolbutamid (50 µM) in INS-1 Zellen gemacht werden (Abel et al. 1996). Daraus kann abgeleitet werden, dass AG weder Einfluss auf die Glucose-induzierten Oszillationen der $[Ca^{2+}]_c$ noch auf die GSIS und das Membranpotential in $SUR^{-/-}$ β-Zellen und Langerhans-Inseln hat und zeigt deutlich, dass AG eigenständig und ohne Anwesenheit von SST seine hemmenden Effekte auf die SSK ausübt. Unumstritten ist ebenfalls die Involvierung eines SST-R-Subtyps, der jedoch im Rahmen dieser Arbeit nicht näher charakterisiert wurde. Allerdings ist nicht gänzlich auszuschließen, dass der GHS-R1a in δ-Zellen exprimiert ist und der von den Arbeitsgruppen Adriaenssens *et al.* und DiGruccio *et al*. postulierte Signalweg auch stattfindet (Adriaenssens et al. 2016, DiGruccio et al. 2016).

Da die Population an β-Zellen mit etwa 60-80 % je nach Spezies (Stefan et al. 1983, Cabrera et al. 2006) sehr hoch ist, ist die Möglichkeit, dass sich bei Messungen mit β-Zellclustern α- oder δ-Zellen in der unmittelbaren Umgebung befanden, zwar möglich, aber nicht unbedingt bei jeder Messung zu erwarten. Es ist unwahrscheinlich, dass die potentielle Nähe anderer Zellpopulationen die Effekte von AG ausgelöst haben, insbesondere in Anbetracht der Tatsache, dass die Wirkung von AG in allen Messung erkenntlich waren, in denen aus Langerhans-Inseln vereinzelte β-Zellcluster verwendet worden sind und die

Erniedrigung der Insulinsekretion in Gegenwart von AG auch in der β-Zelllinie MIN6 zu beobachten war (Abb. 4A). Gegen die Involvierung von α-Zellen spricht, dass diese vorwiegend bei niedrigen Glucosekonzentrationen elektrisch aktiv sind (Nadal et al. 1999, Barg et al. 2000, Quesada et al. 2006). Die Beteiligung von δ-Zellen in sämtlichen Messreihen, in denen aus Langerhans-Inseln vereinzelte β-Zellcluster benutzt worden sind, ist in Anbetracht des geringen Anteils, den δ-Zellen an der endokrinen Zellpopulation ausmachen, ebenfalls fraglich (Barg et al. 2000).

In murinen β-Zellen konnten alle Subtypen des SST-R nachgewiesen werden, wobei der SST-R5 der funktional wichtigste Subtyp zu sein scheint (Norman et al. 2002, Strowski et al. 2003, Tirone et al. 2003, Ludvigsen et al. 2004, Wang et al. 2005), während in humanen β-Zellen der SST-R2 dominant ist (Kailey et al. 2012). Diese Ergebnisse sind in Kongruenz mit der Hypothese der Heteromerisation von GHS-R1a und SST-R5, wie sie Park und Kollegen postulieren. Allerdings widerlegen diese Ergebnisse die Arbeitshypothese von Adriaenssen *et al.* und DiGruccio *et al.*, welche in murinen β-Zellen den SST-R5 gar nicht und stattdessen den SST-R3 als dominanten Subtyp nachgewiesen haben. In murinen β-Zellen konnten Rorsman und Ashcroft wiederum fast ausschließlich mRNA des SST-R3 und in nur geringem Ausmaß den GHS-R1a nachweisen (Rorsman and Ashcroft 2018). DiGruccio und Kollegen begründen zusätzlich die Involvierung des SST-R3 bei der Wirkung von AG mit den Beobachtungen, die sie bei Verwendung des SST-R3-Antagonisten SST3-ODN-8 (Reubi et al. 2000) in WT Mäusen *in vitro* machten (DiGruccio et al. 2016). Bei näherer Betrachtung der dargestellten Ergebnisse wird jedoch ersichtlich, dass die Arbeitsgruppe nicht präsentiert, wie der SST-R3-Antagonist allein die GSIS beeinflusst. Sie zeigt Daten, in denen AG (100 nM) und SST3-ODN-8 (100 nM) gemeinsam verwendet worden sind und die Kombination aus beiden Peptiden zwar nicht signifikant, aber tendenziell die GSIS erhöhte. Daraus kann nicht valide abgeleitet werden, ob nicht der Antagonist allein die GSIS bereits derart stark beeinflusst, dass die Wirkung von AG überdeckt wird oder ob tatsächlich ein Antagonismus vorliegt.

Der Vergleich der Ergebnisse der $[Ca^{2+}]_c$-Messungen von AG und SST in β-Zellen von $SUR^{-/-}$ Mäusen (Abb. 12C, 12D und M-AG Fig. 4A, AB) verdeutlicht, dass die Effekte auf die SSK nicht durch SST, sondern AG in β-Zellen verursacht werden. Die Wirkung von SST ist, im Gegensatz zu AG, nicht über den K_{ATP}-Kanal vermittelt, wodurch der Einfluss von AG auf das Pankreas nicht ausschließlich durch SST erklärt werden kann. Die hier präsentierten Daten lassen darauf schließen, dass die Wirkung von AG nicht durch die Bindung von AG an den $G_{αq}$-gekoppelten GHS-R1a in δ-Zellen und die damit induzierte Freisetzung von SST zustande kommt, welches anschließend parakrin auf $G_{αi}$-gekoppelte SST-Rs in β-Zellen einwirkt. Sie rücken vielmehr die postulierte Heteromerisationstheorie von Park und Kollegen in den Fokus (Park et al. 2012). Diese Theorie beschreibt, wie weiter oben erwähnt, dass unter Bedingungen, in denen das Verhältnis von AG zu SST hoch ist, der GHS-R1a ($G_{αq}$-gekoppelt) und SST-R5 ($G_{αi}$-gekoppelt) heteromerisieren. Dieses Verhältnis ist wiederum abhängig von der Energiebilanz bzw. Glucosekonzentration. In Nüchternphasen, wenn folglich die Glucosekonzentration niedrig ist, wird AG ausgeschüttet und etabliert über das SST-R5 und GHS-R1a Heteromer die $G_{αi}$-Signalkopplung und inhibiert die GSIS. Die konstitutive Heteromerisation der beiden Rezeptoren erklären Park *et al.* zusätzlich als unter diesen Umständen energetisch bevorzugte Formation von SST-R5 und GHS-R1a im Gegensatz zu Homomeren von SST-R5 und GHS-R1a. Dadurch kann die Erniedrigung der cAMP-Konzentration und somit die hemmende Wirkung von AG auf die SSK von Park *et al.* begründet werden. Wie bereits in Abschnitt 1.2 erwähnt, ist der GHS-R1a, wie viele andere metabotrope Rezeptoren, in der Lage, mit anderen Rezeptoren, wie dem DRD2-R und $5\text{-}HT_{2C}$ zu heteromerisieren, was diese Interaktion ermöglicht (Kern et al. 2012, Schellekens et al. 2013).

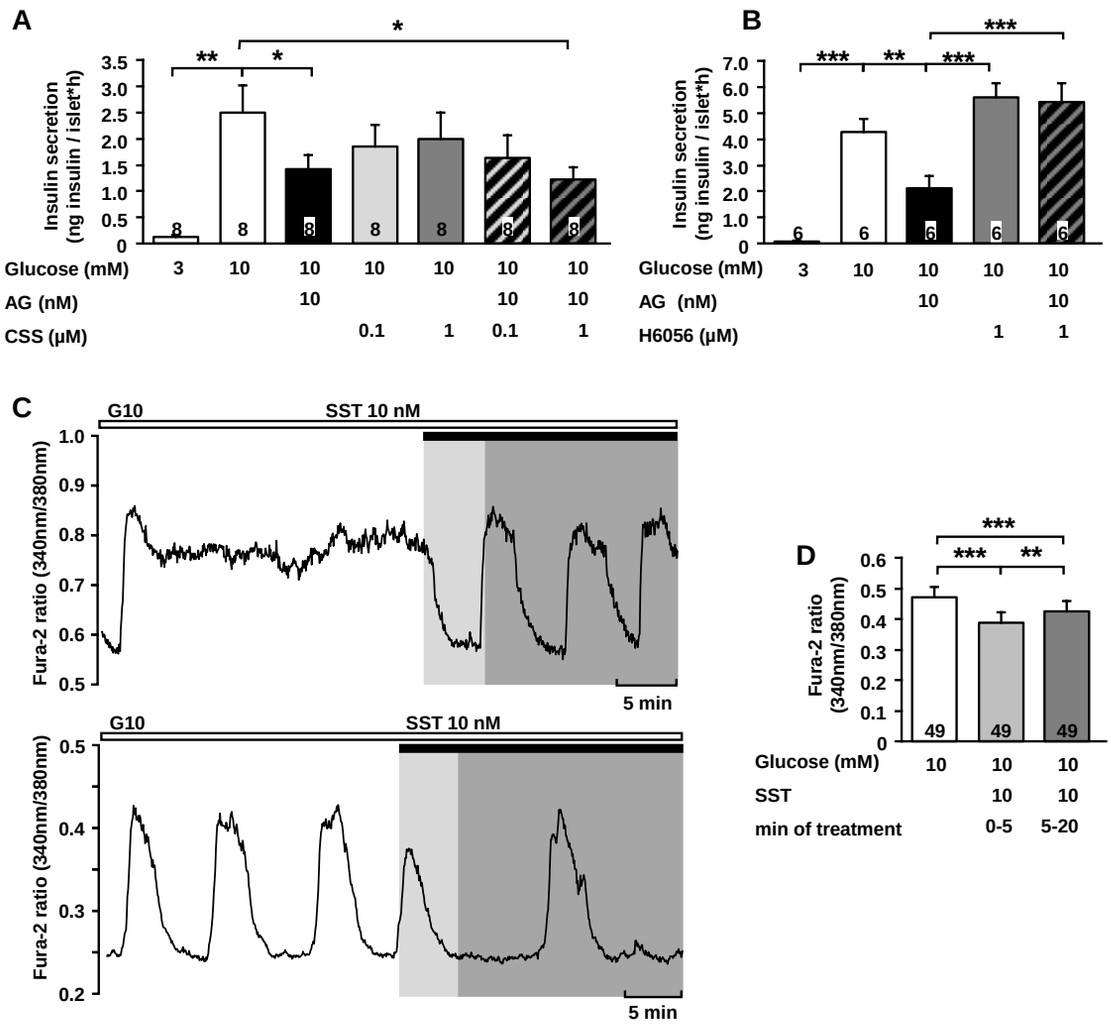

Abb. 12 SST-Rezeptoren sind an der Wirkung von AG beteiligt. SST senkt im Gegensatz zu AG die $[Ca^{2+}]_c$ in β-Zellen aus $SUR^{-/-}$ Mäusen.

A) AG setzt die GSIS unter G10 herab. Der unspezifische SST-R-Antagonist CSS senkt tendenziell die GSIS, erreicht jedoch keine Signifikanz. Die Kombination aus AG und CSS (1 µM) hemmt die GSIS. **B)** AG senkt die GSIS, während der SST-R-Antagonist H6056 allein tendenziell die Insulinsekretion steigert. In Anwesenheit von H6056 hat AG keinen Einfluss auf die GSIS. **C)** Repräsentative Messungen des Effekts von SST auf die Glucose-induzierten Oszillationen der $[Ca^{2+}]_c$ in β-Zellen von $SUR1^{-/-}$ Mäusen. **D)** SST zeigt in den ersten 5 min eine transiente Hemmung der $[Ca^{2+}]_c$ und von Minute 5-20 der Zugabe eine im Vergleich zu den ersten 5 Minuten abgeschwächte, aber persistierende Erniedrigung der $[Ca^{2+}]_c$. Die Angabe n steht für die Anzahl der durchgeführten Messungen mit Langerhans-Inseln oder β-Zellclustern aus mindestens 3 WT oder $SUR^{-/-}$ Mauspräparationen. * $p \leq 0,05$; ** $p \leq 0,01$; *** $p \leq 0,001$

3.6 AG beeinflusst die β-Zellfunktion über den cAMP/PKA Signalweg

Anhand der Ergebnisse der vorangegangenen Abschnitte ist ersichtlich, dass die Wirkung von AG im Zusammenhang mit dem K_{ATP}-Kanal steht. Die Metabolisierung von Glucose zu ATP führt zum Schließen der K_{ATP}-Kanäle und dem Einstrom von Ca^{2+} durch L-Typ Ca^{2+}-Kanäle. Der second messenger cAMP potenziert die durch Ca^{2+}-vermittelten Signale (Hellman et al. 1974, Wollheim and Sharp 1981, Schuit and Pipeleers 1985, Henquin 2000, Tengholm 2012). AG ist nur wirksam in Gegenwart von Glucosekonzentrationen, die über dem Schwellenwert liegen, wie die Ergebnisse aus 3.1 belegen. Das legt den Schluss nahe, dass AG mit amplifizierenden Signalwegen, genaugenommen mit cAMP, interferiert. Die Generierung von cAMP erfolgt durch Aktivierung der membranständigen AC, welche ATP zu cAMP cyclisiert. Anschließend aktiviert cAMP die Effektorproteine PKA und exchange protein directly activated by cAMP (Epac). Über PKA werden Zielstrukturen phosphoryliert und dadurch beispielsweise die Aktivität von spannungsabhängigen K_v-Kanälen herabgesetzt (MacDonald et al. 2002) und die Öffnungswahrscheinlichkeit sowie Leitfähigkeit von L-Typ Ca^{2+}-Kanälen erhöht (Kanno et al. 1998, Bunemann et al. 1999, Fuller et al. 2014). Die PKA reguliert auch die Aktivität von K_{ATP}-Kanälen durch Phosphorylierung der Kir6.2 oder SUR1 UE, wobei die durch PKA-vermittelte Modulation der K_{ATP}-Kanäle von der ADP-Konzentration abhängig ist (Beguin et al. 1999, Lin et al. 2000, Light et al. 2002, Tinker et al. 2018). Zusätzlich beeinflusst PKA die Mobilisierung der Insulin-haltigen Granula durch Interaktion mit ethylmaleimide-sensitive factor attachment protein receptor (SNARE) bzw. synaptosomal protein of 25 kDa (SNAP-25) (Renstrom et al. 1997, Vikman et al. 2009).

Epac2 ist die dominant vorkommende Form im Pankreas (de Rooij et al. 1998, Kawasaki et al. 1998, Ueno et al. 2001) und aktiviert die kleine GTPase Rap1, die wiederum die PLCε mobilisiert (Holz et al. 2006, Leech et al. 2010). Außerdem hat Epac2 Einfluss auf die Exozytose, indem es mit dem Rab3 Effektorprotein RIM2 interagiert (Shibasaki et al. 2007). Zusammengefasst erhöhen und modulieren somit Epac2 und PKA die GSIS.

Die Hydrolyse von cAMP zu 5´AMP erfolgt durch PDEs (Sams and Montague 1972, Heimann et al. 2010, Tengholm and Gylfe 2017) und erniedrigt dadurch die Insulinsekretion. Die PDEs sind mit mehreren Subtypen in pankreatischen Langerhans-Inseln vertreten, von denen insbesondere PDE3B der wichtigste Subtyp ist (Pyne and Furman 2003).

Summa summarum gibt es für AG somit die Möglichkeiten, mit PKA oder Epac2 zu interferieren oder die PDE zu stimulieren. Um diese Möglichkeiten zu eruieren wurde die GSIS mit AG (10 nM) in Langerhans-Inseln von Epac2$^{-/-}$-Mäusen und von WT Mäusen in Gegenwart des zellpermeablen cAMP-Analogons dibutyryl-cAMP (db-cAMP) (1 mM) durchgeführt, welches die PKA stimuliert, oder aber in Gegenwart des PDE-Inhibitors 3-Isobutyl-1-methylxanthin (IBMX) (50 µM). Sowohl die Verwendung von db-cAMP als auch von IBMX antagonisierte die insulinsekretionsinhibierende Wirkung von AG (10 nM) unter G10 (M-AG: Fig. 6A, 6B), während in Langerhans-Inseln aus Epac2$^{-/-}$ Mäusen AG (10 nM) weiterhin die GSIS reduzierte (M-AG: Fig. 6C).

Dezaki und Kollegen führten cAMP Messungen in MIN6 durch, in denen AG (10 nM) in G11 die Glucose-induzierte Erhöhung der $[cAMP]_c$ hemmte (Dezaki et al. 2011). Im perfundierten Rattenpankreas und in aus Ratten isolierten Langerhans-Inseln benutzte diese Arbeitsgruppe ebenfalls db-cAMP und konnte damit auch die Effekte von AG auf die GSIS hemmen. Neben db-cAMP fand bei ihren Experimenten der AC-Inhibitor MDL-12330A und der PKA-Aktivator 6-Phe-cAMP Verwendung, wodurch sie den cAMP/PKA-abhängigen Wirkmechanismus von AG nachweisen konnten.

Zusammengenommen verdeutlichen diese Resultate, dass AG mit dem amplifizierenden cAMP/PKA-Signalweg interferiert. Dieser Signalweg ist β-zellspezifisch, was durch die eigenen Ergebnisse (Abb. 4A) und die $[cAMP]_c$-Messungen von Dezaki *et al.* in MIN6-Zellen gestützt wird (Dezaki et al. 2011). Durch die Hemmung der AC werden die durch cAMP und PKA ausgelösten Signalkaskaden abgeschwächt und damit u.a. der Einfluss von AG auf den K_{ATP}-Kanal erklärt (Abschnitt 3.4 und 3.4.1.).

3.7. Zusammenfassung der Ergebnisse

Die hier vorliegenden Ergebnisse klären auf, dass die AG-Wirkung in β-Zellen nur erfolgreich inhibiert werden kann, wenn nicht nur ein Antagonist des GHS-R1a Einsatz findet, sondern auch die konstitutive Aktivität mit Hilfe eines inversen Agonisten unterdrückt wird.

Außerdem wurde gezeigt, dass DAG im 2:1 Verhältnis zu AG die Effekte von AG in Bezug auf V_m, $[Ca^{2+}]_c$ und GSIS nivelliert. Bei Vorliegen des Nährstoff-induzierten Zellstresses im GLTx-Modell ist nur die Kombination von DAG und AG im selben Verhältnis in der Lage, die Glucose-induzierten Oszillationen der $[Ca^{2+}]$ zu erhalten. Diese Beobachtung steht in Übereinstimmung mit anderen Veröffentlichungen, welche nachweisen, dass es bei an Diabetes mellitus Typ 2 und an Adipositas erkrankten Personen zu einer Verschiebung des DAG zu AG Verhältnisses zu Ungunsten von DAG kommt, wodurch ein relativer DAG-Mangel entsteht (Review von Delhanty et al. 2014). Dadurch ist die Hypothese naheliegend, dass die Wiederherstellung des physiologischen DAG zu AG Verhältnisses die durch Übergewicht und Diabetes mellitus Typ 2 ausgelösten Folgen abschwächen und sich positiv auf die Insulinresistenz auswirken kann.

Diese Arbeit spezifiziert den Wirkmechanismus von AG dahingehend, dass AG indirekt K_{ATP}-Kanäle öffnet (Abb. 10C-J) und über Hemmung der AC mit dem cAMP/PKA Weg die GSIS erniedrigt (M-AG: Fig. 7A-C). Durch die Erniedrigung der cAMP-Konzentration und der damit einhergehend herabgesetzten PKA-Aktivität kann auch die Wirkung von AG auf den K_{ATP}-Kanal erklärt werden. Die Hemmung der AC-Aktivität und dadurch verringerte cAMP-Generierung (Dessauer et al. 2002) wird durch $G_{\alpha i}$-gekoppelte Rezeptoren vermittelt. Kanonisch ist der GHS-R1a, beispielsweise im Hypothalamus, $G_{\alpha q}$-gekoppelt (Date et al. 2000b, Hawley et al. 2005). Dieser Signalweg kann folgerichtig nicht die inhibierenden Effekte von AG auf die GSIS erklären. Die Heteromerisationstheorie von Park und Kollegen (Park et al. 2012) des $G_{\alpha q}$-gekoppelten GHS-R1a und des $G_{\alpha i}$-gekoppelten SST-R5 bietet eine Erklärung, welche hier weitgehend von den eigenen Ergebnissen unterstützt wird. Dem dient insbesondere der Nachweis, dass SST-Rs beteiligt sind, wie die eigenen GSIS-Experimente mit H6056 zeigen (Abb. 12B). Inwiefern die Heteromerisation von GHS-R1a und SST-R von dem Verhältnis von SST zu

AG abhängt, wie es Park *et al.* beschreiben, kann im Rahmen dieser Arbeit nicht näher ausgeführt werden. Es konnte jedoch mit Hilfe der eigenen Ergebnisse bei Messungen der $[Ca^{2+}]_c$ beobachtet werden, dass Interaktionen zwischen SST und AG auftreten (Abb. 11A-D). Diese Arbeit zeigt mittels der Experimente in $SUR1^{-/-}$ Mäusen, dass die Wirkung von AG auf pankreatische β-Zellen nicht ausschließlich durch SST vermittelt wird, da SST im Gegensatz zu AG unter diesen Bedingungen die $[Ca^{2+}]_c$ weiterhin erniedrigt (Abb. 12C, 12D und M-AG Fig. 4A, AB). Es kann aber nicht ausgeschlossen werden, dass der GHS-R1a ebenfalls in SST-sekretierenden δ-Zellen exprimiert ist und somit AG über dortige Ligandbindung parakrine SST-Effekte auf β-Zellen ausübt, wie es die Arbeitsgruppen von Adriaenssens und DiGruccio postulieren (Adriaenssens et al. 2016, DiGruccio et al. 2016).

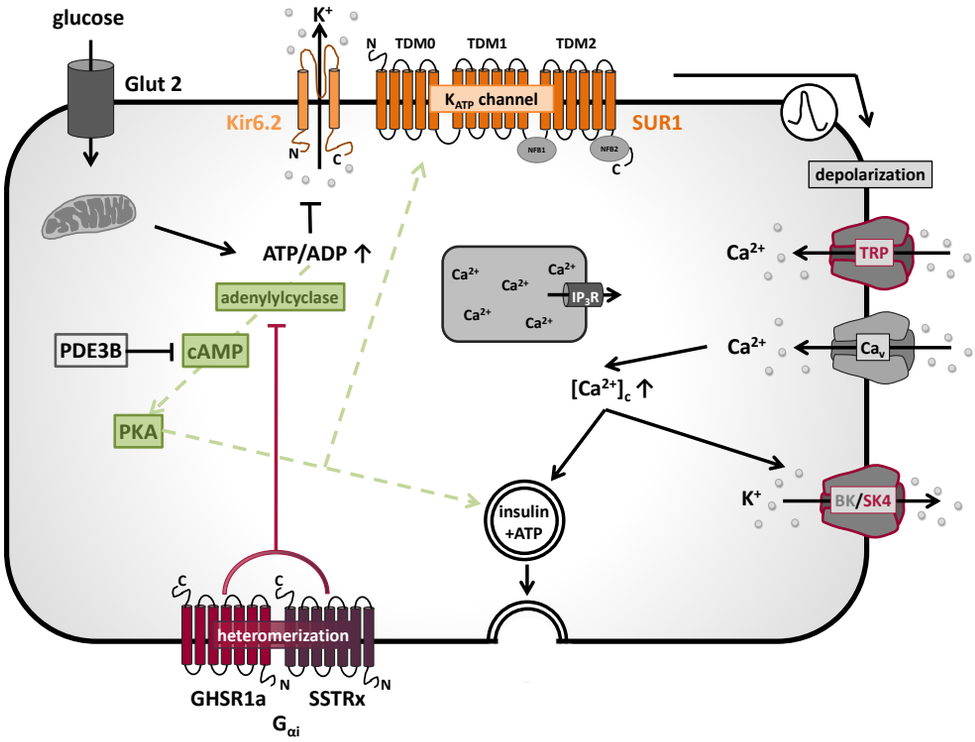

Abb. 13 Darstellung der Beeinflussung der Stimulus-Sekretions-Kopplung in β-Zellen durch AG

Durch Heteromerisation des GHS-R1a und eines SST-R-Subtypen (SSTRx) wird unter stimulatorischen Glucosekonzentrationen in Anwesenheit von AG über den dadurch etablierten $G_{\alpha i}$-gekoppelten Signalweg die AC gehemmt, wodurch die cAMP-Konzentration und PKA-Aktivität abnimmt und folglich amplifizierende Signalkaskaden abgeschwächt werden. Die Wirkung von AG involviert den K_{ATP}-Kanal, indem der K_{ATP}-Strom durch AG erhöht wird. Möglicherweise begünstigt AG auch den K^+-Ausstrom durch K^+-Kanäle, wie SK4-Kanäle oder inhibiert TRP-Kanäle, wodurch der depolarisierende Strom reduziert wird.

4 Literaturverzeichnis

Abegg, K., L. Bernasconi, M. Hutter, L. Whiting, C. Pietra, C. Giuliano, T. A. LutzT. Riediger (2017). Ghrelin receptor inverse agonists as a novel therapeutic approach against obesity-related metabolic disease. Diabetes Obes Metab 19(12): 1740-1750.

Abel, K. B., S. LehrS. Ullrich (1996). Adrenaline, not somatostatin-induced hyperpolarization is accompanied by a sustained inhibition of insulin secretion in INS-1 cells. Activation of sulphonylurea K-ATP(+) channels is not involved. Pflugers Archiv-European Journal of Physiology 432(1): 89-96.

Adriaenssens, A. E., B. Svendsen, B. Y. Lam, G. S. Yeo, J. J. Holst, F. ReimannF. M. Gribble (2016). Transcriptomic profiling of pancreatic alpha, beta and delta cell populations identifies delta cells as a principal target for ghrelin in mouse islets. Diabetologia 59(10): 2156-2165.

Aguilar-Bryan, L.J. Bryan (1999). Molecular biology of adenosine triphosphate-sensitive potassium channels. Endocr Rev 20(2): 101-135.

Alberti, K. G., N. J. Christensen, S. E. Christensen, A. P. Hansen, J. Iversen, K. Lundbaek, K. Seyer-HansenH. Orskov (1973). Inhibition of insulin secretion by somatostatin. Lancet 2(7841): 1299-1301.

Allas, S., T. Delale, N. Ngo, M. Julien, P. Sahakian, J. Ritter, T. AbribatA. J. van der Lely (2016). Safety, tolerability, pharmacokinetics and pharmacodynamics of AZP-531, a first-in-class analogue of unacylated ghrelin, in healthy and overweight/obese subjects and subjects with type 2 diabetes. Diabetes Obes Metab 18(9): 868-874.

Anderson, K. A., T. J. Ribar, F. Lin, P. K. Noeldner, M. F. Green, M. J. Muehlbauer, L. A. Witters, B. E. KempA. R. Means (2008). Hypothalamic CaMKK2 contributes to the regulation of energy balance. Cell Metab 7(5): 377-388.

Angelidis, G., V. ValotassiouP. Georgoulias (2010). Current and potential roles of ghrelin in clinical practice. J Endocrinol Invest 33(11): 823-838.

Ariyasu, H., K. Takaya, T. Tagami, Y. Ogawa, K. Hosoda, T. Akamizu, M. Suda, T. Koh, K. Natsui, S. Toyooka, G. Shirakami, T. Usui, A. Shimatsu, K. Doi, H. Hosoda, M. Kojima, K. KangawaK. Nakao (2001). Stomach is a major source of circulating ghrelin, and feeding state determines plasma ghrelin-like immunoreactivity levels in humans. J Clin Endocrinol Metab 86(10): 4753-4758.

Arvanitakis, L., E. Geras-RaakaM. C. Gershengorn (1998). Constitutively signaling G-protein-coupled receptors and human disease. Trends in Endocrinology and Metabolism 9(1): 27-31.

Asakawa, A., A. Inui, M. Fujimiya, R. Sakamaki, N. Shinfuku, Y. Ueta, M. M. MeguidM. Kasuga (2005). Stomach regulates energy balance via acylated ghrelin and desacyl ghrelin. Gut 54(1): 18-24.

Asakawa, A., A. Inui, T. Kaga, G. Katsuura, M. Fujimiya, M. A. FujinoM. Kasuga (2003). Antagonism of ghrelin receptor reduces food intake and body weight gain in mice. Gut 52(7): 947-952.

Ashcroft, F. M., D. E. HarrisonS. J. H. Ashcroft (1984). Glucose Induces Closure of Single Potassium Channels in Isolated Rat Pancreatic Beta-Cells. Nature 312(5993): 446-448.

Barazzoni, R., M. Zanetti, C. Ferreira, P. Vinci, A. Pirulli, M. Mucci, F. Dore, M. Fonda, B. Ciocchi, L. CattinG. Guarnieri (2007). Relationships between desacylated and acylated ghrelin and insulin sensitivity in the metabolic syndrome. Journal of Clinical Endocrinology & Metabolism 92(10): 3935-3940.

Barg, S., J. Galvanovskis, S. O. Gopel, P. RorsmanL. Eliasson (2000). Tight coupling between electrical activity and exocytosis in mouse glucagon-secreting alpha-cells. Diabetes 49(9): 1500-1510.

Barroso Oquendo, M., N. Layer, R. Wagner, P. Krippeit-DrewsG. Drews (2018). Energy depletion and not ROS formation is a crucial step of glucolipotoxicity (GLTx) in pancreatic beta cells. Pflugers Arch 470(3): 537-547.

Bednarek, M. A., S. D. Feighner, S. S. Pong, K. K. McKee, D. L. Hreniuk, M. V. Silva, V. A. Warren, A. D. Howard, L. H. Van Der PloegJ. V. Heck (2000). Structure-function studies on the new growth hormone-releasing peptide, ghrelin: minimal sequence of ghrelin necessary for activation of growth hormone secretagogue receptor 1a. J Med Chem 43(23): 4370-4376.

Beguin, P., K. Nagashima, M. Nishimura, T. GonoiS. Seino (1999). PKA-mediated phosphorylation of the human K-ATP channel: separate roles of Kir6.2 and SUR1 subunit phosphorylation. Embo Journal 18(17): 4722-4732.

Bender, B. J., G. Vortmeier, S. Ernicke, M. Bosse, A. Kaiser, S. Els-Heindl, U. Krug, A. Beck-Sickinger, J. MeilerD. Huster (2019). Structural Model of Ghrelin Bound to its G Protein-Coupled Receptor. Structure 27(3): 537-544 e534.

Binette, T. M., J. M. DufourG. S. Korbutt (2001). In vitro maturation of neonatal porcine islets - A novel model for the study of islet development and xenotransplantation. Bioartificial Organs Iii: Tissue Sourcing, Immunoisolation, and Clinical Trials 944: 47-61.

Blijdorp, K., A. J. van der Lely, M. M. van den Heuvel-Eibrink, T. M. Huisman, A. P. N. Themmen, P. J. D. DelhantyS. J. C. M. M. Neggers (2013). Desacyl ghrelin is influenced by changes in insulin concentration during an insulin tolerance test. Growth Hormone & Igf Research 23(5): 193-195.

Bosco, D., M. Armanet, P. Morel, N. Niclauss, A. Sgroi, Y. D. Muller, L. Giovannoni, G. ParnaudT. Berney (2010). Unique arrangement of alpha- and beta-cells in human islets of Langerhans. Diabetes 59(5): 1202-1210.

Brazeau, P., W. Vale, R. Burgus, N. Ling, M. Butcher, J. RivierR. Guillemin (1973). Hypothalamic polypeptide that inhibits the secretion of immunoreactive pituitary growth hormone. Science 179(4068): 77-79.

Briggs, D. I., P. J. Enriori, M. B. Lemus, M. A. CowleyZ. B. Andrews (2010). Diet-induced obesity causes ghrelin resistance in arcuate NPY/AgRP neurons. Endocrinology 151(10): 4745-4755.

Brissova, M., M. J. Fowler, W. E. Nicholson, A. Chu, B. Hirshberg, D. M. HarlanA. C. Powers (2005). Assessment of human pancreatic islet architecture and composition by laser scanning confocal microscopy. J Histochem Cytochem 53(9): 1087-1097.

Broglio, F., E. Arvat, A. Benso, C. Gottero, G. Muccioli, M. Papotti, A. J. van der Lely, R. DeghenghiE. Ghigo (2001). Ghrelin, a natural GH secretagogue produced by the stomach, induces hyperglycemia and reduces insulin secretion in humans. J Clin Endocrinol Metab 86(10): 5083-5086.

Broglio, F., C. Gottero, F. Prodam, C. Gauna, G. Muccioli, M. Papotti, T. Abribat, A. J. Van der LelyE. Ghigo (2004a). Non-acylated ghrelin counteracts the metabolic but not the neuroendocrine response to acylated ghrelin in humans. Journal of Clinical Endocrinology & Metabolism 89(6): 3062-3065.

Broglio, F., C. Gottero, F. Prodam, C. Gauna, G. Muccioli, M. Papotti, T. Abribat, A. J. Van Der LelyE. Ghigo (2004b). Non-acylated ghrelin counteracts the metabolic but not the neuroendocrine response to acylated ghrelin in humans. J Clin Endocrinol Metab 89(6): 3062-3065.

Bruno, J. F., Y. Xu, J. SongM. Berelowitz (1992). Molecular cloning and functional expression of a brain-specific somatostatin receptor. Proc Natl Acad Sci U S A 89(23): 11151-11155.

Bunemann, M., B. L. Gerhardstein, T. Y. GaoM. M. Hosey (1999). Functional regulation of L-type calcium channels via protein kinase A-mediated phosphorylation of the beta(2) subunit. Journal of Biological Chemistry 274(48): 33851-33854.

Cabral, A., P. N. De FrancescoM. Perello (2015). Brain circuits mediating the orexigenic action of peripheral ghrelin: narrow gates for a vast kingdom. Front Endocrinol (Lausanne) 6: 44.

Cabrera, O., D. M. Berman, N. S. Kenyon, C. Ricordi, P. O. BerggrenA. Caicedo (2006). The unique cytoarchitecture of human pancreatic islets has implications for islet cell function. Proc Natl Acad Sci U S A 103(7): 2334-2339.

Callaghan, B.J. B. Furness (2014). Novel and conventional receptors for ghrelin, desacyl-ghrelin, and pharmacologically related compounds. Pharmacol Rev 66(4): 984-1001.

Callahan, H. S., D. E. Cummings, M. S. Pepe, P. A. Breen, C. C. MatthysD. S. Weigle (2004). Postprandial suppression of plasma ghrelin level is proportional to ingested caloric load but does not predict intermeal interval in humans. Journal of Clinical Endocrinology & Metabolism 89(3): 1319-1324.

Chanoine, J. P.A. C. Wong (2004). Ghrelin gene expression is markedly higher in fetal pancreas compared with fetal stomach: effect of maternal fasting. Endocrinology 145(8): 3813-3820.

Chao, C. S., Z. L. Loomis, J. E. LeeL. Sussel (2007). Genetic identification of a novel NeuroD1 function in the early differentiation of islet alpha, PP and epsilon cells. Dev Biol 312(2): 523-532.

Chow, K. B., J. Sun, K. M. Chu, W. Tai Cheung, C. H. ChengH. Wise (2012). The truncated ghrelin receptor polypeptide (GHS-R1b) is localized in the endoplasmic reticulum where it forms heterodimers with ghrelin receptors (GHS-R1a) to attenuate their cell surface expression. Mol Cell Endocrinol 348(1): 247-254.

Clement, J. P. t., K. Kunjilwar, G. Gonzalez, M. Schwanstecher, U. Panten, L. Aguilar-BryanJ. Bryan (1997). Association and stoichiometry of K(ATP) channel subunits. Neuron 18(5): 827-838.

Cortelazzi, D., V. Cappiello, P. S. Morpurgo, S. Ronzoni, M. S. N. De Santis, I. Cetin, P. Beck-PeccozA. Spada (2003). Circulating levels of ghrelin in human fetuses. European Journal of Endocrinology 149(2): 111-116.

Cowley, M. A., R. G. Smith, S. Diano, M. Tschöp, N. Pronchuk, K. L. Grove, C. J. Strasburger, M. Bidlingmaier, M. Esterman, M. L. Heiman, L. M. Garcia-Segura, E. A. Nillni, P. Mendez, M. J. Low, P. Sotonyi, J. M. Friedman, H. Liu, S. Pinto, W. F. Colmers, R. D. ConeT. L. Horvath (2003). The distribution and mechanism of action of ghrelin in the CNS demonstrates a novel hypothalamic circuit regulating energy homeostasis. Neuron 37(4): 649-661.

Cummings, D. E.J. Overduin (2007). Gastrointestinal regulation of food intake. J Clin Invest 117(1): 13-23.

Cummings, D. E., J. Q. Purnell, R. S. Frayo, K. Schmidova, B. E. WisseD. S. Weigle (2001). A preprandial rise in plasma ghrelin levels suggests a role in meal initiation in humans. Diabetes 50(8): 1714-1719.

D'Amour, K. A., A. G. Bang, S. Eliazer, O. G. Kelly, A. D. Agulnick, N. G. Smart, M. A. Moorman, E. Kroon, M. K. CarpenterE. E. Baetge (2006). Production of pancreatic hormone-expressing endocrine cells from human embryonic stem cells. Nat Biotechnol 24(11): 1392-1401.

Damian, M., J. Marie, J. P. Leyris, J. A. Fehrentz, P. Verdie, J. Martinez, J. L. BaneresS. Mary (2012). High constitutive activity is an intrinsic feature of ghrelin

receptor protein: a study with a functional monomeric GHS-R1a receptor reconstituted in lipid discs. J Biol Chem 287(6): 3630-3641.

Damian, M., S. Mary, M. Maingot, C. M'Kadmi, D. Gagne, J. P. Leyris, S. Denoyelle, G. Gaibelet, L. Gavara, M. Garcia de Souza Costa, D. Perahia, E. Trinquet, B. Mouillac, S. Galandrin, C. Gales, J. A. Fehrentz, N. Floquet, J. Martinez, J. MarieJ. L. Baneres (2015). Ghrelin receptor conformational dynamics regulate the transition from a preassembled to an active receptor:Gq complex. Proc Natl Acad Sci U S A 112(5): 1601-1606.

Date, Y., M. Kojima, H. Hosoda, A. Sawaguchi, M. S. Mondal, T. Suganuma, S. Matsukura, K. KangawaM. Nakazato (2000a). Ghrelin, a novel growth hormone-releasing acylated peptide, is synthesized in a distinct endocrine cell type in the gastrointestinal tracts of rats and humans. Endocrinology 141(11): 4255-4261.

Date, Y., N. Murakami, M. Kojima, T. Kuroiwa, S. Matsukura, K. KangawaM. Nakazato (2000b). Central effects of a novel acylated peptide, ghrelin, on growth hormone release in rats. Biochem Biophys Res Commun 275(2): 477-480.

de la Cour, C. D., P. NorlenR. Hakanson (2007). Secretion of ghrelin from rat stomach ghrelin cells in response to local microinfusion of candidate messenger compounds: a microdialysis study. Regul Pept 143(1-3): 118-126.

de Rooij, J., F. J. T. Zwartkruis, M. H. G. Verheijen, R. H. Cool, S. M. B. Nijman, A. WittinghoferJ. L. Bos (1998). Epac is a Rap1 guanine-nucleotide-exchange factor directly activated by cyclic AMP. Nature 396(6710): 474-477.

De Vriese, C., F. Gregoire, R. Lema-Kisoka, M. Waelbroeck, P. RobberechtC. Delporte (2004). Ghrelin degradation by serum and tissue homogenates: identification of the cleavage sites. Endocrinology 145(11): 4997-5005.

Delhanty, P. J., S. J. NeggersA. J. van der Lely (2014). Should we consider des-acyl ghrelin as a separate hormone and if so, what does it do? Front Horm Res 42: 163-174.

Dessauer, C. W., M. Chen-GoodspeedJ. Chen (2002). Mechanism of G alpha(i)-mediated inhibition of type V adenylyl cyclase. Journal of Biological Chemistry 277(32): 28823-28829.

Detimary, P., P. GilonJ. C. Henquin (1998). Interplay between cytoplasmic Ca2+ and the ATP/ADP ratio: a feedback control mechanism in mouse pancreatic islets. Biochemical Journal 333: 269-274.

Dezaki, K., B. Damdindorj, H. Sone, O. Dyachok, A. Tengholm, E. Gylfe, T. Kurashina, M. Yoshida, M. KakeiT. Yada (2011). Ghrelin attenuates cAMP-PKA signaling to evoke insulinostatic cascade in islet beta-cells. Diabetes 60(9): 2315-2324.

Dezaki, K., H. Hosoda, M. Kakei, S. Hashiguchi, M. Watanabe, K. KangawaT. Yada (2004). Endogenous ghrelin in pancreatic islets restricts insulin release by

attenuating Ca2+ signaling in beta-cells: implication in the glycemic control in rodents. Diabetes 53(12): 3142-3151.

Dezaki, K., M. KakeiT. Yada (2007). Ghrelin uses G alpha(i2) and activates voltage-dependent K+ channels to attenuate glucose-induced Ca2+ signaling and insulin release in islet beta-cells - Novel signal transduction of ghrelin. Diabetes 56(9): 2319-2327.

DiGruccio, M. R., A. M. Mawla, C. J. Donaldson, G. M. Noguchi, J. Vaughan, C. Cowing-Zitron, T. van der MeulenM. O. Huising (2016). Comprehensive alpha, beta and delta cell transcriptomes reveal that ghrelin selectively activates delta cells and promotes somatostatin release from pancreatic islets. Mol Metab 5(7): 449-458.

Drews, G., P. Krippeit-DrewsM. Düfer (2010). Electrophysiology of Islet Cells. Islets of Langerhans 654: 115-163.

Dubois, M., P. Vacher, B. Roger, D. Huyghe, B. Vandewalle, J. Kerr-Conte, F. Pattou, N. Moustaid-MoussaJ. C. Lang (2007). Glucotoxicity inhibits late steps of insulin exocytosis. Endocrinology 148(4): 1605-1614.

Dunne, M. J.O. H. Petersen (1986). Intracellular Adp Activates K+ Channels That Are Inhibited by Atp in an Insulin-Secreting Cell-Line. Febs Letters 208(1): 59-62.

Egido, E. M., J. Rodriguez-Gallardo, R. A. SilvestreJ. Marco (2002). Inhibitory effect of ghrelin on insulin and pancreatic somatostatin secretion. Eur J Endocrinol 146(2): 241-244.

Ellis, C., J. G. LyonG. S. Korbutt (2016). Optimization and Scale-up Isolation and Culture of Neonatal Porcine Islets: Potential for Clinical Application. Cell Transplant 25(3): 539-547.

Engelstoft, M. S., W. M. Park, I. Sakata, L. V. Kristensen, A. S. Husted, S. Osborne-Lawrence, P. K. Piper, A. K. Walker, M. H. Pedersen, M. K. Nohr, J. Pan, C. J. Sinz, P. E. Carrington, T. E. Akiyama, R. M. Jones, C. Tang, K. Ahmed, S. Offermanns, K. L. Egerod, J. M. ZigmanT. W. Schwartz (2013a). Seven transmembrane G protein-coupled receptor repertoire of gastric ghrelin cells. Mol Metab 2(4): 376-392.

Engelstoft, M. S., W. M. Park, I. Sakata, L. V. Kristensen, A. S. Husted, S. Osborne-Lawrence, P. K. Piper, A. K. Walker, M. H. Pedersen, M. K. Nohr, J. Pan, C. J. Sinz, P. E. Carrington, T. E. Akiyama, R. M. Jones, C. Tang, K. Ahmed, S. Offermanns, K. L. Egerod, J. M. ZigmanT. W. Schwartz (2013b). Seven transmembrane G protein-coupled receptor repertoire of gastric ghrelin cells. Molecular Metabolism 2(4): 376-392.

Esler, W. P., J. Rudolph, T. H. Claus, W. Tang, N. Barucci, S. E. Brown, W. Bullock, M. Daly, L. Decarr, Y. Li, L. Milardo, D. Molstad, J. Zhu, S. J. Gardell, J. N. LivingstonL. J. Sweet (2007). Small-molecule ghrelin receptor antagonists

improve glucose tolerance, suppress appetite, and promote weight loss. Endocrinology 148(11): 5175-5185.

Fernandez, G., A. Cabral, M. P. Cornejo, P. N. De Francesco, G. Garcia-Romero, M. ReynaldoM. Perello (2016). Des-Acyl Ghrelin Directly Targets the Arcuate Nucleus in a Ghrelin-Receptor Independent Manner and Impairs the Orexigenic Effect of Ghrelin. J Neuroendocrinol 28(2): 12349.

Fuller, M. D., Y. Fu, T. ScheuerW. A. Catterall (2014). Differential regulation of Ca(V)1.2 channels by cAMP-dependent protein kinase bound to A-kinase anchoring proteins 15 and 79/150. Journal of General Physiology 143(3): 315-324.

Gagnon, J.Y. Anini (2012). Insulin and Norepinephrine Regulate Ghrelin Secretion from a Rat Primary Stomach Cell Culture. Endocrinology 153(8): 3646-3656.

Gales, C., J. J. J. Van Durm, S. Schaak, S. Pontier, Y. Percherancier, M. Audet, H. ParisM. Bouvier (2006). Probing the activation-promoted structural rearrangements in preassembled receptor-G protein complexes. Nature Structural & Molecular Biology 13(9): 778-786.

Garrino, M. G., T. D. PlantJ. C. Henquin (1989). Effects of Putative Activators of K+ Channels in Mouse Pancreatic Beta-Cells. British Journal of Pharmacology 98(3): 957-965.

Gauna, C., P. J. Delhanty, L. J. Hofland, J. A. Janssen, F. Broglio, R. J. Ross, E. GhigoA. J. van der Lely (2005). Ghrelin stimulates, whereas des-octanoyl ghrelin inhibits, glucose output by primary hepatocytes. J Clin Endocrinol Metab 90(2): 1055-1060.

Gauna, C., F. M. Meyler, J. A. Janssen, P. J. Delhanty, T. Abribat, P. van Koetsveld, L. J. Hofland, F. Broglio, E. GhigoA. J. van der Lely (2004). Administration of acylated ghrelin reduces insulin sensitivity, whereas the combination of acylated plus unacylated ghrelin strongly improves insulin sensitivity. J Clin Endocrinol Metab 89(10): 5035-5042.

Gauna, C., B. van de Zande, A. van Kerkwijk, A. P. Themmen, A. J. van der LelyP. J. Delhanty (2007). Unacylated ghrelin is not a functional antagonist but a full agonist of the type 1a growth hormone secretagogue receptor (GHS-R). Mol Cell Endocrinol 274(1-2): 30-34.

Gnanapavan, S., B. Kola, S. A. Bustin, D. G. Morris, P. McGee, P. Fairclough, S. Bhattacharya, R. Carpenter, A. B. GrossmanM. Korbonits (2002). The tissue distribution of the mRNA of ghrelin and subtypes of its receptor, GHS-R, in humans. J Clin Endocrinol Metab 87(6): 2988.

Gong, Z., M. Yoshimura, S. Aizawa, R. Kurotani, J. M. Zigman, T. Sakail. Sakata (2014). G protein-coupled receptor 120 signaling regulates ghrelin secretion in vivo and in vitro. Am J Physiol Endocrinol Metab 306(1): E28-35.

Granata, R., F. Settanni, L. Biancone, L. Trovato, R. Nano, F. Bertuzzi, S. Destefanis, M. Annunziata, M. Martinetti, F. Catapano, C. Ghe, J. Isgaard, M. Papotti, E. GhigoG. Muccioli (2007). Acylated and unacylated ghrelin promote proliferation and inhibit apoptosis of pancreatic beta-cells and human islets: involvement of 3',5'-cyclic adenosine monophosphate/protein kinase A, extracellular signal-regulated kinase 1/2, and phosphatidyl inositol 3-Kinase/Akt signaling. Endocrinology 148(2): 512-529.

Granata, R., F. Settanni, M. Julien, R. Nano, G. Togliatto, A. Trombetta, D. Gallo, L. Piemonti, M. F. Brizzi, T. Abribat, A. J. van Der LelyE. Ghigo (2012). Des-acyl ghrelin fragments and analogues promote survival of pancreatic beta-cells and human pancreatic islets and prevent diabetes in streptozotocin-treated rats. J Med Chem 55(6): 2585-2596.

Grant, M.U. Kumar (2010). The role of G-proteins in the dimerisation of human somatostatin receptor types 2 and 5. Regulatory Peptides 159(1-3): 3-8.

Green, B. D.D. J. Grieve (2018). Biochemical properties and biological actions of obestatin and its relevence in type 2 diabetes. Peptides 100: 249-259.

Grundy, S. M. (2006). Metabolic syndrome: connecting and reconciling cardiovascular and diabetes worlds. J Am Coll Cardiol 47(6): 1093-1100.

Guan, X. M., H. Yu, O. C. Palyha, K. K. McKee, S. D. Feighner, D. J. Sirinathsinghji, R. G. Smith, L. H. Van der PloegA. D. Howard (1997). Distribution of mRNA encoding the growth hormone secretagogue receptor in brain and peripheral tissues. Brain Res Mol Brain Res 48(1): 23-29.

Gutierrez, J. A., P. J. Solenberg, D. R. Perkins, J. A. Willency, M. D. Knierman, Z. Jin, D. R. Witcher, S. Luo, J. E. OnyiaJ. E. Hale (2008). Ghrelin octanoylation mediated by an orphan lipid transferase. Proc Natl Acad Sci U S A 105(17): 6320-6325.

Hansen, T. K., R. Dall, H. Hosoda, M. Kojima, K. Kangawa, J. S. ChristiansenJ. O. Jorgensen (2002). Weight loss increases circulating levels of ghrelin in human obesity. Clin Endocrinol (Oxf) 56(2): 203-206.

Haspel, D., P. Krippeit-Drews, L. Aguilar-Bryan, J. Bryan, G. DrewsM. Düfer (2005). Crosstalk between membrane potential and cytosolic Ca2+ concentration in beta cells from Sur1-/- mice. Diabetologia 48(5): 913-921.

Hassouna, T., K. L. Seeberger, B. SalamaG. S. Korbutt (2018). Functional Maturation and In Vitro Differentiation of Neonatal Porcine Islet Grafts. Transplantation 102(10): e413-e423.

Hawley, S. A., D. A. Pan, K. J. Mustard, L. Ross, J. Bain, A. M. Edelman, B. G. FrenguelliD. G. Hardie (2005). Calmodulin-dependent protein kinase kinase-beta is an alternative upstream kinase for AMP-activated protein kinase. Cell Metabolism 2(1): 9-19.

Heimann, E., H. A. Jones, S. Resjo, V. C. Manganiello, L. StensonE. Degerman (2010). Expression and regulation of cyclic nucleotide phosphodiesterases in human and rat pancreatic islets. PLoS One 5(12): e14191.

Heller, R. S., M. Jenny, P. Collombat, A. Mansouri, C. Tomasetto, O. D. Madsen, G. Mellitzer, G. GradwohlP. Serup (2005). Genetic determinants of pancreatic epsilon-cell development. Dev Biol 286(1): 217-224.

Hellman, B., L. A. Idahl, A. Lernmarkl. B. Taljedal (1974). The pancreatic beta-cell recognition of insulin secretagogues: does cyclic AMP mediate the effect of glucose? Proc Natl Acad Sci U S A 71(9): 3405-3409.

Henquin, J. C. (1978). D-Glucose Inhibits Potassium Efflux from Pancreatic-Islet Cells. Nature 271(5642): 271-273.

Henquin, J. C. (1990). Role of Voltage-Dependent and Ca-2+-Dependent K+ Channels in the Control of Glucose-Induced Electrical-Activity in Pancreatic B-Cells. Pflugers Archiv-European Journal of Physiology 416(5): 568-572.

Henquin, J. C. (2000). Triggering and amplifying pathways of regulation of insulin secretion by glucose. Diabetes 49(11): 1751-1760.

Heppner, K. M., C. L. Piechowski, A. Muller, N. Ottaway, S. Sisley, D. L. Smiley, K. M. Habegger, P. T. Pfluger, R. DiMarchi, H. Biebermann, M. H. Tschöp, D. A. SandovalD. Perez-Tilve (2014). Both Acyl and Des-Acyl Ghrelin Regulate Adiposity and Glucose Metabolism via Central Nervous System Ghrelin Receptors. Diabetes 63(1): 122-131.

Hill, J. T., C. S. Chao, K. R. Anderson, F. Kaufman, C. W. JohnsonL. Sussel (2010). Nkx2.2 Activates the Ghrelin Promoter in Pancreatic Islet Cells. Molecular Endocrinology 24(2): 381-390.

Hoang, D. T., H. Matsunari, M. Nagaya, H. Nagashima, J. M. Millis, P. Witkowski, V. Periwal, M. HaraJ. Jo (2014). A conserved rule for pancreatic islet organization. PLoS One 9(10): e110384.

Holst, B., N. D. Holliday, A. Bach, C. E. Elling, H. M. CoxT. W. Schwartz (2004). Common structural basis for constitutive activity of the ghrelin receptor family. J Biol Chem 279(51): 53806-53817.

Holz, G. G., G. Kang, M. Harbeck, M. W. RoeO. G. Chepurny (2006). Cell physiology of cAMP sensor Epac. Journal of Physiology-London 577(1): 5-15.

Hosoda, H., M. Kojima, H. MatsuoK. Kangawa (2000). Ghrelin and des-acyl ghrelin: two major forms of rat ghrelin peptide in gastrointestinal tissue. Biochem Biophys Res Commun 279(3): 909-913.

Hosoda, H., M. Kojima, T. Mizushima, S. ShimizuK. Kangawa (2003). Structural divergence of human ghrelin. Identification of multiple ghrelin-derived molecules produced by post-translational processing. J Biol Chem 278(1): 64-70.

Howard, A. D., S. D. Feighner, D. F. Cully, J. P. Arena, P. A. Liberator, C. I. Rosenblum, M. Hamelin, D. L. Hreniuk, O. C. Palyha, J. Anderson, P. S. Paress, C. Diaz, M. Chou, K. K. Liu, K. K. McKee, S. S. Pong, L. Y. Chaung, A. Elbrecht, M. Dashkevicz, R. Heavens, M. Rigby, D. J. Sirinathsinghji, D. C. Dean, D. G. Melillo, A. A. Patchett, R. Nargund, P. R. Griffin, J. A. DeMartino, S. K. Gupta, J. M. Schaeffer, R. G. SmithL. H. Van der Ploeg (1996). A receptor in pituitary and hypothalamus that functions in growth hormone release. Science 273(5277): 974-977.

Hsu, W. H., H. D. Xiang, A. S. Rajan, D. L. KunzeA. E. Boyd, 3rd (1991). Somatostatin inhibits insulin secretion by a G-protein-mediated decrease in Ca2+ entry through voltage-dependent Ca2+ channels in the beta cell. J Biol Chem 266(2): 837-843.

Inhoff, T., H. Monnikes, S. Noetzel, A. Stengel, M. Goebel, Q. T. Dinh, A. Riedl, N. Bannert, A. S. Wisser, B. Wiedenmann, B. F. Klapp, Y. TacheP. Kobelt (2008). Desacyl ghrelin inhibits the orexigenic effect of peripherally injected ghrelin in rats. Peptides 29(12): 2159-2168.

Ishihara, H., T. Asano, K. Tsukuda, H. Katagiri, K. Inukai, M. Anai, M. Kikuchi, Y. Yazaki, J. I. MiyazakiY. Oka (1993). Pancreatic Beta-Cell Line Min6 Exhibits Characteristics of Glucose-Metabolism and Glucose-Stimulated Insulin-Secretion Similar to Those of Normal Islets. Diabetologia 36(11): 1139-1145.

Jacobson, D. A.L. H. Philipson (2007). TRP channels of the pancreatic beta cell. Handb Exp Pharmacol(179): 409-424.

Jensen, B. S., D. Strobaek, P. Christophersen, T. D. Jorgensen, C. Hansen, A. Silahtaroglu, S. P. OlesenP. K. Ahring (1998). Characterization of the cloned human intermediate-conductance Ca2+-activated K+ channel. American Journal of Physiology-Cell Physiology 275(3): C848-C856.

Julien, M., R. G. Kay, P. J. Delhanty, S. Allas, R. Granata, C. Barton, S. Constable, E. Ghigo, A. J. van der LelyT. Abribat (2012). In vitro and in vivo stability and pharmacokinetic profile of unacylated ghrelin (UAG) analogues. Eur J Pharm Sci 47(4): 625-635.

Kaczmarek, P., L. K. Malendowicz, M. Fabis, A. Ziolkowska, E. Pruszynska-Oszmalek, M. Sassek, T. Wojciechowicz, D. Szczepankiewicz, K. Andralojc, T. Szkudelski, M. Z. StrowskiK. W. Nowak (2009). Does Somatostatin Confer Insulinostatic Effects of Neuromedin U in the Rat Pancreas? Pancreas 38(2): 208-212.

Kailey, B., M. van de Bunt, S. Cheley, P. R. Johnson, P. E. MacDonald, A. L. Gloyn, P. RorsmanM. Braun (2012). SSTR2 is the functionally dominant

somatostatin receptor in human pancreatic beta- and alpha-cells. Am J Physiol Endocrinol Metab 303(9): E1107-1116.

Kanno, T., S. Suga, J. Wu, M. KimuraM. Wakui (1998). Intracellular cAMP potentiates voltage-dependent activation of L-type Ca2+ channels in rat islet beta-cells. Pflugers Arch 435(4): 578-580.

Kawasaki, H., G. M. Springett, N. Mochizuki, S. Toki, M. Nakaya, M. Matsuda, D. E. HousmanA. M. Graybiel (1998). A family of cAMP-binding proteins that directly activate Rap1. Science 282(5397): 2275-2279.

Kelpe, C. L., P. C. Moore, S. D. Parazzoli, B. Wicksteed, C. J. RhodesV. Poitout (2003). Palmitate inhibition of insulin gene expression is mediated at the transcriptional level via ceramide synthesis. Journal of Biological Chemistry 278(32): 30015-30021.

Kern, A., R. Albarran-Zeckler, H. E. WalshR. G. Smith (2012). Apo-Ghrelin Receptor Forms Heteromers with DRD2 in Hypothalamic Neurons and Is Essential for Anorexigenic Effects of DRD2 Agonism. Neuron 73(2): 317-332.

Kirchner, H., J. A. Gutierrez, P. J. Solenberg, P. T. Pfluger, T. A. Czyzyk, J. A. Willency, A. Schurmann, H. G. Joost, R. J. Jandacek, J. E. Hale, M. L. HeimanM. H. Tschöp (2009). GOAT links dietary lipids with the endocrine control of energy balance. Nat Med 15(7): 741-745.

Kojima, M., H. Hosoda, Y. Date, M. Nakazato, H. MatsuoK. Kangawa (1999). Ghrelin is a growth-hormone-releasing acylated peptide from stomach. Nature 402(6762): 656-660.

Kojima, M.K. Kangawa (2005). Ghrelin: structure and function. Physiol Rev 85(2): 495-522.

Korbutt, G. S. (2009). The International Xenotransplantation Association consensus statement on conditions for undertaking clinical trials of porcine islet products in type 1 diabetes--chapter 3: Pig islet product manufacturing and release testing. Xenotransplantation 16(4): 223-228.

Krippeit-Drews, P., M. DüferG. Drews (2000). Parallel oscillations of intracellular calcium activity and mitochondrial membrane potential in mouse pancreatic B-cells. Biochem Biophys Res Commun 267(1): 179-183.

Kurashina, T., K. Dezaki, M. Yoshida, R. Sukma Rita, K. Ito, M. Taguchi, R. Miura, M. Tominaga, S. Ishibashi, M. KakeiT. Yada (2015). The beta-cell GHSR and downstream cAMP/TRPM2 signaling account for insulinostatic and glycemic effects of ghrelin. Sci Rep 5: 14041.

Lacraz, G., F. Figeac, J. Movassat, N. Kassis, J. Coulaud, A. Galinier, C. Leloup, D. Bailbe, F. Homo-DelarcheB. Portha (2009). Diabetic beta-Cells Can

Achieve Self-Protection against Oxidative Stress through an Adaptive Up-Regulation of Their Antioxidant Defenses. PLoS One 4(8).

Lameloise, N., P. Muzzin, M. PrentkiF. Assimacopoulos-Jeannet (2001). Uncoupling protein 2: A possible link between fatty acid excess and impaired glucose-induced insulin secretion? Diabetes 50(4): 803-809.

Leech, C. A., O. G. ChepurnyG. G. Holz (2010). Epac2-Dependent Rap1 Activation and the Control of Islet Insulin Secretion by Glucagon-Like Peptide-1. Vitamins and Hormones: Incretins and Insulin Secretion 84: 279-302.

Leung, P. K., K. B. Chow, P. N. Lau, K. M. Chu, C. B. Chan, C. H. ChengH. Wise (2007). The truncated ghrelin receptor polypeptide (GHS-R1b) acts as a dominant-negative mutant of the ghrelin receptor. Cell Signal 19(5): 1011-1022.

Light, P. E., J. E. M. Fox, M. J. RiedelM. B. Wheeler (2002). Glucagon-like peptide-1 inhibits pancreatic ATP-sensitive potassium channels via a protein kinase A- and ADP-dependent mechanism. Molecular Endocrinology 16(9): 2135-2144.

Lim, C. T., B. Kola, A. GrossmanM. Korbonits (2011). The expression of ghrelin O-acyltransferase (GOAT) in human tissues. Endocr J 58(8): 707-710.

Lin, Y. F., Y. N. JanL. Y. Jan (2000). Regulation of ATP-sensitive potassium channel function by protein kinase A-mediated phosphorylation in transfected HEK293 cells. Embo Journal 19(5): 942-955.

Liu, B., E. A. GarciaM. Korbonits (2011). Genetic studies on the ghrelin, growth hormone secretagogue receptor (GHSR) and ghrelin O-acyl transferase (GOAT) genes. Peptides 32(11): 2191-2207.

Longo, K. A., S. Charoenthongtrakul, D. J. Giuliana, E. K. Govek, T. McDonagh, Y. Qi, P. S. DiStefanoB. J. Geddes (2008). Improved insulin sensitivity and metabolic flexibility in ghrelin receptor knockout mice. Regul Pept 150(1-3): 55-61.

Lu, X., X. Zhao, J. Feng, A. P. Liou, S. Anthony, S. Pechhold, Y. Sun, H. LuS. Wank (2012). Postprandial inhibition of gastric ghrelin secretion by long-chain fatty acid through GPR120 in isolated gastric ghrelin cells and mice. Am J Physiol Gastrointest Liver Physiol 303(3): G367-376.

Ludvigsen, E., R. Olsson, M. Stridsberg, E. T. JansonS. Sandler (2004). Expression and distribution of somatostatin receptor subtypes in the pancreatic islets of mice and rats. J Histochem Cytochem 52(3): 391-400.

Lunney, J. K. (2007). Advances in swine biomedical model genomics. Int J Biol Sci 3(3): 179-184.

M'Kadmi, C., J. P. Leyris, L. Onfroy, C. Gales, A. Sauliere, D. Gagne, M. Damian, S. Mary, M. Maingot, S. Denoyelle, P. Verdie, J. A. Fehrentz, J.

Martinez, J. L. BaneresJ. Marie (2015). Agonism, Antagonism, and Inverse Agonism Bias at the Ghrelin Receptor Signaling. J Biol Chem 290(45): 27021-27039.

MacDonald, P. E., A. M. F. SalapatekM. B. Wheeler (2002). Glucagon-like peptide-1 receptor activation antagonizes voltage-dependent repolarizing K+ currents in beta-cells - A possible glucose-dependent insulinotropic mechanism. Diabetes 51: S443-S447.

Martens, G. A., Y. Cai, S. Hinke, G. Stange, M. Van de CasteeleD. Pipeleers (2005). Glucose suppresses superoxide generation in metabolically responsive pancreatic beta cells. Journal of Biological Chemistry 280(21): 20389-20396.

Mary, S., J. A. Fehrentz, M. Damian, G. Gaibelet, H. Orcel, P. Verdie, B. Mouillac, J. Martinez, J. MarieJ. L. Baneres (2013). Heterodimerization with Its splice variant blocks the ghrelin receptor 1a in a non-signaling conformation: a study with a purified heterodimer assembled into lipid discs. J Biol Chem 288(34): 24656-24665.

Mastracci, T. L., K. R. Anderson, J. B. PapizanL. Sussel (2013). Regulation of Neurod1 Contributes to the Lineage Potential of Neurogenin3+ Endocrine Precursor Cells in the Pancreas. Plos Genetics 9(2).

Millington, G. W. M. (2007). The role of proopiomelanocortin (POMC) neurones in feeding behaviour. Nutrition & Metabolism 4.

Mizutani, M., K. Atsuchi, A. Asakawa, N. Matsuda, M. Fujimura, A. Inui, I. KatoM. Fujimiya (2009). Localization of acyl ghrelin- and des-acyl ghrelin-immunoreactive cells in the rat stomach and their responses to intragastric pH. Am J Physiol Gastrointest Liver Physiol 297(5): G974-980.

Mosa, R., L. Huang, H. Li, M. Grist, D. LeRoithC. Chen (2017). Long-term treatment with the ghrelin receptor antagonist, [D-Lys3]-GHRP-6 does not improve glucose homeostasis in non-obese diabetic MKR mice. Am J Physiol Regul Integr Comp Physiol: ajpregu 00157 02017.

Murakami, T., S. Hitomi, A. Ohtsuka, T. TaguchiT. Fujita (1997). Pancreatic insulo-acinar portal systems in humans, rats, and some other mammals: scanning electron microscopy of vascular casts. Microsc Res Tech 37(5-6): 478-488.

Nadal, A., I. QuesadaB. Soria (1999). Homologous and heterologous asynchronicity between identified alpha-, beta- and delta-cells within intact islets of Langerhans in the mouse. J Physiol 517 (Pt 1): 85-93.

Nagamatsu, S., Y. Nakamichi, C. Yamamura, S. Matsushima, T. Watanabe, S. Ozawa, H. FurukawaH. Ishida (1999). Decreased expression of t-SNARE, syntaxin 1, and SNAP-25 in pancreatic beta-cells is involved in impaired insulin secretion from diabetic GK rat islets - Restoration of decreased t-SNARE proteins improves impaired insulin secretion. Diabetes 48(12): 2367-2373.

Navarro, G., D. Aguinaga, E. Angelats, M. Medrano, E. Moreno, J. Mallol, A. Cortes, E. I. Canela, V. Casado, P. J. McCormick, C. LluisS. Ferre (2016). A Significant Role of the Truncated Ghrelin Receptor GHS-R1b in Ghrelin-induced Signaling in Neurons. J Biol Chem 291(25): 13048-13062.

Nenquin, M., A. Szollosi, L. Aguilar-Bryan, J. BryanJ. C. Henquin (2004). Both triggering and amplifying pathways contribute to fuel-induced insulin secretion in the absence of sulfonylurea receptor-1 in pancreatic beta-cells. J Biol Chem 279(31): 32316-32324.

Nishi, Y., H. Hiejima, H. Hosoda, H. Kaiya, K. Mori, Y. Fukue, T. Yanase, H. Nawata, K. KangawaM. Kojima (2005). Ingested medium-chain fatty acids are directly utilized for the acyl modification of ghrelin. Endocrinology 146(5): 2255-2264.

Nobles, M., A. BeniansA. Tinker (2005). Heterotrimeric G proteins precouple with G protein-coupled receptors in living cells. Proceedings of the National Academy of Sciences of the United States of America 102(51): 18706-18711.

Noe, B. D. (1981). Synthesis of one form of pancreatic islet somatostatin predominates. J Biol Chem 256(18): 9397-9400.

Norman, M., S. Moldovan, V. Seghers, X. P. Wang, F. J. DeMayoF. C. Brunicardi (2002). Sulfonylurea receptor knockout causes glucose intolerance in mice that is not alleviated by concomitant somatostatin subtype receptor 5 knockout. Ann Surg 235(6): 767-774.

Olofsson, C. S., S. Collins, M. Bengtsson, L. Eliasson, A. Salehi, K. Shimomura, A. Tarasov, C. Holm, F. AshcroftP. Rorsman (2007a). Long-term exposure to glucose and lipids inhibits glucose-induced insulin secretion downstream of granule fusion with plasma membrane. Diabetes 56(7): 1888-1897.

Olofsson, C. S., S. Collins, M. Bengtsson, L. Eliasson, A. Salehi, K. Shimontura, A. Tarasov, C. Hoim, F. AshcroftP. Rorsman (2007b). Long-term exposure to glucose and lipids inhibits glucose-induced insulin secretion downstream of granule fusion with plasma membrane. Diabetes 56(7): 1888-1897.

Orgaard, A.J. J. Holst (2017). The role of somatostatin in GLP-1-induced inhibition of glucagon secretion in mice. Diabetologia 60(9): 1731-1739.

Otto, B., U. Cuntz, E. Fruehauf, R. Wawarta, C. Folwaczny, R. L. Riepl, M. L. Heiman, P. Lehnert, M. FichterM. Tschöp (2001). Weight gain decreases elevated plasma ghrelin concentrations of patients with anorexia nervosa. Eur J Endocrinol 145(5): 669-673.

Ozcan, B., S. J. Neggers, A. R. Miller, H. C. Yang, V. Lucaites, T. Abribat, S. Allas, M. Huisman, J. A. Visser, A. P. Themmen, E. J. Sijbrands, P. J. DelhantyA. J. van der Lely (2014). Does des-acyl ghrelin improve glycemic

control in obese diabetic subjects by decreasing acylated ghrelin levels? Eur J Endocrinol 170(6): 799-807.

Pacifico, L., E. Poggiogalle, F. Costantino, C. Anama, F. Ferraro, F. ChiarelliC. Chiesa (2009a). Acylated and nonacylated ghrelin levels and their associations with insulin resistance in obese and normal weight children with metabolic syndrome. European Journal of Endocrinology 161(6): 861-870.

Pacifico, L., E. Poggiogalle, F. Costantino, C. Anania, F. Ferraro, F. ChiarelliC. Chiesa (2009b). Acylated and nonacylated ghrelin levels and their associations with insulin resistance in obese and normal weight children with metabolic syndrome. Eur J Endocrinol 161(6): 861-870.

Pantel, J., M. Legendre, S. Cabrol, L. Hilal, Y. Hajaji, S. Morisset, S. Nivot, M. P. Vie-Luton, D. Grouselle, M. de Kerdanet, A. Kadiri, J. Epelbaum, Y. Le BoucS. Amselem (2006). Loss of constitutive activity of the growth hormone secretagogue receptor in familial short stature. J Clin Invest 116(3): 760-768.

Park, S., H. Jiang, H. ZhangR. G. Smith (2012). Modification of ghrelin receptor signaling by somatostatin receptor-5 regulates insulin release. Proc Natl Acad Sci U S A 109(46): 19003-19008.

Patel, Y. C. (1999). Somatostatin and its receptor family. Front Neuroendocrinol 20(3): 157-198.

Patel, Y. C., M. T. Greenwood, A. Warszynska, R. PanettaC. B. Srikant (1994). All five cloned human somatostatin receptors (hSSTR1-5) are functionally coupled to adenylyl cyclase. Biochem Biophys Res Commun 198(2): 605-612.

Patel, Y. C.S. Reichlin (1978). Somatostatin in hypothalamus, extrahypothalamic brain, and peripheral tissues of the rat. Endocrinology 102(2): 523-530.

Perreault, M., N. Istrate, L. Wang, A. J. Nichols, E. TozzoA. Stricker-Krongrad (2004). Resistance to the orexigenic effect of ghrelin in dietary-induced obesity in mice: reversal upon weight loss. Int J Obes Relat Metab Disord 28(7): 879-885.

Philippaert, K.R. Vennekens (2018). The Role of TRP Channels in the Pancreatic Beta-Cell. Neurobiology of Trp Channels: 229-250.

Poitout, V., J. Amyot, M. Semache, B. Zarrouki, D. HagmanG. Fontes (2010). Glucolipotoxicity of the pancreatic beta cell. Biochimica Et Biophysica Acta-Molecular and Cell Biology of Lipids 1801(3): 289-298.

Poitout, V., D. Hagman, R. Stein, I. Artner, R. P. RobertsonJ. S. Harmon (2006). Regulation of the insulin gene by glucose and fatty acids. Journal of Nutrition 136(4): 873-876.

Poitout, V.R. P. Robertson (2008). Glucolipotoxicity: fuel excess and beta-cell dysfunction. Endocr Rev 29(3): 351-366.

Pyne, N. J.B. L. Furman (2003). Cyclic nucleotide phosphodiesterases in pancreatic islets. Diabetologia 46(9): 1179-1189.

Qin, K., C. M. Dong, G. Y. WuN. A. Lambert (2011). Inactive-state preassembly of G(q)-coupled receptors and G(q) heterotrimers. Nature Chemical Biology 7(10): 740-747.

Quesada, I., M. G. Todorova, P. Alonso-Magdalena, M. Beltra, E. M. Carneiro, F. Martin, A. NadalB. Soria (2006). Glucose induces opposite intracellular Ca2+ concentration oscillatory patterns in identified alpha- and beta-cells within intact human islets of Langerhans. Diabetes 55(9): 2463-2469.

Rae, J., K. Cooper, P. GatesM. Watsky (1991). Low Access Resistance Perforated Patch Recordings Using Amphotericin-B. Journal of Neuroscience Methods 37(1): 15-26.

Reimer, M. K., G. PaciniB. Ahren (2003). Dose-dependent inhibition by ghrelin of insulin secretion in the mouse. Endocrinology 144(3): 916-921.

Renstrom, E., L. EliassonP. Rorsman (1997). Protein kinase A-dependent and -independent stimulation of exocytosis by cAMP in mouse pancreatic B-cells. J Physiol 502 (Pt 1): 105-118.

Reubi, J. C., J. C. Schaer, S. Wenger, C. Hoeger, J. Erchegyi, B. WaserJ. Rivier (2000). SST3-selective potent peptidic somatostatin receptor antagonists. Proceedings of the National Academy of Sciences of the United States of America 97(25): 13973-13978.

Rigamonti, A. E., A. I. Pincelli, B. Corra, R. Viarengo, S. M. Bonomo, D. Galimberti, M. Scacchi, E. Scarpini, F. CavagniniE. E. Muller (2002). Plasma ghrelin concentrations in elderly subjects: comparison with anorexic and obese patients. J Endocrinol 175(1): R1-5.

Rindi, G., V. Necchi, A. Savio, A. Torsello, M. Zoli, V. Locatelli, F. Raimondo, D. CocchiE. Solcia (2002). Characterisation of gastric ghrelin cells in man and other mammals: studies in adult and fetal tissues. Histochemistry and Cell Biology 117(6): 511-519.

Ritz-Laser, B., P. Meda, I. Constant, N. Klages, A. Charollais, A. Morales, C. Magnan, A. KtorzaJ. Philippe (1999). Glucose-induced preproinsulin gene expression is inhibited by the free fatty acid palmitate. Endocrinology 140(9): 4005-4014.

Robertson, R., H. Zhou, T. ZhangJ. S. Harmon (2007). Chronic oxidative stress as a mechanism for glucose toxicity of the beta cell in type 2 diabetes. Cell Biochem Biophys 48(2-3): 139-146.

Robertson, R. P., J. Harmon, P. O. TranV. Poitout (2004). Beta-cell glucose toxicity, lipotoxicity, and chronic oxidative stress in type 2 diabetes. Diabetes 53 Suppl 1: S119-124.

Rocheville, M., D. C. Lange, U. Kumar, R. Sasi, R. C. PatelY. C. Patel (2000). Subtypes of the somatostatin receptor assemble as functional homo- and heterodimers. Journal of Biological Chemistry 275(11): 7862-7869.

Rodriguez, A., J. Gomez-Ambrosi, V. Catalan, M. J. Gil, S. Becerril, N. Sainz, C. Silva, J. Salvador, I. ColinaG. Fruhbeck (2009). Acylated and desacyl ghrelin stimulate lipid accumulation in human visceral adipocytes. International Journal of Obesity 33(5): 541-552.

Rorsman, P.F. M. Ashcroft (2018). Pancreatic beta-Cell Electrical Activity and Insulin Secretion: Of Mice and Men. Physiol Rev 98(1): 117-214.

Rorsman, P.M. O. Huising (2018). The somatostatin-secreting pancreatic delta-cell in health and disease. Nat Rev Endocrinol 14(7): 404-414.

Rorsman, P.E. Renstrom (2003). Insulin granule dynamics in pancreatic beta cells. Diabetologia 46(8): 1029-1045.

Rorsman, P.G. Trube (1985). Glucose dependent K+-channels in pancreatic beta-cells are regulated by intracellular ATP. Pflugers Arch 405(4): 305-309.

Sakata, I., K. Nakamura, M. Yamazaki, M. Matsubara, Y. Hayashi, K. KangawaT. Sakai (2002). Ghrelin-producing cells exist as two types of cells, closed- and opened-type cells, in the rat gastrointestinal tract. Peptides 23(3): 531-536.

Sakata, I., J. Yang, C. E. Lee, S. Osborne-Lawrence, S. A. Rovinsky, J. K. ElmquistJ. M. Zigman (2009). Colocalization of ghrelin O-acyltransferase and ghrelin in gastric mucosal cells. Am J Physiol Endocrinol Metab 297(1): E134-141.

Sakata, N., G. YoshimatsuS. Kodama (2019). Development and Characteristics of Pancreatic Epsilon Cells. Int J Mol Sci 20(8).

Samols, E., J. I. Stagner, R. B. EwartV. Marks (1988). The order of islet microvascular cellular perfusion is B----A----D in the perfused rat pancreas. J Clin Invest 82(1): 350-353.

Sams, D. J.W. Montague (1972). The role of adenosine 3':5'-cyclic monophosphate in the regulation of insulin release. Properties of islet-cell adenosine 3':5'-cyclic monophosphate phosphodiesterase. Biochem J 129(4): 945-952.

Schellekens, H., W. E. van Oeffelen, T. G. DinanJ. F. Cryan (2013). Promiscuous dimerization of the growth hormone secretagogue receptor (GHS-R1a) attenuates ghrelin-mediated signaling. J Biol Chem 288(1): 181-191.

Schopfer, L. M., O. LockridgeS. Brimijoin (2015). Pure human butyrylcholinesterase hydrolyzes octanoyl ghrelin to desacyl ghrelin. Gen Comp Endocrinol 224: 61-68.
Schuit, F. C.D. G. Pipeleers (1985). Regulation of Adenosine-3',5'-Monophosphate Levels in the Pancreatic B-Cell. Endocrinology 117(3): 834-840.

Seghers, V., M. Nakazaki, F. DeMayo, L. Aguilar-BryanJ. Bryan (2000). Sur1 knockout mice. A model for K(ATP) channel-independent regulation of insulin secretion. J Biol Chem 275(13): 9270-9277.

Seifert, R.K. Wenzel-Seifert (2002). Constitutive activity of G-protein-coupled receptors: cause of disease and common property of wild-type receptors. Naunyn-Schmiedebergs Archives of Pharmacology 366(5): 381-416.

Shibasaki, T., H. Takahashi, T. Miki, Y. Sunaga, K. Matsumura, M. Yamanaka, C. Zhang, A. Tamamoto, T. Satoh, J. MiyazakiS. Seino (2007). Essential role of Epac2/Rap1 signaling in regulation of insulin granule dynamics by cAMP. Proc Natl Acad Sci U S A 104(49): 19333-19338.

Shiiya, T., M. Nakazato, M. Mizuta, Y. Date, M. S. Mondal, M. Tanaka, S. Nozoe, H. Hosoda, K. KangawaS. Matsukura (2002). Plasma ghrelin levels in lean and obese humans and the effect of glucose on ghrelin secretion. J Clin Endocrinol Metab 87(1): 240-244.

Shimon, I., X. YanS. Melmed (1998). Human fetal pituitary expresses functional growth hormone-releasing peptide receptors. J Clin Endocrinol Metab 83(1): 174-178.

Shiota, C., O. Larsson, K. D. Shelton, M. Shiota, A. M. Efanov, M. Hoy, J. Lindner, S. Kooptiwut, L. Juntti-Berggren, J. Gromada, P. O. BerggrenM. A. Magnuson (2002). Sulfonylurea receptor type 1 knock-out mice have intact feeding-stimulated insulin secretion despite marked impairment in their response to glucose. J Biol Chem 277(40): 37176-37183.

Shuto, Y., T. Shibasaki, A. Otagiri, H. Kuriyama, H. Ohata, H. Tamura, J. Kamegai, H. Sugihara, S. Oikawal. Wakabayashi (2002). Hypothalamic growth hormone secretagogue receptor regulates growth hormone secretion, feeding, and adiposity. J Clin Invest 109(11): 1429-1436.

Smit, M. J., H. F. Vischer, R. A. Bakker, A. Jongejan, H. Timmerman, L. PardoR. Leurs (2007). Pharmacogenomic and structural analysis of constitutive g protein-coupled receptor activity. Annu Rev Pharmacol Toxicol 47: 53-87.

Smith, P. A., F. M. AshcroftP. Rorsman (1990a). Simultaneous Recordings of Glucose Dependent Electrical-Activity and Atp-Regulated K+-Currents in Isolated Mouse Pancreatic Beta-Cells. Febs Letters 261(1): 187-190.

Smith, P. A., K. Bokvist, P. Arkhammar, P. O. BerggrenP. Rorsman (1990b). Delayed rectifying and calcium-activated K+ channels and their significance for

action potential repolarization in mouse pancreatic beta-cells. J Gen Physiol 95(6): 1041-1059.

Somvanshi, R. K., S. A. War, N. Chaudhari, X. F. QiuU. Kumar (2011). Receptor specific crosstalk and modulation of signaling upon heterodimerization between beta(1)-adrenergic receptor and somatostatin receptor-5. Cellular Signalling 23(5): 794-811.

Stefan, Y., S. Grasso, A. PerreletL. Orci (1983). A quantitative immunofluorescent study of the endocrine cell populations in the developing human pancreas. Diabetes 32(4): 293-301.

Steiner, D. J., A. Kim, K. MillerM. Hara (2010). Pancreatic islet plasticity: interspecies comparison of islet architecture and composition. Islets 2(3): 135-145.

Strowski, M. Z., M. Kohler, H. Y. Chen, M. E. Trumbauer, Z. Li, D. Szalkowski, S. Gopal-Truter, J. K. Fisher, J. M. Schaeffer, A. D. Blake, B. B. ZhangH. A. Wilkinson (2003). Somatostatin receptor subtype 5 regulates insulin secretion and glucose homeostasis. Mol Endocrinol 17(1): 93-106.

Swindle, M. M., A. Makin, A. J. Herron, F. J. Clubb, Jr.K. S. Frazier (2012). Swine as models in biomedical research and toxicology testing. Vet Pathol 49(2): 344-356.

Swisa, A., D. Avrahami, N. Eden, J. Zhang, E. Feleke, T. Dahan, Y. Cohen-Tayar, M. Stolovich-Rain, K. H. Kaestner, B. Glaser, R. Ashery-PadanY. Dor (2017). PAX6 maintains beta cell identity by repressing genes of alternative islet cell types. Journal of Clinical Investigation 127(1): 230-243.

Tanaka, M., T. Naruo, D. Yasuhara, Y. Tatebe, N. Nagai, T. Shiiya, M. Nakazato, S. MatsukuraS. Nozoe (2003). Fasting plasma ghrelin levels in subtypes of anorexia nervosa. Psychoneuroendocrinology 28(7): 829-835.

Taylor, M. S., Y. Hwang, P. Y. Hsiao, J. D. BoekeP. A. Cole (2012). Ghrelin O-acyltransferase assays and inhibition. Methods Enzymol 514: 205-228.

Taylor, M. S., T. R. Ruch, P. Y. Hsiao, Y. Hwang, P. Zhang, L. Dai, C. R. Huang, C. E. Berndsen, M. S. Kim, A. Pandey, C. Wolberger, R. Marmorstein, C. Machamer, J. D. BoekeP. A. Cole (2013). Architectural organization of the metabolic regulatory enzyme ghrelin O-acyltransferase. J Biol Chem 288(45): 32211-32228.

Tengholm, A. (2012). Cyclic AMP dynamics in the pancreatic beta-cell. Ups J Med Sci 117(4): 355-369.

Tengholm, A.E. Gylfe (2017). cAMP signalling in insulin and glucagon secretion. Diabetes Obes Metab 19 Suppl 1: 42-53.

Tinker, A., Q. Aziz, Y. W. LiM. Specterman (2018). ATP-Sensitive Potassium Channels and Their Physiological and Pathophysiological Roles. Comprehensive Physiology 8(4): 1463-1511.

Tirone, T. A., M. A. Norman, S. Moldovan, F. J. DeMayo, X. P. WangF. C. Brunicardi (2003). Pancreatic somatostatin inhibits insulin secretion via SSTR-5 in the isolated perfused mouse pancreas model. Pancreas 26(3): e67-73.

Toshinai, K., M. S. Mondal, M. Nakazato, Y. Date, N. Murakami, M. Kojima, K. KangawaS. Matsukura (2001). Upregulation of Ghrelin expression in the stomach upon fasting, insulin-induced hypoglycemia, and leptin administration. Biochem Biophys Res Commun 281(5): 1220-1225.

Tschöp, M., D. L. SmileyM. L. Heiman (2000). Ghrelin induces adiposity in rodents. Nature 407(6806): 908-913.

Tschöp, M., R. Wawarta, R. L. Riepl, S. Friedrich, M. Bidlingmaier, R. LandgrafC. Folwaczny (2001a). Post-prandial decrease of circulating human ghrelin levels. J Endocrinol Invest 24(6): RC19-21.

Tschöp, M., C. Weyer, P. A. Tataranni, V. Devanarayan, E. RavussinM. L. Heiman (2001b). Circulating ghrelin levels are decreased in human obesity. Diabetes 50(4): 707-709.

Tsuboi, T., M. A. Ravier, L. E. PartonG. A. Rutter (2006). Sustained exposure to high glucose concentrations modifies glucose signaling and the mechanics of secretory vesicle fusion in primary rat pancreatic beta-cells. Diabetes 55(4): 1057-1065.

Ueno, H., T. Shibasaki, T. Iwanaga, K. Takahashi, Y. Yokoyama, L. M. Liu, N. Yokoi, N. Ozaki, S. Matsukura, H. YanoS. Seino (2001). Characterization of the gene EPAC2: Structure, chromosomal localization, tissue expression, and identification of the liver-specific isoform. Genomics 78(1-2): 91-98.

Unger, R. H.S. Grundy (1985). Hyperglycaemia as an inducer as well as a consequence of impaired islet cell function and insulin resistance: implications for the management of diabetes. Diabetologia 28(3): 119-121.

Velasco, J. M.O. H. Petersen (1987). Voltage-Activation of High-Conductance K+ Channel in the Insulin-Secreting Cell-Line Rinm5f Is Dependent on Local Extracellular Ca-2+ Concentration. Biochimica Et Biophysica Acta 896(2): 305-310.

Vikman, J., H. Svensson, Y. C. Huang, Y. Kang, S. A. Andersson, H. Y. GaisanoL. Eliasson (2009). Truncation of SNAP-25 reduces the stimulatory action of cAMP on rapid exocytosis in insulin-secreting cells. American Journal of Physiology-Endocrinology and Metabolism 297(2): E452-E461.

Vogalis, F., Y. ZhangR. K. Goyal (1998). An intermediate conductance K+ channel in the cell membrane of mouse intestinal smooth muscle. Biochimica Et Biophysica Acta-Biomembranes 1371(2): 309-316.

Wang, Q., L. Elghazi, S. Martin, I. Martins, R. S. Srinivasan, X. Geng, M. Sleeman, P. Collombat, J. HoughtonB. Sosa-Pineda (2008). ghrelin is a novel target of Pax4 in endocrine progenitors of the pancreas and duodenum. Developmental Dynamics 237(1): 51-61.

Wang, X. P., J. Yang, M. A. Norman, J. Magnusson, F. J. DeMayoF. C. Brunicardi (2005). SSTR5 ablation in islet results in alterations in glucose homeostasis in mice. Febs Letters 579(14): 3107-3114.

Watt, H. L., G. D. KharmateU. Kumar (2009). Somatostatin receptors 1 and 5 heterodimerize with epidermal growth factor receptor: Agonist-dependent modulation of the downstream MAPK signalling pathway in breast cancer cells. Cellular Signalling 21(3): 428-439.

Wierup, N., F. SundlerR. S. Heller (2014). The islet ghrelin cell. J Mol Endocrinol 52(1): R35-49.

Wierup, N., H. Svensson, H. MulderF. Sundler (2002). The ghrelin cell: a novel developmentally regulated islet cell in the human pancreas. Regul Pept 107(1-3): 63-69.

Wierup, N., S. Yang, R. J. McEvilly, H. MulderF. Sundler (2004). Ghrelin is expressed in a novel endocrine cell type in developing rat islets and inhibits insulin secretion from INS-1 (832/13) cells. J Histochem Cytochem 52(3): 301-310.

Willesen, M. G., P. KristensenJ. Romer (1999). Co-localization of growth hormone secretagogue receptor and NPY mRNA in the arcuate nucleus of the rat. Neuroendocrinology 70(5): 306-316.

Williams, D. L., D. E. Cummings, H. J. GrillJ. M. Kaplan (2003). Meal-related ghrelin suppression requires postgastric feedback. Endocrinology 144(7): 2765-2767.

Wolf, E., C. Braun-Reichhart, E. StreckelS. Renner (2014). Genetically engineered pig models for diabetes research. Transgenic Res 23(1): 27-38.

Wollheim, C. B.G. W. G. Sharp (1981). Regulation of Insulin Release by Calcium. Physiological Reviews 61(4): 914-973.

Yamada, Y., S. Kagimoto, A. Kubota, K. Yasuda, K. Masuda, Y. Someya, Y. Ihara, Q. Li, H. Imura, S. Seinoet al. (1993). Cloning, functional expression and pharmacological characterization of a fourth (hSSTR4) and a fifth (hSSTR5) human somatostatin receptor subtype. Biochem Biophys Res Commun 195(2): 844-852.

Yamada, Y., S. R. Post, K. Wang, H. S. Tager, G. I. BellS. Seino (1992). Cloning and functional characterization of a family of human and mouse somatostatin receptors expressed in brain, gastrointestinal tract, and kidney. Proc Natl Acad Sci U S A 89(1): 251-255.

Yanagi, S., T. Sato, K. KangawaM. Nakazato (2018). The Homeostatic Force of Ghrelin. Cell Metab 27(4): 786-804.

Yang, J., M. S. Brown, G. Liang, N. V. GrishinJ. L. Goldstein (2008). Identification of the acyltransferase that octanoylates ghrelin, an appetite-stimulating peptide hormone. Cell 132(3): 387-396.

Zerangue, N., B. Schwappach, Y. N. JanL. Y. Jan (1999). A new ER trafficking signal regulates the subunit stoichiometry of plasma membrane K(ATP) channels. Neuron 22(3): 537-548.

Zhang, J. V., P. G. Ren, O. Avsian-Kretchmer, C. W. Luo, R. Rauch, C. KleinA. J. Hsueh (2005). Obestatin, a peptide encoded by the ghrelin gene, opposes ghrelin's effects on food intake. Science 310(5750): 996-999.

Zhang, Q., M. Bengtsson, C. Partridge, A. Salehi, M. Braun, R. Cox, L. Eliasson, P. R. Johnson, E. Renstrom, T. Schneider, P. O. Berggren, S. Gopel, F. M. AshcroftP. Rorsman (2007). R-type Ca(2+)-channel-evoked CICR regulates glucose-induced somatostatin secretion. Nat Cell Biol 9(4): 453-460.

Zhao, T. J., I. Sakata, R. L. Li, G. S. Liang, J. A. Richardson, M. S. Brown, J. L. GoldsteinJ. M. Zigman (2010). Ghrelin secretion stimulated by beta(1)-adrenergic receptors in cultured ghrelinoma cells and in fasted mice. Proceedings of the National Academy of Sciences of the United States of America 107(36): 15868-15873.

Zhou, Y. P.V. Grill (1995). Long term exposure to fatty acids and ketones inhibits B-cell functions in human pancreatic islets of Langerhans. J Clin Endocrinol Metab 80(5): 1584-1590.

Zhu, X., Y. Cao, K. VoogdD. F. Steiner (2006). On the processing of proghrelin to ghrelin. J Biol Chem 281(50): 38867-38870.

5 Danksagung

Diese Arbeit wurde von Februar 2016 bis Oktober 2019 unter der wissenschaftlichen Anleitung von Prof. Dr. Gisela Drews am pharmazeutischen Institut der Eberhard Karls Tübingen angefertigt.

Ich bedanke mich ganz besonders bei Prof. Dr. Gisela Drews. Bereits bei der Durchführung meines Wahlpflichtfachs im Rahmen des Pharmaziestudiums fühlte ich mich unter ihrer Leitung und im Arbeitskreis sehr wohl und freute mich umso mehr, als ich meine Promotion bei ihr absolvieren durfte. Die gute Ansprechbarkeit, die interessanten Diskussionen, in denen jeder Gedanke genannt werden durfte und das gegenseitig entgegengebrachte Vertrauen werden diese Zeit immer unvergesslich für mich machen.
Ebenso möchte ich mich bei Prof. Dr. Peter Krippeit-Drews herzlich bedanken, der mir die technischen Geräte der Elektrophysiologie geduldig – auch mehrmals – erklärte und sofort zur Stelle war, wenn Reparaturen anstanden. An dieser Stelle möchte ich Prof. Dr. Gisela Drews und Prof. Dr. Peter Krippeit-Drews zusammen für ihre allgemeinen Erläuterungen der Materie bedanken, die mir so manche Grundlagen und wissenschaftlichen Details verständlicher machten.

Ich bedanke mich sehr bei Prof. Dr. Susanne Ullrich, welche als meine zweite Betreuerin fungierte.

Bei JProf. Dr. Leonard Kaysser und Prof. Harald Groß bedanke ich mich sehr dafür, dass sie bei meiner mündlichen Verteidigung der Doktorarbeit als Prüfer fungierten.

Ein Dank geht auch an die Mitarbeiter des Arbeitskreises von Prof. Dr. Martina Düfer aus Münster, mit denen ich mehrfach korrespondierte. Dabei möchte ich insbesondere Theresa Hoffmeister danken, dass ich an ihrem Forschungsthema mitwirken durfte und Anne Gresch für das geduldige Zusenden der MIN6.

Ich bedanke mich sehr bei Dr. Cita Bleile und Dr. Jonas Maczewksy, welche mich in alle Methoden, die ich benötigte, einlernten und jederzeit für Fragen offen waren. Jelena Sikimic möchte ich für die gute Zusammenarbeit danken, welche mir immer eine Freude war. Vielen Dank für die lustigen Momente im Labor, egal wie widrig die Umstände waren.

Ich danke Isolde Breuning für die vielen RIAs und ihre tolle Arbeit. Zusätzlich zu ihr möchte ich auch Ilona Böhler für die gute Betreuung unserer Mäuse in der Tierhaltung Dank zukommen lassen.

Besondere Erwähnung sollen meine liebsten Freunde erfahren: Kojo, Anja und Celi. Ihr begleitet nun stellenweise seit vielen Jahren meinen akademischen Werdegang und ich kann mir eurer Liebe und Unterstützung immer gewiss sein. Danke für alles!

Ohne meinen Mann hätte ich vieles in den letzten Jahren nicht im Ansatz so glimpflich gemeistert. Du zähmst meine wirren Gedanken und stützt mich in jeglicher Hinsicht. Bis die Welt für uns verbrennt und darüber hinaus, mein Liebster.

Außerdem möchte ich meinen Eltern von ganzem Herzen danken. Ihr habt die Grundpfeiler dafür gelegt, dass ich all dies erreichen konnte, seid immer für mich da und unterstützt mich ganz egal, welche Hürde sich mir entgegenstellt. Meiner Missis gebührt noch ein besonderer Dank für ihr hervorragendes Lektorat und unermüdliches Lesen meiner Doktorarbeit.

Herzlichen Dank an alle Leser und Kommentatoren meiner Doktorarbeit: Kojo, Doro, Alex, Haaga, Mailin und Angela. Insbesondere ist dabei Angela hervorzuheben, welche in einer atemberaubenden Geschwindigkeit meine Doktorarbeit kommentierte und in einer ungeahnten Teamarbeit mit meiner Missis großartige Arbeit geleistet hat.

Dorothea Dickmann und Philipp Schmidt möchte ich für das Lektorat meiner Doktorarbeit besonderen Dank zukommen lassen.

6 Lebenslauf

Persönliche Daten

Name:	Julia Marion Kaiser
Geburtsdatum:	15.08.1988
Geburtsort:	Malsch
Staatsangehörigkeit:	deutsch

Ausbildung und beruflicher Werdegang

02/2016-10/2019	Promotion an der Eberhard Karls Universität Tübingen, Mathematisch-Naturwissenschaftliche Fakultät, pharmazeutisches Institut, Lehrstuhl für Pharmakologie, Toxikologie und klinische Pharmazie, Prof. Dr. Gisela Drews
11/2014-11/2015	Pharmazeutin im Praktikum in der Bären Apotheke Tübingen, Herrenberg und Rottenburg 12/2015 3. Staatsexamen, Stuttgart
04/2010-09/2014	Studium der Pharmazie an der Eberhard Karls Universität Tübingen 09/2014 2.Staatsexamen, Tübingen 08/2012 1.Staatsexamen, Tübingen
09/2007-02/2010	Ausbildung zur Pharmazeutisch-Technischen Assistentin (PTA) an der Carl-Engler Schule, Karlsruhe 02/2010 Abschlussprüfung, Karlsruhe 08/2009-02/2010 PTA im Praktikum in der Stadtapotheke Kuppenheim

09/1999-07/2007 Schulbildung am Tulla-Gymnasium in Rastatt

07/2007 Abitur, Rastatt

7 Veröffentlichungen

S. Undank, J. Kaiser, J. Sikimic, M. Düfer, P. Krippeit-Drews, G. Drews (2017). Atrial Natriuretic Peptide Affects Stimulus-Secretion Coupling of Pancreatic β-Cells. Diabetes 66(11):2840-2848

C. Bauer, J. Kaiser, J. Sikimic, P. Krippeit-Drews, M. Düfer, G. Drews (2018). ATP mediates a negative autocrine signal on stimulus-secretion coupling in mouse pancreatic β-cells. Endocrine: 1-14

J. Maczewsky, J. Kaiser, A. Gresch, F. Gerst, M. Düfer, P. Krippeit-Drews, G. Drews (2018).
TGR5 Activation Promotes Stimulus-Secretion Coupling of Pancreatic β-Cells via a PKA-Dependent Pathway. Diabetes 68(2):324-336

8 Anhang

Liste der Manuskripte:

1. M-AG

J. Kaiser, P. Krippeit-Drews, G. Drews (2019)

Ghrelin Influences β-cell Function by Interference with K_{ATP}-Channels. Paper in preparation

2. M-ANP

S. Undank, J. Kaiser, J. Sikimic, M. Düfer, P. Krippeit-Drews, G. Drews (2017).

Atrial Natriuretic Peptide Affects Stimulus-Secretion Coupling of Pancreatic β-Cells. Diabetes 66(11):2840-2848

3. M-ATP

C. Bauer, J. Kaiser, J. Sikimic, P. Krippeit-Drews, M. Düfer, G. Drews (2018).

ATP mediates a negative autocrine signal on stimulus-secretion coupling in mouse pancreatic β-cells. Endocrine: 1-14

4. M-TGR5

J. Maczewsky, J. Kaiser, A. Gresch, F. Gerst, M. Düfer, P. Krippeit-Drews, G. Drews (2018).

TGR5 Activation Promotes Stimulus-Secretion Coupling of Pancreatic β-Cells via a PKA-Dependent Pathway. Diabetes 68(2):324-336

5. M-FXR

T. Hoffmeister, J. Kaiser, G. Drews, M. Düfer

Interactions between Atorvastatin and the Farnesoid X Receptor Impair Insulinotropic Effects of Bile Acids and Modulate Diabetogenic Risk. Submitted paper.

8.1 M-AG - Ghrelin influences β-cell function by interference with K_{ATP} channels

J. Kaiser, P. Krippeit-Drews, G. Drews

Institute of Pharmacy, Department of Pharmacology, University of Tübingen, Tübingen, Germany

Paper in preparation

Abstract

Objective Acyl-ghrelin (AG) is well known as a hunger-inducing hormone on hypothalamic neurons. Meanwhile it has become evident, that AG is produced in the pancreas as well and influences β-cell function. For many years it was well accepted that AG decreases glucose-stimulated insulin secretion (GSIS) via the growth hormone secretagogue receptor 1a (GHSR1a) coupled to the $G_{\alpha i}$/cAMP pathway which modulates TRPM2 channel activity. This assumption was recently challenged by the discovery of GHSR1a expression in δ-cells. Accordingly, AG induces the secretion of somatostatin which in turn, acts in a paracrine manner on β-cells and inhibits GSIS.

Aims This study aimed to further elucidate how AG interferes with β-cell function.

Methods Patch-clamp and fluorescence techniques and a radioimmune assay were used to determine the cytosolic Ca^{2+} concentration ($[Ca^{2+}]_c$), GSIS, and electrophysiological parameters in β-cells or islets of WT, SUR1-KO and Epac2-KO mice.

Results AG hyperpolarized the membrane potential and decreased $[Ca^{2+}]_c$ and GSIS at a stimulatory glucose concentration. These effects were abolished in β-cells and islets from SUR1-KO mice. AG had no influence on K_{ATP} single channel current in excised patches, but increased K_{ATP} current in a whole-cell configuration

with intact metabolism. Desacyl-ghrelin (DAG) counteracted the effects of AG. The influence of AG on the membrane potential and GSIS could only be averted in the combined presence of a GHSR1a antagonist and an inverse agonist. Furthermore, the inhibition of GSIS by AG could be prevented in the presence of db-cAMP or IBMX and with the somatostatin (SST) receptor 2-5 (SSTR2-5) antagonist H6056. SST did not mimic the effects of AG in β-cells of SUR1-KO mice.

Conclusion These data indicate that AG indirectly opens K_{ATP} channels probably by interference with the cAMP/PKA pathway resulting in a decrease of $[Ca^{2+}]_c$ and GSIS. The experiments with SUR1-KO β-cells point to a direct effect of AG on β-cells and not to an effect by AG-induced SST release from δ-cells. Nevertheless, SST receptors may be involved in the effect of AG, possibly by heteromerization of AG and SST receptors.

Introduction

The peptide hormone ghrelin (**gr**owth **h**ormone **rel**ease **in**ducing), discovered in 1999, is named after the observation that it stimulates growth hormone receptors. The active form is acylated ghrelin (acyl-ghrelin, AG). Meanwhile, it is well-known as an important orexigenic hormone, which is mainly produced in the X/A like cells within the oxyntic glands of the stomach (1, 2). The amino-acid precursor preproghrelin is cleaved into the peptides AG and obestatin, a pleiotropic peptide whose receptor is still unknown (3). The posttranslational acylation of AG with a fatty acid, preferably octanoic acid, occurs via the membrane-bound O-acyltransferase (MBOAT) ghrelin-O-acyltransferase (GOAT).

AG secretion plays a decisive role in the brain-gut axis and is dependent on the nutritional state. Plasma AG concentration rises before food intake and rapidly decreases postprandially. AG induces the secretion of the appetite stimulators e.g. agouti-related peptide (AgRP) and neuropeptide Y (NPY) which are expressed in neurons in the feeding center of the hypothalamus (4). Accordingly, changes in the AG concentration may be related to diseases such as obesity, type 2 diabetes (T2D) or Prader-Willi syndrome and interfering with its receptor may present an interesting therapeutic approach.

Soon after the discovery of AG it became evident that it is expressed in a distinct cell type of the pancreas, the so-called AG-expressing cells or ε-cells (5, 6). This discovery suggests a paracrine influence of AG on other pancreatic cell types.

Desacyl-ghrelin (DAG) is the degradation product of AG by desoctanoylation in plasma (7, 8). It is the most dominant isoform of AG in the plasma and was long time considered to be biologically inactive because of the missing evidence of DAG binding to GHSR1a at physiological concentrations. It is still questionable whether DAG is able to bind to the GHSR1a (9) or has its own, yet unknown receptor. However, studies revealed that the plasma DAG concentration is decreased in obese patient compared to normal-weight subjects, whereas the plasma AG concentration remains more or less unchanged shifting the DAG:AG ratio to higher values (10, 11). Moreover, DAG is able to antagonize the action of AG concerning its diabetogenic effects and detrimental action on insulin sensitivity (12-14). Accordingly, modulation of the DAG:AG ratio could be an interesting therapeutic approach.

The expression pattern of the receptor of AG, the growth hormone secretagogue receptor 1a (GHSR1a), is still a matter of debate, i.e. it is largely unclear by which receptors AG exerts its distinct effects in different tissues outside the hypothalamus. Dezaki and colleagues reported that AG diminished glucose-stimulated insulin secretion (GSIS) via binding on GHSR1a in β-cells. Instead of the well-established canonically $G_{\alpha q}$ signaling pathway known from other tissues, GHSR1a in β-cells is suggested to display an unique coupling to the $G_{\alpha i}$/cAMP pathway with subsequent modulation of ion channel activities including TRPM2 and K_v2.1 channels (15, 16). Park *et al.* concluded that the GHSR1a expressed in β-cells heterodimerizes with the somatostatin receptor 5 (SSTR5) and establishes a $G_{\alpha i}$- or $G_{\alpha q}$-coupled signaling pathway depending on the energy balance, or more precisely, the ratio of AG:SST (17). Recently, Adriannssen *et al.* and DiGruccio *et al.* postulated, by using transcriptomic profiling, that the GHSR1a is not expressed in β-cells but in δ-cells (18, 19). According to their hypothesis AG induces the secretion of somatostatin (SST) *via* binding to the canonically $G_{\alpha i}$-coupled GHSR1a receptor. Subsequently, SST binds to SSTRs in β-cells and inhibits GSIS. Consequently, AG does not modulate β-cell function directly, but *via* a paracrine

action mediated *via* SST. Taken together, the mode of action of AG remains contradictorily and not completely understood. This study has the objective to address these conflicts and clarify, how AG influences β-cell function as well as the role of DAG and the importance of GHSR1a in AG action.

Research Design and Methods

Animal and Islet Preparation

C57Bl/6N Wild type (WT), SUR1-KO and Epac2-KO mice with C57Bl/6N background were bred in the animal facility of the Department of Pharmacology at the University of Tübingen in Germany. The principles of laboratory animal care were followed (NIH publication No. 85-23, revised 1985) and the experiments were conducted according German laws. Isolation and culture were performed as previously described (20). Islets of Langerhans were dispersed to small cell clusters by trypsin treatment.

Solutions and Chemicals

Recordings of $[Ca^{2+}]_c$ and measurements of K_{ATP} current and membrane potential (V_m) in the perforated-patch configuration were performed with a bath solution that contained (in mM): 140 NaCl, 5 KCl, 1.2 $MgCl_2$, 2.5 $CaCl_2$, glucose as indicated, and 10 HEPES, pH 7.4, adjusted with NaOH.

Krebs-Ringer HEPES solution (KRH) for insulin secretion was composed of (in mM): 120 NaCl, 4.7 KCl, 1.1 MgCl2, 2.5 CaCl2, glucose as indicated, 10 HEPES, and 0.5% BSA, pH 7.4, adjusted with NaOH. For recording of cell-attached K_{ATP} current and V_m pipette solution consisted of (in mM): 10 KCl, 10 NaCl, 70 K_2SO_4, 4 $MgCl_2$, 2 $CaCl_2$, 10 EGTA, 20 HEPES, and amphotericin B (250 µg/mL), pH 7.15, adjusted with KOH.

Murine islets and islet cell clusters were cultured in RPMI 1640 (11.1 mM glucose) enriched with 10% FCS and 1% penicillin/streptomycin. For the patch-clamp recordings in the inside/out configuration ATP-containing and ATP-free bath solution was composed of (in mM): 130 KCl, 4.6 $CaCl_2$, 10 EDTA, and 20 HEPES with pH adjusted to 7.2 with KOH. Pipette solution for the inside/out configuration

contained (in mM) 130 KCl, 1.2 MgCl2, 2 CaCl2, 10 EGTA, and 10 HEPES, pH was adjusted to 7.4 with KOH.

Acyl-ghrelin (human) was obtained from Biomol (Hamburg, Germany). Desacyl-ghrelin (human) and K-(D1-NaI)-FwLL-NH_2 was purchased from Tocris Bioscience (Wiesbaden-Nordstadt, Germany), [D-Lys^3]-GHRP-6 and H6056 was from Bachem (Bubendorf, Switzerland). Fura-2 acetoxymethylester (Fura-2-AM) was ordered from Biotrend (Köln, Germany). RPMI 1640 medium, FCS, penicillin/streptomycin, and trypsin was from Invitrogen (Karlsruhe, Germany). All other chemicals were purchased from Sigma-Aldrich (Taufkirchen, Germany) or Carl Roth (Karlsruhe, Germany) in the purest form available.

Determination of $[Ca^{2+}]_c$

$[Ca^{2+}]_c$ was measured in β-cell clusters at 37°C after incubation with 5 µM fura-2 AM for 35 min. Fura-2 AM was excited alternately at 340 nm or 380 nm and emission filtered (LP515). $[Ca^{2+}]_c$ was calculated as the ratio of the emitted light at 340 nm and 380 nm, respectively. Emission was measured by a digital camera (Imago CCD; TILL phototonics). Equipment and software from TILL photonics and Visitron Systems, respectively, were used. To compare $[Ca^{2+}]_c$ under different experimental conditions, mean $[Ca^{2+}]_c$ was calculated for 15 min before solution change if not indicated otherwise.

Insulin secretion

Details for insulin secretion in steady-state incubations have been described previously (21). Isolated islets from WT mice were kept overnight in RPMI1640 culture medium with 11.1 mM glucose. Islets were incubated in batches of five in triplicate in 1 ml KRH with substances as indicated for 1 h at 37°C. For determination of the secreted insulin a radioimmune assay (RIA, Merck Millipore) was performed with rat insulin as standard.

Patch-clamp measurements

K_{ATP} whole-cell currents and single channel activity and V_m were recorded with an EPC-9 patch-clamp amplifier using Patchmaster software (HEKA, Lambrecht,

Germany). For measurements of $V_{m,}$ patch-clamp recordings were performed in the perforated-patch configuration in the current clamp mode at the holding current of 0 mA. For determination of V_m average plateau potential was evaluated 1 min before solution change. Action potential firing was determined by counting spikes 1 min before solution change. For determination of the K_{ATP} whole-cell current, pulses of 300 ms were performed every 15 s from the holding potential at -70 to -60 and -80 mV. The amplitude of currents elicited by voltage steps from the holding potential to -60 mV was taken for evaluation. Data of the last three pulses in each interval were averaged. Single channel activity was measured in the inside/out patch configuration at a holding potential of -50 mV. Under this condition K_{ATP} channel currents were about -4 pA, corresponding to a single-channel conductance of 80 pS. Inward currents are shown as downward deflections. For determination of mean current density, the current during the last 30 sec before solution change was evaluated. Patch pipettes were pulled from borosilicate glass capillaries (Harvard Apparatus, March-Hugstetten, Germany) and had a resistance of 6–8 MΩ for inside/out patch measurements and 2-5 MΩ for perforated-patch measurements, respectively.

Data evaluation and statistical analysis

Each series of experiments were performed with isolated islets of Langerhans or β-cell clusters from at least three independent preparations. Means ± SEM are given for the indicated number of experiments. For paired values statistical differences was assessed by Student´s t-test. ANOVA followed by Student-Newman-Keuls test was made for multiple comparisons. *P values* ≤ 0.05 were considered significant.

Results

AG negatively affects stimulus-secretion coupling (SSC) of pancreatic β-cells of WT mice

In pancreatic β-cells fluctuations of the membrane potential (V_m) govern oscillations in cytosolic Ca^{2+} concentration ($[Ca^{2+}]_c$) which finally trigger insulin secretion. To evaluate the effects of AG on SSC first $[Ca^{2+}]_c$ and V_m were determined. AG (10 nM) diminished typical glucose-stimulated oscillation of $[Ca^{2+}]_c$ at 10 mM glucose in

WT β-cells (Fig. 1A). The mean Ca^{2+} concentration determined as the fura-2 AM ratio (340 nm/380 nm) was decreased from 0.63 ± 0.03 under control conditions to 0.58 ± 0.03 in the presence of AG (Fig. 1B). This is due to the effect of AG on V_m. The addition of AG hyperpolarized V_m from -37.78 ± 2.12 mV in the presence of 10 mM glucose to -53.00 ± 2.61 mV with AG (Fig. 1C) and lowered action potential (AP) frequency from 40 ± 8.03 APs/min at 10 mM glucose to 6.44 ± 11.37 APs/min with AG (Fig. 1D). Consequently, AG attenuated steady-state GSIS at suprathreshold glucose concentration (10 mM glucose: 3.89 ± 0.8 ng insulin/(islet*h) *vs.* 10 mM glucose with AG: 3.01 ± 0.69 ng insulin/(islet*h)) (Fig. 1E). AG had no effect at a low or threshold glucose concentration (3 and 6 mM glucose, respectively) and shows a tendency to diminish secretion at 8 mM glucose, a concentration directly above the threshold. Overall, AG attenuated important parameters of SSC and thus exerted insulinostatic effects on pancreatic β-cells of WT mice.

DAG antagonizes the effect of AG on SSC in pancreatic β-cells

The metabolite DAG is the most dominant circulating form of AG in the plasma. DAG (20 nM) alone increased mean $[Ca^{2+}]_c$ from 0.69 ± 0.03 to 0.75 ± 0.03 and prevented the AG-induced decrease of $[Ca^{2+}]_c$. DAG had no impact on cell membrane potential. The addition of AG in the presence of DAG did not alter V_m (-44.50 ± 2.47 mV at 10 mM glucose *vs.* -45.50 ± 2.32 mV with DAG *vs.* -45.33 ± 2.06 mV with DAG + AG) (Fig. 2C, 2D).

DAG (10 and 20 nM) showed a tendency to increase steady-state GSIS in whole islets but this effect did not reach significance (1.83 ± 0.16 ng insulin/(islet*h) at 10 mM glucose *vs*. 2.10 ± 0.28 ng insulin/(islet*h) in the presence of 10 nM DAG and 2.23 ± 0.36 ng insulin/(islet*h) with 20 nM DAG, respectively) (Fig. 2E). The addition of AG in the presence of DAG did not affect GSIS (Fig. 2F) (2.62 ± 0.25 ng insulin/(islet*h) at 10 mM glucose and 2.33 ± 0.31 ng insulin/(islet*h) with DAG and AG), while AG alone elicited the above described inhibitory action. Taken together, the data point to an AG-counteracting effect of DAG in b-cells.

The effect of AG can be inhibited in the presence of an antagonist and an inverse agonist of the GHSR1a

The receptor of AG, GHSR1a, is not only expressed in the arcuate nucleus of the hypothalamus (22), but probably also in the pancreas (23), however, the data about the expression in the pancreas are conflicting. We used the peptidyl antagonist [D-Lys^3]-GHRP-6 to evaluate, whether the effect of AG is mediated *via* GHSR1a in β-cells. Measurements of $[Ca^{2+}]_c$ revealed that the $[Ca^{2+}]_c$-diminishing effect of AG was not averted in all experiments by [D-Lys^3]-GHRP-6 in β-cells of WT mice (Fig. 3A, 3B). [D-Lys^3]-GHRP-6 increased mean $[Ca^{2+}]_c$ from 0.64 ± 0.02 in the presence of 10 mM glucose to 0.69 ± 0.02 while the subsequent addition of AG decreased mean $[Ca^{2+}]_c$ to 0.65 ± 0.02. This dual effect was even more evident in cell membrane potential measurements (Fig. 3C): in 5 out of 10 recordings AG still hyperpolarized the membrane potential and decreased action potential frequency in the presence of the GHSR1a antagonist. In the summary of all experiments under this condition (Fig. 3D) [D-Lys^3]-GHRP-6 alone had no effect on V_m but AG elicited a significant hyperpolarization (-38.10 ± 1.58 mV at 10 mM glucose *vs.* -38.00 ± 1.61 mV with [D-Lys3]-GHRP-6 *vs*. -48.20 ± 3.51 mV with [D-Lys^3]-GHRP-6 + AG). These results were reproducible with the non-peptidyl GHSR1a antagonist YIL 781 (n=8, data not show) excluding a specific [D-Lys^3]-GHRP-6 phenomenon. We took into consideration that the GHSR1a exhibits a high constitutive activity, which is about 50% of the activity achieved by AG binding to the GHSR1a (24). The inverse agonist K-(D1-NaI)-FwLL-NH_2 stabilizes the inactive conformation of the GHSR1a but still allows AG to bind to the receptor (24, 25). Patch-clamp experiments revealed that K-(D1-NaI)-FwLL-NH_2 alone had no influence on V_m (n=6, data not shown). The combination of the inverse agonist and the peptidyl antagonist finally averted the effect of AG on V_m in every recording (-40.57 mV ± 2.72 at 10 mM glucose *vs.* -39 mV ± 3.32 with K-(D1-NaI)-FwLL-NH_2 and [D-Lys3]-GHRP-6 *vs.* -40.29 ± 3.01 mV with K-(D1-NaI)-FwLL-NH_2, D-Lys3]-GHRP-6 and AG). One typical recording of this series is shown in Fig. 3E and the summary of all data of this series in Fig. 3F. These results were reflected by the GSIS. As expected, AG attenuated GSIS in the presence of 10 mM glucose and

this reduction was only partially inhibited by the GHSR1a antagonist [D-Lys3]-GHRP-6 (Fig. 3G). A complete inhibition of the AG-effect on insulin secretion was achieved by the combination of the inverse agonist K-(D1-NaI)-FwLL-NH_2 and the GHSR1a antagonist [D-Lys3]-GHRP-6 (Fig. 3G).

These results underline the importance of the constitutive activity of the GHSR1a in the mode of action of AG, not only in tissues like the arcuate nucleus, but also in pancreatic β-cells.

AG shows no effect in b-cells and islets of SUR1-KO mice

The inwardly rectifying K_{ATP} channels play a crucial role in the SSC. They are only transported to the cell surface, if they are correctly assembled in the ER, consistent of four SUR1 and four Kir6.2 subunits (26). Therefore, mice lacking the ABCC8 gene, encoding the SUR1 subunit, have no functional K_{ATP} channels in b-cells (27). Interestingly, SUR1-KO mice react nearly physiologically to glucose stimuli, but show higher basal insulin secretion at low glucose concentration and slightly reduced insulin release at higher glucose concentration (28-30). Contrary to the results of AG in cell material from WT mice, AG did not alter $[Ca^{2+}]_c$ in β-cells isolated from SUR1-KO mice (Fig. 4 A,B). Determination of membrane potential revealed that AG slightly depolarized V_m from -37 ± 1.82 mV in the presence of 10 mM glucose to -34.56 ± 1.94 mV after addition of AG (Fig. 4C,D). AG had no influence on steady-state GSIS in whole islets of SUR1-KO mice (2.02 ± 0.35 ng insulin/(islet*h) at 10 mM glucose *vs*. 2.00 ± 0.268 ng insulin/(islet*h) with AG) (Fig. 4E). These results point to a K_{ATP} channel-modulated pathway of AG.

AG interacts indirectly with K_{ATP} channels

To elucidate if AG directly targets K_{ATP} channels, recordings with excised patches in the inside/out patch configuration were performed (Fig. 5A,B). As expected, K_{ATP} channels are open in the absence of ATP and closed by the addition of the nucleotide (0.1-1mM). The addition of AG in the presence of ATP did not open K_{ATP} channels and thus did not affect single channel activity (24.13 ± 8.22 pA without ATP *vs.* 1.11 ± 0.33 pA with ATP *vs.* 2.65 ± 1.14 pA with ATP and AG), which

excludes a direct interaction of AG with K_{ATP} channels. To evaluate, whether AG modulates K_{ATP} channel activity indirectly e.g. *via* second messenger pathways, we measured the current in the perforated-patch configuration. AG increased the current from 9.24 ± 1.86 pA under control conditions to 164.99 ± 24.05 pA with AG. The addition of the specific K_{ATP} channel inhibitor tolbutamide showed that the AG-provoked effect is not completely abolished (3.48 ± 0.63 pA under control conditions *vs.* 346.32 ± 47.87 pA with AG *vs.* 144.16 ± 35.06 pA with tolbutamide and AG) suggesting the activation of a sulfonylurea-resistant component by AG. Furthermore, the data indicate that AG rely on intact β-cell metabolism to be effective and is not able to alter K_{ATP} channel opening or single channel activity directly.

The potential influence of SST and SST-R

According to the hypothesis of Adriannssen *et al*. and DiGruccio *et al.* (18, 19), AG does not act on β-cells but on d-cells and SST mediates the AG effect by its paracrine influence on β-cells. Although our observation that K_{ATP} channels are critical for the action of AG does not support this theory, we repeated the $[Ca^{2+}]_c$ experiments shown in Fig. 4A, 4B with SST (10 nM) in β-cells of SUR1-KO mice (Fig. 6). In β-cell clusters, which exhibited a plateau phase, the addition of SST interrupted the plateau phase and showed ongoing oscillations of $[Ca^{2+}]_c$ (Fig. 6A). In β-cell clusters, which displayed oscillatory activity, SST led to a transient inhibition of the oscillations and decreased mean $[Ca^{2+}]_c$ from 0.47 ± 0.03 at 10 mM glucose to 0.39 ± 0.03 with SST in the first 5 min and to 0.42 ± 0.04 in the 5-20 min interval (Fig. 6B). Overall, 10 nM SST diminished $[Ca^{2+}]_c$ in β-cell clusters of SUR1-KO mice. This contrasts the findings with AG that does not affect $[Ca^{2+}]_c$ in β-cell clusters of SUR1-KO mice. This observation points to different modes of action of both hormones in β-cells.

H6056 is a specific antagonist for SSTR2 but can act as antagonist on SSTR2-5 when used in a higher concentration range, as in the following experiment. Unexpectedly, the inhibiting effect of AG on GSIS is abolished in the presence of

H6056 (Fig. 6C). This finding may exclude the participation of SST in the mode of action of AG but questions a possible involvement of the SSTRs.

AG inhibits GSIS via the cAMP/PKA pathway

The GHSR1a is a G-protein coupled receptor, canonically linked to $G_{\alpha q}$ such as in AgRP and NPY neurons. The binding of AG to GHSR1a activates PLC and therefore increases $[Ca^{2+}]_c$ (31-33). Hence, the $G_{\alpha q}$ pathway would rather result in an increase of GSIS instead of the observed reduction of insulin secretion. Dezakis and Kurashinas group presented evidence for the coupling of the GHSR1a to G_{ai} in β-cells and thus cAMP as a downstream target of AG (15, 16). To evaluate cAMP-dependent pathways we performed insulin secretion in the presence of the cAMP analogue db-cAMP as well as with the phosphodiesterase (PDE) inhibitor IBMX in isolated islets of WT mice. AG no longer decreased GSIS when a cAMP reduction is counteracted by excess cAMP due to addition of db-cAMP or IBMX (Fig. 7A,B). cAMP could influence β-cell function *via* a PKA-dependent pathway or a PKA-independent pathway, i.e. Epac (exchange protein activated directly by cAMP), whereas Epac2 represents the most abundant form in the pancreas (34). AG still diminished GSIS in isolated islets of Epac2-KO mice (Fig. 7C). Taken together, AG interacts with the amplifying cAMP pathway in a PKA-dependent manner by inhibition of adenylate cyclase which in turn decreases cAMP concentration and attenuates insulin secretion.

Discussion

AG exhibits insulinostatic effects via interaction with K_{ATP} channels in a PKA-dependent manner

We demonstrated with our $[Ca^{2+}]_c$ and V_m experiments performed with cell clusters from SUR1-KO mice and K_{ATP} current measurements with cells of WT mice that AG mediates its effect *via* K_{ATP}-channels. AG was not able to modulate K_{ATP} single channel activity in excised patches excluding a direct interaction of AG with K_{ATP}

channels. However, AG modulated K_{ATP} channels when second messenger pathways were active. The results of GSIS in the presence of the PDE inhibitor IBMX and the cAMP-analogue db-cAMP suggest that AG interferes with the amplifying cAMP pathway. This is supported by Dezaki *et al*., which postulated a PTX-sensitive pathway and observed a decrease in glucose-induced cAMP production with 10 nM AG in MIN6 cells as well as in isolated rat islets (15). PKA and Epac are downstream targets of cAMP, both present in b-cells. Our results suggest that the interference of AG is primarily PKA-dependent because AG attenuated GSIS in isolated islets of Epac2-KO mice. The diminution of cAMP due to inhibition of adenylate cyclase activity followed by decreased PKA activity probably accounts for the interaction of AG with K_{ATP} channels. Our current measurements in the presence of tolbutamide revealed that AG not only affects K_{ATP} channels but stimulates another current component. Dezaki and colleagues proposed that AG opens K_v channels and inhibits TRPM2 channels (16, 36). Regarding our experimental protocol, the involvement of voltage-dependent K_v channels in the AG effect on β-cells seems unlikely but does not exclude the participation of TRP channels or voltage-independent, Ca^{2+}-activated K^+ channels like SK4 channels.

The involvement of GHSR1a and SSTR in the mode of action of AG

Constitutive activity is well known as an intrinsic feature of many metabotropic receptors and peculiarly of GHSR1a. The GHSR1a displays a high basal activation of $G_{\alpha q}$ and PLC turnover in the absence of AG e.g. in the hypothalamus (24, 25). Dezaki *et al.* averted the AG-evoked diminution of $[Ca^{2+}]_c$ and decrease of blood glucose concentration by the sole use of the receptor antagonist [D-Lys^3]-GHRP-6 (37). At first sight, this is in accordance with our results of $[Ca^{2+}]_c$ measurements, whereas determination of GSIS and particularly V_m revealed, that the effect of AG cannot be completely blocked in the presence of a non-peptidyl or peptidyl GHSR1a antagonist alone (Fig. 3C, 3D, 3G). Our data clearly show that a complete block of the AG effects on different parameters of SSC can only be achieved by

suppressing the basal activity of the GHSR1a together with a receptor antagonist. The data prove that AG mediates its effects in β-cells by binding to GHSR1a.

Our data with the SSTR antagonist H6056 points to an involvement of SSTRs in the action of AG. There is conflicting evidence regarding the subtypes of SSTR expressed in murine β-cells. For many years it was well accepted that SSTR5 is the dominant subtype in mouse β-cells (38-40). However, transcriptomic profiling by DiGruccio *et al.* and Adriaenssens *et al.* revealed that SSTR3 is the most abundant subtype in β-cells. SSTR5 was hardly detected in these studies (18, 19). These results are supported by Rorsman and Ashcroft (41). The data about heteromerization of SSTR5 and GHSR1a in dependence of the AG:SST ratio published by Park and colleagues in 2012 provides a suitable model explaining the involvement of both receptors (17). According to this model SST and AG mediate regulation of β-cell function *via* energy-dependent heteromerization of the canonically $G_{\alpha q}$ coupled GHSR1a and the canonically $G_{\alpha i}$ coupled SSTR5. Under low energy conditions, the GHSR1a:SSTR5 heteromer provides the $G_{\alpha i}$ signaling, which explains the attenuation of GSIS by endogenous AG.

Evidence for direct action of AG on β-cells

According to the hypothesis of DiGruccio *et al*. and Adriaenssens *et al.* circulating AG binds to GHSR1a in δ-cells, promoting SST secretion which binds to SSTR3 in β-cells (18, 19). Our data revealed that SST but not AG affects $[Ca^{2+}]_c$ in β-cells isolated from SUR1-KO mice which speaks against an indirect effect of AG mediated by somatostatin released from δ-cells. Evidently, the effect of SST on β-cells, in contrast to that of AG, is not mediated by K_{ATP} channels. Our $[Ca^{2+}]_c$ experiments in SUR1-KO mice are in agreement with studies from Kailey *et al.* and Abel *et al.* who showed that SST still hyperpolarized membrane potential and abolished action potential firing in human β-cells and INS-1 cells in the presence of the K_{ATP} channel inhibitor tolbutamide (42, 43).

We cannot rule out that other endocrine cells, besides β-cells, remain in the cell clusters after trypsin treatment of isolated islets. Evidently, β-cells represent the

dominant cell population in islets of Langerhans, whereas δ-cells are only a minority (44, 45). It seems unlikely that δ-cells were present in every cell cluster under investigation, but the effects of AG were consistently observable. Apart from that, the group of Dezaki (15) and our workgroup could confirm that AG inhibits insulin secretion in MIN6 cells (n=5, data not shown), which also points to a β-cell specific interaction.

Taken together, we did not find evidence, that SST primarily contributes to the effect of AG, but cannot exclude, that GHSR1a is expressed in δ-cells as well and establishes the signaling cascade postulated by DiGruccio *et al.* and Adriaenssens *et al.*(18, 19).

The role of the DAG:AG ratio in the efficiency of AG

Degradation of AG to DAG by carboxypeptidase and butyrylcholinesterase occurs in the plasma (7, 8), so it is likely that AG is mainly to be accountable for influencing β-cell function in the endocrine pancreas. DAG alone did not exhibit noteworthy effects on SSC but averted respectively antagonized the influence of AG on $[Ca^{2+}]_c$, V_m and GSIS (Fig. 2A-D, 2F). So far, no specific DAG receptor is known. An antagonism of DAG *via* interaction with the GHSR1a was questioned in some studies, yet it was shown that DAG can act as an agonist on GHSR1a (9). Binding of DAG to the GHSR1a seems unlikely in a low concentration range but was observed at higher concentrations by Gauna and colleagues (9). The acylated fatty acid chain on the peptide seems to accelerates the binding to GHSR1a (46), which makes a possible interaction of DAG with this receptor questionable or just possible at higher concentration range, as proposed from Gauna and coworkers, while our observations would favor an antagonism of DAG in regard of the actions of AG. Our own observation clearly speak for an antagonism between AG and DAG also it remains unclear at which step of the signaling pathway this antagonism occurs. Evidently, the DAG:AG ratio plays an important role concerning insulin resistance and hyperglycemia (12). It is suggested, that obesity and T2D result in a relative DAG deficiency which decreases the DAG:AG ratio and favors the aforementioned pathophysiological conditions (10-12). These findings led to first

therapeutic approaches: AZP-531 (livoletide) is the first DAG analogue tested in a clinical phase 2b/3 study on food-related behavior in patients with Prader-Willi syndrome, a disease which is characterized with hyperphagia (47). In 2016, Allas and colleagues conducted a phase 1-2 study with AZP-531 in obese subjects and subjects with T2D as well which revealed that AZP-531 shows the tendency to be beneficial in subjects with impaired glucose tolerance (48).

In summary, to our knowledge, this is the first study showing the involvement of K_{ATP} channels in the action of ghrelin on SSC in b-cells. The effect is indirect, probably mediated by reduced PKA activity. Our data are in favor for a direct action of AG on b-cells and do not support the hypothesis that AG exerts an effect on b-cell function *via* SST release from d-cells. Nevertheless SSTRs may be involved in the effects of AG on b-cells via receptor heteromerization. Moreover, our data suggest an antagonism between AG and DAG.

Author´s contribution

J.K. researched data and wrote the manuscript; P.K.-D. contributed to the discussion and the study design. G.D. designed the study, wrote and edited the manuscript and contributed to the discussion.

Acknowledgments

We thank and are grateful to Isolde Breuning for her excellent technical assistance.

References

1. Kojima, M., H. Hosoda, Y. Date, M. Nakazato, H. Matsuo and K. Kangawa (1999). Ghrelin is a growth-hormone-releasing acylated peptide from stomach. Nature 402(6762): 656-660.

2. Date, Y., M. Kojima, H. Hosoda, A. Sawaguchi, M. S. Mondal, T. Suganuma, S. Matsukura, K. Kangawa and M. Nakazato (2000). Ghrelin, a novel growth hormone-releasing acylated peptide, is synthesized in a distinct endocrine cell type in the gastrointestinal tracts of rats and humans. Endocrinology 141(11): 4255-4261.

3. Green, B. D. and D. J. Grieve (2018). Biochemical properties and biological actions of obestatin and its relevence in type 2 diabetes. Peptides 100: 249-259.

4. Cowley, M. A., R. G. Smith, S. Diano, M. Tschöp, N. Pronchuk, K. L. Grove, C. J. Strasburger, M. Bidlingmaier, M. Esterman, M. L. Heiman, L. M. Garcia-Segura, E. A. Nillni, P. Mendez, M. J. Low, P. Sotonyi, J. M. Friedman, H. Liu, S. Pinto, W. F. Colmers, R. D. Cone and T. L. Horvath (2003). The distribution and mechanism of action of ghrelin in the CNS demonstrates a novel hypothalamic circuit regulating energy homeostasis. Neuron 37(4): 649-661.

5. Wierup, N., H. Svensson, H. Mulder and F. Sundler (2002). The ghrelin cell: a novel developmentally regulated islet cell in the human pancreas. Regul Pept 107(1-3): 63-69.

6. Heller, R. S., M. Jenny, P. Collombat, A. Mansouri, C. Tomasetto, O. D. Madsen, G. Mellitzer, G. Gradwohl and P. Serup (2005). Genetic determinants of pancreatic epsilon-cell development. Dev Biol 286(1): 217-224.

7. Schopfer, L. M., O. Lockridge and S. Brimijoin (2015). Pure human butyrylcholinesterase hydrolyzes octanoyl ghrelin to desacyl ghrelin. Gen Comp Endocrinol 224: 61-68.

8. De Vriese, C., F. Gregoire, R. Lema-Kisoka, M. Waelbroeck, P. Robberecht and C. Delporte (2004). Ghrelin degradation by serum and tissue homogenates: identification of the cleavage sites. Endocrinology 145(11): 4997-5005.

9. Gauna, C., B. van de Zande, A. van Kerkwijk, A. P. Themmen, A. J. van der Lely and P. J. Delhanty (2007). Unacylated ghrelin is not a functional antagonist but a full agonist of the type 1a growth hormone secretagogue receptor (GHS-R). Mol Cell Endocrinol 274(1-2): 30-34.

10. Barazzoni, R., M. Zanetti, C. Ferreira, P. Vinci, A. Pirulli, M. Mucci, F. Dore, M. Fonda, B. Ciocchi, L. Cattin and G. Guarnieri (2007). Relationships between desacylated and acylated ghrelin and insulin sensitivity in the metabolic syndrome. Journal of Clinical Endocrinology & Metabolism 92(10): 3935-3940.

11. Pacifico, L., E. Poggiogalle, F. Costantino, C. Anama, F. Ferraro, F. Chiarelli and C. Chiesa (2009). Acylated and nonacylated ghrelin levels and their associations with insulin resistance in obese and normal weight children with metabolic syndrome. European Journal of Endocrinology 161(6): 861-870.

12. Delhanty, P. J., S. J. Neggers and A. J. van der Lely (2014). Should we consider des-acyl ghrelin as a separate hormone and if so, what does it do? Front Horm Res 42: 163-174.

13. Broglio, F., C. Gottero, F. Prodam, C. Gauna, G. Muccioli, M. Papotti, T. Abribat, A. J. Van der Lely and E. Ghigo (2004). Non-acylated ghrelin counteracts the metabolic but not the neuroendocrine response to acylated ghrelin in humans. Journal of Clinical Endocrinology & Metabolism 89(6): 3062-3065.

14. Gauna, C., F. M. Meyler, J. A. Janssen, P. J. Delhanty, T. Abribat, P. van Koetsveld, L. J. Hofland, F. Broglio, E. Ghigo and A. J. van der Lely (2004). Administration of acylated ghrelin reduces insulin sensitivity, whereas the combination of acylated plus unacylated ghrelin strongly improves insulin sensitivity. J Clin Endocrinol Metab 89(10): 5035-5042.

15. Dezaki, K., B. Damdindorj, H. Sone, O. Dyachok, A. Tengholm, E. Gylfe, T. Kurashina, M. Yoshida, M. Kakei and T. Yada (2011). Ghrelin attenuates cAMP-PKA signaling to evoke insulinostatic cascade in islet beta-cells. Diabetes 60(9): 2315-2324.

16. Kurashina, T., K. Dezaki, M. Yoshida, R. Sukma Rita, K. Ito, M. Taguchi, R. Miura, M. Tominaga, S. Ishibashi, M. Kakei and T. Yada (2015). The beta-cell GHSR and downstream cAMP/TRPM2 signaling account for insulinostatic and glycemic effects of ghrelin. Sci Rep 5: 14041.

17. Park, S., H. Jiang, H. Zhang and R. G. Smith (2012). Modification of ghrelin receptor signaling by somatostatin receptor-5 regulates insulin release. Proc Natl Acad Sci U S A 109(46): 19003-19008.

18. DiGruccio, M. R., A. M. Mawla, C. J. Donaldson, G. M. Noguchi, J. Vaughan, C. Cowing-Zitron, T. van der Meulen and M. O. Huising (2016). Comprehensive alpha, beta and delta cell transcriptomes reveal that ghrelin selectively activates delta cells and promotes somatostatin release from pancreatic islets. Mol Metab 5(7): 449-458.

19. Adriaenssens, A. E., B. Svendsen, B. Y. Lam, G. S. Yeo, J. J. Holst, F. Reimann and F. M. Gribble (2016). Transcriptomic profiling of pancreatic alpha, beta and delta cell populations identifies delta cells as a principal target for ghrelin in mouse islets. Diabetologia 59(10): 2156-2165.

20. Gier, B., P. Krippeit-Drews, T. Sheiko, L. Aguilar-Bryan, J. Bryan, M. Düfer and G. Drews (2009). Suppression of KATP channel activity protects murine pancreatic beta cells against oxidative stress. J Clin Invest 119(11): 3246-3256.

21. Maczewsky, J., J. Sikimic, C. Bauer, P. Krippeit-Drews, C. Wolke, U. Lendeckel, W. Barthlen and G. Drews (2017). The LXR Ligand T0901317 Acutely Inhibits Insulin Secretion by Affecting Mitochondrial Metabolism. Endocrinology 158(7): 2145-2154.

22. Willesen, M. G., P. Kristensen and J. Romer (1999). Co-localization of growth hormone secretagogue receptor and NPY mRNA in the arcuate nucleus of the rat. Neuroendocrinology 70(5): 306-316.

23. Gnanapavan, S., B. Kola, S. A. Bustin, D. G. Morris, P. McGee, P. Fairclough, S. Bhattacharya, R. Carpenter, A. B. Grossman and M. Korbonits (2002). The tissue distribution of the mRNA of ghrelin and subtypes of its receptor, GHS-R, in humans. J Clin Endocrinol Metab 87(6): 2988.

24. Damian, M., J. Marie, J. P. Leyris, J. A. Fehrentz, P. Verdie, J. Martinez, J. L. Baneres and S. Mary (2012). High constitutive activity is an intrinsic feature of ghrelin receptor protein: a study with a functional monomeric GHS-R1a receptor reconstituted in lipid discs. J Biol Chem 287(6): 3630-3641.

25. Callaghan, B. and J. B. Furness (2014). Novel and conventional receptors for ghrelin, desacyl-ghrelin, and pharmacologically related compounds. Pharmacol Rev 66(4): 984-1001.

26. Zerangue, N., B. Schwappach, Y. N. Jan and L. Y. Jan (1999). A new ER trafficking signal regulates the subunit stoichiometry of plasma membrane K(ATP) channels. Neuron 22(3): 537-548.

27. Seghers, V., M. Nakazaki, F. DeMayo, L. Aguilar-Bryan and J. Bryan (2000). Sur1 knockout mice. A model for K(ATP) channel-independent regulation of insulin secretion. J Biol Chem 275(13): 9270-9277.

28. Shiota, C., O. Larsson, K. D. Shelton, M. Shiota, A. M. Efanov, M. Hoy, J. Lindner, S. Kooptiwut, L. Juntti-Berggren, J. Gromada, P. O. Berggren and M. A. Magnuson (2002). Sulfonylurea receptor type 1 knock-out mice have intact feeding-stimulated insulin secretion despite marked impairment in their response to glucose. J Biol Chem 277(40): 37176-37183.

29. Haspel, D., P. Krippeit-Drews, L. Aguilar-Bryan, J. Bryan, G. Drews and M. Düfer (2005). Crosstalk between membrane potential and cytosolic Ca2+ concentration in beta cells from Sur1-/- mice. Diabetologia 48(5): 913-921.

30. Nenquin, M., A. Szollosi, L. Aguilar-Bryan, J. Bryan and J. C. Henquin (2004). Both triggering and amplifying pathways contribute to fuel-induced insulin secretion in the absence of sulfonylurea receptor-1 in pancreatic beta-cells. J Biol Chem 279(31): 32316-32324.

31. Anderson, K. A., T. J. Ribar, F. Lin, P. K. Noeldner, M. F. Green, M. J. Muehlbauer, L. A. Witters, B. E. Kemp and A. R. Means (2008). Hypothalamic CaMKK2 contributes to the regulation of energy balance. Cell Metab 7(5): 377-388.

32. Hawley, S. A., D. A. Pan, K. J. Mustard, L. Ross, J. Bain, A. M. Edelman, B. G. Frenguelli and D. G. Hardie (2005). Calmodulin-dependent protein kinase kinase-beta is an alternative upstream kinase for AMP-activated protein kinase. Cell Metabolism 2(1): 9-19.

33. Date, Y., N. Murakami, M. Kojima, T. Kuroiwa, S. Matsukura, K. Kangawa and M. Nakazato (2000). Central effects of a novel acylated peptide, ghrelin, on growth hormone release in rats. Biochem Biophys Res Commun 275(2): 477-480.

34. Ueno, H., T. Shibasaki, T. Iwanaga, K. Takahashi, Y. Yokoyama, L. M. Liu, N. Yokoi, N. Ozaki, S. Matsukura, H. Yano and S. Seino (2001). Characterization of the gene EPAC2: Structure, chromosomal localization, tissue expression, and identification of the liver-specific isoform. Genomics 78(1-2): 91-98.

35. Tinker, A., Q. Aziz, Y. W. Li and M. Specterman (2018). ATP-Sensitive Potassium Channels and Their Physiological and Pathophysiological Roles. Comprehensive Physiology 8(4): 1463-1511.

36. Dezaki, K., M. Kakei and T. Yada (2007). Ghrelin uses G alpha(i2) and activates voltage-dependent K+ channels to attenuate glucose-induced Ca2+ signaling and insulin release in islet beta-cells - Novel signal transduction of ghrelin. Diabetes 56(9): 2319-2327.

37. Dezaki, K., H. Hosoda, M. Kakei, S. Hashiguchi, M. Watanabe, K. Kangawa and T. Yada (2004). Endogenous ghrelin in pancreatic islets restricts insulin release by attenuating Ca2+ signaling in beta-cells: implication in the glycemic control in rodents. Diabetes 53(12): 3142-3151.

38. Strowski, M. Z., M. Kohler, H. Y. Chen, M. E. Trumbauer, Z. Li, D. Szalkowski, S. Gopal-Truter, J. K. Fisher, J. M. Schaeffer, A. D. Blake, B. B. Zhang and H. A. Wilkinson (2003). Somatostatin receptor subtype 5 regulates insulin secretion and glucose homeostasis. Mol Endocrinol 17(1): 93-106.

39. Tirone, T. A., M. A. Norman, S. Moldovan, F. J. DeMayo, X. P. Wang and F. C. Brunicardi (2003). Pancreatic somatostatin inhibits insulin secretion via SSTR-5 in the isolated perfused mouse pancreas model. Pancreas 26(3): e67-73.

40. Wang, X. P., J. Yang, M. A. Norman, J. Magnusson, F. J. DeMayo and F. C. Brunicardi (2005). SSTR5 ablation in islet results in alterations in glucose homeostasis in mice. Febs Letters 579(14): 3107-3114.

41. Rorsman, P. and F. M. Ashcroft (2018). Pancreatic beta-Cell Electrical Activity and Insulin Secretion: Of Mice and Men. Physiol Rev 98(1): 117-214.

42. Abel, K. B., S. Lehr and S. Ullrich (1996). Adrenaline, not somatostatin-induced hyperpolarization is accompanied by a sustained inhibition of insulin secretion in INS-1 cells. Activation of sulphonylurea K-ATP(+) channels is not involved. Pflugers Archiv-European Journal of Physiology 432(1): 89-96.

43. Kailey, B., M. van de Bunt, S. Cheley, P. R. Johnson, P. E. MacDonald, A. L. Gloyn, P. Rorsman and M. Braun (2012). SSTR2 is the functionally dominant somatostatin receptor in human pancreatic beta- and alpha-cells. Am J Physiol Endocrinol Metab 303(9): E1107-1116.

44. Barg, S., J. Galvanovskis, S. O. Gopel, P. Rorsman and L. Eliasson (2000). Tight coupling between electrical activity and exocytosis in mouse glucagon-secreting alpha-cells. Diabetes 49(9): 1500-1510.

45. Cabrera, O., D. M. Berman, N. S. Kenyon, C. Ricordi, P. O. Berggren and A. Caicedo (2006). The unique cytoarchitecture of human pancreatic islets has implications for islet cell function. Proc Natl Acad Sci U S A 103(7): 2334-2339.

46. Hosoda, H., M. Kojima, T. Mizushima, S. Shimizu and K. Kangawa (2003). Structural divergence of human ghrelin. Identification of multiple ghrelin-derived molecules produced by post-translational processing. J Biol Chem 278(1): 64-70.

47. Allas, S., A. Caixas, C. Poitou, M. Coupaye, D. Thuilleaux, F. Lorenzini, G. Diene, A. Crino, F. Illouz, G. Grugni, D. Potvin, S. Bocchini, T. Delale, T. Abribat and M. Tauber (2018). AZP-531, an unacylated ghrelin analog, improves food-related behavior in patients with Prader-Willi syndrome: A randomized placebo-controlled trial. PLoS One 13(1): e0190849.

48. Allas, S., T. Delale, N. Ngo, M. Julien, P. Sahakian, J. Ritter, T. Abribat and A. J. van der Lely (2016). Safety, tolerability, pharmacokinetics and pharmacodynamics of AZP-531, a first-in-class analogue of unacylated ghrelin, in healthy and overweight/obese subjects and subjects with type 2 diabetes. Diabetes Obes Metab 18(9): 868-874.

49. Abegg, K., L. Bernasconi, M. Hutter, L. Whiting, C. Pietra, C. Giuliano, T. A. Lutz and T. Riediger (2017). Ghrelin receptor inverse agonists as a novel therapeutic approach against obesity-related metabolic disease. Diabetes Obes Metab 19(12): 1740-1750.

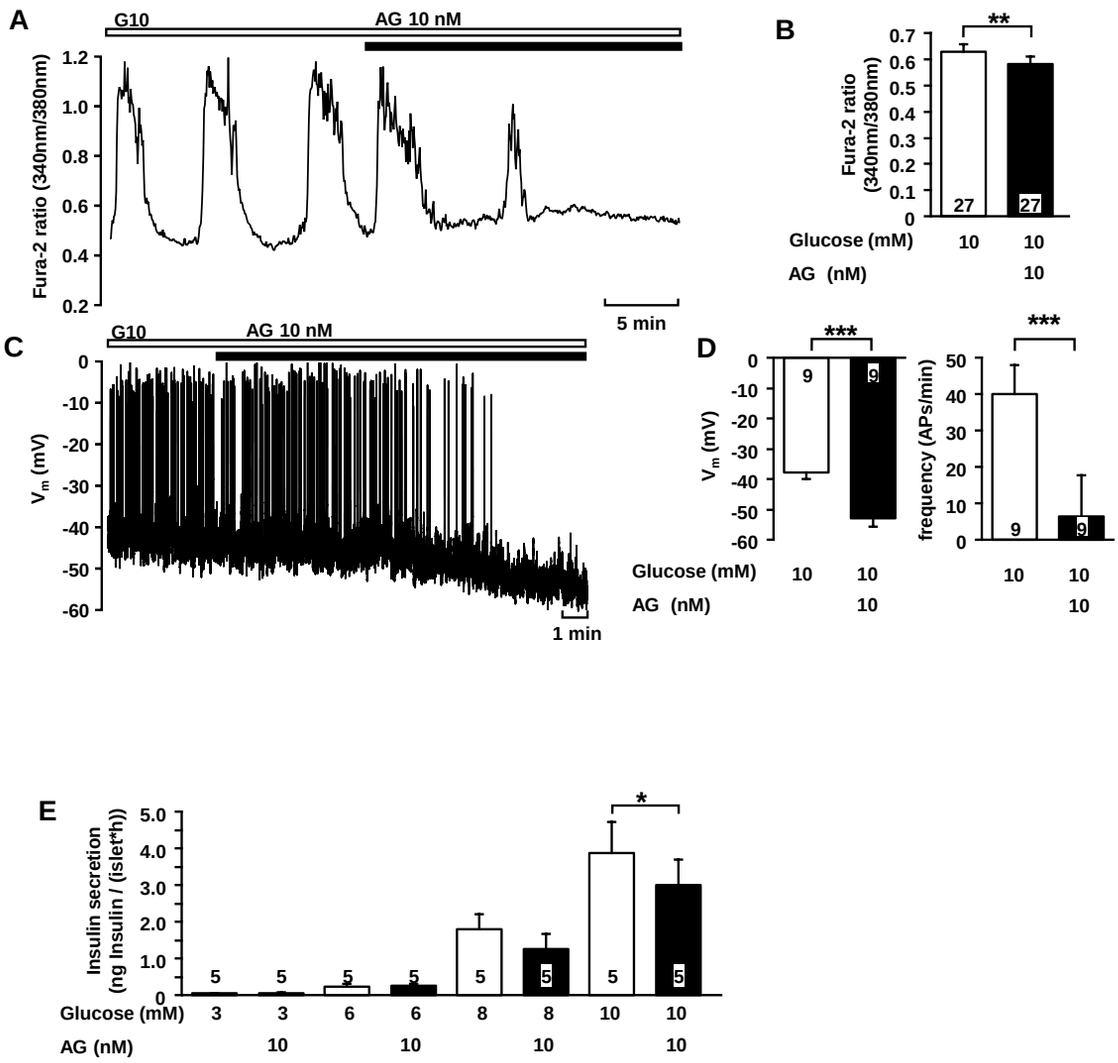

Fig. 1: AG exerts a negative impact on SSC of β-cells of WT mice

A) Representative measurement showing the inhibition of glucose-induced oscillations of $[Ca^{2+}]_c$ in β-cells of WT mice in the presence of AG at 10 mM glucose (G10). B) Summary of all experiment of this series. C) Representative measurement of the hyperpolarizing effect of AG on the membrane potential and the decrease in action potential frequency at 10 mM glucose in β-cells of WT mice. D) Summary of all experiments of this series. E) AG decreased GSIS under steady-state conditions in isolated islets of WT mice at suprathreshold glucose concentration. The numbers in the columns indicate the number of experiments with different β-cell clusters or isolated islets from at least 3 mice. **P ≤ 0.05; **P ≤ 0.01; ***P ≤ 0.001.*

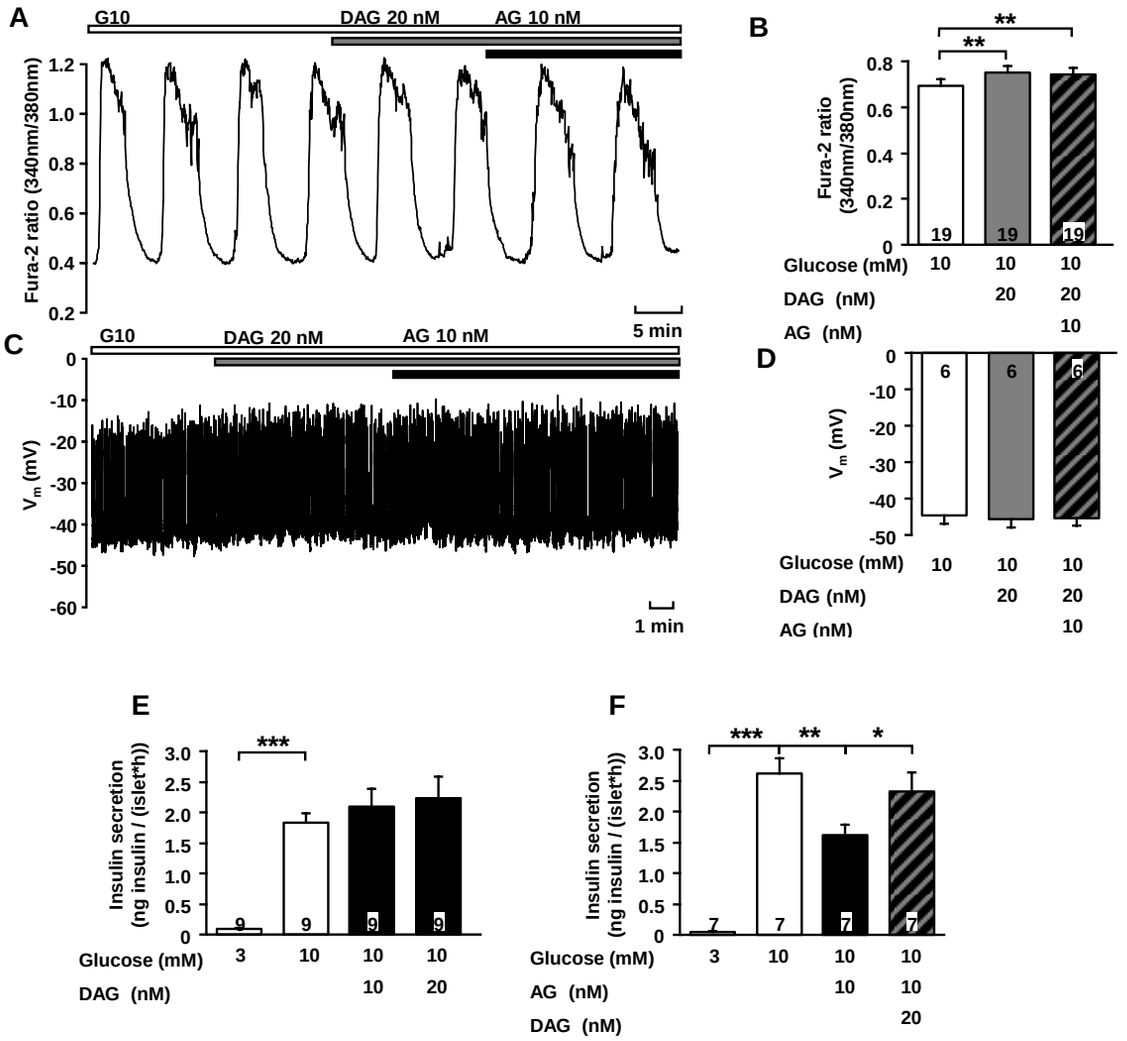

Fig. 2: DAG interferes with the effect of AG on β-cells

A) Representative measurement of glucose-induced oscillations of $[Ca^{2+}]_c$ in β-cells with DAG and AG. DAG alone did not affect glucose-induced oscillations of $[Ca^{2+}]_c$. In the presence of DAG, AG no longer decreased glucose-induced oscillations of $[Ca^{2+}]_c$, demonstrating the counteracting potential of DAG. B) Summary of all measurements of mean $[Ca^{2+}]_c$ with DAG and AG. C) Representative measurement of the effect of DAG and AG on membrane potential in the presence of 10 mM glucose (G10). DAG suppressed the AG-induced effects on membrane potential and action potential frequency. D) Summary of all experiments of the membrane potential series with DAG and AG. E) DAG tended to increase GSIS under steady-state conditions but did not alter GSIS significantly. F) In the presence of DAG, AG did not decrease GSIS in the presence of 10 mM glucose. The numbers in the columns indicate the number of experiments with different β-cell clusters or isolated islets from at least 3 mice. **P ≤ 0.05; **P ≤ 0.01; ***P ≤ 0.001.*

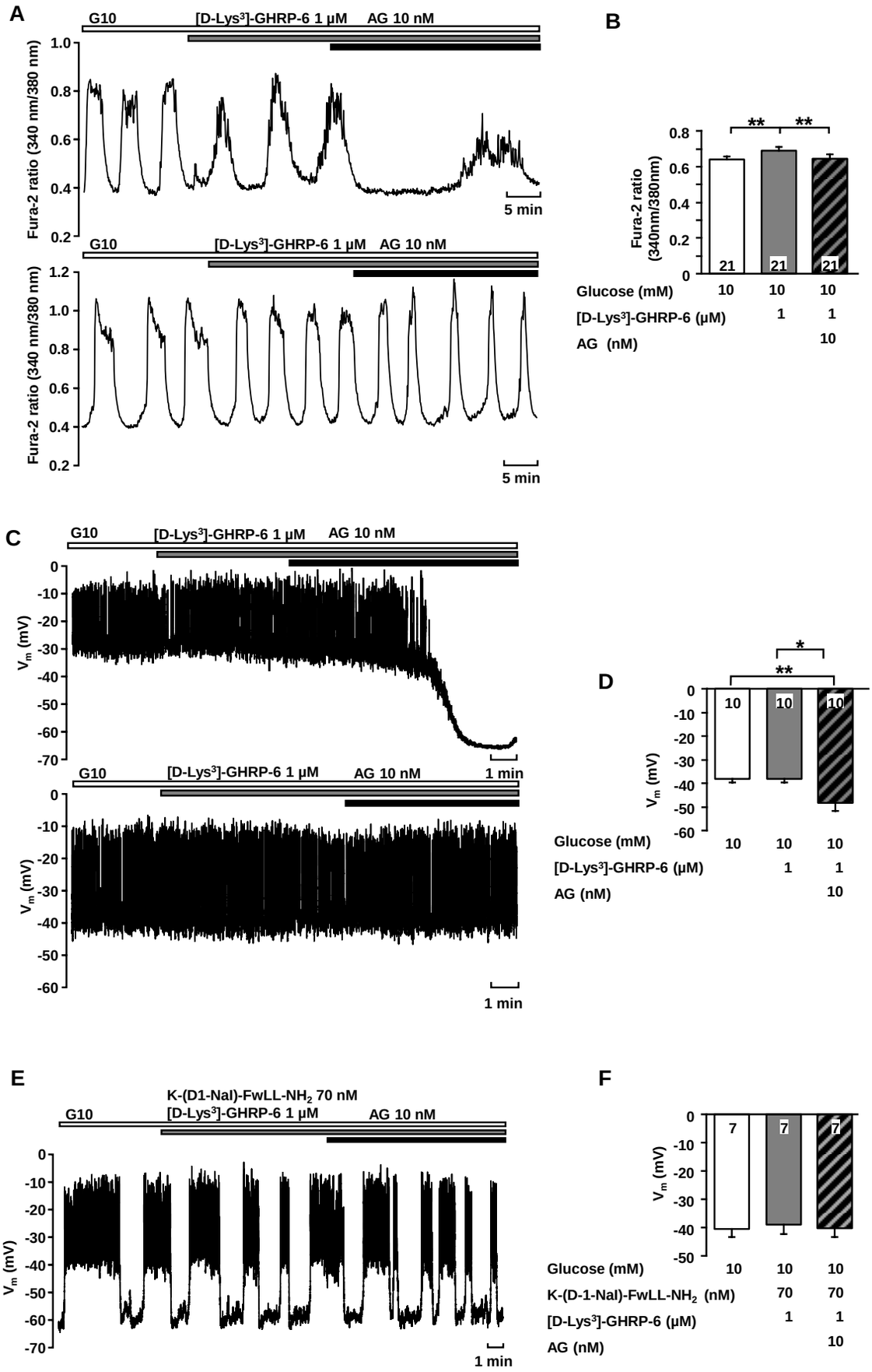
A
G10
[D-Lys³]-GHRP-6 1 µM
AG 10 nM
Fura-2 ratio (340 nm/380 nm)
5 min
B
Fura-2 ratio (340nm/380nm)
**
**
21
Glucose (mM)
[D-Lys³]-GHRP-6 (µM)
AG (nM)
C
Vm (mV)
1 min
D
*
**
10
E
K-(D1-Nal)-FwLL-NH2 70 nM
F
7
Glucose (mM)
K-(D-1-Nal)-FwLL-NH2 (nM)

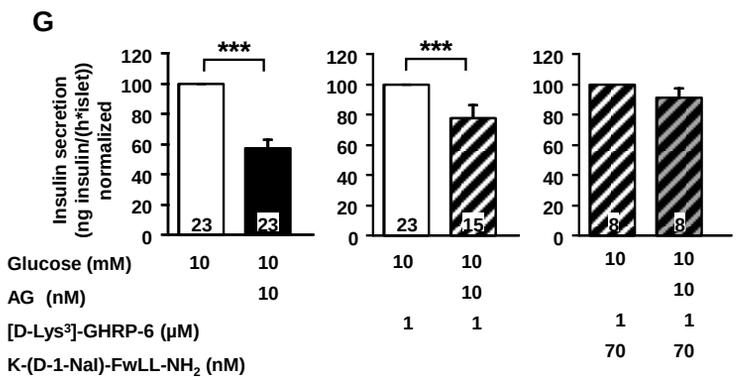

Fig. 3: The action of AG on SSC can be averted by a combination of an antagonist and an inverse agonist of the GHSR1a

A) Representative measurements of glucose-induced oscillations of $[Ca^{2+}]_c$ in the presence of [D-Lys^3]-GHRP-6 and AG in the presence of 10 mM glucose (G10). The inhibition of glucose-induced oscillations of $[Ca^{2+}]$ can occur even in the presence of the GHSR1a antagonist (8 out of 21 measurements). The GHSR1a antagonist [D-Lys3]-GHRP-6 alone is not sufficient to inhibit the effect of AG in every measurement of glucose-induced oscillations of $[Ca^{2+}]_c$. B) Summary of all experiment of this series with determination of $[Ca^{2+}]_c$. C) Representative measurements of the effect of [D-Lys^3]-GHRP-6 and AG on the membrane potential in the presence of 10 mM glucose. [D-Lys^3]-GHRP-6 itself did not affect the membrane potential and could inhibit the effect of AG in 5 out 10 measurements. D) Summary of all experiments of the membrane potential measurements with [D-Lys^3]-GHRP-6 and AG. E) Representative measurement of the effect of K-(D1-NaI)-FwLL-NH_2 as inverse agonist of the GHSR1a, [D-Lys^3]-GHRP-6 as antagonist of the GHSR1a and AG on the membrane potential at 10 mM glucose. F) Summary of all experiments of this series of V_m measurements. G) AG decreased GSIS significantly at G10. The addition of the GHSR1a antagonist [D-Lys^3]-GHRP-6 could not completely avert the effect of AG. The combination of K-(D1-NaI)-FwLL-NH_2 and [D-Lys^3]-GHRP-6 prevented the AG-evoked decrease of the GSIS at 10 mM glucose. The numbers in the columns indicate the number of experiments with different β-cell clusters or isolated islets from at least 3 mice. **P ≤ 0.05; **P ≤ 0.01; ***P ≤ 0.001*

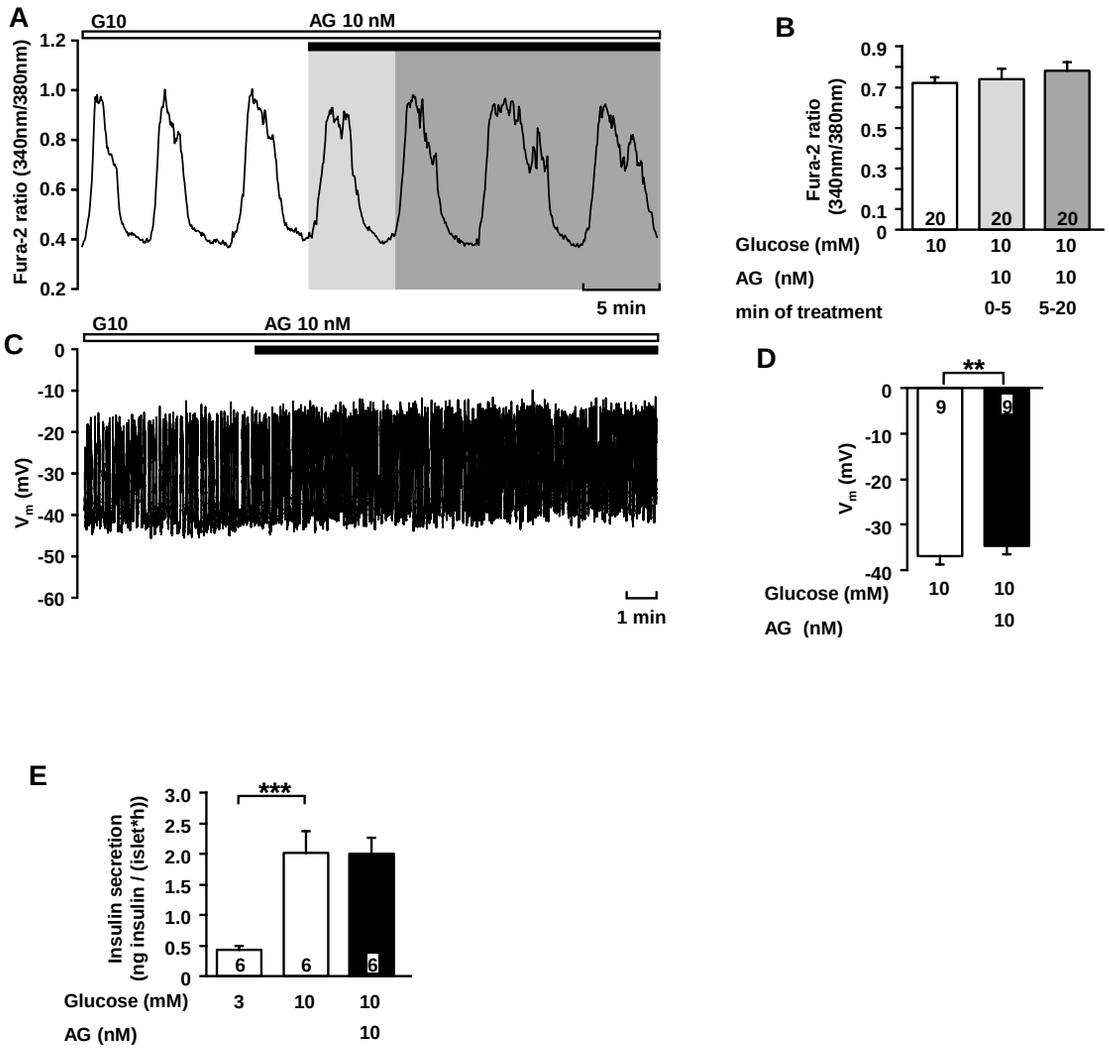

Fig. 4: The negative effect of AG on SSC is abolished in β-cells and isolated islets from SUR1-KO mice

A) Representative measurement of glucose-induced oscillations of $[Ca^{2+}]_c$ in β-cells of SUR1-KO mice in the presence of AG. AG had no significant effect. B) Summary of all experiments of measurements of mean $[Ca^{2+}]_c$ with AG in β-cells of SUR1-KO mice. C) Representative measurement of the effect of AG on membrane potential in the presence of 10 mM glucose (G10). AG slightly depolarized V_m. D) Summary of all experiments of membrane potential measurements with AG in β-cells of SUR1-KO mice. E) AG has no effect in GSIS in isolated islets of SUR1-KO mice at 10 mM glucose. The numbers in the columns indicate the number of experiments with different β-cell clusters or isolated islets from at least 3 mice. ***P ≤ 0.01; ***P ≤ 0.001.*

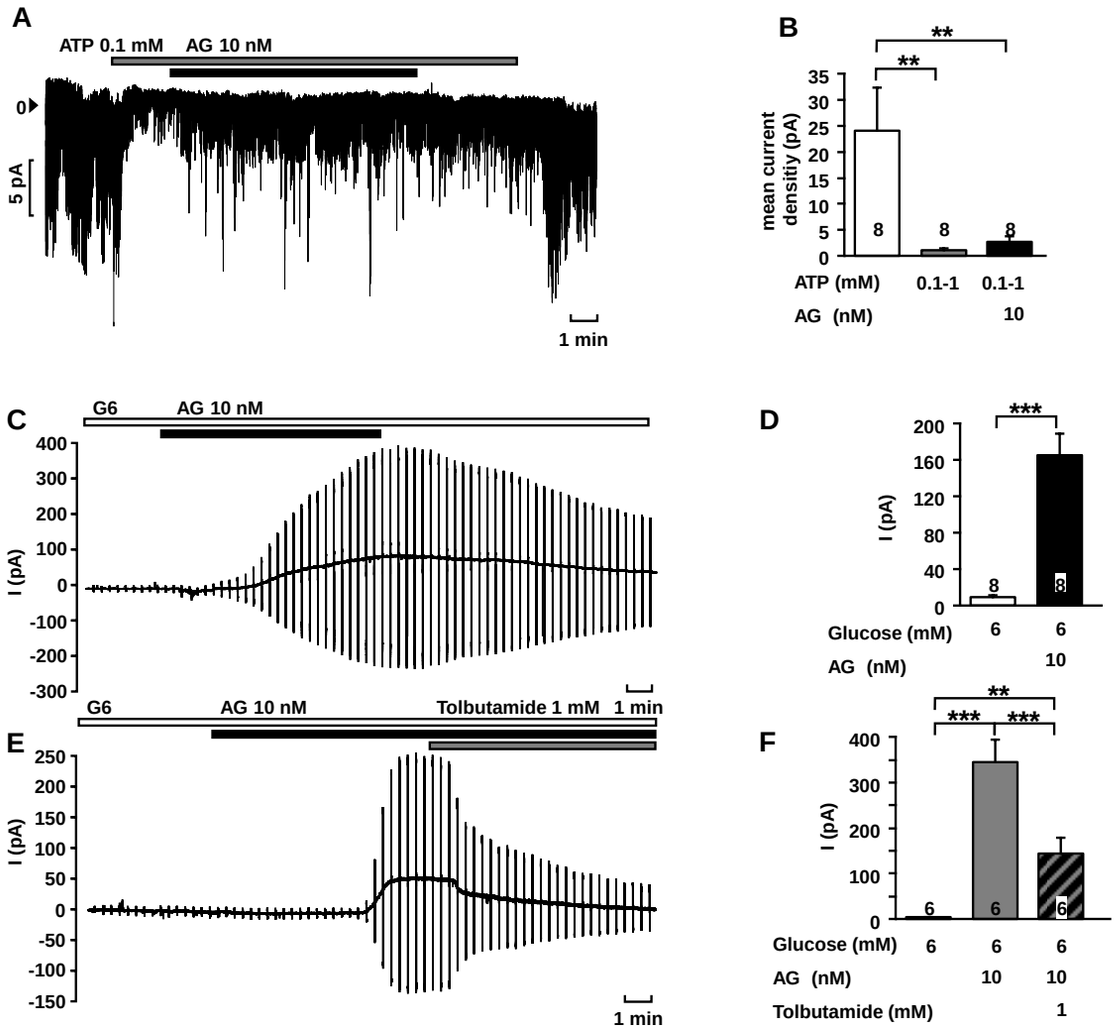

Fig. 5: AG modulates K_{ATP} channels indirectly

A) Representative measurement of K_{ATP} channel activity in the inside/out patch configuration in β-cells of WT mice. ATP closed most K_{ATP} channels. The addition of AG slightly increased current density but did not open K_{ATP} channels. B) Summary of all experiment performed under these conditions with AG and ATP in β-cells of WT mice. C) Representative measurement of K_{ATP} current in the perforated-patch configuration with AG in β-cells of WT mice. In the presence of 6 mM glucose (G6) most K_{ATP} channels are closed and therefore the K_{ATP} current is low. After application of AG the current increased. D) Summary of all experiments of this series with AG. E) Representative measurement of K_{ATP} current in the perforated-patch configuration with AG and tolbutamide. The AG-evoked increase of K_{ATP} current is partially diminished after application of tolbutamide. F) Summary of all experiments performed under this condition. The numbers in the columns indicate the number of experiments with different β-cell clusters from at least 3 mice. ***P ≤ 0.01; ***P ≤ 0.001*

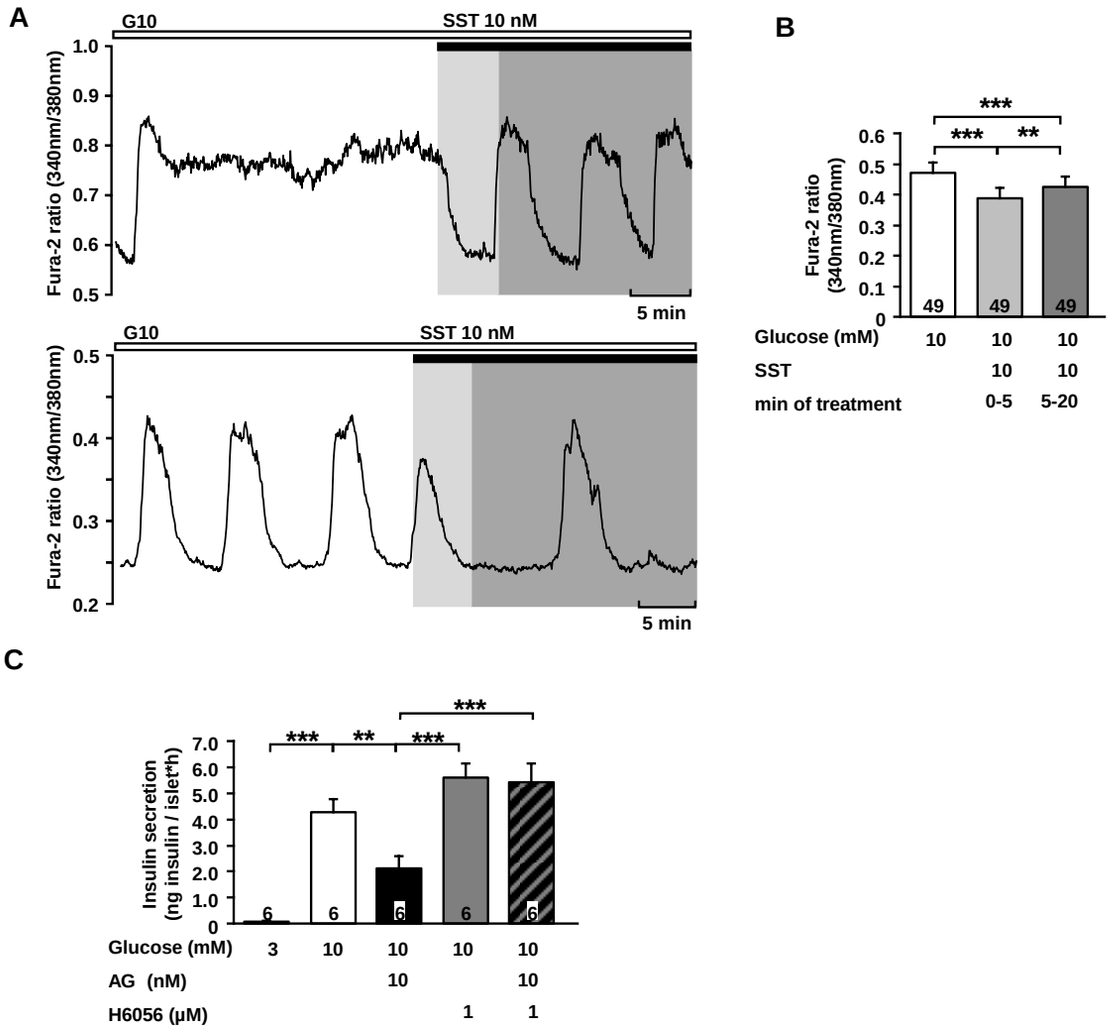

Fig. 6: The effect of AG is not mediated via SST, but possibly SSTR is involved

A) Representative measurement showing the attenuation of glucose-induced oscillations of $[Ca^{2+}]_c$ in β-cells of SUR1-KO by SST. B) Summary of all experiments of this series of measurements of mean $[Ca^{2+}]_c$ with SST in β-cells of SUR1-KO mice. The effect of SST was separately calculated for the intervals 0-5 min and 5-20 min. C) AG did not diminish GSIS in the presence of the SSTR2-5 antagonist H6056 in whole islets of WT mice. The numbers in the columns indicate the number of experiments with different β-cell clusters or isolated islets from at least 3 mice. ***P ≤ 0.01; ***P ≤ 0.001*

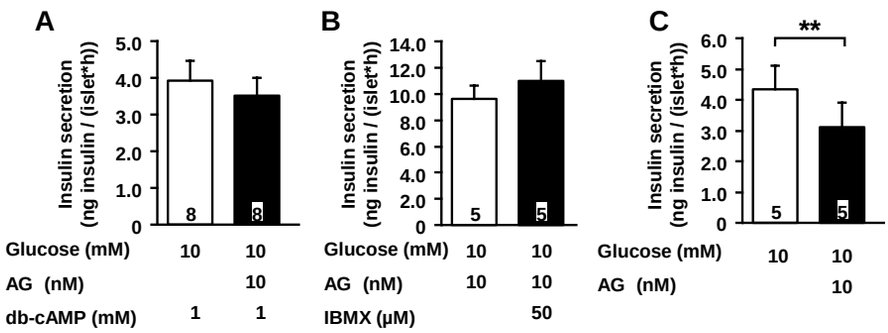

Fig. 7: AG modulates β-cell function via the cAMP/PKA pathway

A) AG did not alter GSIS in the presence of the cAMP-analogue db-cAMP in whole islets of WT mice in the presence of 10 mM glucose (G10). B) The PDE-inhibitor IBMX averted the GSIS-diminishing effect of AG at 10 mM glucose. C) AG decreased GSIS in whole islets of Epac2-KO mice at 10 mM glucose. The numbers in the columns indicate the number of experiments with isolated islets from at least 3 mice. ***P ≤ 0.01*

8.2 M-ANP - Atrial Natriuretic Peptide Affects Stimulus-Secretion Coupling of Pancreatic β-Cells

Sabrina Undank[1], Julia Kaiser[1], Jelena Sikimic[1], Martina Düfer[2], Peter Krippeit-Drews[1] and Gisela Drews[1]

[1]Institute of Pharmacy, Department of Pharmacology, University of Tübingen, Tübingen, Germany; [2]Department of Pharmaceutical and Medical Chemistry, University of Münster, Münster, Germany

Published: Diabetes 2017 Nov; 66(11): 2840-2848. doi: 10.2337/db17-0392

Abstract

Atrial natriuretic peptide (ANP) influences glucose homeostasis and possibly acts as a link between the cardiovascular system and metabolism, especially in metabolic disorders like diabetes. The current study evaluated effects of ANP on β-cell function by the use of a β-cell–specific knockout of the ANP receptor with guanylate cyclase activity (βGC-A-KO). ANP augmented insulin secretion at the threshold glucose concentration of 6 mmol/L and decreased K_{ATP} single-channel activity in β-cells of control mice but not of βGC-A-KO mice. In wild-type β-cells but not β-cells lacking functional K_{ATP} channels (SUR1-KO), ANP increased electrical activity, suggesting no involvement of other ion channels. At 6 mmol/L glucose, ANP readily elicited Ca^{2+} influx in control β-cells. This effect was blunted in β-cells of βGC-A-KO mice, and the maximal cytosolic Ca^{2+} concentration was lower. Experiments with inhibitors of protein kinase G (PKG), protein kinase A (PKA), phosphodiesterase 3B (PDE3B), and a membrane-permeable cyclic guanosine monophosphate (cGMP) analog on K_{ATP} channel activity and insulin secretion point to participation of the cGMP/PKG and cAMP/PKA/Epac (exchange protein directly activated by cAMP) directly activated by cAMP Epac pathways in the effects of ANP on β-cell function; the latter seems to prevail. Moreover, ANP potentiated the effect of glucagon-like peptide 1 (GLP-1) on glucose-induced insulin secretion, which could be caused by a cGMP-mediated inhibition of PDE3B, which in turn reduces cAMP degradation.

Introduction

ANP plays an important role in the regulation of blood volume and blood pressure (1). ANP also is involved in the regulation of food intake and lipid and glucose homeostasis. Cellular effects of ANP are mediated by a plasma membrane–associated receptor with guanylate cyclase activity (GC-A receptor). Thus, activation of the receptor results in an increased cyclic guanosine monophosphate (cGMP) concentration. GC-A receptors are expressed in murine β- and α-cells and in the insulin-secreting tumor cell line INS-1E (2). However, functional studies about effects of ANP on β-cells are controversial. In cultured mouse islets, ANP increases glucose-stimulated insulin secretion (GSIS), and the effect is suggested to be mediated by closure of K_{ATP} channels and an increase of the cytosolic Ca^{2+} concentration ($[Ca^{2+}]_c$) (3). In the current study, β-cells of a global GC-A receptor knockout mouse (GC-A-KO) have been used to investigate the link between this receptor and islet function. The interpretation of the data is somewhat limited because a global GC-A-KO can alter systemic parameters, including blood pressure and lipid and glucose homeostasis (e.g., through effects on insulin resistance), which can retroact on the functional status of β-cells before islet isolation. A weak insulinotropic effect also has been observed in perfused rat pancreas (4), and another study reported marked hypoglycemia after intravenous ANP infusion in rats (5). On the contrary, acute incubation of isolated rat islets with ANP did not influence insulin secretion (6,7), and long-term culture with ANP even inhibited insulin production and GSIS (7). In healthy male volunteers, infusion of ANP slightly elevated plasma insulin and moderately increased blood glucose concentrations (8–10). Taken together, the mode of action on pancreatic islets remains to be elucidated.

In vitro data with isolated islets and/or β-cells are sparse, and the experiments with ANP infusion are difficult to interpret because one cannot discriminate between effects on β-cells and effects on peripheral organs or blood flow. Long-term effects were studied in mouse models lacking the GC-A receptor; however, the data are inconsistent. Global homozygous GC-A receptor deletion has led to enhanced fasted blood glucose concentration, whereas glucose tolerance and insulin sensitivity remained unchanged in GC-A-KO mice after 12 weeks of high-fat or

standard diet compared with control mice (3). In contrast, mice with heterozygous receptor deletion that were not hypertensive developed impaired glucose tolerance after a high-fat diet (11). Humans with genetic variants predisposing to low plasma concentrations of ANP and brain natriuretic peptide (BNP) (mainly secreted by the heart) exhibit a high risk for the development of hypertension and heart hypertrophy (12,13). Epidemiological studies also found an association between low ANP (and BNP) plasma concentrations and obesity, insulin resistance, and the metabolic syndrome (14–16). According to the concept of Gruden et al. (17), the lack of the beneficial effects of the natriuretic peptides on adipose tissue, skeletal muscle, and β-cells promotes the development of type 2 diabetes. The current study takes advantage of a β-cell–specific GC-A-KO (βGC-A-KO) mouse to clarify the effects of ANP on stimulus-secretion coupling of β-cells.

Research Design and Methods

Mice

C57BL/6N mice (wild type [WT]) were bred in the animal facility of the Department of Pharmacology at the University of Tübingen in Germany. GC-A-KO mice and their WT littermates (*l*-WT) were provided by Dr. M. Kuhn (Physiological Department, University of Würzburg, Würzburg, Germany). As previously described (18), βGC-A-KO mice were generated by crossing rat insulin II promoter (RIP)-Cre mice (RIP-Cre founders of the Herrera strain) (19) with floxed GC-A mice of a C57BL/6/Sv129 background (20). Deletion of GC-A protein in islet cells was verified by immunohistochemistry (18). The Guide for the Care and Use of Laboratory Animals and German laws were followed.

Cell and Islet Preparation

The details for cell and islet preparation have been previously described (21). Briefly, collagenase was injected into the ductus pancreaticus, and exocrine tissue was digested for ~5 min. Islets were handpicked, and clusters/single cells were made by trypsin digestion of islets.

Solutions and Chemicals

Standard whole-cell and cell-attached recordings were done with a bath solution that contained (in mmol/L) 140 NaCl, 5 KCl, 1.2 $MgCl_2$, 2.5 $CaCl_2$, or 10 $CaCl_2$ (for measurements of membrane potential), glucose as indicated, and 10 HEPES, pH adjusted to 7.4 with NaOH. The same bath solution was used for the determination of $[Ca^{2+}]_c$ and the mitochondrial membrane potential ($\Delta\Psi$). The pipette solution for standard whole-cell measurements of K_{ATP} currents contained (in mmol/L) 130 KCl, 4 $MgCl_2$, 2 $CaCl_2$, 10 EGTA, 20 HEPES, and Na_2ATP as indicated, pH adjusted to 7.15 with KOH. For cell-attached recordings, the pipette solution contained (in mmol/L) 130 KCl, 1.2 $MgCl_2$, 2 $CaCl_2$, 10 EGTA, and 20 HEPES, pH adjusted to 7.4 with KOH. Cell membrane potential recordings were performed with amphotericin B (250 µg/mL) in the pipette solution, which contained (in mmol/L): 10 KCl, 10 NaCl, 70K_2SO_4, 4 $MgCl_2$, 2 $CaCl_2$, 10 EGTA, and 20 HEPES, pH adjusted to 7.15 with KOH. Fura-2 acetoxymethylester was obtained from Molecular Probes (Eugene, OR). RPMI1640 medium was from PromoCell (Heidelberg, Germany), penicillin/streptomycin from Gibco BRL (Karlsruhe, Germany), atrial natriuretic factor (1-28) (mouse, rabbit, rat) trifluoroacetate salt from Bachem (Weil am Rhein, Germany), Rp-8-Br-PET-cGMPS from Biolog (Bremen, Germany), and PKI 14-22 amide, myristoylated (myr-PKI) from Tocris Bioscience (Wiesbaden, Germany). All other chemicals were purchased from Sigma (Deisenhofen, Germany) or Merck (Darmstadt, Germany) in the purest form available.

Patch-Clamp Recordings

K_{ATP} currents and membrane potentials were recorded with an EPC-9 patch-clamp amplifier by using PATCHMASTER software (HEKA Elektronik, Lambrecht, Germany). Channel activity of the single channels was measured at the actual membrane potential in the cell-attached mode. Point-by-point analysis of the current traces reveals an open probability (P_o) owing to all active channels (N) in the patch and is thus presented as NP_o. Whole-cell K_{ATP} current was evoked by 300-ms voltage steps from −70 to −60 mV and −80 mV. Under these conditions, the current is completely blockable by K_{ATP} channel inhibitors (22).

Measurements of the Mitochondrial ΔΨ

Mitochondrial ΔΨ was measured as Rh123 fluorescence at 480-nm excitation wavelength as previously described (23).

Measurement of $[Ca^{2+}]_c$

Details have been previously described (21). In brief, cells were loaded with 5 µmol/L Fura-2 acetoxymethylester for 30 min at 37°C. Fluorescence was excited at a 340- and 380-nm wavelength, and fluorescence emission was filtered (LP515) and measured by a digital camera. $[Ca^{2+}]_c$ was calibrated in vitro by using Fura-2 pentapotassium salt (24).

Measurement of Insulin Secretion

Details for steady-state incubations have been previously described (21). For perifusions, 50 islets were placed in a bath chamber and perifused with 3 mmol/L glucose for 60 min before the beginning of the experiment. Samples for the determination of insulin were taken every 2 min.

Statistics

Each series of experiments was performed with islets or islet cells of at least three independent preparations. Mean ± SEM is given for the indicated number of experiments. Statistical significance of differences was assessed by Student *t* test for paired values. Multiple comparisons were made by ANOVA followed by Student-Newman-Keuls test. $P \leq 0.05$ was considered significant.

Results

ANP Increases Insulin Secretion and $[Ca^{2+}]_c$ at a Threshold Glucose Concentration

Insulin secretion of isolated mouse islets was measured in vitro to evaluate whether GC-A receptor stimulation by ANP results in changed insulin secretion. First, ANP was added in the second phase of insulin release after increasing the glucose concentration from 3 to 10 mmol/L (Fig. 1*A*). Under these conditions ANP

increased insulin secretion induced by 10 mmol/L glucose from 7.6 ± 1.2 to 8.7 ± 1.3 pg insulin/(islet · min) ($P \leq 0.001$) and insulin area under the curve (AUC) (Fig. 1*B*). For these experiments, islets from C57BL/6N mice (WT) were used. ANP effects at a threshold glucose concentration of 6 mmol/L were tested in steady-state incubation. In islets of *I*-WT, ANP significantly increased insulin secretion from 0.24 ± 0.06 to 0.33 ± 0.07 ng insulin/(islet · h) ($P \leq 0.05$), whereas it was ineffective in islets from βGC-A-KO mice [0.24 ± 0.04 vs. 0.23 ± 0.06 ng insulin/(islet · h)] (Fig. 1*C*). The stimulating effect of ANP also was absent in islets from SUR1-KO mice that lacked functional K_{ATP} channels (Supplementary Fig. 1*A*).

$[Ca^{2+}]_c$ was measured in the presence of 6 mmol/L glucose in islet cell clusters of *I*-WT and βGC-A-KO mice. In 6 mmol/L glucose, $[Ca^{2+}]_c$ was at basal values in most cells (i.e., no oscillations occurred). These cells with basal Ca^{2+} concentration were selected for investigation of the effect of ANP (Fig. 1*D*). Glucose at a concentration of 15 mmol/L was added at the end of each experiment to test whether cells were metabolically intact and thus able to show a response to ANP. Maximal $[Ca^{2+}]_c$ ($max[Ca^{2+}]_c$) before (basal) and after application of ANP was calculated for each of the 76 and 74 experiments performed with *I*-WT and βGC-A-KO cells, respectively. The mean of the $max[Ca^{2+}]_c$ is an indirect measure for the percentage of ANP-responsive cells because it mirrors the number of responsive cells (Fig. 1*E*). Figure 1*D* shows the typical response to ANP for cell clusters of each genotype. The summary of the data is shown in Fig. 1*E*. In *I*-WT β-cells, ANP increased $max[Ca^{2+}]_c$ from 68 ± 4 to 270 ± 33 nmol/L ($P \leq 0.001$). Switching to the bath solution with ANP also augmented $max[Ca^{2+}]_c$ in βGC-A-KO β-cells from 68 ± 4 to 135 ± 23 nmol/L ($P \leq 0.01$). This increase in the βGC-A-KO β-cells is significantly lower than that in the *I*-WT β-cells. Of note, the mean value for $max[Ca^{2+}]_c$ for βGC-A-KO cells in Fig. 1*E* is not 0, which may be a result of spontaneous Ca^{2+} transients occurring sporadically in single cells or small clusters after a change in bath solution from a stimulatory glucose concentration to a threshold concentration for induction of Ca^{2+} oscillations. To emphasize the significance of the data, we also calculated the percentage of cells for each of the three mouse preparations per genotype, which was 42 ± 12% for *I*-WT cells and 11 ± 5% for β-GC-A-KO

cells. Because of the high variability between days and the small and limited number of mice, this data evaluation was not statistically significant (*P* = 0.08).

ANP Decreases K_{ATP} Channel Activity in a GC-A Receptor–Dependent Manner

K_{ATP} channel activity was measured with β-cells from WT mice in the cell-attached mode in the presence of 0.5 mmol/L glucose to test whether ANP affects these channels. ANP at a concentration of 10 nmol/L reduced the NP_o from 100% under control conditions to 62 ± 10% (*P* ≤ 0.01) (Fig. 2*A* and *B*). Changes in K_{ATP} channel activity can be caused by altered mitochondrial metabolism (25). Therefore, the effects of ANP on the mitochondrial ΔΨ were measured, which can be taken to estimate mitochondrial ATP production (26). Neither in the presence of 15 mmol/L glucose nor in the presence of 4 mmol/L glucose did 10 nmol/L ANP alter ΔΨ (Supplementary Fig. 2). These data argue against an influence of ANP on ATP formation. To examine whether the GC-A receptor is involved in the inhibitory effect of ANP, β-cells from βGC-A-KO mice and *l*-WT mice were used. In *l*-WT β-cells, NP_o was reduced from 100% to 29 ± 11% (*P* ≤ 0.01) (Fig. 2*C* and *D*) upon addition of 10 nmol/L ANP. In contrast, ANP was without effect in βGC-A-KO β-cells (100% vs. 119 ± 15%) (Fig. 2*E* and *F*). In accordance with K_{ATP} single-channel current measurements, ANP increased the electrical activity of β-cells of WT mice. The fraction of plateau phase (FOPP), which is the percentage of time with spike activity, increased from 47 ± 5% to 65 ± 5% (*P* ≤ 0.05) (Fig. 3*A* and *B*). However, ANP did not change electrical activity in β-cells obtained from SUR1-KO mice (Fig. 3*C* and *D*). In these experiments, β-cells did not oscillate because the membrane potential is more depolarized in this genotype. Therefore, data were analyzed by determining the number of action potentials 2 min before change of the bath solution.

The global GC-A-KO leads to reduced expression of the K_{ATP} channel subunits SUR1 and Kir6.2 in β-cells (3). To elucidate a possible difference in K_{ATP} current density between the two genotypes, the maximal K_{ATP} current that developed after formation of the standard whole-cell configuration was measured without ATP in the patch pipette in *l*-WT (Fig. 4*A*) and βGC-A-KO β-cells (Fig. 4*B*). The data

revealed no difference in the K_{ATP} current density (21 ± 2 vs. 23 ± 1 pA/pF in *I*-WT and βGC-A-KO, respectively) (Fig. 4*C*).

Involvement of the cGMP/PKG and cAMP/PKA Pathways in the Effect of ANP in β-Cells

Because GCs synthesize the second messenger cGMP (27), we tested whether cGMP can mimic the effect of ANP on K_{ATP} channels. The membrane-permeable analog 8-Br-cGMP reduced NP_o of β-cells from *I*-WT mice in the cell-attached configuration from 100% to 72 ± 8% ($P \leq 0.05$) (Fig. 5*A* and *B*). Preincubation of the cells with the PKG inhibitor Rp-8 completely blunted the effect of ANP on K_{ATP} channel activity of β-cells from WT mice measured in the cell-attached configuration (100% vs. 110 ± 23%) (Fig. 5*C* and *D*), indicating the dependence of the effect of ANP on K_{ATP} channels on this protein kinase. However, ANP still increased insulin secretion in the presence of Rp-8 and 6 mmol/L glucose [0.14 ± 0.03 to 0.19 ± 0.03 ng insulin/(islet · h); $P \leq 0.05$] (Fig. 5*E*). Besides stimulating the PKG, cGMP can activate or inhibit various types of phosphodiesterases (PDEs) (28). With respect to insulin secretion, PDE3B is the most important PDE in β-cells (29), which is inhibited by cGMP (28). Because inhibition of PDE3B should inhibit the degradation of cAMP, cGMP and cAMP signaling pathways may converge on this PDE. Thus, ANP may affect the cAMP concentration and, consequently, insulin secretion by a PKA-dependent pathway. The specific PDE3B blocker cilostamide markedly increased insulin secretion in the presence of 10 mmol/L glucose, showing that this pathway is present in β-cells (Supplementary Fig. 3*A*). After inhibition of PDE3B by cilostamide, ANP no longer was able to increase insulin secretion (Supplementary Fig. 3*B*), pointing to a significant role of cAMP in the ANP effect on insulin secretion. Treatment of the cells with the PKA inhibitor myr-PKI did not suppress the inhibitory effect of ANP on K_{ATP} channel activity of β-cells from WT mice (85 ± 15% vs. 28 ± 12% with myr-PKI vs. with myr-PKI and ANP, respectively; $P \leq 0.01$) (Fig. 5*F* and *G*). Insulin secretion was not significantly enhanced by ANP in the presence of myr-PKI, but a tendency was discernible (Fig. 5*H*). Figure 6 demonstrates the well-known effect that glucagon-like peptide 1 (GLP-1) potentiates GSIS. Of note, Fig. 6 also shows that the action of GLP-1 on

secretion is augmented by 90-min preincubation of the cells with ANP [1.7 ± 0.2 vs. 2.3 ± 0.4 ng insulin/(islet · h) with GLP-1 vs. with GLP-1 and ANP, respectively; $P \leq 0.05$]. Ten-minute preincubation with ANP was ineffective [3.2 ± 0.4 vs. 3.2 ± 0.6 ng insulin/(islet · h); $n = 6$]; after 20 min preincubation, a tendency to increase the action of GLP-1 appeared [1.7 ± 0.4 vs. 2.0 ± 0.5 ng insulin/(islet · h); $n = 12$]. The potentiating action of ANP on the GLP-1 effect was absent in islets from SUR1-KO mice, pointing to a significant role of K_{ATP} channels in this intensification (Supplementary Fig. 1*B*). The potentiating effect is most likely a result of inhibition of the PDE3B by cGMP (see above) and increased cAMP concentration. It can be mimicked by cilostamide. Insulin secretion amounted to 1.6 ± 0.2 ng insulin/(islet · h) with GLP-1 alone versus 3.8 ± 0.2 ng insulin/(islet · h) with GLP-1 and cilostamide ($P \leq 0.001$) (Supplementary Fig. 3*A*).

Discussion

Effects of ANP at the Threshold Concentration of Glucose

An ANP-induced increase in insulin secretion was easier to detect at 6 mmol/L glucose, the threshold concentration for the induction of insulin secretion, than at 10 mmol/L glucose. Identical steady-state incubation experiments with 10 mmol/L glucose did not reveal a significant increase in insulin secretion (data not shown). However, with 10 mmol/L glucose, an effect of ANP could be detected in perifusion experiments. This kind of experiment allows discrimination between the effects of a drug on first and second phase of secretion. The results revealed an increase of GSIS by ANP in the second phase. Ropero et al. (3) showed an augmentation of insulin secretion by ANP in steady-state experiments in the presence of the threshold concentration of 7 mmol/L glucose but did not mention whether other glucose concentrations were tried. ANP seems to be less effective on insulin secretion than on other parameters of the stimulus-secretion coupling, which may be due to insulin secretion being measured with whole islets and, for example, membrane potential or $[Ca^{2+}]_c$ with dispersed cells. The capsule of connective tissue that surrounds the islets can restrain access of drugs to islet cells.

Therefore, one should keep in mind that in vivo ANP reaches the cells through the capillaries, not across the capsule.

The particular effectiveness of ANP at the threshold glucose concentration also is assessed with $[Ca^{2+}]_c$ measurements. ANP considerably increased max$[Ca^{2+}]_c$ above the basal values obtained at 6 mmol/L. The special physiological role of ANP in β-cells possibly augments GSIS in a coordinated action, with incretins at blood glucose concentrations occurring at the beginning of a meal. In humans with metabolic disorders, low plasma concentrations of ANP (14–16) may contribute to the impairment of insulin secretion in addition to a reduced incretin effect.

Involvement of the GC-A Receptor/cGMP/PKG Pathway in Effects of ANP on β-Cell Function

The patch-clamp data clearly demonstrate that ANP-mediated inhibition of K_{ATP} single-channel activity is caused by activation of GC-A receptors on β-cells because the effect is abolished in βGC-A-KO cells. K_{ATP} channel current density was the same in both genotypes, which contrasts findings in β-cells with a global GC-A-KO, showing diminished K_{ATP} channel activity and reduced expression of both K_{ATP} channel subunits compared with WT cells (3). The findings may explain the higher rate of insulin secretion in islets of the global GC-A receptor KO compared with WT islets, an effect not observed in the β-cell–specific KO model (Fig. 1*C*). As expected, the inhibitory effect of ANP on K_{ATP} channel activity was accompanied by a depolarization of the plasma membrane and an increase in $[Ca^{2+}]_c$ and insulin secretion attributable to GC-A activation. ANP did not affect membrane potentials of cells from SUR1-KO mice, suggesting that ANP does not influence the activity of other ion channels than K_{ATP} channels. Stimulation of GC-A receptors should result in an increase in the cGMP concentration. Dankworth (18) showed that the ANP-induced increase in cGMP is much higher in islets of *l*-WT mice than in those of βGC-A-KO mice. The inhibitory effect of ANP on K_{ATP} channels was mimicked by a membrane-permeable cGMP analog and completely blocked by the PKG inhibitor Rp-8, strongly suggesting the involvement of the GC-A/cGMP/PKG signaling pathway in the action of ANP on β-cell K_{ATP} channels (Fig.

7). This pathway also is proposed for the rapid action of estrogen (30) and the effect caused by small amounts of nitric oxide (31) on β-cell function. Which PKG is involved in this pathway in β-cells is unknown, and Rp-8 is not isoform specific. Because two studies exclude the expression of PKGI in β-cells (32,33), PKGII is the most likely candidate. Pancreatic K_{ATP} channels comprise SUR1 (sulfonylurea receptor) and Kir6.2 (inwardly rectifying K^+ channel) subunits. PKG is proposed to have dual effects in regulating SUR1/Kir6.2 channels: indirect activation of the channels by phosphorylation of cellular compounds not directly linked to K_{ATP} channels and inhibition by phosphorylation of channel proteins or tightly coupled proteins (34). In pancreatic β-cells, we, like Ropero et al. (35), found that the latter pathway seems to prevail. After preincubation with Rp-8, ANP still significantly augmented insulin secretion (Fig. 5*E*), which apparently contrasts with the patch-clamp data. Considering that cGMP inhibits the PDE3B (28), an increase in insulin secretion could be explained by increased cAMP concentration and activation of PKA (see below). The data even suggest that the cGMP/cAMP signaling pathway is more important for the final ANP effects on β-cell function than the cGMP/K_{ATP} pathway.

Effects of ANP on the cAMP Signaling Pathway

ANP can increase the cAMP concentration through GC-A receptor activation, cGMP formation, and inhibition of the PDE3B by reducing cAMP degradation. Inhibition of PKA did not influence the inhibitory effect of ANP on K_{ATP} channel activity, making a direct link between PKA and K_{ATP} channels unlikely (Fig. 5*F* and *G*). From these patch-clamp experiments, one would expect that ANP still activates insulin secretion when PKA is blocked. In our experiments, there was a tendency but no significant effect (Fig. 5*H*). However, PKA directly interferes with exocytosis (e.g., by increasing the Ca^{2+} sensitivity of the exocytotic machinery) (36). This effect may be alleviated by PKA inhibition. The experiments with cilostamide support the hypothesis that the increase of the cAMP concentration is an essential step in the action of ANP. In the presence of cilostamide, ANP did not enhance insulin secretion, most likely because PDE3B is fully inhibited and cAMP maximally increased under these conditions. The current data suggest that ANP augments

cAMP through cGMP-mediated inhibition of the PDE3B. cAMP activates the PKA, which influences exocytosis, and exchange protein activated by cAMP (Epac), which interferes with K_{ATP} channels by rendering them more sensitive to ATP (37) (Fig. 7). The cAMP/Epac/K_{ATP} pathway seems to be indispensable for the action of ANP on β-cell function and to prevail in the cAMP/PKA/exocytosis pathway because ANP did not increase insulin secretion in islets from SUR1-KO mice (Supplementary Fig. 1*A*). The cGMP/cAMP pathway is mediated by the ANP-induced activation of the GC-A receptor because ANP-induced augmentation of insulin secretion is completely blunted in islets from βGC-A-KO mice (Fig. 1*C*).

The incretin hormone GLP-1 increases insulin secretion by increasing the cAMP concentration. This effect is potentiated by preincubation with ANP. A significant potentiating effect was seen after 90 min of preincubation with ANP at room temperature. Twenty minutes of preincubation led at least to a tendency to potentiate the action of the incretin hormone. We assume that penetration through the capsule is slow (see above), especially at room temperature. Although we cannot entirely rule out a genomic effect for this potentiation, a cytosolic interaction of the hormones seems much more likely. The ANP/cGMP/PDE3B/cAMP pathway may also be involved in the additive effect of ANP and GLP-1 in β-cells. This assumption is confirmed by the observation that the PDE3B inhibitor cilostamide potentiates the GLP-1 effect on GSIS. Our hypothesis is in accordance with earlier findings. Overexpression of PDE3B in insulin-secreting rat insulinoma cells leads to a decrease of cAMP concentration and GSIS. Furthermore, the ability of GLP-1 to potentiate insulin secretion is impaired (38). Thus, we assume that ANP inhibits PDE3B, which leads to reduced degradation of cAMP and finally increases the effectiveness of GLP-1 (Fig. 7). Because this potentiation requires K_{ATP} channels, it is most likely mediated by the cAMP/Epac/K_{ATP} pathway.

In conclusion, the data point to a dual action of ANP in pancreatic β-cells (Fig. 7): *1*) ANP activates the GC-A/cGMP/PKG pathway wherein phosphorylation by PKG blocks K_{ATP} channels and *2*) ANP inhibits PDE3B and thus increases cAMP concentration, which positively influences insulin secretion through the PKA and

Epac pathway. The second pathway seems to be essential for ANP-mediated enhancement of insulin secretion.

Acknowledgments. The authors thank Isolde Breuning, Institute of Pharmacy, University of Tübingen, for excellent technical support. The authors thank Dr. Michaela Kuhn, Physiological Department, University of Würzburg for kindly providing the knockout mice and corresponding littermates.

Funding. This work was supported by Deutsche Forschungsgemeinschaft grant DR 225/9-1 (to G.D.).

Duality of Interest. No potential conflicts of interest relevant to this article were reported.

Author Contributions. S.U., J.K., and J.S. researched data. M.D. contributed to the discussion and study design and edited the manuscript. P.K.-D. evaluated data and edited the manuscript. G.D. designed the study, wrote and edited the manuscript, and contributed to the discussion. G.D. is the guarantor of this work and, as such, had full access to all the data in the study and takes responsibility for the integrity of the data and the accuracy of the data analysis.

References

1. Kuhn M. Molecular physiology of membrane guanylyl cyclase receptors. *Physiol Rev* 2016;96:751–804pmid:27030537

2. You H, Laychock SG. Atrial natriuretic peptide promotes pancreatic islet beta-cell growth and Akt/Foxo1a/cyclin D2 signaling. *Endocrinology* 2009;150:5455–5465pmid:19837876

3. Ropero AB, Soriano S, Tudurí E, et al. The atrial natriuretic peptide and guanylyl cyclase-A system modulates pancreatic beta-cell function. *Endocrinology* 2010;151:3665–3674pmid:20555029

4. Fehmann HC, Noll B, Göke R, Göke B, Trautmann ME, Arnold R. Atrial natriuretic factor has a weak insulinotropic action in the isolated perfused rat pancreas. *Res Exp Med (Berl)* 1990;190:253–258pmid:2145621

5. Carlsson PO, Andersson A, Jansson L. Cardiac natriuretic peptides and pancreatic islet blood flow in anesthetized rats. *Horm Metab Res* 2001;33:181–185pmid:11355754

6. Verspohl EJ, Ammon HP. Atrial natriuretic peptide (ANP) acts via specific binding sites on cGMP system of rat pancreatic islets without affecting insulin release. *Naunyn Schmiedebergs Arch Pharmacol* 1989;339:348–353pmid:2542810

7. You H, Laychock SG. Long-term treatment with atrial natriuretic peptide inhibits ATP production and insulin secretion in rat pancreatic islets. *Am J Physiol Endocrinol Metab* 2011;300:E435–E444pmid:20959527

8. Birkenfeld AL, Budziarek P, Boschmann M, et al. Atrial natriuretic peptide induces postprandial lipid oxidation in humans. *Diabetes* 2008;57:3199–3204pmid:18835931

9. Uehlinger DE, Weidmann P, Gnädinger MP, et al. Increase in circulating insulin induced by atrial natriuretic peptide in normal humans. *J Cardiovasc Pharmacol* 1986;8:1122–1129pmid:2434736

10. Birkenfeld AL, Boschmann M, Moro C, et al. Beta-adrenergic and atrial natriuretic peptide interactions on human cardiovascular and metabolic regulation. *J Clin Endocrinol Metab* 2006;91:5069–5075pmid:16984990

11. Miyashita K, Itoh H, Tsujimoto H, et al. Natriuretic peptides/cGMP/cGMP-dependent protein kinase cascades promote muscle mitochondrial biogenesis and prevent obesity. *Diabetes* 2009;58:2880–2892pmid:19690065

12. Kato N, Sugiyama T, Morita H, et al. Genetic analysis of the atrial natriuretic peptide gene in essential hypertension. *Clin Sci (Lond)* 2000;98:251–258pmid:10677382

13. Rubattu S, Bigatti G, Evangelista A, et al. Association of atrial natriuretic peptide and type a natriuretic peptide receptor gene polymorphisms with left ventricular mass in human essential hypertension. *J Am Coll Cardiol* 2006;48:499–505pmid:16875975

14. Das SR, Drazner MH, Dries DL, et al. Impact of body mass and body composition on circulating levels of natriuretic peptides: results from the Dallas Heart Study. Circulation 2005;112:2163–2168pmid:16203929

15. Khan AM, Cheng S, Magnusson M, et al. Cardiac natriuretic peptides, obesity, and insulin resistance: evidence from two community-based studies. J Clin Endocrinol Metab 2011;96:3242–3249pmid:21849523

16. Wang TJ, Larson MG, Levy D, et al. Impact of obesity on plasma natriuretic peptide levels. *Circulation* 2004;109:594–600pmid:14769680

17. Gruden G, Landi A, Bruno G. Natriuretic peptides, heart, and adipose tissue: new findings and future developments for diabetes research. *Diabetes Care* 2014;37:2899–2908pmid:25342830

18. Dankworth B. Charakterisierung der dynamischen Interaktion des Guanyl Cyclase-A (GC-A)-Rezeptors mit den Transient Receptor Potential Canonical Type 3 und Type 6 (TRPC3/C6)-Kanälen und Generierung von β-Zell-spezifischen GC-A-knockout-Mäusen sowie die Analyse der Bedeutung von ANP für die Insulin-Homöostase unter pathophysiologischen Bedingungen. Würzburg, Germany, University of Würzburg, 2013

19. Herrera PL. Adult insulin- and glucagon-producing cells differentiate from two independent cell lineages. *Development* 2000;127:2317–2322pmid:10804174

20. Holtwick R, Gotthardt M, Skryabin B, et al. Smooth muscle-selective deletion of guanylyl cyclase-A prevents the acute but not chronic effects of ANP on blood pressure. *Proc Natl Acad Sci U S A* 2002;99:7142–7147pmid:11997476

21. Gier B, Krippeit-Drews P, Sheiko T, et al. Suppression of KATP channel activity protects murine pancreatic beta cells against oxidative stress. *J Clin Invest* 2009;119:3246–3256pmid:19805912

22. Garrino MG, Plant TD, Henquin JC. Effects of putative activators of K+ channels in mouse pancreatic beta-cells. *Br J Pharmacol* 1989;98:957–965pmid:2531623

23. Edalat A, Schulte-Mecklenbeck P, Bauer C, et al. Mitochondrial succinate dehydrogenase is involved in stimulus-secretion coupling and endogenous ROS formation in murine beta cells. *Diabetologia* 2015;58:1532–1541pmid:25874444

24. Grynkiewicz G, Poenie M, Tsien RY. A new generation of Ca2+ indicators with greatly improved fluorescence properties. *J Biol Chem* 1985;260:3440–3450pmid:3838314

25. Drews G, Krippeit-Drews P, Düfer M. Electrophysiology of islet cells. In *Islets of Langerhans.* Vol. 1, 2nd ed. Islam MS, Ed. New York, Springer, 2015, p. 249–303

26. Krippeit-Drews P, Düfer M, Drews G. Parallel oscillations of intracellular calcium activity and mitochondrial membrane potential in mouse pancreatic B-cells. *Biochem Biophys Res Commun* 2000;267:179–183pmid:10623595

27. Kuhn M. Function and dysfunction of mammalian membrane guanylyl cyclase receptors: lessons from genetic mouse models and implications for human diseases. *Handb Exp Pharmacol* 2009;(191):47–69pmid:19089325

28. Potter LR, Abbey-Hosch S, Dickey DM. Natriuretic peptides, their receptors, and cyclic guanosine monophosphate-dependent signaling functions. *Endocr Rev* 2006;27:47–72pmid:16291870

29. Pyne NJ, Furman BL. Cyclic nucleotide phosphodiesterases in pancreatic islets. *Diabetologia* 2003;46:1179–1189pmid:12904862

30. Soriano S, Ropero AB, Alonso-Magdalena P, et al. Rapid regulation of K(ATP) channel activity by 17beta-estradiol in pancreatic beta-cells involves the estrogen receptor beta and the atrial natriuretic peptide receptor. *Mol Endocrinol* 2009;23:1973–1982pmid:19855088

31. Sunouchi T, Suzuki K, Nakayama K, Ishikawa T. Dual effect of nitric oxide on ATP-sensitive K+ channels in rat pancreatic beta cells. *Pflugers Arch* 2008;456:573–579pmid:18239934

32. Lutz SZ, Hennige AM, Feil S, et al. Genetic ablation of cGMP-dependent protein kinase type I causes liver inflammation and fasting hyperglycemia. *Diabetes* 2011;60:1566–1576pmid:21464444

33. Leiss V, Friebe A, Welling A, Hofmann F, Lukowski R. Cyclic GMP kinase I modulates glucagon release from pancreatic α-cells. *Diabetes* 2011;60:148–156pmid:20978093

34. Chai Y, Lin YF. Dual regulation of the ATP-sensitive potassium channel by activation of cGMP-dependent protein kinase. *Pflugers Arch* 2008;456:897–915pmid:18231807

35. Ropero AB, Fuentes E, Rovira JM, Ripoll C, Soria B, Nadal A. Non-genomic actions of 17beta-oestradiol in mouse pancreatic beta-cells are mediated by a cGMP-dependent protein kinase. *J Physiol* 1999;521:397–407pmid:10581311

36. Skelin M, Rupnik M. cAMP increases the sensitivity of exocytosis to Ca2+ primarily through protein kinase A in mouse pancreatic beta cells. *Cell Calcium* 2011;49:89–99pmid:21242000

37. Kang G, Leech CA, Chepurny OG, Coetzee WA, Holz GG. Role of the cAMP sensor Epac as a determinant of KATP channel ATP sensitivity in human pancreatic beta-cells and rat INS-1 cells. *J Physiol* 2008;586:1307–1319pmid:18202100

38. Härndahl L, Jing XJ, Ivarsson R, et al. Important role of phosphodiesterase 3B for the stimulatory action of cAMP on pancreatic beta-cell exocytosis and release of insulin. *J Biol Chem* 2002;277:37446–37455pmid:12169692

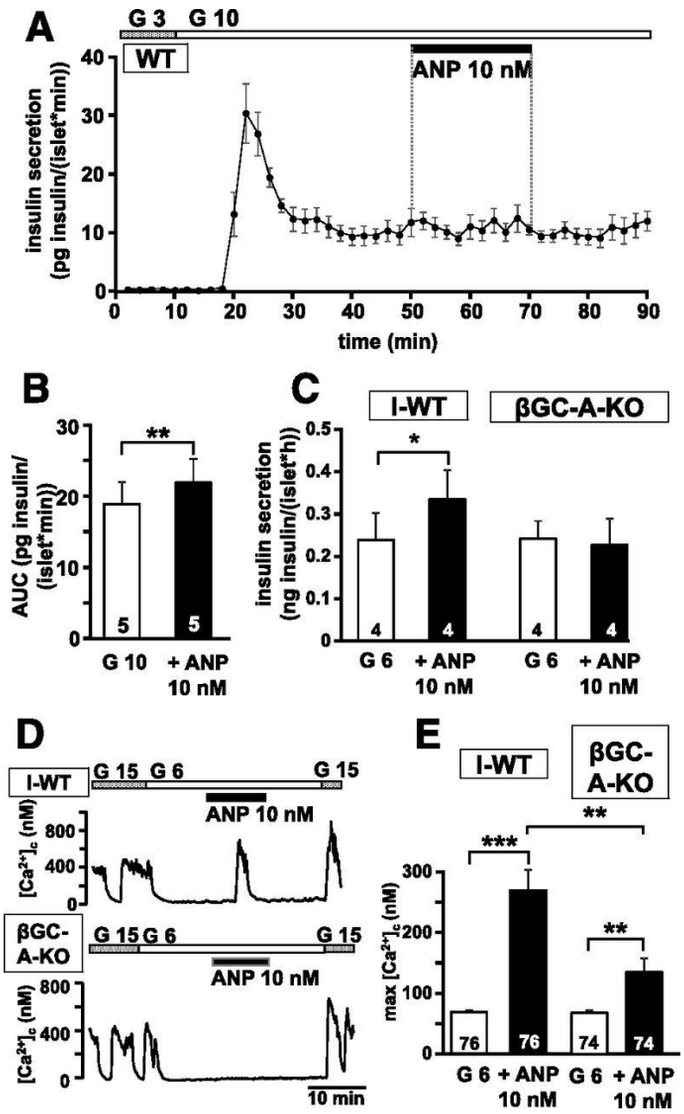

Fig. 1: Effects of ANP on insulin secretion and $[Ca^{2+}]_c$. *A*: Perifusion experiments with WT C57BL/6 islets showing the typical biphasic response of the insulin secretion after augmentation of the glucose concentration from 3 (G 3) to 10 mmol/L (G 10). ANP was added during the second phase as indicated. *B*: Evaluation of the AUCs, which were calculated between minutes 40 and 48 (control) and 60 and 68 (ANP application). *C*: Steady-state insulin secretion measurements at the threshold glucose concentration for the stimulation of insulin secretion with islets from *I*-WT and βGC-A-KO mice. *D*: Measurements of $[Ca^{2+}]_c$ at 6 mmol/L glucose (G 6). The top panel shows a typical recording for an *I*-WT β-cell, and the bottom panel shows a recording for a βGC-A-KO β-cell. Each experiment was started at 15 mmol/L glucose (G 15), where β-cells exhibit oscillations of $[Ca^{2+}]_c$. Lowering the glucose concentration to 6 mmol/L decreased $[Ca^{2+}]_c$ in most cells to basal values. Cells in which oscillations continued were discarded. *E*: Summary of the ANP-induced increase of $[Ca^{2+}]_c$ in *I*-WT and βGC-A-KO β-cells. The numbers within the columns in *B* and *C* are the number of different mice. The numbers within the columns in *E* are the number of different experiments with three different mice. **P* ≤ 0.05, ***P* ≤ 0.01, ****P* ≤ 0.001.

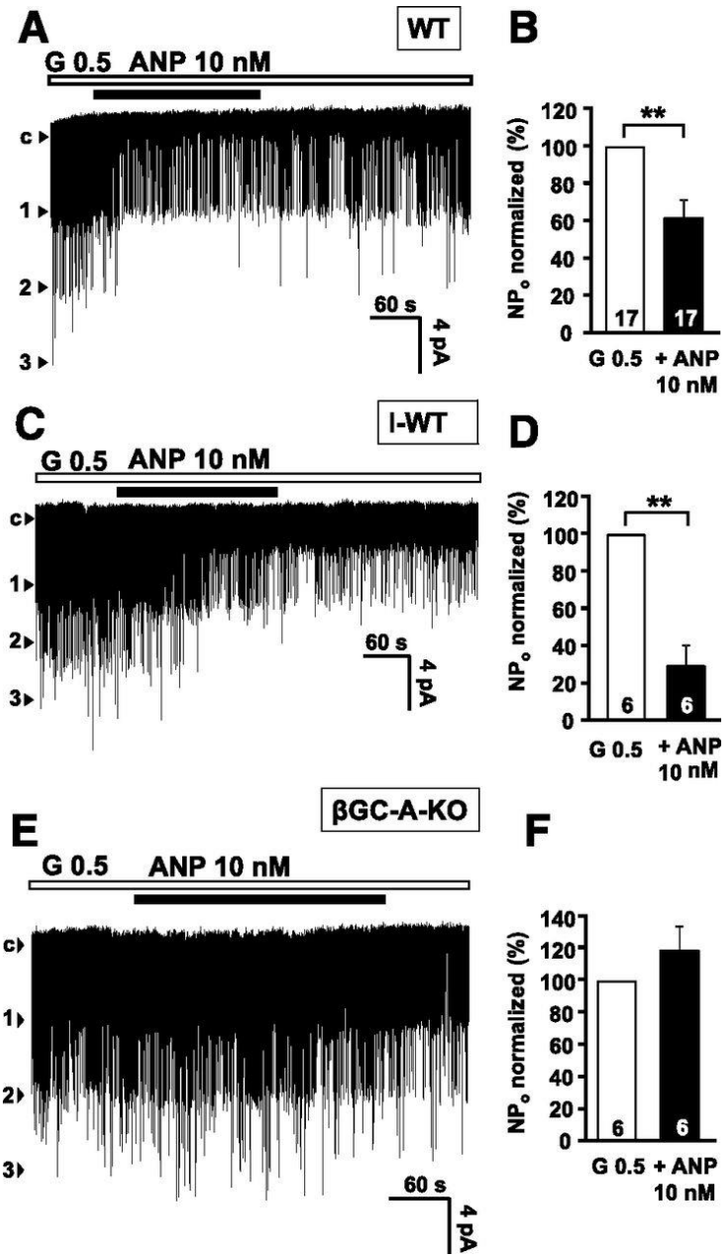

Fig. 2: Effects of ANP on NP_o of single K_{ATP} channels. *A*: Typical K_{ATP} single-channel recording of a WT β-cell in the cell-attached mode, demonstrating the effect of ANP application in the presence of 0.5 mmol/L glucose (G 0.5). *B*: Mean NP_o of all experiments conducted under this condition. NP_o before addition of ANP was normalized to 100%. *C* and *D*: Same experimental protocol with *I*-WT β-cells. *E* and *F*: Same experimental protocol with βGC-A-KO β-cells. The numbers within columns are the number of different cells used for the experiments. In each series, cells of at least three different mice were used. $^{**}P \leq 0.01$. c, closed state of the channel.

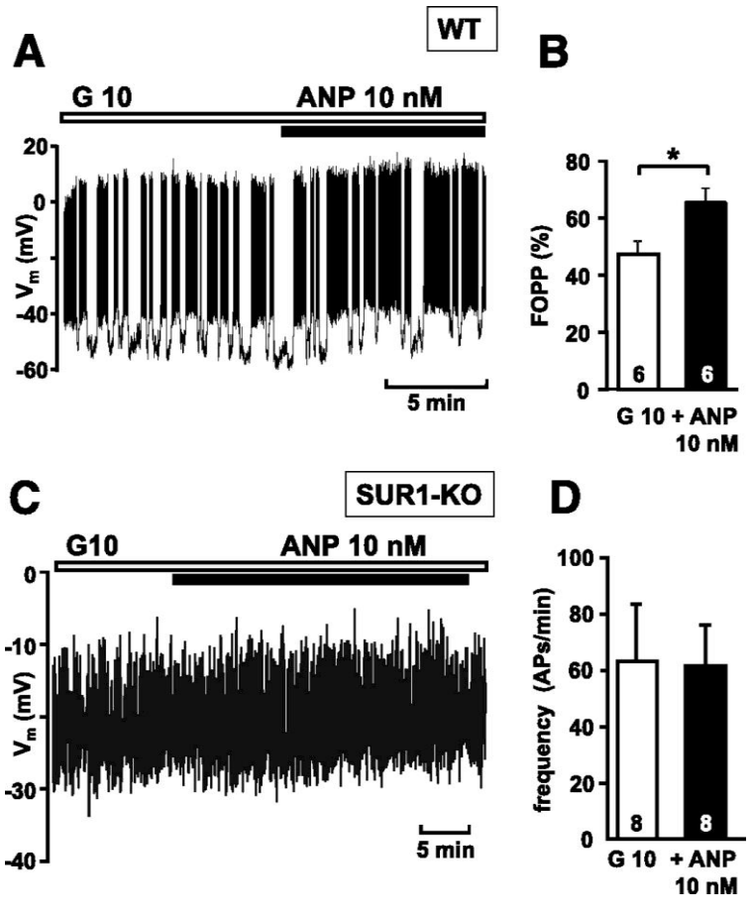

Fig. 3: Influence of ANP on the membrane potential (V_m) in cells from WT and SUR1-KO mice. *A*: Typical recording of V_m in the perforated-patch mode, showing the effect of ANP in the presence of 10 mmol/L glucose (G 10) in a WT β-cell. *B*: Calculation of the mean FOPP (percentage of time with spike activity) for all experiments conducted under this condition. *C*: Typical recording of V_m in the perforated-patch mode, showing the effect of ANP in the presence of G 10 in an SUR1-KO β-cell. *D*: Calculation of the number of action potentials (APs) during the 2 min before change of bath solution for all experiments conducted under this condition. The numbers within columns are the number of different cells used for the experiments. In each series, cells of at least three different mice were used. *$P \leq 0.05$.

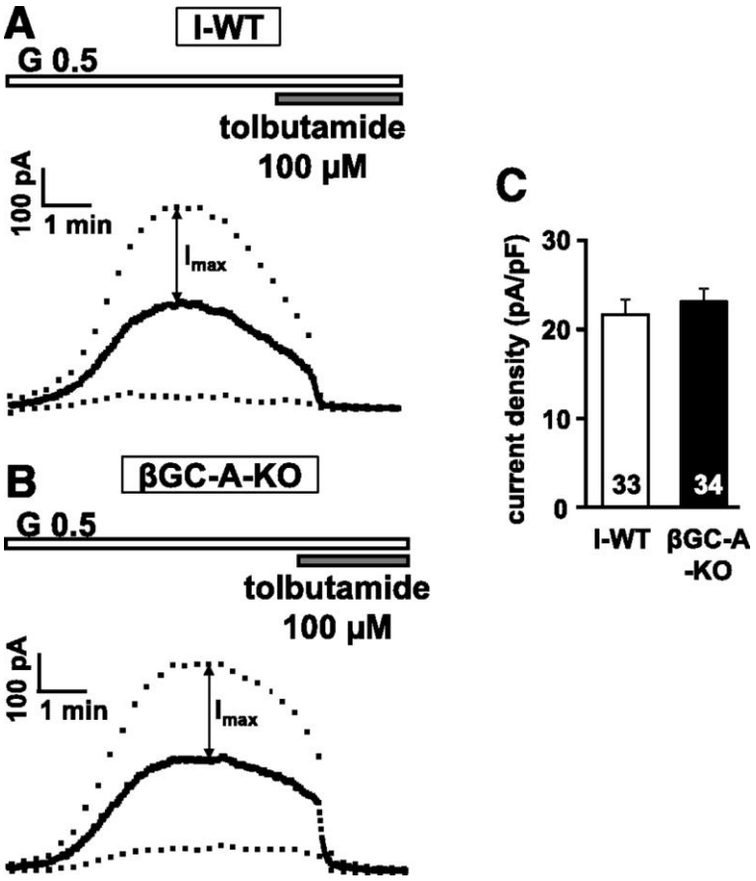

Fig. 4: Maximum K_{ATP} current density evoked by the washout of ATP in the standard whole-cell configuration. After gigaseal formation, the patch under the patch-pipette is ruptured, establishing the standard whole-cell configuration. The cell is dialyzed by the ATP-free pipette solution, completely removing ATP from the cytosol. Thus, the K_{ATP} current measured at −70 mV (solid line) or during voltage steps to −60 mV (upper dotted line) increased, whereas the current at −80 mV did not greatly change because this potential is close to the K^+ equilibrium potential. After a maximum, the current in ATP-free solution usually decreases as a result of an unspecific phenomenon called rundown. *A*: Typical recording from an *I*-WT β-cell. At the end of each experiment, tolbutamide was added to ensure that the entire current is sensitive to ATP. The current elicited by a voltage step from −70 to −60 mV was taken for evaluation. *B*: Typical recording from a βGC-A-KO β-cell. *C*: Summary of the results obtained by all experiments conducted with this protocol. Current density = current / cell capacitance. The numbers within columns are the number of different cells used for the experiments. In each series, cells of at least three different mice were used. G 0.5, 0.5 mmol/L glucose.

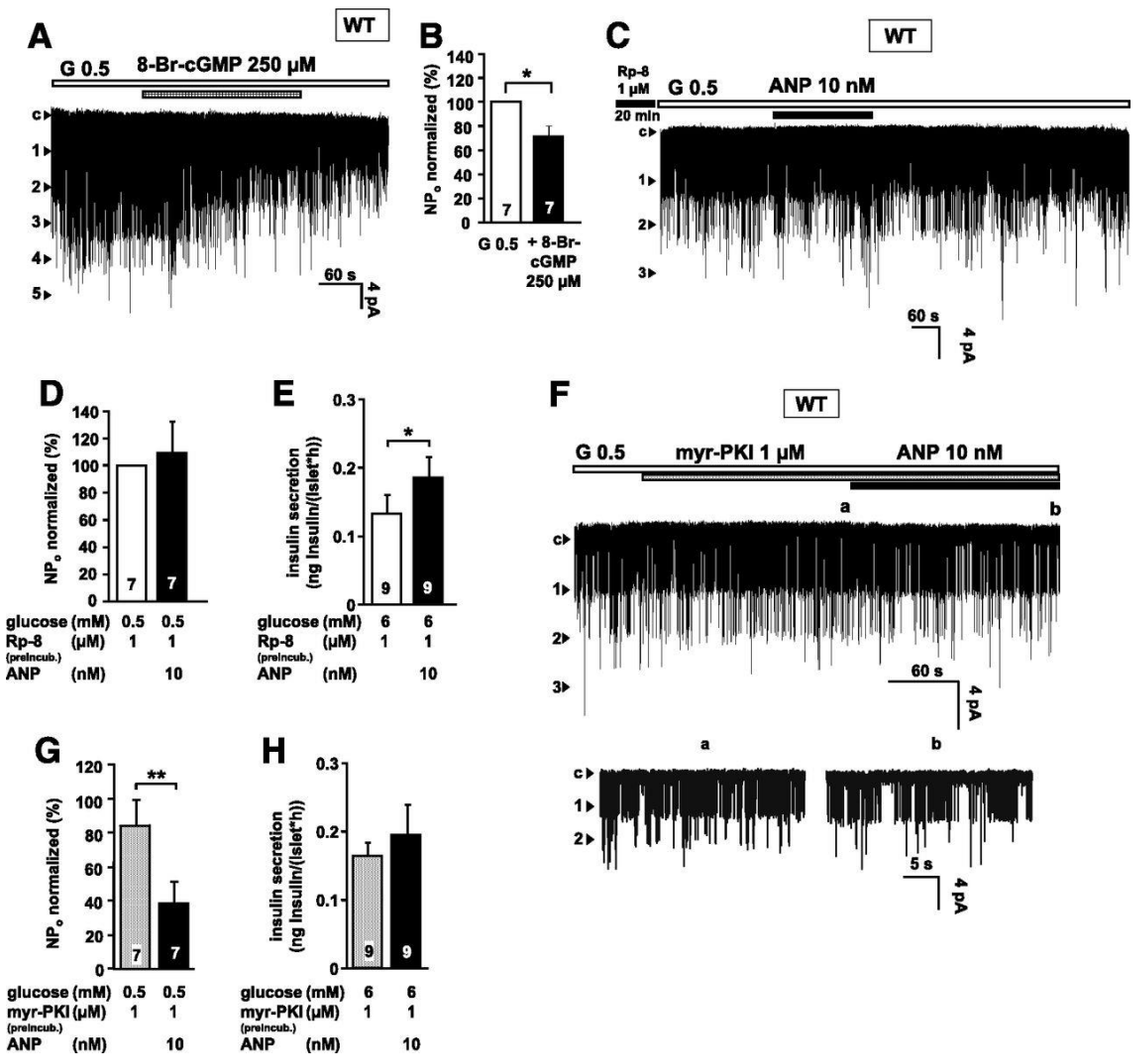

Fig. 5: Involvement of cGMP/PKG and cAMP/PKA signaling pathways in the effect of ANP on the K_{ATP} current and insulin secretion. *A*: Typical recording showing the effect of 8-Br-cGMP on the NP_o of single K_{ATP} channels recorded in the cell-attached mode with a WT β-cell. *B*: Summary of the results. *C*: Typical recording showing the lack of effect of ANP after preincubation with Rp-8 on the NP_o of single K_{ATP} channels recorded in the cell-attached mode of a WT β-cell. *D*: Summary of the results. *E*: ANP effect on insulin secretion in the presence of 6 mmol/L glucose after preincubation of WT islets with Rp-8. *F*: Typical recording showing the effect of ANP in the presence of myr-PKI on the NP_o of single K_{ATP} channels recorded in the cell-attached mode of a WT β-cell. *G*: Summary of the results. *H*: ANP effect on insulin secretion in the presence of 6 mmol/L glucose and after treatment of WT islets with myr-PKI. The numbers within the columns are the number of different experiments with at least three different mice. **P* ≤ 0.05, ***P* ≤ 0.01. c, closed state of the channel; G 0.5, 0.5 mmol/L glucose.

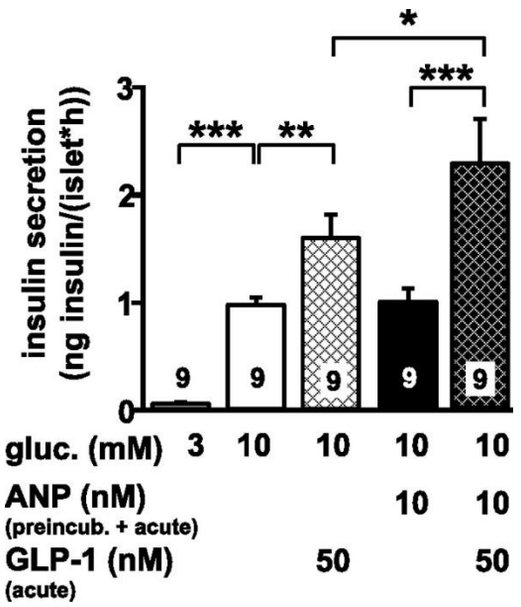

Fig. 6: Enhancement of the cGMP effect by cAMP. Potentiation of GLP-1–induced increase in insulin secretion by 90 min preincubation at room temperature with ANP. The experiments were performed with islets from WT mice. The numbers within columns are the number of different experiments. In each series, islets of at least three different mice were used. *$P \leq 0.05$, **$P \leq 0.01$, ***$P \leq 0.001$.

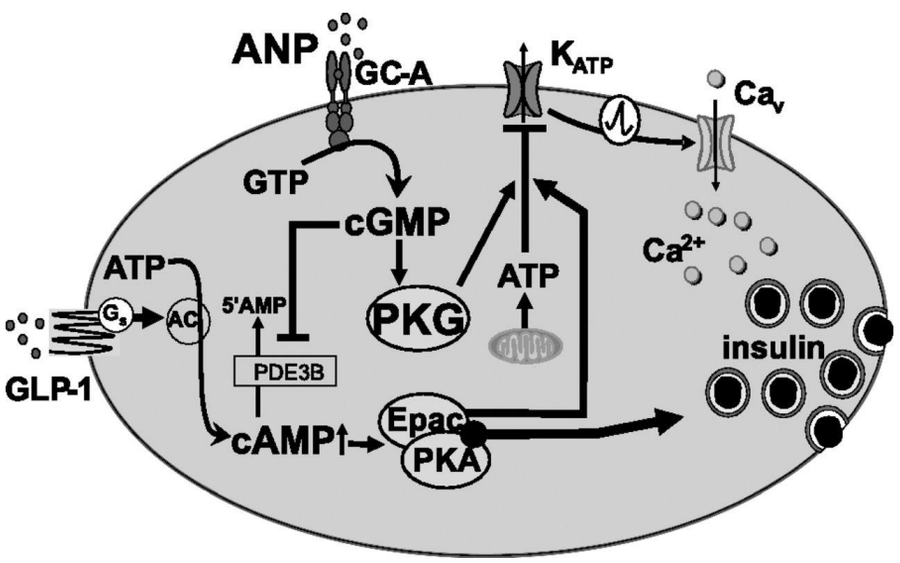

Fig. 7: Model showing how ANP affects stimulus-secretion coupling in β-cells. For details, see discussion. AC, adenylyl cyclase; Ca_v, voltage-dependent Ca channel; G_s, stimulative regulative G-protein.

8.3 M-ATP - ATP mediates a negative autocrine signal on stimulus-secretion coupling in mouse pancreatic β-cells

Bauer C[1], Kaiser J[1], Sikimic J[1], Krippeit-Drews P[1], Düfer M[2], Drews G[1].

[1]Department of Pharmacology, Institute of Pharmacy, University of Tübingen, Auf der Morgenstelle 8, Tübingen, D-72076, Germany; [2]Department of Pharmaceutical and Medicinal Chemistry, University of Münster, Corrensstraße 48, Münster, D-48149, Germany

Published: Endocrine. 2019 Feb;63(2):270-283. doi: 10.1007/s12020-018-1731-0.

Abstract

Purpose

The role of ATP, which is secreted by pancreatic β-cells, is still a matter of debate. It has been postulated that extracellular ATP acts as a positive auto- or paracrine signal in β-cells amplifying insulin secretion. However, there is rising evidence that extracellular ATP may also mediate a negative signal.

Methods

We evaluated whether extracellular ATP interferes with the Ca^{2+}-mediated negative feedback mechanism that regulates oscillatory activity of β-cells.

Results

To experimentally uncover the Ca^{2+}-induced feedback we applied a high extracellular Ca^{2+} concentration. Under this condition ATP (100 µM) inhibited glucose-evoked oscillations of electrical activity and hyperpolarized the membrane potential. Furthermore, ATP acutely increased the interburst phase of Ca^{2+} oscillations and reduced the current through L-type Ca^{2+} channels. Accordingly, ATP (500 µM) decreased glucose-induced insulin secretion. The ATP effect was not mimicked by AMP, ADP, or adenosine. The use of specific agonists and antagonists and mice deficient of large conductance Ca^{2+}-dependent K^+ channels revealed that P2X, but not P2Y receptors, and Ca^{2+}-dependent K^+ channels are

involved in the underlying signaling cascade induced by ATP. The effectiveness of ATP to interfere with parameters of stimulus-secretion coupling is markedly reduced at low extracellular Ca^{2+} concentration.

Conclusion

It is suggested that extracellular ATP which is co-secreted with insulin in a pulsatile manner during glucose-stimulated exocytosis provides a negative feedback signal driving β-cell oscillations in co-operation with Ca^{2+} and other signals.

Abbreviations

V_m	cell membrane potential
$\Delta\psi$	mitochondrial membrane potential
$[Ca^{2+}]_c$	cytosolic Ca^{2+} concentration
BK-KO	BK channel knock-out

Introduction

ATP is the energy source of the cell, but serves as a signaling molecule, too. ATP enriched in insulin-containing granules via a vesicular nucleotide transporter (1) is thus secreted to the cell surface. The ATP concentration within the granules is around 3.5 mM (2). ATP is co-released with insulin (3) or secreted without insulin in a process called kiss-and-run exocytosis (4) where only small molecules are discharged. Extracellular ATP is degraded by specific ecto-nucleotidases (for review see (5)) which contribute to the regulation of the extracellular ATP content. ATP exerts numerous important physiological effects in many mammalian cell types including pancreatic islets (6, 7) via activation of purinergic P2 receptors divided in the P2X and P2Y families with seven and eight subtypes, respectively. P2X receptors are ligand-operated cation channels while P2Y receptors belong to the large group of G-protein-coupled receptors. All these subtypes have been identified in the endocrine pancreas (for review see (7)). The effects of extracellular ATP on β-cell function are numerous, but often controversial depending on the species, cell systems, and experimental conditions. Moreover, activation of different receptor subtypes may induce various and even opposed effects which complicates the understanding of the action of extracellular ATP on β-cell function.

Studies with murine β-cells mainly report an inhibitory effect of extracellular ATP on stimulus-secretion coupling (SSC), but the underlying mechanism is far from being clear. Two studies reported that extracellular ATP reduced insulin secretion of isolated mouse islets despite a reduction of K^+ conductance and K_{ATP} current, respectively (8, 9). Petit et al. (8) assumed that the inhibitory effect of ATP can be attributed to the degradation of ATP to adenosine while Poulsen et al. (9) suggested that it is caused by an interaction with the exocytotic machinery via $P2Y_1$-induced activation of calcineurin. Other groups observed stimulation and inhibition of insulin secretion in dependence of different receptor subtypes (10, 11, 12). Studies with P2Y receptor knockout (KO) mice did not solve the discrepancies since $P2Y_1$ receptor-KO mice show increased glucose-induced insulin secretion while $P2Y_{14}$ receptor-KO mice exhibit decreased secretion (13, 14). In rats the results of extracellular ATP on β-cell function are less controversial and in contrast to mice a stimulatory effect of ATP is supported by most studies (e.g. (15, 16, 17) although participating receptors and involved mechanisms are not entirely clear. IP_3-induced Ca^{2+} mobilization with subsequent activation of Ca^{2+} influx via CRAC channels are mechanisms discussed in this context. ATP-evoked Ca^{2+} release from the endoplasmic reticulum (ER) is observed in mouse, rat, and human β-cells; however, in mouse β-cells this seems not to result in CRAC channel activation (18). Hellman and colleagues (19, 20, 21) suggested that extracellular ATP is involved in the control of the rhythmic activity of β-cells and in the propagation of the oscillations from cell to cell. In the proposed model ATP has a time-dependent dual effect on β-cell function: prompt activation followed by inhibition.

In contrast to other studies, we focused on the influence of the nucleotide on bursting activity of β-cells. In particular, we investigated effects of ATP on β-cell function at conditions with enhanced Ca^{2+}-mediated negative feedback on SSC, especially reflecting the burst phases with action potentials.

Materials and methods

Animals and islet preparation

Islets of Langerhans were isolated from adult C57Bl/6N mice or C57Bl/6N mice with a global knockout of BK channels (BK-KO). The mice were bred in the animal

facility of the Department of Pharmacology at the University of Tübingen. The principles of laboratory animal care (NIH publication no. 85-23, revised 1985) and German laws were followed. Isolation and culture were performed as described previously (22), except, islets of Langerhans were dispersed to single cells or cell clusters by trypsin treatment.

Solutions and chemicals

Recordings of $[Ca^{2+}]_c$ were performed with a bath solution which contained (in mM): 140 NaCl, 5 KCl, 1.2 $MgCl_2$, 10 HEPES; $CaCl_2$, and glucose as indicated, pH 7.4 adjusted with NaOH. The same bath solution was used for the determination of the mitochondrial membrane potential ($\Delta\psi$) and for measurements of membrane potential (V_m) in the perforated-patch configuration. For this purpose, the pipette solution was composed of (in mM): 10 KCl, 10 NaCl, 70 K_2SO_4, 4 $MgCl_2$, 2 $CaCl_2$, 10 EGTA, 20 HEPES, 0.27 amphotericin B, pH adjusted to 7.15 with KOH. For perforated-patch measurements of Ca^{2+} currents a bath solution of the following composition was used (mM): 115 NaCl, 1.2 $MgCl_2$, 10 $CaCl_2$, 10 TEA, 10 glucose, 10 HEPES, pH 7.4 adjusted with NaOH. The respective pipette solution contained (in mM): 10 KCl, 10 NaCl, 70 Cs_2SO_4, 7 $MgCl_2$, 10 HEPES, 0.27 amphotericin B, pH adjusted to 7.15 with NaOH. Krebs–Ringer–Hepes solution for insulin secretion was composed of (in mM): 122 NaCl, 4.7 KCl, 1.1 $MgCl_2$, 10 $CaCl_2$, glucose as indicated, 10 HEPES, 0.5 % bovine serum albumin and pH 7.4 adjusted with NaOH. Adenosine 5′-triposphate (ATP) was obtained from Carl Roth (Karlsruhe, Germany) or Sigma-Aldrich (Taufkirchen, Germany), the $P2X_{1,3}$-agonist α,β-methyleneadenosine 5′-triphosphate (αβ-MeATP) from Tocris Bioscience (Bristol, United Kingdom). Fura-2/AM was either purchased from Biotrend (Köln, Germany) or Sigma-Aldrich (Schnelldorf, Germany). Rhodamine, RPMI 1640 medium, and penicillin/streptomycin was from Invitrogen (Karlsruhe, Germany). All other chemicals were purchased from Sigma-Aldrich or Carl Roth in the purest form available.

Measurements of the mitochondrial membrane potential

$\Delta\Psi$ was measured as rhodamine 123 fluorescence at 480 nm excitation wave length as described in (23). To evaluate the effects, the values were averaged for 60 s at the end of each interval before solution change.

Measurement of $[Ca^{2+}]_c$

$[Ca^{2+}]_c$ was measured by the fura-2 method as described by Grynkiewicz et al. (24). Details are described in (22). In brief, cells were loaded with 5 µM fura-2-AM for 35 min at 37 °C. Fluorescence was excited at 340 and 380 nm, emission was filtered (LP515), and measured by a digital camera. $[Ca^{2+}]_c$ was calculated according to an in vitro calibration with fura2-5K-salt. The area under the curve (AUC) was taken to reveal the effect of ATP or αβ-MeATP on oscillations of the cytosolic Ca^{2+} concentration. The AUC was evaluated in the steady state before the switch to ATP or αβ-MeATP and between min 0 to 5 and 5 to 10 in the presence of the nucleotide. In the experiments with NF-279 the AUC was calculated for 10 min after addition of the drug. In fura-2 measurements with whole islets the fluorescence ratio F340/F380 is given instead of $[Ca^{2+}]_c$.

Patch-clamp measurements

Membrane currents and potentials were recorded with an EPC-9 patch-clamp amplifier using “Patchmaster” software (HEKA, Lambrecht, Germany). For V_m measurements, the plateau potential under control conditions was compared to the maximal hyperpolarization induced by ATP. Where applicable, action potential frequency was determined during a period of 2.5 min before ATP application and separately during the first and second 2.5 min period after addition of ATP. At the high Ca^{2+} concentration of 10 mM the membrane potential oscillated, i.e., burst phases with action potentials changed with silent interburst phases. Under this condition the fraction of plateau phase (FOPP ~ percentage of time with spike activity) was calculated for 2 min before and during min 3 and 5 after drug application. Currents through L-type Ca^{2+} channels were measured using the perforated-patch configuration in the voltage-clamp mode by 50 ms pulses from –70 to 0 mV. The last three currents prior to solution change were used for analysis

of the maximum peak current (I_{peak}), the AUC to determine charge movement, and τ to characterize current inactivation.

Insulin secretion

After preparation islets were kept overnight in RPMI 1640 culture medium with 11.1 mM glucose. Details for steady-state incubations are described in (22). Briefly, insulin secretion under steady-state conditions was measured for 1 h at 37 °C under conditions as indicated. For perifusion experiments 50 islets of Langerhans were perifused continuously with bath solution as described in (23) and test substances as indicated and a sample was taken every 2 min. Levels of insulin were determined by radioimmunoassay (Merck Millipore, Darmstadt, Germany).

Statistics

Each series of experiments was performed with islets of Langerhans or cell clusters from at least three independent preparations unless otherwise indicated. Means ± SEM are given for the indicated number of experiments. Statistical significance of differences was assessed by a Student's *t*-test for paired values. Multiple comparisons were made by ANOVA followed by Student–Newman–Keuls test. *P*-values ≤0.05 were considered significant.

Results

Extracellular ATP affects key parameters of SSC

Cytosolic Ca^{2+} concentration and cell membrane potential

The cell membrane potential (V_m) takes a prominent position within SSC as it connects glucose metabolism to insulin secretion by determining the cytosolic Ca^{2+} concentration ($[Ca^{2+}]_c$). Within the SSC, opening of voltage-dependent L-type Ca^{2+} channels and Ca^{2+} influx represent the decisive trigger for secretion of insulin from storage vesicles. For this reason, alterations of the cytosolic Ca^{2+} concentration ($[Ca^{2+}]_c$) are crucial for insulin secretion. The recording in Fig. 1a shows periodic oscillations of $[Ca^{2+}]_c$ in the presence of 10 mM glucose and 2.5 mM Ca^{2+}. Addition

of ATP in a concentration of 100 µM interrupted this regular pattern so that the next oscillation appeared later and exhibited a smaller amplitude. To quantify this observation, the AUC of $[Ca^{2+}]_c$ was determined before and after addition of ATP (Fig. 1b). The AUC was reduced from 384 ± 27 nM × 5 min under control conditions to 300 ± 29 nM × 5 min during the first 5 min period in the presence of ATP. The AUC amounted to 353 ± 24 nM × 5 min in the second 5 min period of ATP treatment indicating a transient effect of ATP.

The plasma membrane potential V_m was measured in the perforated-patch configuration under the same conditions. The record (Fig. 1c) and the bar chart (Fig. 1d) show that ATP had no effect on V_m (−37 ± 3 mV under control conditions vs. −39 ± 3 mV in the first 2.5 min and −38 ± 4 mV in the second 2.5 min period in the presence of ATP). Likewise, action potential frequency did not change (Fig. 1c, e). It amounted to 3.3 ± 0.6 Hz before ATP application, to 2.9 ± 0.6 Hz during the first 2.5 min period with ATP ($n = 4$, n.s.), and to 3.4 ± 0.5 Hz during the second 2.5 min period with ATP ($n = 4$, n.s.). Under these conditions characteristic slow waves consisting of electrically silent phases (interbursts) and active phases (bursts with action potentials) are hardly detectable (25). Bursting activity can be achieved by increasing the extracellular Ca^{2+} concentration (compare Fig. 1c and Fig. 2c). It is known that $[Ca^{2+}]_c$ affects its own entry via opening of K_{ATP} channels, i.e., it exerts an important feedback control on insulin secretion (26, 27). Increasing the extracellular Ca^{2+} concentration which enhances the Ca^{2+} gradient and thus Ca^{2+} entry augments this feedback mechanism under experimental conditions. To evaluate whether extracellular ATP interferes with this Ca^{2+}-mediated feedback mechanism, it was amplified in the following experiments by applying 10 mM Ca^{2+} in the presence of 10 mM glucose (G10/Ca10). Treatment with 100 µM ATP strongly reduced the AUC of $[Ca^{2+}]_c$ from 414 ± 26 nM × 5 min under control conditions to 188 ± 19 and 319 ± 34 nM × 5 min, respectively, during the first and second 5 min period of ATP addition (Fig. 2a, b). Under these conditions with 10 mM Ca^{2+} the effect of ATP was much larger in the first 5 min period of ATP addition compared to conditions with 2.5 mM Ca^{2+} and remained significant in the second application period. Furthermore, the interburst phase directly after addition of ATP was markedly longer compared to the mean interburst phase under control condition (247±35 vs. 117±21 s, $n = 20$, $P \leq 0.001$). The representative

measurement of electrical activity in Fig. 2c shows characteristic slow waves in the presence of G10/Ca10 as a result of the Ca^{2+} feedback described above. Addition of ATP (100 µM) led to a sustained hyperpolarization of V_m from a plateau potential of −44.2 ± 1.4 to −68.0 ± 3.5 mV (Fig. 2d).

Mitochondrial membrane potential

Hyperpolarization of V_m can be caused by opening of K_{ATP} channels due to a reduction in ATP production. The mitochondrial membrane potential ($\Delta\Psi$) is directly linked to glucose metabolism and ATP production (27) because the electrochemical proton gradient across the inner mitochondrial membrane determines the activity of the F1/F0-ATPase. Increasing glucose concentration caused a hyperpolarization of $\Delta\Psi$, which is indicated by a decrease in rhodamine 123 fluorescence signal and reflects ATP production. On average, the fluorescence signal was lowered from 502 ± 47 a.u. in the presence of 0.5 mM glucose to 412 ± 32 a.u. upon an increase of the glucose concentration to 10 mM ($P \leq 0.001$, $n = 28$). ATP (100 µM) had no effect on $\Delta\Psi$ (409±32 a.u.) ($n = 28$, n.s., data not shown). The experiment was repeated with 500 µM ATP and additionally in 5 mM glucose to create conditions where $\Delta\Psi$ is not that hyperpolarized but ATP did not show any effect (G10/Ca10: 530±35 a.u., G10/Ca10 + 500 µM ATP: 528±34 a.u., $n = 27$, n.s.; G5/Ca10: 550±45 a.u., G5/Ca10 + 500 µM ATP: 552±45 a.u., $n = 16$, n.s., data not shown). Thus, extracellular ATP seems not to affect mitochondrial ATP production.

Current through voltage-dependent Ca^{2+} channels

Next, a possible influence of ATP on Ca^{2+} currents was studied. In Fig. 3a, a typical Ca^{2+} current is shown which was elicited by a 50 ms voltage step from −70 to 0 mV. Under control conditions (black curve) opening of L-type Ca^{2+} channels led to a marked and rapid Ca^{2+} influx followed by a slow current decay due to Ca^{2+}-dependent current inactivation. Addition of ATP (100 µM, dotted curve) reduced the peak Ca^{2+} current (I_{peak}) from −87 ± 8 to −72 ± 9 pA (Fig. 3b) and the charge movement, measured as area under the curve (AUC), from 2.6 ± 0.3 to 2.1 ± 0.2 pC

(Fig. 3c). The Ca^{2+}-dependent inactivation of the channels (28) which was determined by calculating the time constant *τ* was not influenced by ATP (22 ± 3 ms under control conditions vs. 21 ± 2 ms with ATP) (Fig. 3d).

Extracellular ATP reduces insulin secretion

The effect of ATP on insulin secretion was studied in steady state as well as in perifusion experiments. As seen in Fig. 4a, after 1 h steady-state incubation in G15/Ca10, ATP (500 µM and 1 mM) reduced glucose-induced insulin secretion by 26% and 33%, respectively. ATP in a concentration of 100 µM was without effect in these experiments. In contrast to the experiments described before, insulin secretion measurements are performed with whole islets which are encircled by a capsule of connective tissue. Evidently, this capsule impedes diffusion of ATP to the islets cells, an observation that confirms earlier findings (29). To test for this, the Ca^{2+} experiments illustrated in Fig. 2a, b were repeated with whole islets instead of dispersed cells. Indeed, 100 µM ATP did not influence $[Ca^{2+}]_c$ measured with whole islets (as fluorescence ratio F340/F380) (10 mM glucose: 0.48 ± 0.09; after ATP application: 0.48 ± 0.09, $n = 6$ different islets, not shown). This suggestion is supported by the finding that pre-treatment of islets for 1 h with 100 and 200 µM ATP, respectively, reduced the response to a subsequent glucose stimulus (Fig. 4b).

The inhibitory effect of ATP on insulin secretion was not mimicked by AMP, ADP, or adenosine (Suppl. Figure 1). In contrast to ATP, concentrations of adenosine higher than 100 µM increased insulin secretion. Perifusion experiments disclosed that ATP diminished the first and second phase of insulin secretion. Rising the glucose concentration from 3 to 15 mM glucose in the absence (solid curve) and presence of ATP (dotted curve) revealed that the first phase of insulin secretion was markedly reduced by ATP (Fig. 5a). The quantitative analyses of the AUC demonstrated that ATP decreased the first phase of insulin secretion from 61 ± 14 ng insulin/(50 islets × 30 min) to 41 ± 10 ng insulin/(50 islets × 30 min) (Fig. 5b). In Fig. 5c the glucose concentration was first raised from 3 to 15 mM glucose showing the typical biphasic pattern of insulin secretion. The figure shows the

typical steep, transient rise during the first phase followed by a lower but still elevated plateau in the second phase. Addition of ATP at the steady state during the second phase reduced insulin secretion. For further quantification the AUC was calculated for the last 10 min in the absence and presence of ATP, respectively. It decreased from 15 ± 2 ng insulin/(50 islets × 10 min) to 12 ± 2 ng insulin/(50 islets × 10 min) (Fig. 5d).

Extracellular ATP mediates its effects by activation of P2X receptors

The $P2X_{1,3}$ agonist αβ-MeATP was used to test whether ATP-induced effects on SSC are mediated via P2X receptors. As shown in Fig. 6a αβ-MeATP mimicked the effect of ATP on $[Ca^{2+}]_c$ oscillations. αβ-MeATP led to a decrease in the AUC of $[Ca^{2+}]_c$ (Fig. 6b) from 345 ± 22 nM × 5 min under control conditions to 264 ± 33 and 287 ± 30 nM × 5 min, respectively, during the first and second 5 min period in the presence of αβ-MeATP. As observed with ATP, duration of the interburst phase directly after addition of αβ-MeATP was prolonged compared to the mean interburst phase before application of the $P2X_{1,3}$ agonist (240±54 vs. 123±17 s, $n = 16$, $P \leq 0.05$). Furthermore, αβ-MeATP reduced glucose-induced insulin secretion by 36% (from 3.1 ± 0.4 ng insulin/(islet × h) under control conditions to 2.0 ± 0.1 ng insulin/(islet × h) in the presence of αβ-MeATP) after 1 h steady-state incubation in 15 mM glucose and 10 mM Ca^{2+} (Fig. 6c). Insulin secretion experiments with the $P2X_1$ antagonist NF-279 revealed that ATP is no longer able to reduce insulin secretion when $P2X_1$ channels are blocked (Fig. 6d). Insulin secretion in the presence of NF-279 was 2.2 ± 0.2 ng insulin/(islet × h) before and 2.2 ± 0.1 ng insulin/(islet × h) after addition of ATP. In contrast, the $P2X_3$ antagonist RO-3 was not able to suppress the inhibitory effect of extracellular ATP (Fig. 6e). Insulin secretion in the presence of RO-3 was 3.9 ± 0.7 ng insulin/(islet × h) before and 2.4 ± 0.3 ng insulin/(islet × h) after addition of ATP.

The most prominent receptor of the P2Y family in β-cells is the $P2Y_1$ receptor (12, 13, 30). This receptor family is Gq protein-coupled and thus affects intracellular Ca^{2+} stores. We observed a short Ca^{2+} transient after ATP administration (Fig. 2a). This was also present when L-type Ca^{2+} channels were blocked (Suppl. Figure 2A,

B) and is due to ER store depletion (Suppl. Figure 2C, D). However, pre-treatment of β-cells with the SERCA inhibitor thapsigargin did not affect the inhibitory effect of ATP on insulin secretion (Suppl. Figure 2E). Moreover, the inhibitory effect of ATP on insulin secretion was not influenced by the specific $P2Y_1$ receptor antagonist MRS-2179 (Suppl. Figure 2F). Obviously, the P2Y receptor family does not essentially contribute to the inhibitory effect of ATP.

Possible involvement of Ca^{2+}-dependent potassium channels

As P2X receptors are unspecific cation channels leading to a depolarizing cation influx, activation of these receptors seems hard to reconcile with the above-mentioned negative influences of ATP and αβ-MeATP on parameters of SSC. In β-cells several types of Ca^{2+}-dependent K^+ channels are expressed mediating K^+ outflux upon activation including BK channels with large conductance and SK4 channels with intermediate conductance. Both channel types are involved in the regulation of β-cell function (31, 32). To test whether extracellular ATP activates these channels to mediate a negative feedback on SSC, we used β-cells from BK-KO mice and TRAM-34 as a pharmacologic inhibitor of SK4 channels.
Figure 7a shows a measurement of V_m in the perforated-patch configuration with BK-KO β-cells. After SK4 channel inhibition the BK channel-deficient β-cells are rather depolarized and show continuous spike activity. Administration of ATP (100 µM) only led to a transient hyperpolarization of -10.7 ± 2.6 mV in six out of nine experiments (from -39 ± 3 mV in the presence of TRAM-34 in 10 mM glucose and 10 mM Ca^{2+} to -50 ± 3 mV after application of ATP (Fig. 7b)). A slight depolarization (from -34 ± 3 mV in the presence of TRAM-34 to -29 ± 3 mV) was observed in all nine measurements during the last 3 min of ATP addition (Fig. 7c).

In addition, the effect of ATP on Ca^{2+} oscillations is reduced after inhibition of SK4 channels in BK-KO cells. Figure 7d shows Ca^{2+} oscillations in β-cells from BK-KO mice in the presence of TRAM-34. Under these conditions ATP reduced the AUC of $[Ca^{2+}]_c$ only transiently despite of the high extracellular Ca^{2+} concentration (Fig. 7e) which fits to the transient effect of ATP on electrical activity. The AUC decreased from 472 ± 29 nM × 5 min under control conditions with TRAM-34 to

339 ± 20 nM × 5 min in the presence of ATP during the first 5 min application period. In the second 5 min period of ATP addition the AUC of $[Ca^{2+}]_c$ amounted to 439 ± 21 nM × 5 min.

In agreement with the influence of BK and SK4 channels on ATP-induced alterations in $[Ca^{2+}]_c$, the effect of ATP on insulin secretion was reduced after inhibition of these channels. Five hundred micromolar ATP led to a significant reduction of glucose-stimulated insulin secretion which amounted to 34% under control conditions but only to 23% after pharmacological blockage of BK channels with 100 nM iberiotoxin and SK4 channels with 10 µM TRAM-34. In this series of experiments, insulin secretion (15 mM glucose) was reduced by ATP from 4.5 ± 0.5 to 2.9 ± 0.1 ng insulin/(islet × h) ($n = 6$, $P \leq 0.05$). In the presence of TRAM-34 and iberiotoxin the effect of ATP was lower (reduction from 4.2 ± 0.3 to 3.1 ± 0.2 ng insulin/(islet × h), $n = 6$, $P \leq 0.05$, data not shown).

Blockage of $P2X_1$ channels increased electrical activity and $[Ca^{2+}]_c$

According to our hypothesis inhibition of the $P2X_1$ channels should increase electrical activity, the AUC of $[Ca^{2+}]_c$, and insulin secretion. Figure 8a, b reveals that NF-279 indeed augmented the AUC of $[Ca^{2+}]_c$ from 592 ± 35 nM × 10 min under control conditions to 632 ± 45 nM × 10 min in the presence of 5 µM NF-279. Accordingly, the FOPP increased from 46 ± 9 to 56 ± 11% after addition of NF-279 (Fig. 8c, d). Paradoxically, insulin secretion was reduced by NF-279 from 2.81 ± 0.30 to 2.16 ± 0.18 ng insulin/(islet × h) ($n = 6$, $P \leq 0.05$). Since this is unexpected and does not fit to the results obtained with NF-279 on $[Ca^{2+}]_c$ and V_m, it is suggested that this effect is an unspecific Ca^{2+}-independent interaction with the exocytotic machinery. To further strengthen this conclusion, we tested suramin on $[Ca^{2+}]_c$, another frequently used blocker of $P2X_1$ channels, although less specific. Suramin enhanced the AUC of $[Ca^{2+}]_c$ during a 5 min application period in 9 out of 13 cells from 323 ± 29 nM × 5 min to 404 ± 42 nM × 5 min. Subsequent addition of ATP for 5 min in the presence of suramin did not significantly alter the AUC of $[Ca^{2+}]_c$ (Fig. 8e, f).

Discussion

The inhibitory signaling pathway of extracellular ATP

It is well known that signaling through purinergic receptors affects insulin secretion and that ATP released from secretory granules or nerve endings can activate these receptors. Effects on β-cells are mediated by P2X and P2Y receptors but not by P1 receptors (for review see (33)). The physiological significance of activation of purinergic receptors is still debated; stimulation and inhibition of insulin secretion have been reported. The situation is complex because each receptor has many subtypes and subtype expression varies between species and between primary β-cells and insulin-secreting tumor cells.

We have chosen a protocol for our experiments where we stimulated β-cells and islets by glucose and raised Ca^{2+} influx by increasing the electrochemical gradient for Ca^{2+}. This protocol enhances the Ca^{2+}-mediated negative feedback on β-cell function (26) which is most prominent during burst phases with Ca^{2+} action potentials. Under these conditions, extracellular ATP inhibited SSC of β-cells as evidenced by hyperpolarization of V_m, reduced Ca^{2+} influx and AUC of $[Ca^{2+}]_c$ and decreased insulin secretion. This effect was specific for ATP and not mimicked by AMP, ADP, or adenosine suggesting interference of ATP with specific receptors. Our results point to the involvement of $P2X_1$ receptors under these conditions: (1) The $P2X_{1,3}$ agonist αβ-MeATP mimicked the effect of extracellular ATP on insulin secretion. (2) The $P2X_1$ receptor antagonist NF-279 suppressed the effect of ATP on insulin release but not the $P2X_3$ receptor antagonist RO-3. (3) The $P2Y_1$ antagonist MRS-2179 did not influence the effect of ATP on insulin secretion.

The $P2X_1$ receptor is a non-specific cation channel with a relatively high permeability to Ca^{2+} (34). $P2X_1$ receptor activation by extracellular ATP leads to Ca^{2+} influx and the local enhancement of Ca^{2+} in the sub-membrane space obviously influences the activity of other ion channels: (1) Extracellular ATP reduced the charge movement through L-type Ca^{2+} channels. This may be explained by a reduction of the driving force for Ca^{2+} due to the local increase of

the intracellular Ca^{2+} concentration after $P2X_1$ receptor activation. Since Ca^{2+} influx through L-type Ca^{2+} channels constitutes the major trigger signal for insulin secretion (35), reduced influx would diminish secretion. (2) The effectiveness of ATP to inhibit SSC was reduced after genetic and pharmacological deletion of two Ca^{2+}-activated K^+ channels present in β-cells, the BK and SK4 channels. An increase in the current through these channels after $P2X_1$ receptor activation would hyperpolarize the membrane and in turn lower insulin secretion contributing to the negative feedback induced by ATP.

Since the early paper of Gylfe and Hellman (36), who demonstrated that extracellular ATP induces Ca^{2+} release from ER Ca^{2+} stores, a variety of studies has shown similar results. These observations are confirmed by our experiments. Notably, store depletion does not affect the effectiveness of ATP to inhibit insulin secretion. This indicates that the sub-membrane increase in Ca^{2+} is decisive for the effect of ATP.

Physiological significance of extracellular ATP for β-cell oscillations

Oscillatory activity of β-cells is a prerequisite for normal action of insulin and glycemic control. Disturbances in the fluctuations of the parameters of SSC profoundly impair insulin signaling in peripheral tissues and are early events in diabetes (37). We have extensively studied the mechanisms underlying these oscillations earlier (27, 31). In the present paper we suggest a negative feedback for extracellular ATP in synergism with Ca^{2+}, i.e., a role for ATP in the termination of burst phases with action potentials. Partial inhibition of this feedback by blockade of $P2X_1$ channels indeed prolonged burst phases and thus increased electrical activity and the AUC of $[Ca^{2+}]_c$.

An extracellular ATP concentration of 100 µM, as used in the present work, seems not to be extraordinarily high considering that the ATP concentration within exocytotic granules of β-cells is around 3.5 mM (2). In 1998 Hazama and co-workers (38) demonstrated that the ATP concentration at the cell surface is above 25 µM after stimulation of rat β-cells with glucose. They concluded that ATP can

reach concentrations high enough to stimulate purinergic receptors during insulin secretion. Therefore, we used 100 µM ATP to realize an effect of ATP additional to that evoked by endogenous ATP from the granules. In experiments with whole islets, even higher concentrations of ATP (500 µM) were needed, which is most likely due to the capsule of connective tissue surrounding the islets which can form a barrier for molecules like ATP (see also Extracellular ATP reduces insulin secretion). Interestingly, Weitz et al. (6) recently demonstrated that tissue-resident macrophages of islets sense the interstitial ATP concentration. It is concluded that macrophages use ATP as a signal to estimate the activity state of the β-cells via purinergic receptors in order to balance their secretion products which influence β-cell proliferation. To achieve maximum Ca^{2+} signals in macrophages concentrations of ATP up to 1 mM were used.

In most experiments we have used a high extracellular Ca^{2+} concentration of 10 mM to augment the negative feedback mediated by Ca^{2+} which is most important during the burst phases. This feedback is thought to contribute to the initiation of burst termination. Exocytotic vesicles contain 120 mM Ca^{2+} which is mostly bound. Anyhow, the free granular Ca^{2+} concentration reaches 10 mM (2) suggesting that the local Ca^{2+} concentration on the surface of the cells is higher than the bulk Ca^{2+} concentration of the extracellular space. Enhanced local Ca^{2+} concentration steepens the gradient driving Ca^{2+} entry.

Ion flux through P2X receptors is dependent on the extracellular Ca^{2+} concentration, i.e., Ca^{2+} influx through P2X increases concomitantly with rising extracellular Ca^{2+} concentration (39) initiating an inhibitory signaling pathway (see above).

It has been demonstrated that a rise in the mitochondrial Ca^{2+} concentration during a burst phase increases K_{ATP} current and hyperpolarizes V_m to initiate the interburst (40). Based on our current results, it can be concluded that extracellular ATP and fluctuations of the intracellular Ca^{2+} concentration act synergistically to exert a negative feedback that terminates the burst phases and perpetuate oscillatory activity

Proposed model

The negative effects of extracellular ATP on SSC described in the present paper are in accordance with numerous reports in the literature, e.g. (8, 9, 19, 41). This contrasts with findings about stimulating effects of ATP on β-cells in mouse and other species (11, 15, 16, 42, 43, 44). To reconcile these observations it is hypothesized that short ATP pulses stimulate β-cell SSC (42), while longer exposure and higher concentrations induce a negative feedback(19, 20, 21, 30). The authors suggest that this dual effect of extracellular ATP supports the coordination of Ca^{2+} oscillations. Furthermore, it is assumed that short pulses of ATP evoked by kiss-and run exocytosis (45) (where only small molecules like ATP but no insulin is released) or by exocytosis at the beginning of a burst phase activate P2Y receptors. Activation of these receptors increases $[Ca^{2+}]_c$ via Ca^{2+} release from the ER, an effect also seen in our experiments. However, this is not sufficient to potentiate the first phase of insulin release.

Our observation that the effect of extracellular ATP depends on the concentration of extracellular Ca^{2+} underlines the complexity of the action of ATP. At a low extracellular Ca^{2+} concentration ATP hardly affects β-cell SSC. Obviously, an increased extracellular Ca^{2+} concentration is necessary to unveil the ATP-induced negative feedback, i.e. extracellular ATP amplifies the negative feedback on β-cell function induced by high Ca^{2+}, thus contributing to the termination of bursts and the maintenance of β-cell oscillations.

According to our model (Fig. 9) the effect of ATP essentially depends on V_m and activity of Ca^{2+}-dependent ion channels during burst phases. During burst phases quickly enhanced extracellular ATP and Ca^{2+} concentrations and thus marked ATP-mediated Ca^{2+} influx through $P2X_1$ receptors prevail, exerting a negative feedback limiting the burst phase. This involves opening of SK4 and BK channels. The novel proposed feedback mechanism of ATP may offer new approaches to influence the regulation of β-cell activity.

Acknowledgements

We are grateful to Isolde Breuning for excellent technical assistance. BK-KO mice were kindly provided by Prof. Dr. Peter Ruth, Institute of Pharmacy, University of Tübingen.

Author's contribution

C.B., J.K., and J.S. researched data; P.K.-D. evaluated data and edited the manuscript; M.D. contributed to discussion and study design and edited the manuscript; G.D. designed the study, wrote and edited the manuscript, and contributed to discussion. G.D. is the guarantor of this work and, as such, had full access to all the data in the study and takes responsibility for the integrity of the data and the accuracy of the data analysis.

Conflict of interest

The authors declare that they have no conflict of interest.

References

1. K. Sawada, N. Echigo, N. Juge, T. Miyaji, M. Otsuka, H. Omote, A. Yamamoto, Y. Moriyama, Identification of a vesicular nucleotide transporter. *Proc. Natl. Acad. Sci. USA* 105(15), 5683–5686 (2008)

2. J.C. Hutton, E.J. Penn, M. Peshavaria, Low-molecular-weight constituents of isolated insulin-secretory granules. Bivalent cations, adenine nucleotides and inorganic phosphate. *Biochem. J.* 210(2), 297–305 (1983)

3. J.W. Leitner, K.E. Sussman, A.E. Vatter, F.H. Schneider, Adenine nucleotides in the secretory granule fraction of rat islets. *Endocrinology* 96(3), 662–677 (1975)

4.S. Obermuller, A. Lindqvist, J. Karanauskaite, J. Galvanovskis, P. Rorsman, S. Barg, Selective nucleotide-release from dense-core granules in insulin-secreting cells. J*. Cell. Sci.* 118(Pt 18), 4271–4282 (2005)

5. M. Cieslak, K. Roszek, Purinergic signaling in the pancreas and the therapeutic potential of ecto-nucleotidases in diabetes. *Acta Biochim. Pol.* 61(4), 655–662 (2014)

6. J.R. Weitz, M. Makhmutova, J. Almaca, J. Stertmann, K. Aamodt, M. Brissova, S. Speier, R. Rodriguez-Diaz, A. Caicedo, Mouse pancreatic islet macrophages use locally released ATP to monitor beta cell activity. *Diabetologia* 61(1), 182–192 (2018)

7. P. Petit, A.D. Lajoix, R. Gross, P2 purinergic signalling in the pancreatic beta-cell: control of insulin secretion and pharmacology. *Eur. J. Pharm. Sci*. 37(2), 67–75 (2009)

8. P. Petit, G. Bertrand, W. Schmeer, J.C. Henquin, Effects of extracellular adenine nucleotides on the electrical, ionic and secretory events in mouse pancreatic beta-cells. *Br. J. Pharmacol*. 98(3), 875–882 (1989)

9. C.R. Poulsen, K. Bokvist, H.L. Olsen, M. Hoy, K. Capito, P. Gilon, J. Gromada, Multiple sites of purinergic control of insulin secretion in mouse pancreatic beta-cells. *Diabetes* 48(11), 2171–2181 (1999)

10. S. Amisten, S. Meidute-Abaraviciene, C. Tan, B. Olde, I. Lundquist, A. Salehi, D. Erlinge, ADP mediates inhibition of insulin secretion by activation of P2Y13 receptors in mice. *Diabetologia* 53(9), 1927–1934 (2010)

11. M. Ohtani, K. Ohura, T. Oka, Involvement of P2X receptors in the regulation of insulin secretion, proliferation and survival in mouse pancreatic beta-cells. *Cell. Physiol. Biochem.* 28(2), 355–366 (2011)

12. M. Ohtani, J. Suzuki, K.A. Jacobson, T. Oka, Evidence for the possible involvement of the P2Y(6) receptor in Ca (2+) mobilization and insulin secretion in mouse pancreatic islets. *Purinergic Signal* 4(4), 365–375 (2008)

13. C. Leon, M. Freund, O. Latchoumanin, A. Farret, P. Petit, J.P. Cazenave, C. Gachet, The P2Y(1) receptor is involved in the maintenance of glucose homeostasis and in insulin secretion in mice. *Purinergic Signal* 1(2), 145–151 (2005)

14. J. Meister, D. Le Duc, A. Ricken, R. Burkhardt, J. Thiery, H. Pfannkuche, T. Polte, J. Grosse, T. Schoneberg, A. Schulz, The G protein-coupled receptor P2Y14 influences insulin release and smooth muscle function in mice. *J. Biol. Chem.* 289(34), 23353–23366 (2014)

15. F. Blachier, W.J. Malaisse, Effect of exogenous ATP upon inositol phosphate production, cationic fluxes and insulin release in pancreatic islet cells. *Biochim. Biophys. Acta* 970(2), 222–229 (1988)

16. P. Petit, D. Hillaire-Buys, M. Manteghetti, S. Debrus, J. Chapal, M.M. Loubatieres-Mariani, Evidence for two different types of P2 receptors stimulating insulin secretion from pancreatic B cell. *Br. J. Pharmacol.* 125(6), 1368–1374 (1998)

17. P. Petit, M. Manteghetti, R. Puech, M.M. Loubatieres-Mariani, ATP and phosphate-modified adenine nucleotide analogues. Effects on insulin secretion and calcium uptake. *Biochem. Pharmacol.* 36(3), 377–380 (1987)

18. Y.F. Zhao, R. Xu, M. Hernandez, Y. Zhu, C. Chen, Distinct intracellular Ca2+ response to extracellular adenosine triphosphate in pancreatic beta-cells in rats and mice. *Endocrine* 22(3), 185–192 (2003)

19. E. Grapengiesser, H. Dansk, B. Hellman, Pulses of external ATP aid to the synchronization of pancreatic beta-cells by generating premature Ca(2+) oscillations. *Biochem. Pharmacol.* 68(4), 667–674 (2004)

20. B. Hellman, H. Dansk, E. Grapengiesser, Pancreatic beta-cells communicate via intermittent release of ATP. *Am. J. Physiol. Endocrinol. Metab.* 286(5), E759–765 (2004)

21. E. Gylfe, E. Grapengiesser, H. Dansk, B. Hellman, The neurotransmitter ATP triggers Ca2 + responses promoting coordination of pancreatic islet oscillations. *Pancreas* 41(2), 258–263 (2012)

22. B. Gier, P. Krippeit-Drews, T. Sheiko, L. Aguilar-Bryan, J. Bryan, M. Düfer, G. Drews, Suppression of K_{ATP} channel activity protects murine pancreatic beta-cells against oxidative stress. *J. Clin. Invest*. 119(11), 3246–3256 (2009)

23. A. Edalat, P. Schulte-Mecklenbeck, C. Bauer, S. Undank, P. Krippeit-Drews, G. Drews, M. Düfer, Mitochondrial succinate dehydrogenase is involved in stimulus-secretion coupling and endogenous ROS formation in murine beta cells. *Diabetologia* 58(7), 1532–1541 (2015)

24. G. Grynkiewicz, M. Poenie, R.Y. Tsien, A new generation of Ca2+ indicators with greatly improved fluorescence properties. *J. Biol. Chem.* 260(6), 3440–3450 (1985)

25. M. Düfer, D. Haspel, P. Krippeit-Drews, L. Aguilar-Bryan, J. Bryan, G. Drews, Oscillations of membrane potential and cytosolic Ca^{2+} concentration in $SUR1^{-/-}$ beta cells. *Diabetologia* 47(3), 488–498 (2004)

26. J.C. Henquin, Glucose-induced electrical activity in beta-cells. Feedback control of ATP-sensitive K+ channels by Ca2+? [corrected]. *Diabetes* 39(11), 1457–1460 (1990)

27. P. Krippeit-Drews, M. Düfer, G. Drews, Parallel oscillations of intracellular calcium activity and mitochondrial membrane potential in mouse pancreatic B-cells. *Biochem. Biophys. Res. Commun.* 267(1), 179–183 (2000)

28. T.D. Plant, Properties and calcium-dependent inactivation of calcium currents in cultured mouse pancreatic B-cells. *J. Physiol.* 404, 731–747 (1988)

29. Maczewsky, J., Sikimic, J., Bauer, C., Krippeit-Drews, P., Wolke, C., Lendeckel, U., Barthlen, W., Drews, G. The LXR ligand T0901317 acutely inhibits insulin secretion by affecting mitochondrial metabolism. *Endocrinology* (2017)

30. A. Salehi, S.S. Qader, E. Grapengiesser, B. Hellman, Inhibition of purinoceptors amplifies glucose-stimulated insulin release with removal of its pulsatility. *Diabetes* 54(7), 2126–2131 (2005)

31. M. Düfer, B. Gier, D. Wolpers, P. Krippeit-Drews, P. Ruth, G. Drews, Enhanced glucose tolerance by SK4 channel inhibition in pancreatic beta-cells. *Diabetes* 58, 1835–1843 (2009)

32. M. Düfer, Y. Neye, K. Hörth, P. Krippeit-Drews, A. Hennige, H. Widmer, H. McClafferty, M.J. Shipston, H.U. Häring, P. Ruth, G. Drews, BK channels affect glucose homeostasis and cell viability of murine pancreatic beta cells. *Diabetologia* 54(2), 423–432 (2011)

33. G. Burnstock, Purinergic signalling in endocrine organs. *Purinergic Signal* 10(1), 189–231 (2014)

34. G. Burnstock, Purine and pyrimidine receptors. *Cell. Mol. Life Sci*. 64(12), 1471–1483 (2007)

35. S.N. Yang, P.O. Berggren, The role of voltage-gated calcium channels in pancreatic beta-cell physiology and pathophysiology. *Endocr. Rev.* 27(6), 621–676 (2006)

36. E. Gylfe, B. Hellman, External ATP mimics carbachol in initiating calcium mobilization from pancreatic beta-cells conditioned by previous exposure to glucose. *Br. J. Pharmacol.* 92(2), 281–289 (1987)

37. N. Porksen, M. Hollingdal, C. Juhl, P. Butler, J.D. Veldhuis, O. Schmitz, Pulsatile insulin secretion: detection, regulation, and role in diabetes. *Diabetes* 51(Suppl 1), S245–254 (2002)

38. A. Hazama, S. Hayashi, Y. Okada, Cell surface measurements of ATP release from single pancreatic beta cells using a novel biosensor technique. *Pflug. Arch*. 437(1), 31–35 (1998)

39. K. Nakazawa, K. Fujimori, A. Takanaka, K. Inoue, An ATP-activated conductance in pheochromocytoma cells and its suppression by extracellular calcium. *J. Physiol.* 428, 257–272 (1990)

40. J.F. Rolland, J.C. Henquin, P. Gilon, Feedback control of the ATP-sensitive K^+ current by cytosolic Ca^{2+} contributes to oscillations of the membrane potential in pancreatic beta-cells. *Diabetes* 51(2), 376–384 (2002)

41. Q. Gong, M. Kakei, N. Koriyama, M. Nakazaki, S. Morimitsu, K. Yaekura, C. Tei, P2Y-purinoceptor mediated inhibition of L-type Ca2+ channels in rat pancreatic beta-cells. *Cell Struct. Funct.* 25(5), 279–289 (2000)

42. M.C. Jacques-Silva, M. Correa-Medina, O. Cabrera, R. Rodriguez-Diaz, N. Makeeva, A. Fachado, J. Diez, D.M. Berman, N.S. Kenyon, C. Ricordi, A. Pileggi, R.D. Molano, P.O. Berggren, A. Caicedo, ATP-gated P2X3 receptors constitute a positive autocrine signal for insulin release in the human pancreatic beta cell. *Proc. Natl. Acad. Sci. USA* 107(14), 6465–6470 (2010)

43. J. Fernandez-Alvarez, D. Hillaire-Buys, M.M. Loubatieres-Mariani, R. Gomis, P. Petit, P2 receptor agonists stimulate insulin release from human pancreatic islets. *Pancreas* 22(1), 69–71 (2001)

44. Khan, S., Yan-Do, R., Duong, E., Wu, X., Bautista, A., Cheley, S., MacDonald, P.E., Braun, M. Autocrine activation of P2Y receptors couples Ca influx to Ca release in human pancreatic beta cells. *Diabetologia* (2014)

45. P.E. MacDonald, M. Braun, J. Galvanovskis, P. Rorsman, Release of small transmitters through kiss-and-run fusion pores in rat pancreatic beta cells. *Cell. Metab.* 4(4), 283–290 (2006)

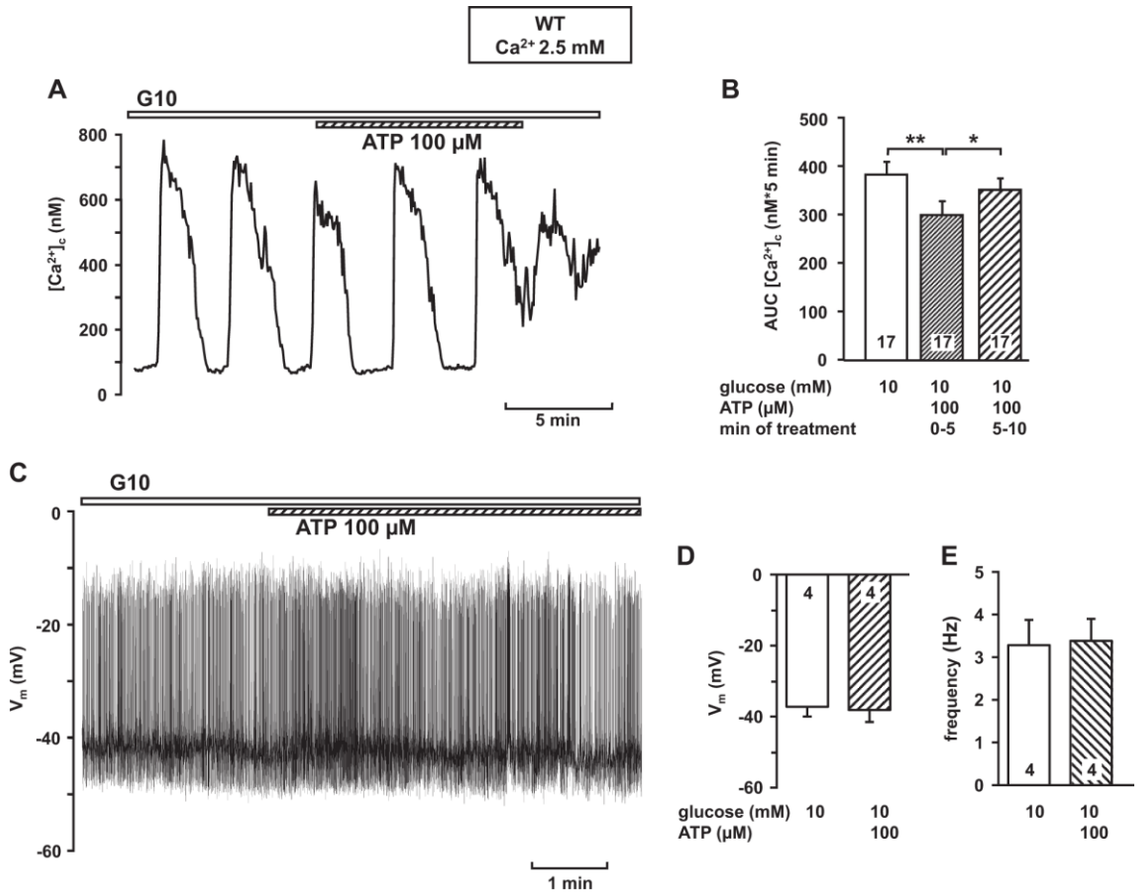

Fig. 1: Extracellular ATP slightly affects V_m and $[Ca^{2+}]_c$ in the presence of 10 mM glucose and 2.5 mM Ca^{2+}. **A** Representative recording presenting regular oscillations of $[Ca^{2+}]_c$. ATP application results in transiently reduced AUC of $[Ca^{2+}]_c$. **B** Summary of the quantitative analysis of the AUC of $[Ca^{2+}]_c$ before and after addition of ATP. **C** ATP does not affect V_m in the presence of 2.5 mM Ca^{2+}. Representative recording showing continuous spike activity in response to 10 mM glucose and 2.5 mM Ca^{2+}, measured in the perforated-patch configuration. **D** Summary of the quantitative analysis of the membrane potential measurements. Values under control condition and after addition of ATP were taken at the plateau potential 2.5 min before solution change. **E** Action potential frequency determined during a period of 2.5 min before ATP application and between min 2.5 and 5 in the presence of ATP. The numbers in the columns indicate the number of experiments with different cell clusters from two to three different preparations. *$P \leq 0.05$, **$P \leq 0.01$

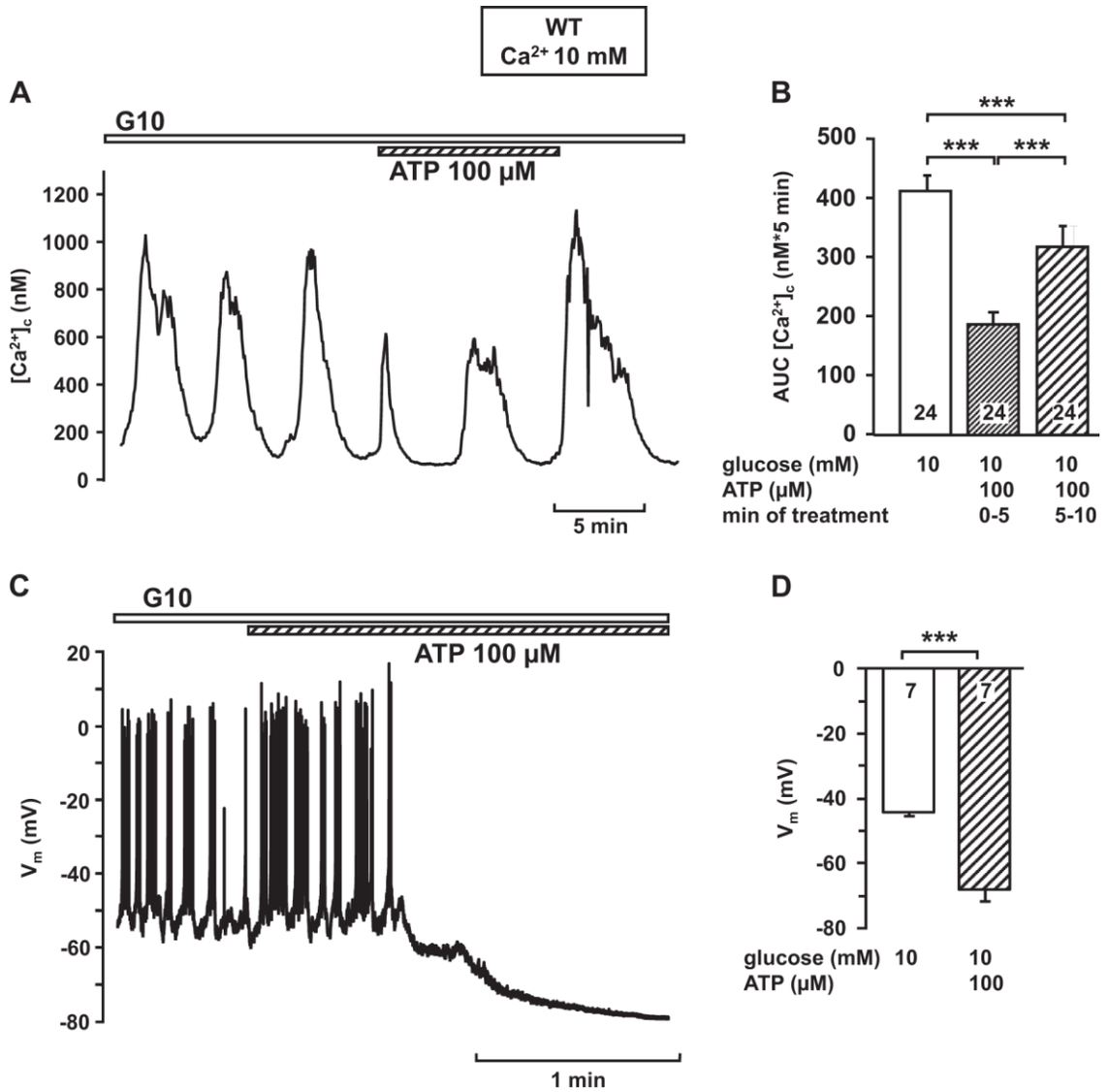

Fig. 2: Enhancing the negative feedback of Ca^{2+} on SSC augments the effectiveness of extracellular ATP on V_m and $[Ca^{2+}]_c$. ATP clearly affects oscillations of $[Ca^{2+}]_c$ and V_m in the presence of 10 mM glucose and 10 mM Ca^{2+}. **A** Representative recording showing regular oscillations of $[Ca^{2+}]_c$. ATP addition leads to a reduction in the AUC of $[Ca^{2+}]_c$. **B** Summary of the quantitative analysis of the AUC of $[Ca^{2+}]_c$ before and after addition of ATP. **C** ATP hyperpolarizes the cell membrane potential (V_m). Representative recording measured in the perforated-patch configuration showing slow waves in response to 10 mM glucose and 10 mM Ca^{2+}. **D** Summary of the quantitative analysis of V_m measurements. Values under control condition were taken at the plateau potential, values after application of ATP at the maximal hyperpolarization. The numbers in the columns indicate the number of experiments with different cell clusters from at least three different mice. ***$P \leq 0.001$

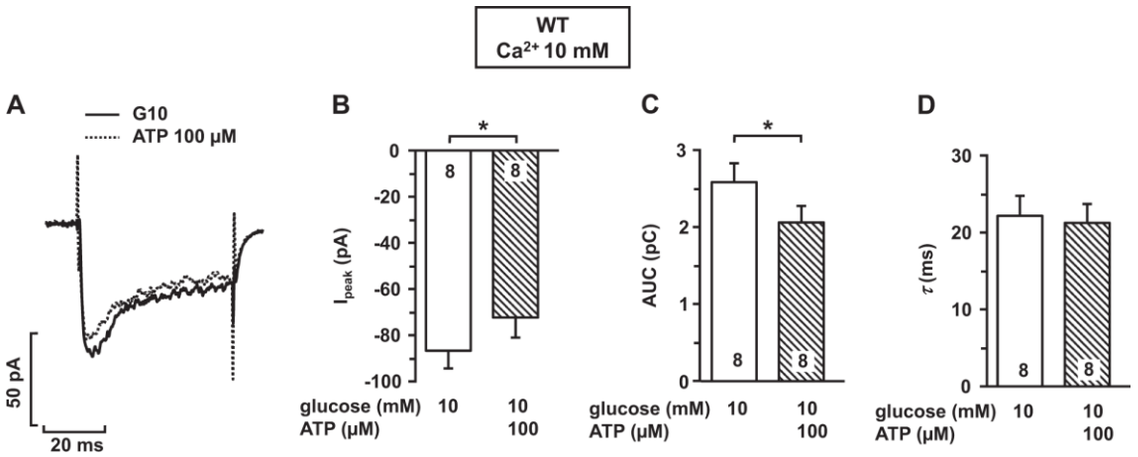

Fig. 3: Extracellular ATP influences currents through L-type Ca^{2+} channels. **A** Representative recordings of I_{Ca} under control conditions (black curve) and after addition of ATP (dotted curve). Currents were elicited by 50 ms voltage steps from –70 to 0 mV. **B**–**D** Summary of the quantitative analysis of the peak current (I_{peak}) (**B**) and the charge movement (determined by the area under the curve (AUC)) (**C**) as well as the inactivation of the currents determined by the time constant τ (**D**). The numbers in the columns indicate the number of experiments with different cell clusters from at least three different mice. *$P \leq 0.05$

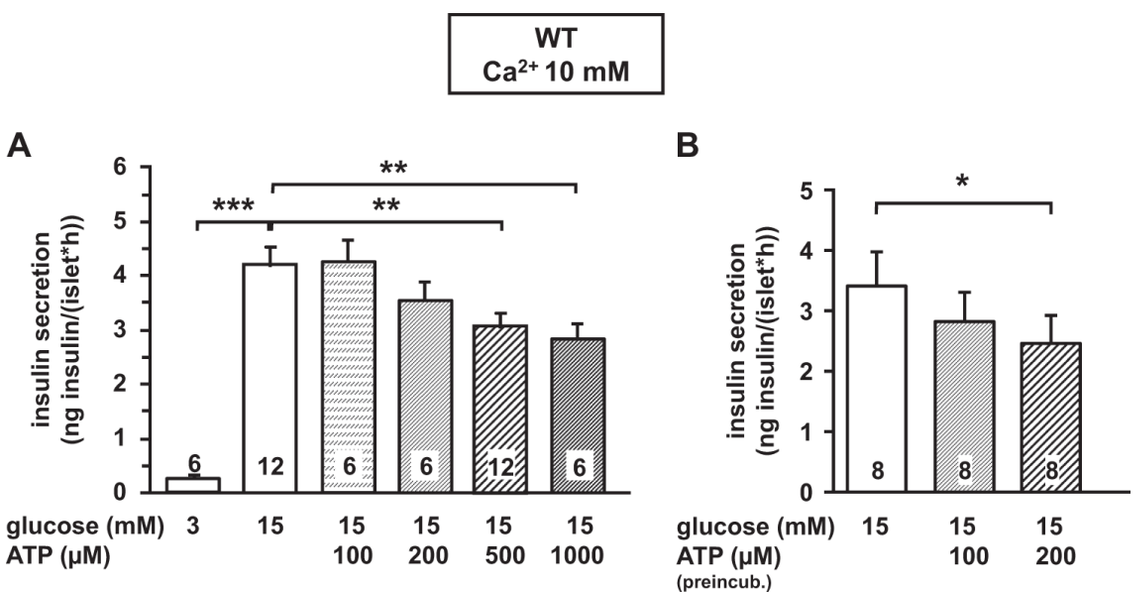

Fig. 4: Extracellular ATP reduces steady-state insulin secretion. **A** ATP dose-dependently decreases insulin secretion in the presence of 15 mM glucose after 1 h incubation under steady-state conditions. **B** Pre-treatment with ATP for 1 h reduces the response to a subsequent glucose stimulus. The numbers in the columns indicate the number of mice. *$P \leq 0.05$, **$P \leq 0.01$, ***$P \leq 0.001$

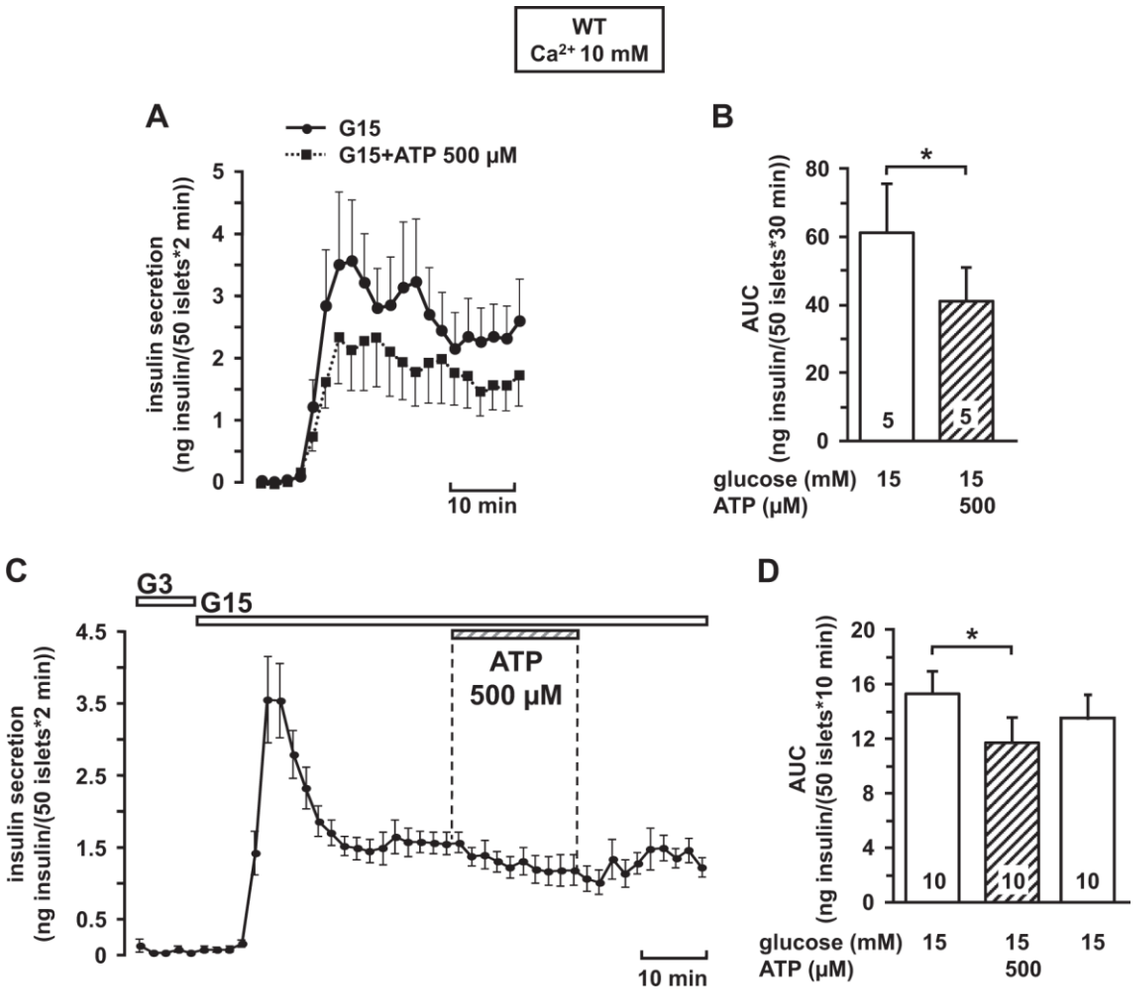

Fig. 5: Extracellular ATP diminishes first and second phase insulin secretion. **A** ATP reduces the first phase of insulin secretion. Curves represent the mean values of first phase insulin secretion. Samples were taken every 2 min. Isolated islets were either perifused with 15 mM glucose without (black curve) or with ATP (dotted curve). In both cases, islets were silenced with 3 mM glucose (±ATP 500 µM) before solution change. **B** Summary of the quantitative analysis determined by the AUC of the first 30 min after changing the glucose concentration from 3 to 15 mM (±ATP 500 µM). **C** ATP reduces the second phase of insulin secretion. The curve represents the mean values of the first and second phase of insulin secretion under control conditions. Administration of ATP in the second phase leads to reduction of insulin secretion. Samples were taken every 2 min. **D** Summary of the quantitative analysis determined by the AUC of the last 10 min under control conditions and ATP administration, respectively. The numbers in the columns indicate the number of mice. *$P \leq 0.05$

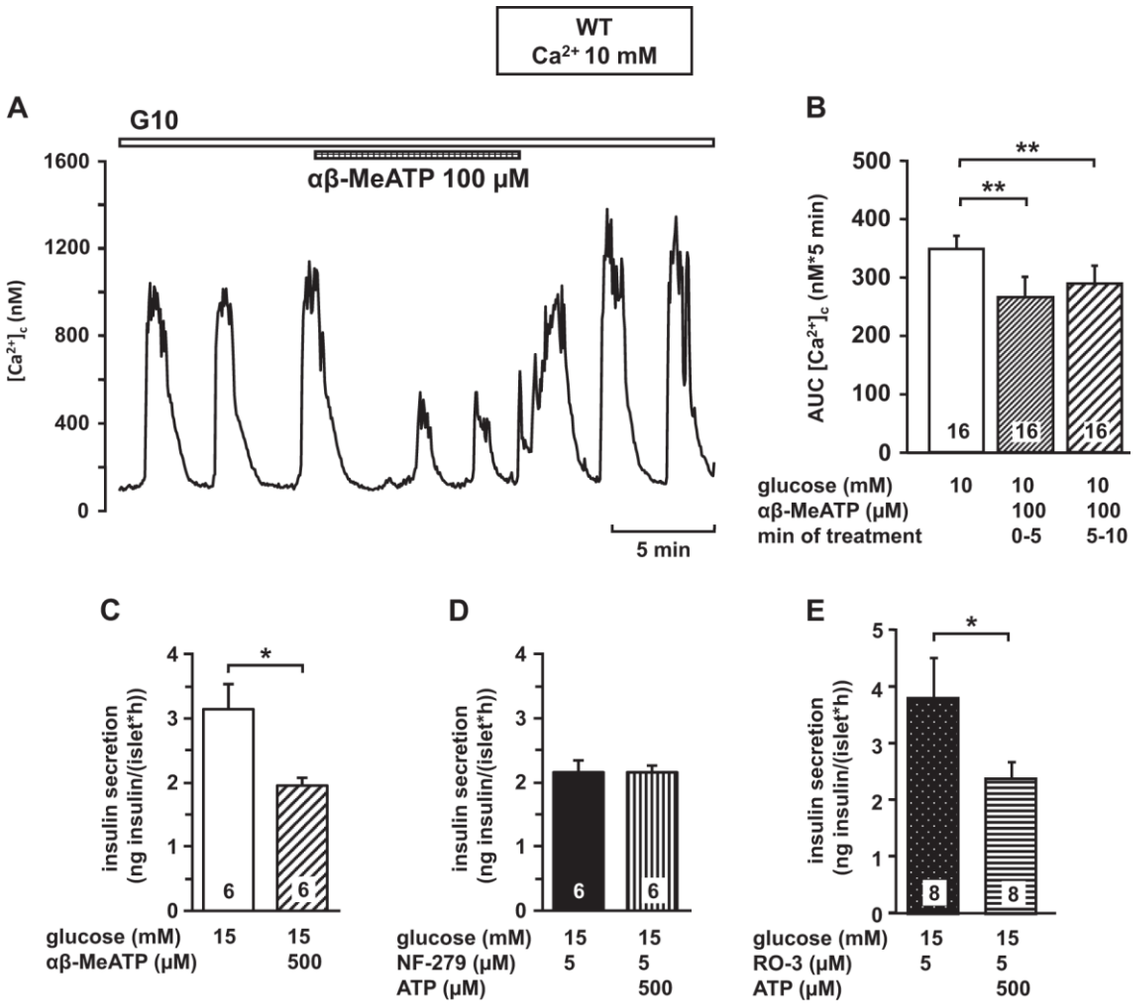

Fig. 6: Extracellular ATP mediates its effects by activating P2X receptors. The $P2X_{1,3}$ agonist αβ-MeATP (100 µM) mimics the effect of ATP on oscillations of $[Ca^{2+}]_c$. **A** Representative recording showing regular oscillations of $[Ca^{2+}]_c$. αβ-MeATP (100 µM) reduced the AUC of $[Ca^{2+}]_c$. **B** Summary of the quantitative analysis of the AUC of $[Ca^{2+}]_c$ before and after application of αβ-MeATP. **C** αβ-MeATP (500 µM) reduces insulin secretion in the presence of 15 mM glucose after 1 h incubation under steady-state conditions. **D** After inhibition of $P2X_1$ channels with the specific antagonist NF-279 (5 µM) ATP has no effect on insulin secretion in 15 mM glucose. **E** The $P2X_3$ receptor blocker RO-3 does not alter the effect of ATP on insulin secretion. The numbers in the columns indicate the number of experiments with different cell clusters from three different mice (**A**, **B**) or the number of mice used for islet preparations (**c**–**e**). $*P \leq 0.05$, $**P \leq 0.01$

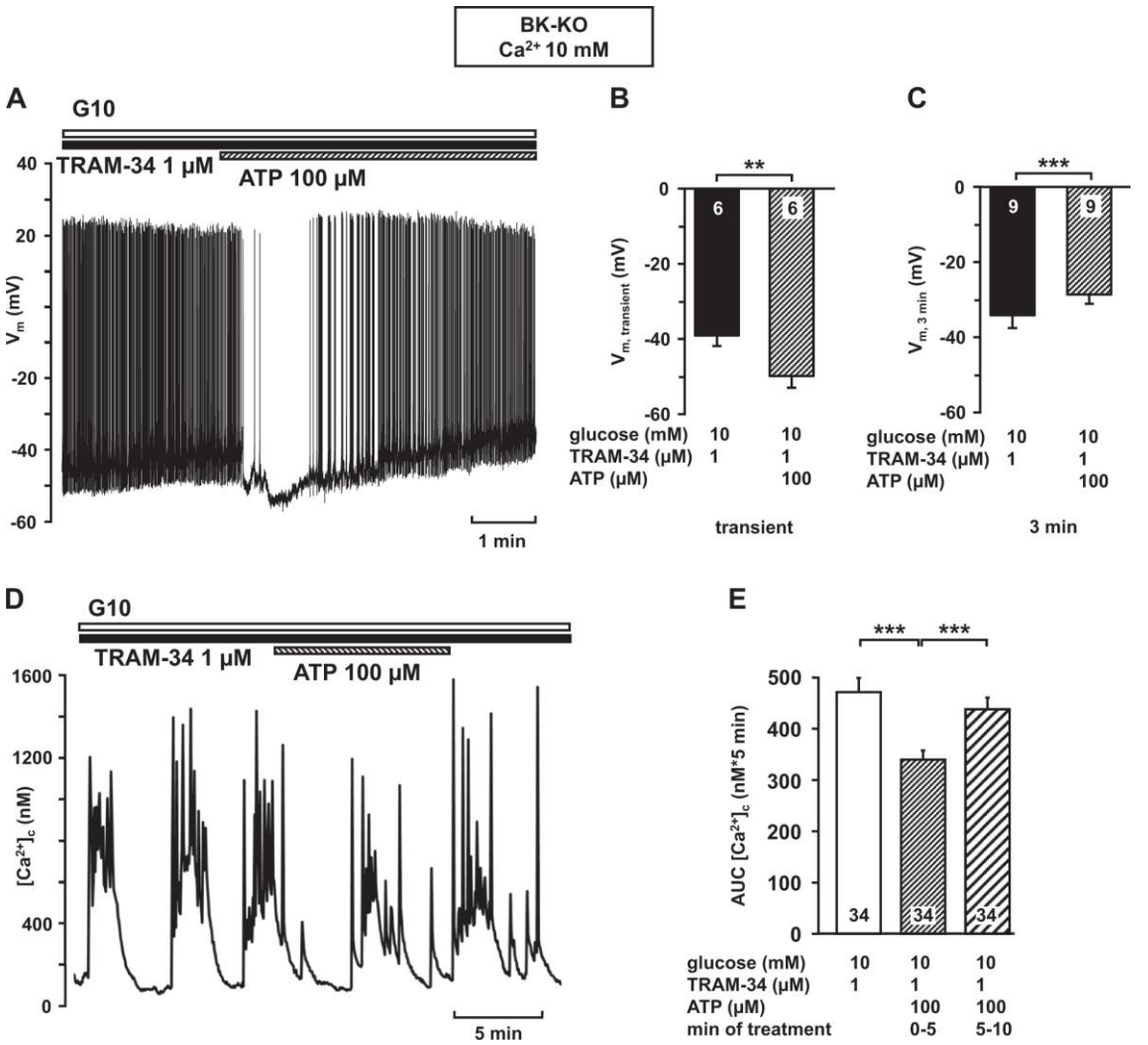

Fig. 7: Possible involvement of Ca^{2+}-dependent potassium channels. **A** The effect of ATP on V_m is reduced after elimination of BK and SK4 channels. Representative recording showing continuous spike activity in β-cells of BK-KO mice after addition of the SK4 channel blocker TRAM-34 measured in the perforated-patch configuration. ATP hyperpolarizes V_m only transiently and leads to a slight depolarization during the last period of administration. **B**, **C** Summary of the quantitative analysis of V_m measurements. Values under control condition were taken at the plateau potential; values under ATP were determined at the minimum of hyperpolarization (**B**) and over the last 3 min of ATP administration (**C**). **D** The effect of ATP on Ca^{2+} oscillations is reduced after inhibition of SK4 channels in BK-KO β-cells. Representative recording showing regularly oscillations of $[Ca^{2+}]_c$ in β-cells of BK-KO mice treated with the SK4 channel blocker TRAM-34. ATP does not cause a significant delay of the start of the next oscillation after ATP administration and reduces its amplitude less pronounced compared to untreated WT β-cells. **E** Summary of the quantitative analysis of the AUC of $[Ca^{2+}]_c$ before and after addition of ATP. The numbers in the columns indicate the number of experiments with different cell clusters from three different mice. $^{**}P \leq 0.01$, $^{***}P \leq 0.001$

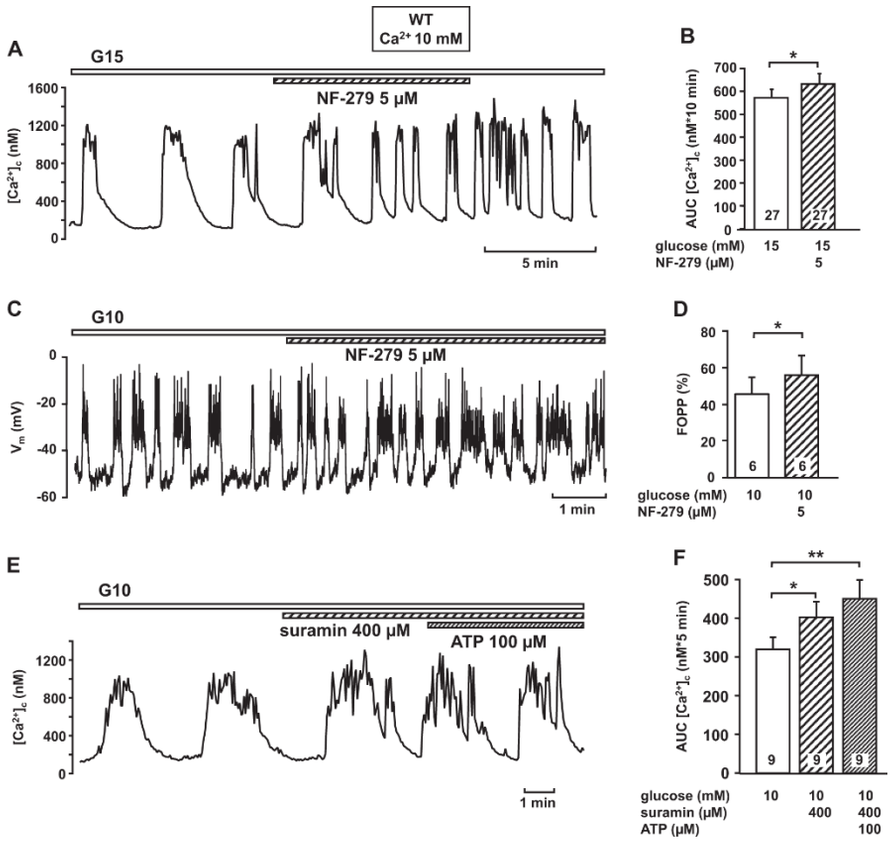

Fig. 8: Blockage of $P2X_1$ channels augments the fraction of plateau phase and the AUC of $[Ca^{2+}]_c$. **A** Representative recording showing regular oscillations of $[Ca^{2+}]_c$. NF-279 (5 µM) increases $[Ca^{2+}]_c$. **B** Summary of the quantitative analysis of the AUC of $[Ca^{2+}]_c$ before and after application of NF-279. **C** Representative recording showing oscillations of V_m with burst and interburst phases. Application of NF-279 (5 µM) augments the fraction of plateau phase (FOPP). **D** Summary of the quantitative analysis of the FOPP before and after application of NF-279. **E** Representative recording demonstrating the effect of suramin (400 µM) on the AUC of $[Ca^{2+}]_c$. **F** Quantitative analysis of the data of this series. The numbers in the columns indicate the number of experiments with different cell clusters from three different mice. $*P \leq 0.05$, $**P \leq 0.01$

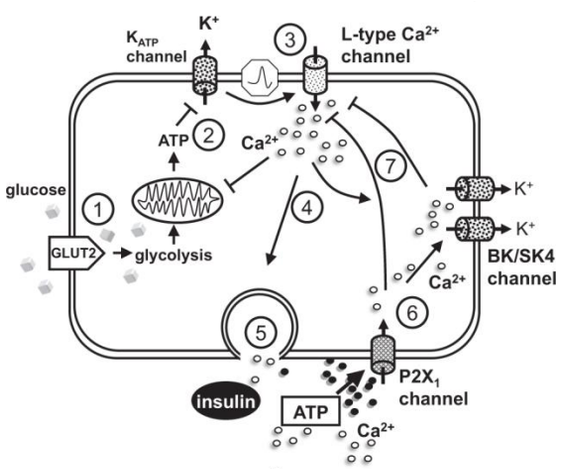

Fig. 9: Proposed model. For details see text

8.4 M-TGR5 - TGR5 Activation Promotes Stimulus-Secretion Coupling of Pancreatic β-Cells via a PKA-Dependent Pathway

Maczewsky J[1], Kaiser J[1], Gresch A[2], Gerst F[3], Düfer M[2], Krippeit-Drews P[1], Drews G[1]

[1]Institute of Pharmacy, Department of Pharmacology, Eberhard Karls University of Tübingen, Tübingen, Germany; [2]Institute of Pharmaceutical and Medicinal Chemistry, Department of Pharmacology, University of Münster, Münster, Germany; [3]Institute for Diabetes Research and Metabolic Diseases, Helmholtz Center Munich, Eberhard Karls University of Tübingen, Tübingen, Germany

Published: Diabetes. 2019 Feb;68(2):324-336. doi: 10.2337/db18-0315

Abstract

The Takeda-G-protein-receptor-5 (TGR5) mediates physiological actions of bile acids. Since it was shown that TGR5 is expressed in pancreatic tissue, a direct TGR5 activation in β-cells is currently postulated and discussed. The current study reveals that oleanolic acid (OLA) affects murine β-cell function by TGR5 activation. Both a $G_{\alpha s}$ inhibitor and an inhibitor of adenylyl cyclase (AC) prevented stimulating effects of OLA. Accordingly, OLA augmented the intracellular cAMP concentration. OLA and two well-established TGR5 agonists, RG239 and tauroursodeoxycholic acid (TUDCA), acutely promoted stimulus-secretion coupling (SSC). OLA reduced K_{ATP} current and elevated current through Ca^{2+} channels. Accordingly, in mouse and human β-cells, TGR5 ligands increased the cytosolic Ca^{2+} concentration by stimulating Ca^{2+} influx. Higher OLA concentrations evoked a dual reaction, probably due to activation of a counterregulating pathway. Protein kinase A (PKA) was identified as a downstream target of TGR5 activation. In contrast, inhibition of phospholipase C and phosphoinositide 3-kinase did not prevent stimulating effects of OLA. Involvement of exchange protein directly activated by cAMP 2 (Epac2) or farnesoid X receptor (FXR2) was ruled out by experiments with knockout mice. The proposed pathway was not influenced by local glucagon-like peptide 1 (GLP-1)

secretion from α-cells, shown by experiments with MIN6 cells, and a GLP-1 receptor antagonist. In summary, these data clearly demonstrate that activation of TGR5 in β-cells stimulates insulin secretion via an AC/cAMP/PKA-dependent pathway, which is supposed to interfere with SSC by affecting K_{ATP} and Ca^{2+} currents and thus membrane potential.

Introduction

In recent years, it became evident that the membrane protein Takeda-G-protein-receptor-5 (TGR5), also known as GPBA, MBAR, or Gpbar1, plays an important role in energy and glucose metabolism (1,2). TGR5 is present in several tissues and cell types including heart, spleen, intestine, macrophages, and pancreas (3,4). The receptor is involved in physiological processes such as inflammation, gallbladder filling, gastrointestinal motility, and thermogenesis (1,5–7). TGR5 stimulates secretion of glucagon-like peptide 1 (GLP-1) from intestinal L cells and thus regulates glucose metabolism (8–10). TGR5 activation leads to energy expenditure, which in turn improves glucose homeostasis (9). Noteworthy, after vertical sleeve gastrectomy, TGR5 contributes to the beneficial effects of the surgery (11).

The endogenous ligands of the receptor are bile acids that potently regulate glucose homeostasis (3). For oleanolic acid (OLA), a triterpene isolated from *Olea europaea* that improves metabolic disorders and has antidiabetes effects (12,13), the situation is less clear. While OLA is proposed to be a TGR5 agonist in pancreatic islets by one study (4), another group excludes an increase in cAMP concentration by OLA normally observed downstream of TGR5 activation (14). In addition, direct effects of OLA on β-cells through increased acetylcholine levels and the muscarinic M_3 receptor were reported (15).

Since it was discovered that TGR5 is present in pancreatic β-cells, several in vitro studies described a direct effect of TGR5 on islet cell function (4,16–18). First, Kumar et al. (4) showed the stimulating effect of TGR5 agonists on insulin secretion in β-cells by an increase of intracellular Ca^{2+} concentration ($[Ca^{2+}]_c$) due

to Ca^{2+} release from intracellular stores. They postulated a pathway through cAMP, exchange protein directly activated by cAMP (Epac), and phospholipase C (PLC) (4). In contrast, another study found that activation of TGR5 by the bile acid tauroursodeoxycholic acid (TUDCA) stimulates insulin secretion via protein kinase A (PKA) (16). This pathway was associated neither with changes in the activity of K_{ATP} channels nor with modified Ca^{2+} signals but included an increase of cAMP, activation of PKA, and phosphorylation of cAMP response element–binding protein (CREBP) (16). Both studies demonstrated TGR5 activation in clonal and murine β-cells, respectively. However, the results point to completely different cAMP-mediated signaling pathways.

It cannot be ruled out that some effects of TGR5 agonists are mediated by the farnesoid X receptor (FXR). Some bile acids are able to rapidly activate a nongenomic FXR-dependent pathway in β-cells (19). FXR and TGR5 are known to influence each other after ligand binding. However, the exact mechanism of this interaction has not been clarified yet (20).

Another in vitro study suggests that stimulating effects of TGR5 agonists in the pancreas are mainly due to GLP-1 released from α-cells that acts in a paracrine manner on β-cells (18). As with GLP-1, activation of TGR5 improves mass and function of β-cells in diabetic mouse models (21). Thus, TGR5 agonists might have a promising therapeutic profile (12).

Taken together, the potential of TGR5 to influence glucose metabolism has been shown in several studies. However, the precise pathways and contribution of different islet cells and peripheral organs are still a matter of debate. Therefore, in the current study the direct effects of OLA and two well-known TGR5 agonists on β-cell stimulus-secretion coupling (SSC) were investigated.

Research Design and Methods

Cell and Islet Preparation

Details are described by Gier et al. (22). In brief, mouse islets were isolated by injecting collagenase (0.5–1 mg/mL) into the pancreas and by handpicking after digestion at 37°C. Male and female wild-type C57Bl/6 (WT) mice were used in equal shares. FXR knockout ($FXR^{-/-}$) mice and Epac2 knockout ($Epac2^{-/-}$) mice are all on a C57Bl/6 background and were housed under same conditions. Mice were bred in the animal facility of the Department of Pharmacology at the University of Tübingen. Principles of laboratory animal care (NIH publication no. 85-23, revised 1985) and German laws were followed. Human islets were provided, by JDRF award 31-2008-416 (European Consortium for Islet Transplantation Islet for Basic Research Program), from the Islet Transplantation Centre (Milan, Italy). Mouse and human islets were dispersed to single cells and cell clusters, respectively, by trypsin treatment.

Solutions and Chemicals

Recordings of $[Ca^{2+}]_c$ were performed with a bath solution that contained (in mmol/L) 140 NaCl, 5 KCl, 1.2 $MgCl_2$, 2.5 $CaCl_2$, glucose as indicated, and 10 HEPES, pH 7.4, adjusted with NaOH. The same bath solution was used for patch clamp measurements to record K_{ATP} current and membrane potential (V_m) in the perforated patch configuration. For Ca^{2+} current measurements in the perforated patch configuration, bath solution consisted of (in mmol/L) 115 NaCl, 1.2 $MgCl_2$, 10 $CaCl_2$, 10 tetraethylammonium chloride, 10 HEPES, 15 glucose, and 0.1 tolbutamide, pH 7.4, adjusted with NaOH. Krebs-Ringer HEPES solution (KRH) for insulin secretion was composed of (in mmol/L) 120 NaCl, 4.7 KCl, 1.1 $MgCl_2$, 2.5 $CaCl_2$, glucose as indicated, 10 HEPES, and 0.5% BSA, pH 7.4, adjusted with NaOH. Pipette solution for cell-attached K_{ATP} current and V_m recordings consisted of (in mmol/L) 10 KCl, 10 NaCl, 70 K_2SO_4, 4 $MgCl_2$, 2 $CaCl_2$, 10 EGTA, 20 HEPES, and 0.27 amphotericin B, pH, adjusted to 7.15 with KOH. For determination of the Ca^{2+} currents, pipette solution was composed of (in mmol/L) 10 KCl, 10 NaCl, 7 $MgCl_2$, 70 Cs_2SO_4, 10 HEPES, and 0.27 amphotericin B, with pH adjusted to 7.15 with NaOH. Murine islet cell clusters and islets were cultured in RPMI 1640 (11.1

mmol/L glucose) enriched with 10% FCS and 1% penicillin/streptomycin. MIN6 cells were incubated in DMEM containing 22.2 mmol/L glucose, 15% FCS, and 1% penicillin/streptomycin. Human islets were kept in Connaught Medical Research Laboratories medium with 5.5 mmol/L glucose.

OLA and NF449 were obtained from Biomol (Hamburg, Germany). Fura-2-acetoxymethyl ester (Flura-2-AM) was purchased from Biotrend (Köln, Germany). Edelfosine and myristoylated protein kinase A inhibitor 14-22 amide (Myr-PKI) were from Tocris (Wiesbaden, Germany). RPMI 1640 medium, FCS, penicillin/streptomycin, and trypsin were from Invitrogen (Karlsruhe, Germany). DMEM medium was from Biozym Scientific (Hessisch Oldendorf, Germany). TUDCA was obtained from Merck (Darmstadt, Germany) and exendin (9-39) amide (exendin 9-39) from Bachem (Bubendorf, Switzerland). The cAMP ELISA kit was from Cayman Chemical, Ann Arbor, MI. All other chemicals were purchased from Sigma-Aldrich (Deisenhofen, Germany) or Merck in the purest form available.

Measurement of $[Ca^{2+}]_c$

Details have previously been published (22). In brief, cells were loaded with 5 µmol/L Fura-2-AM for 35 min at 37°C. Fluorescence was excited at 340 and 380 nm and emission filtered (LP515) and measured by a digital camera. $[Ca^{2+}]_c$ was calculated according to an in vitro calibration. The mean $[Ca^{2+}]_c$ over 10 min at the end of each interval was calculated to compare $[Ca^{2+}]_c$ under different experimental conditions.

Patch Clamp Measurements

Patch pipettes were pulled from borosilicate glass capillaries (Harvard Apparatus, March-Hugstetten, Germany). Ionic currents and V_m were recorded with an EPC-9 patch clamp amplifier using PatchMaster software (HEKA, Lambrecht, Germany). For determination of the K_{ATP} current, pulses of 300 ms were performed every 15 s from the holding potential at −70 to −60 and −80 mV, which is the equivalence potential without any current. The amplitude of currents elicited by voltage steps from the holding potential to −60 mV was taken for evaluation. Data of the last three pulses in each interval were averaged and normalized to the control

condition. Ca^{2+} currents were triggered by 100-ms steps from −70 to 0 mV. K^+ currents were blocked by tetraethylammonium chloride (TEA), K^+-free bath solution, and the K_{ATP} channel antagonist tolbutamide. The maximum Ca^{2+} current was analyzed. For statistics the currents of three succeeding pulses for each measuring point were averaged and data were normalized to the control condition. V_m measurements were evaluated by determination of the plateau potential (from which spikes start) and spike frequency during a 1-min interval after achievement of the maximum OLA effect (minute 4–7 after application). In experiments with KT5720, plateau potential and spike frequency were estimated during 1 min before OLA application and at minute 5–6 after OLA addition.

Insulin Secretion

Details for steady-state incubations have previously been described 23. Briefly, batches of five islets in triplicate were incubated in 1 mL KRH for 1 h at 37°C under conditions indicated. For perifusion experiments, bath chambers were equipped with 50 islets and perifused with KRH under conditions indicated at a rate of 0.7 mL/min at 37°C. Eluate samples were taken every 2 min. MIN6 cells were incubated for 1 h at 37°C under conditions indicated. For determination of the first phase of insulin secretion, AUC was calculated between mins 6 (start of increase) and 21 after the switch to 15 mmol/L glucose.

Insulin was determined by radioimmunoassay (Merck Millipore). Results are presented as the secreted insulin per islet in a specific time. In addition, for MIN6 cells secreted insulin was normalized to the total insulin content and high glucose control condition.

Measurement of cAMP

Batches of 100 islets were incubated in 2 mL KRH for 1 h at 37°C under conditions indicated. Thereafter, buffer was removed and islets were lysed in 0.1 mol/L HCl. Supernatant was used for measuring cAMP by ELISA according to the manufacturer’s protocol.

Statistics

Each series of experiments was performed with islets or islet cells from at least three different mice. Means ± SEM are given for the indicated number of experiments (cell clusters or islets). Statistical significance of differences was assessed by a paired Student *t* test. Multiple comparisons were made by repeated ANOVA followed by the Student-Newman-Keuls test. *P* values ≤0.05 were considered significant.

Results

Effect of OLA on $[Ca^{2+}]_c$ and Insulin Secretion

The triterpene OLA, extracted from olive leaves, is a powerful modulator of glucose homeostasis (12,13). However, it is not clear by which receptors and downstream pathways OLA interferes with SSC. For evaluation of whether OLA affects β-cell function, its effects on $[Ca^{2+}]_c$ and insulin secretion in isolated β-cells and islets, respectively, were investigated. In the presence of 15 mmol/L glucose, $[Ca^{2+}]_c$ oscillated. OLA increased mean $[Ca^{2+}]_c$ in WT mouse β-cells (Fig. 1*A*–*D*). Figure 1*E* and *F* reveals that OLA also augmented $[Ca^{2+}]_c$ in human β-cells. For evaluation of how this change in $[Ca^{2+}]_c$ affects insulin secretion, perifusion experiments with islets of WT mice were performed. Switching from a low to a stimulating glucose concentration evoked the typical biphasic pattern. A first peak secretion (first phase) is followed by consistent release at a lower level (second phase). Addition of 1 µmol/L OLA to the second phase slightly augmented insulin secretion (Fig. 2*A*). The mean insulin secretion rate for 10 min increased from 22 ± 3 pg insulin/(min × islet) under the control condition to 24 ± 3 pg insulin/(min × islet) (Fig. 2*B*). In addition to this small, yet significant, effect, the first phase was analyzed in the presence of 1 µmol/L OLA (Fig. 2*C*). The mean insulin secretion (AUC) during the first 15 min of the first phase of insulin secretion under the high glucose condition was clearly augmented in the presence of 1 µmol/L OLA (37 ± 6 pg insulin/(min × islet)) in comparison with control condition without OLA (27 ± 3 pg insulin/(min × islet)) (Fig. 2*D*).

Steady-state insulin secretion comprises both phases of insulin secretion. Application of 1 µmol/L and 10 µmol/L OLA augmented insulin secretion in the presence of 15 mmol/L glucose to 147 ± 11 and 145 ± 16%, respectively (Fig. 2*E*); 0.1 µmol/L OLA was without effect (113 ± 5%)

The glucose dependency of the drug effect was tested in the presence of 1 µmol/L OLA. OLA did not affect basal insulin secretion at 3 mmol/L glucose but increased it above the threshold concentration for the initiation of insulin secretion (8 mmol/L) and at higher glucose concentrations (Fig. 2*F*).

Dependence of OLA-Mediated Effects on $G_{\alpha s}$ and FXR

OLA structurally resembles bile acids. Since acute effects of bile acids in β-cells can be mediated by FXR (19), a possible interaction of the TGR5 agonist with this receptor was investigated. In β-cells of $FXR^{-/-}$ mice, 1 µmol/L OLA increased mean $[Ca^{2+}]_c$ similarly to the effect in WT mice (Fig. 3*A* and *B*). Accordingly, 1 µmol/L OLA enhanced insulin secretion from islets of $FXR^{-/-}$ mice (Fig. 3*C*).

Since the TGR5 is G_s-coupled, the influence of NF449, an inhibitor of the $G_{\alpha s}$ subunit, on TGR5 activation was investigated to test for this pathway. NF449 (10 µmol/L) did not affect insulin secretion but completely blocked the stimulating effect evoked by OLA in islets of WT mice (Fig. 3*D*).

Confirmation of the Influence of TGR5 Activation on β-Cell Function by Two Other TGR5 Agonists

The synthetic TGR5 agonist RG239 (1 µmol/L) increased mean $[Ca^{2+}]_c$ (Fig. 4*A* and *B*) and insulin secretion (Fig. 4*C*). TUDCA (50 µmol/L), another TGR5 ligand with bile acid structure, provided very similar results for mean $[Ca^{2+}]_c$ (Fig. 4*D* and *E*) and insulin secretion (Fig. 4*F*), emphasizing the significance of TGR5 for β-cell function.

Effects of OLA on K_{ATP} and Ca^{2+} Channel Currents

In the well-accepted model of SSC in β-cells, increased $[Ca^{2+}]_c$ can result from Ca^{2+} influx due to closure of K_{ATP} channels with subsequent opening of voltage-dependent Ca^{2+} channels (VDCCs) or to opening of VDCCs. Activity of both channels can be affected by protein kinases (24–26). Patch clamp measurements showed an acute effect on K_{ATP} current after OLA administration. In recordings with the perforated patch configuration, 1 μmol/L OLA reduced the K_{ATP} current measured in WT β-cells to 54 ± 3% (12.2 ± 1.2 pA) of the control current (100% [22.8 ± 2.4 pA]) in the presence of 0.5 mmol/L glucose (Fig. 5*A* and *B*). The effect was dose dependent. The inhibitory effect of 10 μmol/L OLA on the K_{ATP} current showed a faster onset of action and reduced the current to 22 ± 2% (7.3 ± 1.3 pA) of the control level (100%, 32.9 ± 5.3 pA) (Fig. 5*C* and *D*). The currents were identified as K_{ATP} channel currents by use of the K_{ATP} opener diazoxide at the end of each measurement.

As mentioned above, phosphorylation may influence VDCCs. The peak Ca^{2+} current, measured in the perforated patch configuration, was increased to 118 ± 2% (70.8 ± 9.9 pA) and 122 ± 3% (73.2 ± 10.4 pA) after 2 and 4 min of 1 μmol/L OLA administration, respectively, compared with the control condition (100% [60.5 ± 8.8 pA]) (Fig. 5*E* and *F*). At the higher OLA concentration of 10 μmol/L, peak Ca^{2+} current was augmented after 2 min of drug application but strongly inhibited after 8 min (Fig. 6*A* and *B*). OLA (10 μmol/L) also affected second-phase insulin secretion in a biphasic manner (Fig. 6*C* and *D*). Evidently, higher concentrations of OLA induce a counterregulating pathway. This observation could explain why 10 μmol/L OLA was not more effective than 1 μmol/L with regard to steady-state insulin secretion (Fig. 2*E*).

At first glance, it may seem astonishing that a clear dual effect of 10 μmol/L OLA on $[Ca^{2+}]_c$ is missing (Fig. 1*C*). However, despite the strong inhibition of Ca^{2+} currents by 10 μmol/L OLA (Fig. 6), substantial Ca^{2+} influx may remain. First, K_{ATP} current is also markedly reduced by 10 μmol/L OLA (Fig. 5), prolonging the burst time during which Ca^{2+} channels open (transition from oscillations to a plateau in

the presence of 10 µmol/L OLA shown in Fig. 1*C*). Second, inhibition of K_{ATP} current will further depolarize the cells leading to increased opening of Ca^{2+}- and voltage-dependent K^+ channels of large conductance (BK channels), resulting in enhanced Ca^{2+} influx during a single action potential. This assumption is based on the observation that inhibition of BK channels decreases Ca^{2+} influx (27). Nevertheless, the transient effect of 10 µmol/L OLA on $[Ca^{2+}]_c$ can be detected by evaluating maximum Ca^{2+} concentration. In the experiments presented in Fig. 1, maximum Ca^{2+} increased from 831 ± 45 nmol/L (*n* = 26) in the presence of 15 mmol/L glucose to 1,167 ± 75 nmol/L (*n* = 26, *P* ≤ 0.001) after application of 10 µmol/L OLA if the usual evaluation procedure (last 10 min of the application interval) was used. However, it amounted to 874 ± 68 nmol/L if only the last 2 min of OLA application was evaluated (*n* = 26, not significant vs. 15 mmol/L glucose). This shows a clear reduction of maximum Ca^{2+} concentration over time during OLA application.

K_{ATP} and L-type Ca^{2+} channel currents are two key determinants of the membrane potential of β-cells. Thus, the observed effects on the ion channels should result in changes of the V_m. Figure 6*E–G* reveals that OLA depolarized V_m and increased the number of action potentials. The described effects were completely suppressed in the presence of the established PKA inhibitor, KT5720 (Fig. 6*H–J*), pointing to an involvement of this kinase in the OLA-evoked changes in channel activities.

Influence of OLA-Evoked TGR5 Activation on Adenylyl Cyclase and Epac2

The TGR5 belongs to the group of G_s-coupled receptors. The $G_{\alpha s}$ subunit is known to activate adenylyl cyclase (AC), which leads to cAMP production (3). For verification of this pathway for OLA, the AC inhibitor 2′5′-dideoxyadenosine (DDA) was used in insulin secretion experiments. Remarkably, DDA (100 µmol/L) alone had a stimulating effect on insulin secretion (Fig. 7*A*). In the presence of DDA, OLA no longer stimulated insulin secretion but, rather, reduced it. Furthermore, OLA (1 µmol/L) increased the intracellular cAMP concentration by ~23% in five of six experiments (Fig. 7*B*). In one experiment, we observed a paradoxical decrease of ~10%.

Since Epac is one of the postulated targets of cAMP, islets and β-cells of Epac2$^{-/-}$ mice were used to investigate an involvement of this protein in the OLA-activated pathway. Epac2 is the most abundant isoform in β-cells (28). $[Ca^{2+}]_c$ measurements did not reveal any influence of Epac2 on the stimulating effect of 1 μmol/L OLA (Fig. 7*C*). Moreover, the stimulating effects of OLA and RG239 on insulin secretion were still present in islets from Epac2$^{-/-}$ mice (Fig. 7*D*).

Involvement of PKA in the Signaling Cascade Downstream TGR5 Activation

For further evaluation of a possible participation of PKA in the TGR5 signaling pathway, the established PKA inhibitors Myr-PKI and KT5720 were tested on OLA-evoked insulin secretion. Myr-PKI itself increased insulin secretion, while KT5720 alone was without a significant effect compared with the respective control conditions in WT islets. Both inhibitors suppressed the stimulatory effect of 1 μmol/L OLA in the presence of 15 mmol/L glucose (Fig. 8*A* and *B*). OLA even inhibited insulin secretion under these conditions. Since PLC is supposed to be involved in the TGR5 pathway according to Kumar et al. (4), the PLC inhibitor edelfosine was applied. In contrast to PKA inhibitors, edelfosine (10 μmol/L) did not prevent the stimulation evoked by 1 μmol/L OLA (Fig. 8*C* [same controls as in Fig. 8*A*]).

Phosphoinositide 3-kinase (PI3K) is also proposed to be involved in the signaling pathway downstream of TGR5 activation. The PI3K inhibitor wortmannin did not prevent but even amplified the OLA effect on insulin secretion (Fig. 8*D* [same controls as in Fig. 8*B*]). Neither edelfosine nor wortmannin alone changed insulin secretion induced by 15 mmol/L glucose.

α-Cells and GLP-1 Are Not Involved in Effects of OLA in β-Cells

α-Cells can secrete GLP-1, and activation of TGR5 is known to increase GLP-1 production and secretion (18). For exclusion of the possibility that GLP-1 contributes to the OLA-evoked effects in β-cells, the GLP-1 receptor antagonist exendin 9-39 was used in secretion experiments. Exendin 9-39 did not prevent the

stimulating effect of 1 µmol/L OLA on insulin secretion (Fig. 9*A*). The potency of the inhibitor exendin 9-39 at the GLP-1 receptor was proved by the fact that the stimulation of 50 nmol/L GLP-1 was completely blocked by the antagonist (Fig. 9*B* [same controls as in Fig. 9*A*]). Notably, 100 nmol/L exendin 9-39 alone did not significantly alter the amount of secreted insulin. For circumvention of a possible influence of α-cells, the β-cell line MIN6 was used to perform insulin secretion experiments. Insulin secretion of MIN6 cells was dependent on the glucose concentration (insulin levels reached 26.6 ± 2.9% at a low glucose concentration compared with levels at a stimulatory concentration of 15 mmol/L glucose). Application of 1 and 10 µmol/L OLA significantly increased insulin secretion to 111.5 ± 3.0 and 121.4 ± 7.8%, respectively, compared with 15 mmol/L glucose alone (Fig. 9*C*). These experiments support the assumption that the TGR5 agonist OLA acts directly on β-cells.

Discussion

OLA Directly Stimulates β-Cells by Binding to the TGR5

During the last decades, it became evident that TGR5 agonists are important contributors to the regulation of glucose metabolism. Several studies have shown reduction of blood glucose concentration and improvement of the energy expenditure by TGR5 agonists (9,12,29). TGR5 activation in L cells crucially affects GLP-1 secretion (30). Here, we identify OLA as a TGR5 agonist of β-cells and show a stimulating effect of OLA and two other TGR5 agonists, RG239 and TUDCA, on islets of Langerhans in vitro excluding factors like GLP-1 secreted from L cells. TGR5 activation concurrently affects several parameters of SSC including current through K_{ATP} channels and VDCCs and, as a result, V_m. Changes in the activity of these channels are followed by enhanced $[Ca^{2+}]_c$ and insulin secretion. Kumar et al. (4) also demonstrated a direct effect on isolated β-cells after TGR5 agonist administration. In their study, OLA leads to enhanced glucose-induced insulin secretion; however, an increase in $[Ca^{2+}]_c$ is only shown at substimulatory glucose concentration and is attributed to release from intracellular Ca^{2+} stores.

This effect cannot account for increased insulin secretion after stimulation of β-cells with glucose. In contrast, our data clearly show that enhanced Ca^{2+} influx contributes to increased $[Ca^{2+}]_c$ after TGR5 activation at a stimulatory glucose concentration and not at basal one.

In α-cells, alternative splicing of proglucagon enables synthesis and secretion of GLP-1 (17). Kumar et al. (18) observed an increased GLP-1 secretion from pancreatic α-cells after TGR5 activation. They suggest that this is mediated via the cAMP/Epac/PLC-dependent pathway. Moreover, synthesis of GLP-1 in α-cells was stimulated by the cAMP/PKA/phosphorylated CREBP cascade. The authors provide evidence that this pathway is activated by hyperglycemia (18). To examine a possible GLP-1–mediated stimulation of insulin secretion after TGR5 activation under physiological conditions, we blocked the GLP-1 receptor by the antagonist exendin 9-39 (31). Since exendin 9-39 did not prevent the effect of OLA, we conclude that OLA stimulates insulin secretion independent of GLP-1 receptor activation. Kumar et al. (18) performed a similar experiment with human islets but with a higher concentration of exendin 9-39 and after culturing the islets in the presence of 25 mmol/L glucose for 7 days. They claim that in this glucotoxic model, exendin 9-39 reduces the effect of the TGR5 agonist INT-777; however, this reduction is marginal and insulin release is still approximately twofold higher compared with the effect of glucose alone. Our view that the effects of TGR5 agonists are not mediated by GLP-1 released by α-cells is further supported by the observation that OLA increased insulin secretion of MIN6 cells. The MIN6 cell line solely consists of clonal β-cells, and an effect of locally secreted GLP-1 from other cell types can be ruled out (32).

TGR5 agonists are structural analogs of bile acids, the endogenous activators of TGR5. Bile acids acutely affect additional targets regulating glucose metabolism, particularly the FXR (19,33). In β-cells, Vettorazzi et al. (16) found that TUDCA activates a TGR5-dependent pathway and suggested that FXR is not involved. In the current study, the involvement of FXR was excluded owing to experiments with a $FXR^{-/-}$ mouse model. Teodoro et al. (14) also showed a stimulating effect of OLA on insulin secretion but excluded increased cAMP concentration and thus

involvement of the TGR5 as explanation for this observation. In contrast, our results with inhibitors of the $G_{\alpha s}$ subunit and the AC clearly indicate a TGR5-dependent pathway for OLA.

OLA Acts via a cAMP/PKA-Dependent Pathway

The TGR5/$G_{\alpha s}$/AC pathway results in increased cAMP concentrations (5,34). This fits well with the OLA-induced increase of the cAMP concentration and the loss of efficacy of OLA after inhibition of AC in our experiments. Enhanced cAMP levels are known to activate PKA and/or Epac, which is also described for β-cells (4,16,30). Kumar et al. (4) exclude any influence of OLA on PKA in β-cells but describe a pathway via Epac, followed by PLC activation, which leads to enhanced insulin secretion. This suggestion is based on a single series of secretion experiments with MIN6 cells and the high concentration of 50 µmol/L OLA (4). Moreover, Kumar et al. (4) blocked the effect of 50 µmol/L OLA with the PLC antagonist U73122. However, the used concentration of U73122 can exert unspecific effects, such as modulation of transient receptor potential melastatin 3/4 (TRPM3/4) channels as well as stimulation of inositol triphosphate synthesis and mobilization of Ca^{2+} from intracellular stores (35–37).

To clarify the discrepancy in our results, we used an Epac2$^{-/-}$ mouse model. Epac2 is more abundant compared with Epac1 and is an important target of cAMP in β-cells (28,30). Since TGR5 agonists effectively enhanced $[Ca^{2+}]_c$ and insulin secretion in β-cells and islets of Epac2$^{-/-}$ mice, an involvement of Epac2 seems to be unlikely. Nevertheless, a possible influence of Epac1 should be considered. Likewise, PLC blockade by edelfosine did not suppress the OLA effect on insulin secretion, also speaking against an involvement of the Epac/PLC pathway after TGR5 activation.

PI3K has been identified as another downstream target of Epac in processes like angiogenesis or stem cell differentiation (38,39). The PI3K inhibitor wortmannin revealed that PI3K seems not to be involved in stimulating effects of OLA.

We identified PKA as the downstream kinase in the TGR5/cAMP pathway. OLA completely lost the stimulating effect on insulin secretion after PKA inhibition with two different PKA inhibitors, Myr-PKI and KT5720. This is supported by findings of Vettorazzi et al. (16), who showed that the TGR5 agonist TUDCA was ineffective in stimulating insulin secretion in the presence of the PKA inhibitor H89. Worth mentioning, the link between cAMP and PKA is clearly demonstrated for the GLP-1 pathway in β-cells (40,41).

The puzzling observation that inhibition of AC or PKA leads to stimulation of insulin secretion may be due to a cross talk between cAMP and cGMP as described for other organs (42,43), especially activation of a cGMP-specific PDE by PKA (44,45). Inhibition of PKA would thus increase cGMP concentration, leading to protein kinase G (PKG)-dependent closure of K_{ATP} channels (46). Inhibition of the AC by DDA would also reduce PKA activity with similar consequences at least for the cGMP/PKG/K_{ATP} channel signaling pathway. Remarkably, during inhibition of the AC/cAMP/PKA pathway, OLA is not without effect but exerts inhibition of insulin secretion. This is most likely due to the biphasic effect of OLA. Apparently, after inhibition of the stimulatory pathway the inhibitory one that is PKA independent prevails.

K_{ATP} and VDCCs Mediate Stimulating Effects of OLA

Although presenting results in favor of the PKA pathway, Vettorazzi et al. (16) did not find any changes in K_{ATP} channel activity or $[Ca^{2+}]_c$ after TGR5 activation in β-cells. In our experiments, OLA caused both a distinct reduction of the K_{ATP} current and an increase in Ca^{2+} current, probably due to phosphorylation of both channel proteins by PKA. After PKA activation, K_{ATP} channel activity is reduced, resulting in membrane depolarization and enhanced insulin secretion (24). Suitably, OLA-evoked changes in V_m, which are a result of the effects on the channels, are suppressed by the PKA inhibitor KT5720.

The VDCC in pancreatic islet cells is a possible target to control insulin secretion (47). Phosphorylation of VDCCs could affect channel activity, thus increasing the Ca^{2+} current (25,26). It is worth mentioning that the effect of OLA on VDCCs is not secondary to inhibition of K_{ATP} channels, since the latter were not functional under the relevant experimental conditions. Thus, K_{ATP} channel closure and VDCC activation together cause increased $[Ca^{2+}]_c$ followed by enhanced insulin secretion. Since OLA increases $[Ca^{2+}]_c$ in human β-cells, it is to be assumed that the suggested mechanism is also relevant for human β-cells. The proposed direct interaction of PKA with ion channels would result in a rapid effect after TGR5 activation. However, we cannot exclude that other mechanisms besides changes in ion channel activity contribute to the stimulatory effects of TGR5 activation. The cAMP-PKA pathway can directly increase granule exocytosis by enhancing the sensitivity of the exocytotic machinery to Ca^{2+} (48,49). Two other groups postulated modified protein synthesis by PKA-mediated phosphorylation of CREBP (16,18). Such a mechanism is inconsistent with the rapid effects on SSC starting within seconds. However, protein synthesis may account for effects on exocytosis after prolonged exposure to TGR5 agonists (14,16,18).

In summary, we clearly demonstrated that OLA affects β-cell SSC via TGR5 activation and that TGR5 agonists directly stimulate β-cells to secrete insulin. The data suggest a pathway including AC activation, PKA, closure of K_{ATP}, and opening of Ca^{2+} channels and increased Ca^{2+} influx. This insulinotropic effect opens new possibilities for pharmaceutical applications of drugs like OLA.

Acknowledgments. The authors thank Isolde Breuning for excellent and skillful technical assistance. The authors thank Jelena Sikimic for performing some of the experiments with human islet cells and Friederike Anna Steudel and Nia Blackwell for careful and excellent revision of the manuscript, all from Institute of Pharmacy, Department of Pharmacology, Eberhard Karls University of Tübingen.

Funding. This work was supported by a grant from the DFG (Deutsche Forschungsgemeinschaft) (DR 225/11-1 to G.D.).

Duality of Interest. No potential conflicts of interest relevant to this article were reported.

Author Contributions. J.M. researched data and wrote and edited the manuscript. J.K., A.G., and F.G. researched data. M.D. and P.K.-D. contributed to discussion and study design and edited the manuscript. G.D. designed the study, wrote and edited the manuscript, and contributed to discussion. G.D. is the guarantor of this work and, as such, had full access to all the data in the study and takes responsibility for the integrity of the data and the accuracy of the data analysis.

References

1. Watanabe M, Houten SM, Mataki C, et al. Bile acids induce energy expenditure by promoting intracellular thyroid hormone activation. *Nature* 2006;439:484–489

2. Katsuma S, Hirasawa A, Tsujimoto G. Bile acids promote glucagon-like peptide-1 secretion through TGR5 in a murine enteroendocrine cell line STC-1. *Biochem Biophys Res Commun* 2005;329:386–390

3. Kawamata Y, Fujii R, Hosoya M, et al. A G protein-coupled receptor responsive to bile acids. *J Biol Chem* 2003;278:9435–9440

4. Kumar DP, Rajagopal S, Mahavadi S, et al. Activation of transmembrane bile acid receptor TGR5 stimulates insulin secretion in pancreatic β cells. *Biochem Biophys Res Commun* 2012;427:600–605

5. Pols TW, Nomura M, Harach T, et al. TGR5 activation inhibits atherosclerosis by reducing macrophage inflammation and lipid loading. *Cell Metab* 2011;14:747–757

6. Vors C, Pineau G, Drai J, et al. Postprandial endotoxemia linked with chylomicrons and lipopolysaccharides handling in obese versus lean men: a lipid dose-effect trial. *J Clin Endocrinol Metab* 2015;100:3427–3435

7. Li T, Holmstrom SR, Kir S, et al. The G protein-coupled bile acid receptor, TGR5, stimulates gallbladder filling. *Mol Endocrinol* 2011;25:1066–1071

8. Harach T, Pols TW, Nomura M, et al. TGR5 potentiates GLP-1 secretion in response to anionic exchange resins. *Sci Rep* 2012;2:430

9. Thomas C, Gioiello A, Noriega L, et al. TGR5-mediated bile acid sensing controls glucose homeostasis. *Cell Metab* 2009;10:167–177

10. Parker HE, Wallis K, le Roux CW, Wong KY, Reimann F, Gribble FM. Molecular mechanisms underlying bile acid-stimulated glucagon-like peptide-1 secretion. *Br J Pharmacol* 2012;165:414–423

11. McGavigan AK, Garibay D, Henseler ZM, et al. TGR5 contributes to glucoregulatory improvements after vertical sleeve gastrectomy in mice. *Gut* 2017;66:226–234

12. Castellano JM, Guinda A, Delgado T, Rada M, Cayuela JA. Biochemical basis of the antidiabetic activity of oleanolic acid and related pentacyclic triterpenes. *Diabetes* 2013;62:1791–1799

13. Sato H, Genet C, Strehle A, et al. Anti-hyperglycemic activity of a TGR5 agonist isolated from Olea europaea. *Biochem Biophys Res Commun* 2007;362:793–798

14. Teodoro T, Zhang L, Alexander T, Yue J, Vranic M, Volchuk A. Oleanolic acid enhances insulin secretion in pancreatic beta-cells. *FEBS Lett* 2008;582:1375–1380

15. Hsu JH, Wu YC, Liu IM, Cheng JT. Release of acetylcholine to raise insulin secretion in Wistar rats by oleanolic acid, one of the active principles contained in Cornus officinalis. *Neurosci Lett* 2006;404:112–116

16. Vettorazzi JF, Ribeiro RA, Borck PC, et al. The bile acid TUDCA increases glucose-induced insulin secretion via the cAMP/PKA pathway in pancreatic beta cells. *Metabolism* 2016;65:54–63

17. Whalley NM, Pritchard LE, Smith DM, White A. Processing of proglucagon to GLP-1 in pancreatic α-cells: is this a paracrine mechanism enabling GLP-1 to act on β-cells? *J Endocrinol* 2011;211:99–106

18. Kumar DP, Asgharpour A, Mirshahi F, et al. Activation of transmembrane bile acid receptor TGR5 modulates pancreatic islet alpha cells to promote glucose homeostasis. *J Biol Chem* 2016;291:6626–6640

19. Düfer M, Hörth K, Wagner R, et al. Bile acids acutely stimulate insulin secretion of mouse β-cells via farnesoid X receptor activation and K(ATP) channel inhibition. *Diabetes* 2012;61:1479–1489

20. Pathak P, Liu H, Boehme S, et al. Farnesoid X receptor induces Takeda G-protein receptor 5 cross-talk to regulate bile acid synthesis and hepatic metabolism. *J Biol Chem* 2017;292:11055–11069

21. Zheng C, Zhou W, Wang T, et al. A novel TGR5 activator WB403 promotes GLP-1 secretion and preserves pancreatic β-cells in type 2 diabetic mice. *PLoS One* 2015;10:e0134051

22. Gier B, Krippeit-Drews P, Sheiko T, et al. Suppression of KATP channel activity protects murine pancreatic beta cells against oxidative stress. *J Clin Invest* 2009;119:3246–3256
23. Maczewsky J, Sikimic J, Bauer C, et al. The LXR ligand T0901317 acutely inhibits insulin secretion by affecting mitochondrial metabolism. *Endocrinology* 2017;158:2145–2154

24. Light PE, Manning Fox JE, Riedel MJ, Wheeler MB. Glucagon-like peptide-1 inhibits pancreatic ATP-sensitive potassium channels via a protein kinase A- and ADP-dependent mechanism. *Mol Endocrinol* 2002;16:2135–2144

25. Leiser M, Fleischer N. cAMP-dependent phosphorylation of the cardiac-type alpha 1 subunit of the voltage-dependent Ca2+ channel in a murine pancreatic beta-cell line. *Diabetes* 1996;45:1412–1418

26. Fuller MD, Fu Y, Scheuer T, Catterall WA. Differential regulation of CaV1.2 channels by cAMP-dependent protein kinase bound to A-kinase anchoring proteins 15 and 79/150. *J Gen Physiol* 2014;143:315–324

27. Düfer M, Neye Y, Hörth K, et al. BK channels affect glucose homeostasis and cell viability of murine pancreatic beta cells. *Diabetologia* 2011;54:423–432

28. Sugawara K, Shibasaki T, Takahashi H, Seino S. Structure and functional roles of Epac2 (Rapgef4). *Gene* 2016;575:577–583

29. Thomas C, Pellicciari R, Pruzanski M, Auwerx J, Schoonjans K. Targeting bile-acid signalling for metabolic diseases. *Nat Rev Drug Discov* 2008;7:678–693

30. Dzhura I, Chepurny OG, Leech CA, et al. Phospholipase C-ε links Epac2 activation to the potentiation of glucose-stimulated insulin secretion from mouse islets of Langerhans. *Islets* 2011;3:121–128

31. Thorens B, Porret A, Bühler L, Deng SP, Morel P, Widmann C. Cloning and functional expression of the human islet GLP-1 receptor. Demonstration that exendin-4 is an agonist and exendin-(9-39) an antagonist of the receptor. *Diabetes* 1993;42:1678–1682

32. Miyazaki J, Araki K, Yamato E, et al. Establishment of a pancreatic beta cell line that retains glucose-inducible insulin secretion: special reference to expression of glucose transporter isoforms. *Endocrinology* 1990;127:126–132

33. Schittenhelm B, Wagner R, Kähny V, et al. Role of FXR in β-cells of lean and obese mice. *Endocrinology* 2015;156:1263–1271

34. Bala V, Rajagopal S, Kumar DP, et al. Release of GLP-1 and PYY in response to the activation of G protein-coupled bile acid receptor TGR5 is mediated by Epac/PLC-ε pathway and modulated by endogenous H2S. *Front Physiol* 2014;5:420

35. Leitner MG, Michel N, Behrendt M, et al. Direct modulation of TRPM4 and TRPM3 channels by the phospholipase C inhibitor U73122. *Br J Pharmacol* 2016;173:2555–2569

36. Horowitz LF, Hirdes W, Suh BC, Hilgemann DW, Mackie K, Hille B. Phospholipase C in living cells: activation, inhibition, Ca2+ requirement, and regulation of M current. *J Gen Physiol* 2005;126:243–262

37. Hildebrandt JP, Plant TD, Meves H. The effects of bradykinin on K+ currents in NG108-15 cells treated with U73122, a phospholipase C inhibitor, or neomycin. *Br J Pharmacol* 1997;120:841–850

38. Namkoong S, Kim CK, Cho YL, et al. Forskolin increases angiogenesis through the coordinated cross-talk of PKA-dependent VEGF expression and Epac-mediated PI3K/Akt/eNOS signaling. *Cell Signal* 2009;21:906–915

39. Tang Z, Shi D, Jia B, et al. Exchange protein activated by cyclic adenosine monophosphate regulates the switch between adipogenesis and osteogenesis of human mesenchymal stem cells through increasing the activation of phosphatidylinositol 3-kinase. *Int J Biochem Cell Biol* 2012;44:1106–1120

40. Kashima Y, Miki T, Shibasaki T, et al. Critical role of cAMP-GEFII--Rim2 complex in incretin-potentiated insulin secretion. *J Biol Chem* 2001;276:46046–46053

41. Renström E, Eliasson L, Rorsman P. Protein kinase A-dependent and -independent stimulation of exocytosis by cAMP in mouse pancreatic B-cells. *J Physiol* 1997;502:105–118

42. Weber S, Zeller M, Guan K, Wunder F, Wagner M, El-Armouche A. PDE2 at the crossway between cAMP and cGMP signalling in the heart. *Cell Signal* 2017;38:76–84

43. Pelligrino DA, Wang Q. Cyclic nucleotide crosstalk and the regulation of cerebral vasodilation. *Prog Neurobiol* 1998;56:1–18

44. Corbin JD, Turko IV, Beasley A, Francis SH. Phosphorylation of phosphodiesterase-5 by cyclic nucleotide-dependent protein kinase alters its catalytic and allosteric cGMP-binding activities. *Eur J Biochem* 2000;267:2760–2767

45. Murthy KS. Activation of phosphodiesterase 5 and inhibition of guanylate cyclase by cGMP-dependent protein kinase in smooth muscle. *Biochem J* 2001;360:199–208

46. Undank S, Kaiser J, Sikimic J, Düfer M, Krippeit-Drews P, Drews G. Atrial natriuretic peptide affects stimulus-secretion coupling of pancreatic β-cells. *Diabetes* 2017;66:2840–2848

47. Gromada J, Bokvist K, Ding WG, et al. Adrenaline stimulates glucagon secretion in pancreatic A-cells by increasing the Ca2+ current and the number of granules close to the L-type Ca2+ channels. *J Gen Physiol* 1997;110:217–228

48. Skelin M, Rupnik M. cAMP increases the sensitivity of exocytosis to Ca2+ primarily through protein kinase A in mouse pancreatic beta cells. *Cell Calcium* 2011;49:89–99

49. Kasai H, Suzuki T, Liu TT, Kishimoto T, Takahashi N. Fast and cAMP-sensitive mode of Ca(2+)-dependent exocytosis in pancreatic beta-cells. *Diabetes* 2002;51(Suppl. 1):S19–S24

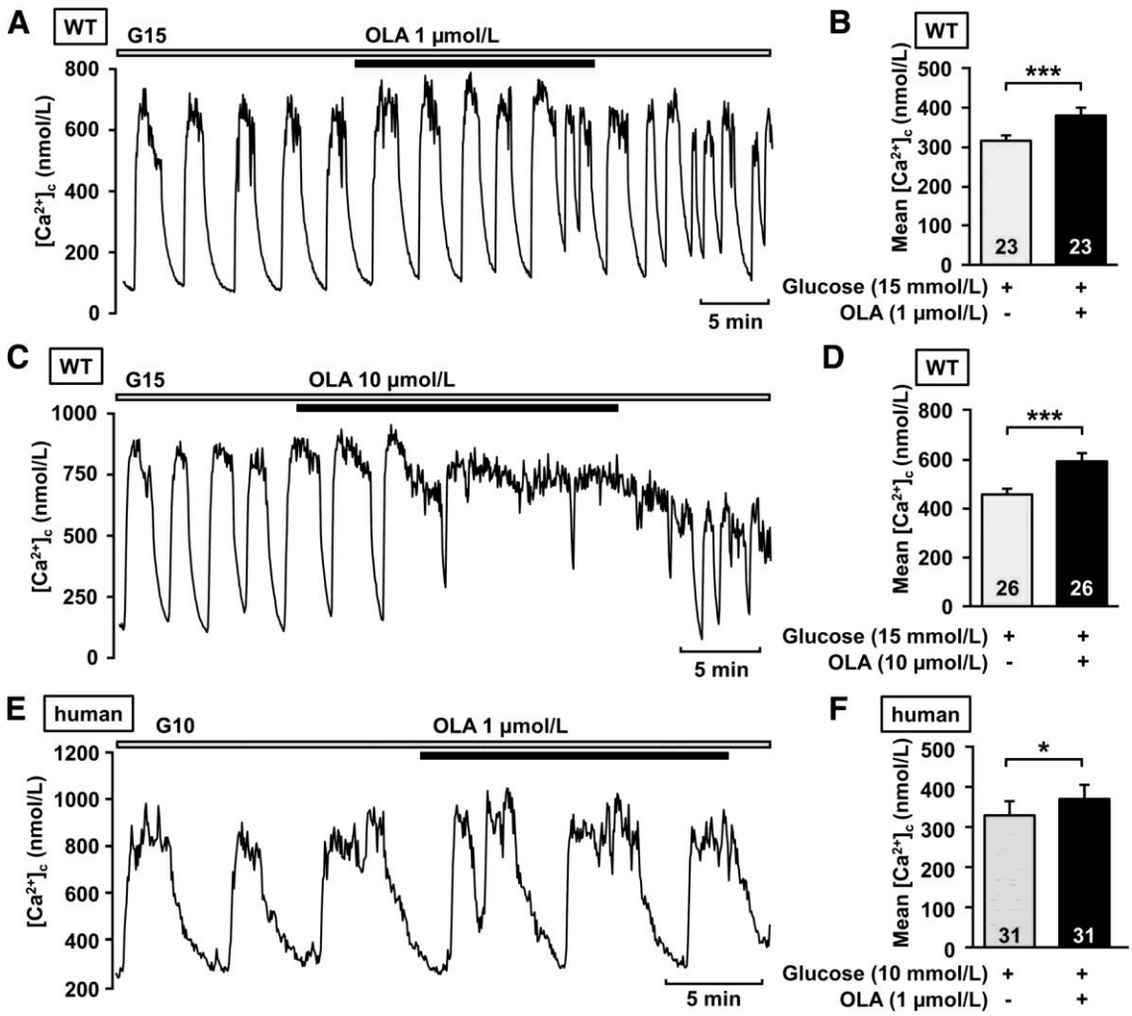

Fig. 1: OLA increases $[Ca^{2+}]_c$ of mouse and human β-cells. *A*: Representative measurement showing enhancement of glucose-induced oscillations of $[Ca^{2+}]_c$ in a mouse β-cell by OLA (1 µmol/L) in the presence of 15 mmol/L glucose. *B*: Summary of all experiments of this series. *C* and *D*: Effect of OLA (10 µmol/L) in the presence of 15 mmol/L glucose. *E*: Representative experiment showing the effect of 1 µmol/L OLA on a human β-cell in the presence of 10 mmol/L glucose. *F*: Summary of all experiments of this series. The number in the columns indicates the number of experiments with different cell clusters from three to four mice. Experiments with human β-cells were performed with dispersed islets from one organ donor. **P* ≤ 0.05; ****P* ≤ 0.001.

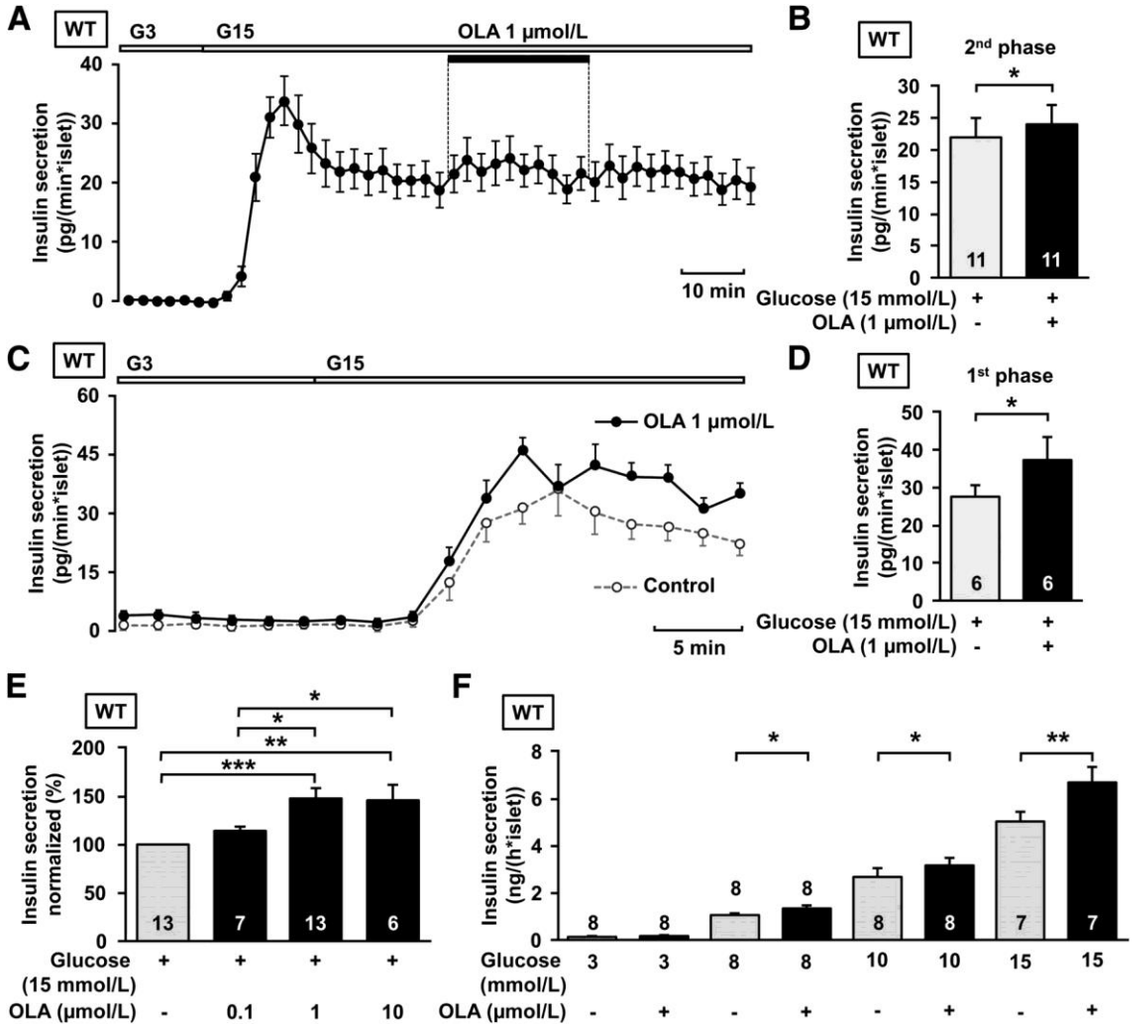

Fig. 2: OLA stimulates insulin secretion in mouse islets. *A*: Averaged curve showing the stimulating effect of OLA on insulin secretion in perifusion experiments. OLA (1 µmol/L) was applied during the second phase of insulin secretion. *B*: Mean insulin secretion rate was analyzed for 10 min before and after addition of OLA in the second phase of insulin secretion. *C*: For evaluation of the effect on the first phase of insulin secretion, OLA (1 µmol/L) was added before the increase of the glucose concentration. Curves showing the first phase of insulin secretion averaged, with OLA and without OLA. *D*: Mean insulin secretion rate during the first 15 min of the first phase of insulin secretion in the presence of 15 mmol/L glucose with and without OLA was analyzed. *E*: Steady-state glucose-induced insulin secretion measured for 1 h is enhanced by 1 and 10 µmol/L OLA but not by 0.1 µmol/L. *F*: Glucose dependency of the OLA effect (1 µmol/L) on steady-state insulin secretion. The number in the columns indicates the number of experiments with islets from 6–13 mice. **P* ≤ 0.05; ***P* ≤ 0.01; ****P* ≤ 0.001.

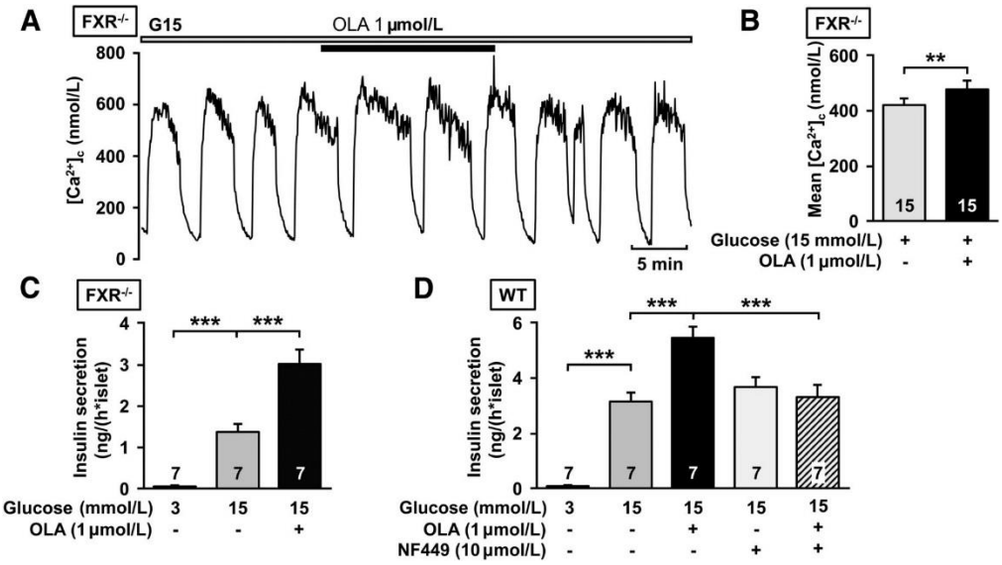

Fig. 3: A $G_{\alpha s}$-coupled receptor but not FXR is the target of OLA. *A*: Representative trace showing the effect of OLA (1 µmol/L) in the presence of 15 mmol/L glucose on a β-cell of an $FXR^{-/-}$ mouse. *B*: Summary of all experiments of this series. *C*: Steady-state glucose-induced insulin secretion from islets of $FXR^{-/-}$ mice is enhanced by OLA (1 µmol/L). *D*: Inhibition of $G_{\alpha s}$ by NF449 (10 µmol/L) prevents the stimulating effect of OLA (1 µmol/L) on insulin secretion in islets from WT mice. The number in the columns indicates the number of experiments with different cell clusters or islets from four to six mice. $^{**}P \leq 0.01$; $^{***}P \leq 0.001$.

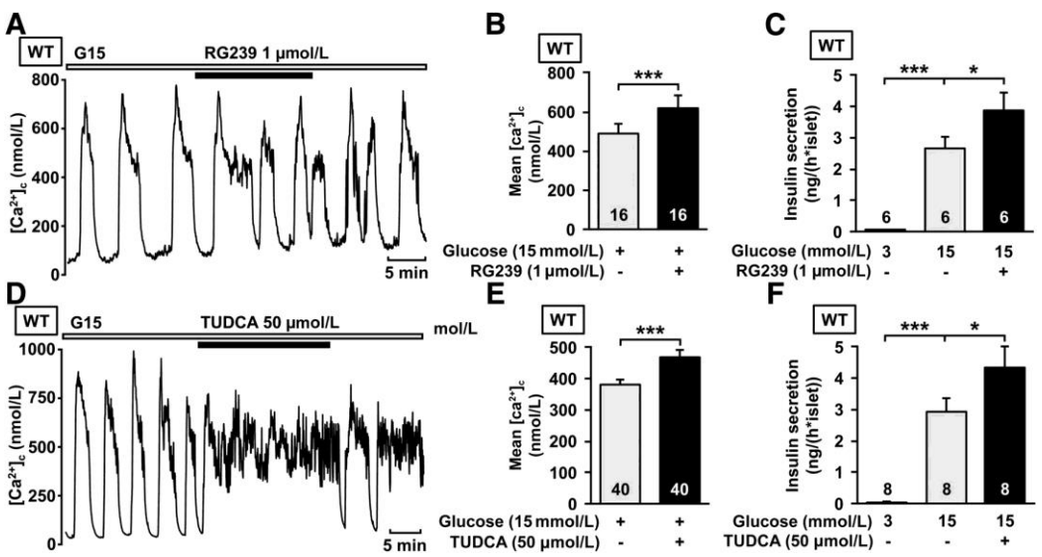

Fig. 4: Different TGR5 agonists mimic stimulating effects on $[Ca^{2+}]_c$ and insulin secretion in β-cells. *A*: Representative measurement showing enhancement of glucose-induced oscillations of $[Ca^{2+}]_c$ by RG239 (1 µmol/L) in the presence of 15 mmol/L glucose. *B*: Summary of all experiments of this series. *C*: Steady-state glucose-induced insulin secretion is stimulated by RG239 compared with control islets. *D*: Representative measurement showing the stimulating effect on glucose-induced oscillations of $[Ca^{2+}]_c$ by TUDCA (50 µmol/L) in the presence of 15 mmol/L glucose. *E*: Summary of all experiments of this series. *F*: Steady-state glucose-induced insulin secretion is increased by TUDCA. The number in the columns indicates the number of experiments with different cell clusters or islets from three to six mice. $^{*}P \leq 0.05$; $^{***}P \leq 0.001$.

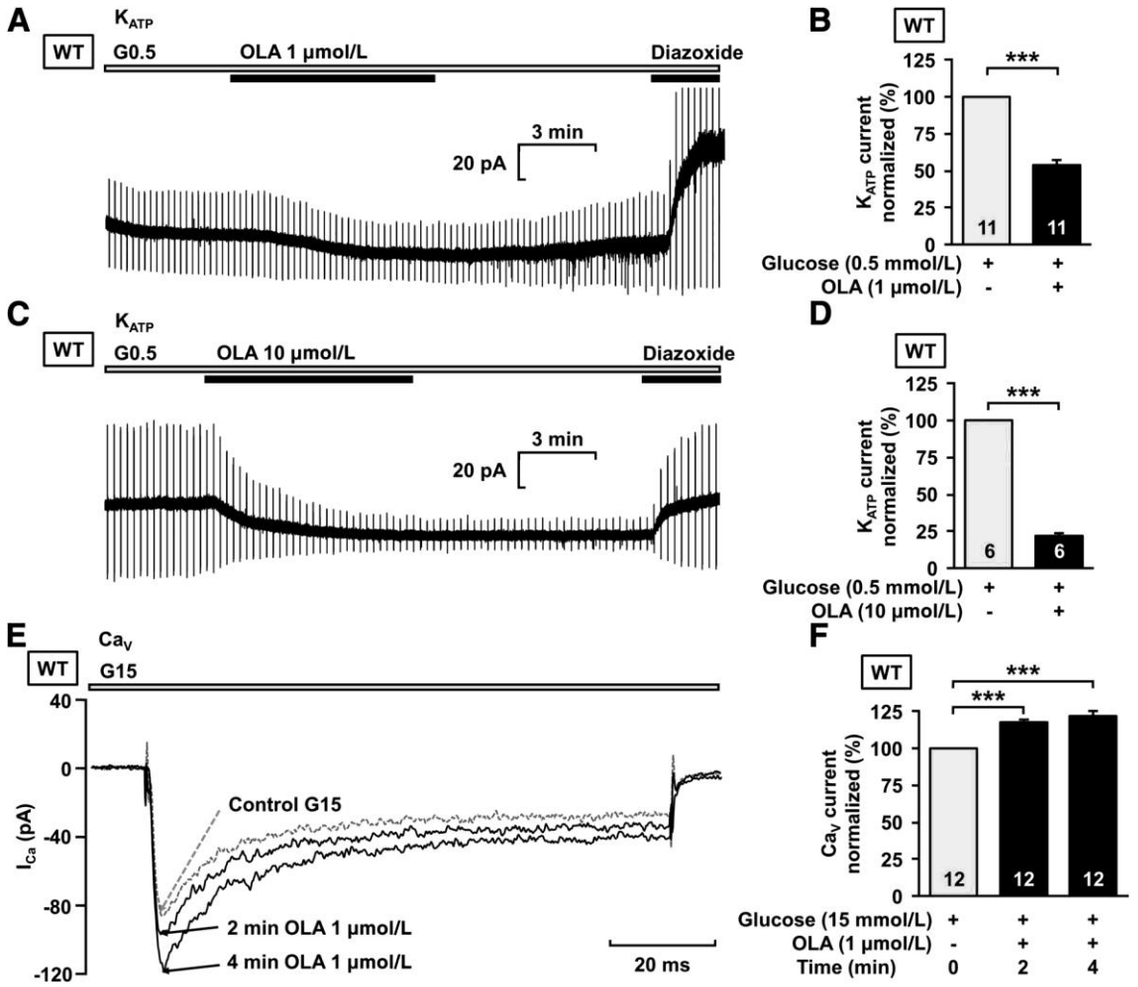

Fig. 5: OLA acutely affects K_{ATP} and Ca^{2+} currents of mouse β-cells. *A*: Representative experiment showing K_{ATP} current measured in the perforated-patch configuration of the patch-clamp technique. Administration of OLA (1 µmol/L) leads to reduction of K_{ATP} current in the presence of 0.5 mmol/L glucose. The current is identified as K_{ATP} current by the specific K_{ATP} channel opener diazoxide (250 µmol/L). *B*: Summary of all experiments of this series, normalized to the current under control condition. *C* and *D*: Increased concentration of OLA (10 µmol/L) amplifies the reduction of the K_{ATP} current. *E*: Currents through VDCCs were measured in the perforated-patch configuration. The representative measurement shows an enhancement of the maximal Ca^{2+} current during OLA administration compared with control condition in the presence of 15 mmol/L glucose. *F*: Summary of all experiments of this series at different time points of OLA application, normalized to the current under control condition. The number in the columns indicates the number of experiments with different cell clusters from three to four mice. ***$P \leq 0.001$.

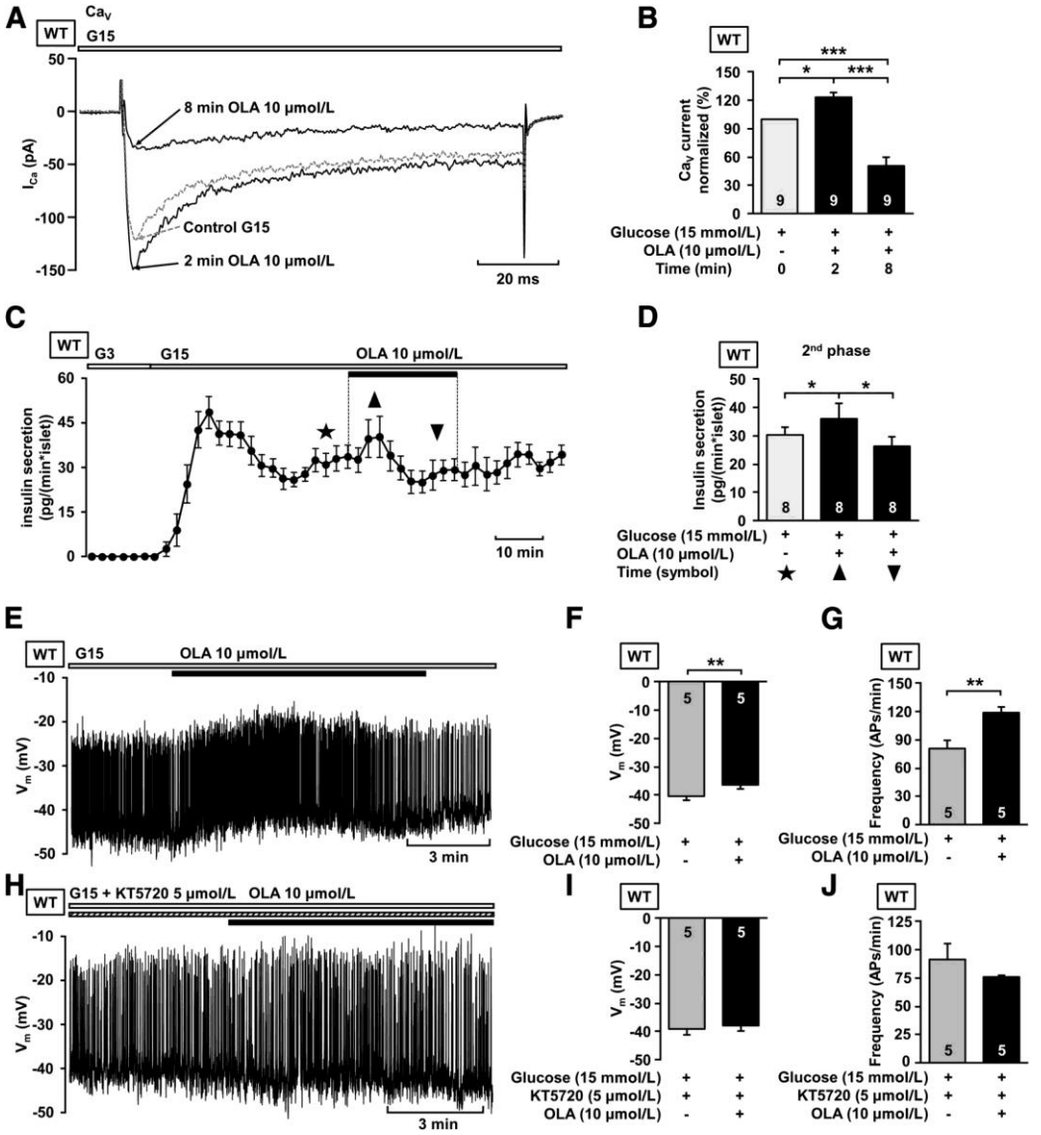

Fig. 6: OLA (10 µmol/L) induces a biphasic effect on Ca^{2+} currents and insulin secretion and depolarized V_m. *A*: Currents through VDCCs were measured in the perforated patch configuration. The representative measurement shows an enhancement of the maximal Ca^{2+} current after 2 min of OLA administration (10 µmol/L) compared with the control condition in the presence of 15 mmol/L glucose. Eight minutes of OLA application clearly reduced the current. *B*: Summary of all experiments of this series at different time points of OLA application, normalized to the current under the control condition. *C*: Averaged curve showing the transient stimulating effect of 10 µmol/L OLA on the second phase of insulin secretion in perifusion experiments. *D*: Mean insulin secretion rate was assessed at the time intervals indicated by the symbols. ★, 10 min before OLA application; ▲, 5 min after OLA application; ▼; 10 min before washout OLA-evoked changes in V_m were suppressed by PKA inhibition. *E*: Representative experiment showing that OLA (10 µmol/L) depolarized V_m and increased action potential frequency. *F*: Summary of the results concerning the plateau potential. *G*: Summary of the results concerning spike frequency. AP, action potential. *H*: Representative experiment in the presence of KT5720 (5 µmol/L) showing that the inhibitor suppresses the OLA effect. *I* and *J*: Summary of the results of this series. The number in the columns indicates the number of experiments with different cell clusters or islets from four to six mice. **P* ≤ 0.05; ***P* ≤ 0.01; ****P* ≤ 0.001.

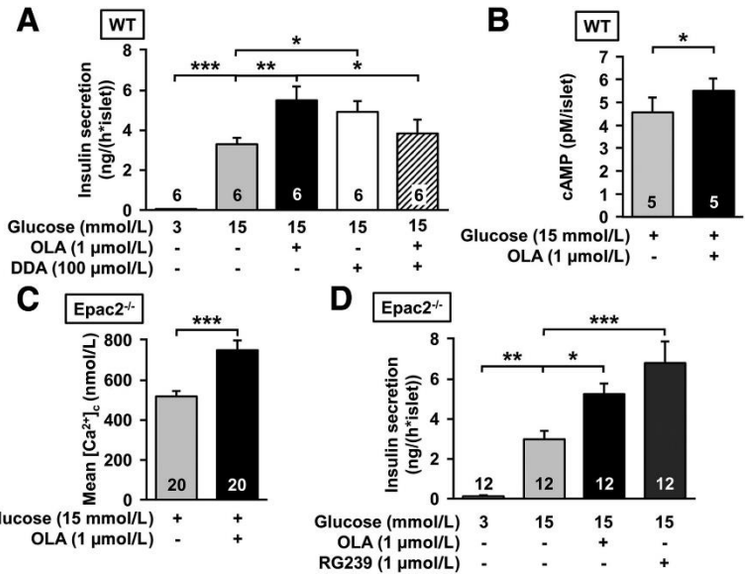

Fig. 7: Inhibition of the AC but not the knockout of Epac2 prevents the effect of OLA. *A*: Inhibition of the AC with DDA (100 µmol/L) prevents the stimulatory effect of OLA (1 µmol/L) on insulin secretion of islets from WT mice. *B*: OLA (1 µmol/L) increases the intracellular cAMP concentration in islets from WT mice in the presence of 15 mmol/L glucose. *C*: Effect of OLA (1 µmol/L) on $[Ca^{2+}]_c$ in the presence of 15 mmol/L glucose in β-cells from Epac2$^{-/-}$ mice. *D*: In islets of Epac2$^{-/-}$ mice, steady-state glucose-induced insulin secretion is increased by OLA (1 µmol/L) and RG239 (1 µmol/L) compared with control islets. The number in the columns indicates the number of experiments with different cell clusters or islets from three to six mice. *$P \leq 0.05$; **$P \leq 0.01$; ***$P \leq 0.001$.

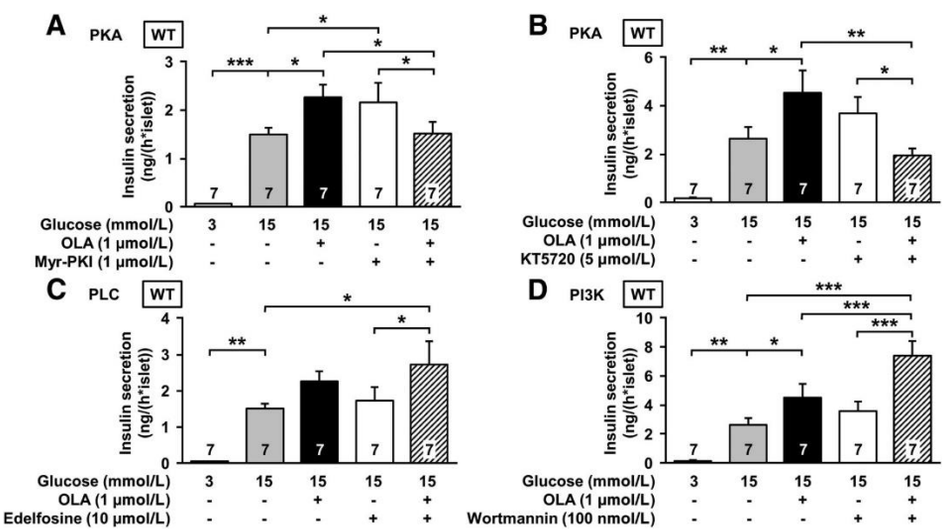

Fig. 8: Stimulating effects of OLA on insulin secretion are mediated by PKA but not by PLC or PI3K. Experiments were performed with islets from WT mice. *A*: The PKA antagonist Myr-PKI (1 µmol/L) eliminates the increasing effect of OLA. *B*: Another PKA antagonist, KT5720 (5 µmol/L), also prevents the stimulation by OLA. *C*: The PLC antagonist edelfosine (10 µmol/L) does not influence the effect of OLA. *D*: The PI3K inhibitor wortmannin (100 nmol/L) does not reduce the stimulation by OLA. The number in the columns indicates the number of experiments with different islets from six mice. *$P \leq 0.05$; **$P \leq 0.01$; ***$P \leq 0.001$.

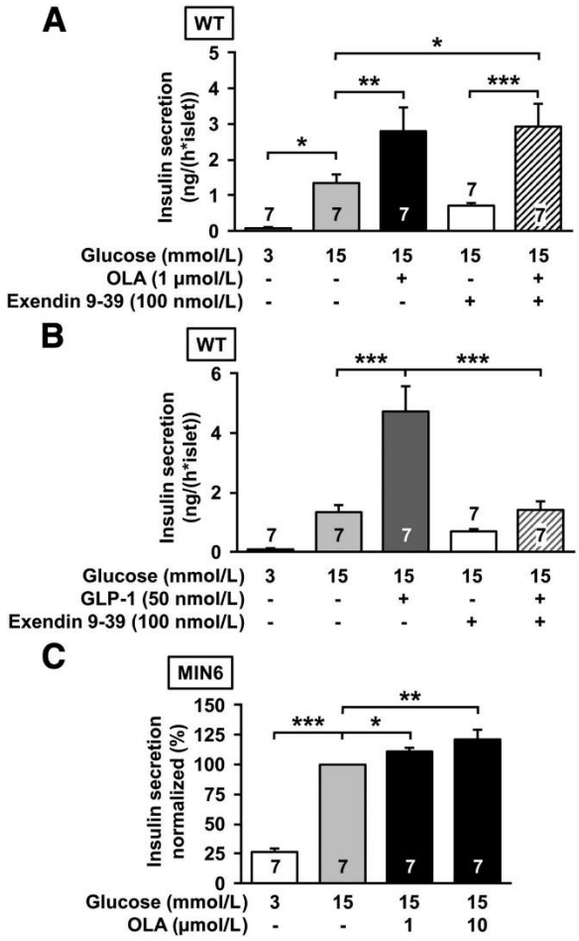

Fig. 9: The stimulating effect of OLA on β-cells is not mediated by GLP-1 from α-cells. *A*: Inhibition of the GLP-1 receptor by the antagonist exendin 9-39 (100 nmol/L) in WT islets does not influence the OLA-mediated increase of insulin secretion. *B*: The potential of exendin 9-39 (100 nmol/L) to inhibit the GLP-1 receptor is demonstrated by the abolishment of the GLP-1–induced (50 nmol/L) increase in insulin secretion. *C*: In MIN6 cells, glucose-induced insulin secretion (15 mmol/L glucose) is increased by OLA. The number in the columns indicates the number of experiments. Islets for the series with exendin 9-39 were from seven different mice. **P* ≤ 0.05; ***P* ≤ 0.01; ****P* ≤ 0.001.

8.5 M-FXR – Interactions between Atorvastatin and the Farnesoid X Receptor Impair Insulinotropic Effects of Bile Acids and Modulate Diabetogenic Risk

T. Hoffmeister[1], J. Kaiser[2], G. Drews[2], M. Düfer[1]

Institute of Pharmaceutical and Medicinal Chemistry, Department of Pharmacology, Münster, Germany[1] and Institute of Pharmacy, Department of Pharmacology and Clinical Pharmacy, Tübingen, Germany[2]

Abstract:

Bile acids such as chenodeoxycholic acid (CDC) acutely enhance insulin secretion via the farnesoid X receptor (FXR). Statins, which are frequently prescribed for type 2 diabetic patients suffering from dyslipidemia, are known for their diabetogenic risk and are reported to interact with the FXR. Our study investigates whether this interaction is relevant for beta cell signaling and plays a role for negative effects of statins on glycemic control. Experiments were performed with islets and islet cells from C57BL/6 wildtype and FXR knock-out mice. Culturing islets with atorvastatin (15 µM) for 24 h decreased glucose-stimulated insulin secretion by approximately 30 %. Prolonged exposure for 7 d lowered the concentration necessary for impairment of insulin release to 150 nM. After 24-h culture of islets with atorvastatin, the ability of CDC (500 nM) to elevate $[Ca^{2+}]_c$ was diminished and the potentiating effect on insulin secretion was completely lost. Though not a prerequisite, FXR seems to influence the degree of damage caused by atorvastatin in dependence of its interaction with CDC: Preparations responding to CDC with an increase in insulin secretion under control conditions were less impaired by atorvastatin than preparations that were non-responsive to CDC. Extended stimulation of FXR by the synthetic agonist GW4064, which is suggested to induce translocation of FXR from the cytosol into the nucleus, increased the inhibitory effect of atorvastatin. In conclusion, atorvastatin inhibits insulin release and prevents positive effects of bile acids on beta cell function. Both interactions may contribute to progression of type 2 diabetes mellitus.

1. Introduction

Statins as LDL-cholesterol lowering drugs are in broad clinical use. Their beneficial effects concerning prevention of cardiovascular risk are undisputed (Pedersen *et al*., 1994; Sever *et al*., 2003), nevertheless certain side effects have to be considered (Thompson *et al*., 2016). A meta-analysis of 13 statin trials with 91140 participants provides clear evidence that the risk to develop type 2 diabetes mellitus increases in patients during long-term statin therapy (Sattar *et al*., 2010).

Particularly, lipophilic statins such as atorvastatin are assumed to influence islet function in a detrimental way (Yada *et al*., 1999; Yaluri *et al*., 2015; Urbano *et al*., 2017). Whether this is associated with the hydroxy-methyl-glutaryl coenzyme A (HMG-CoA) reductase inhibition or results from off-target effects, remains controversial. Partly the effects are closely linked to the mode of action of statins (Urbano *et al*., 2017), partly the observed effects are not reversible by a co-culture with mevalonate (Yaluri *et al*., 2015). Interestingly, it was shown that statins interact with pathways regulated by the farnesoid X receptor (FXR). Fu *et al.* reported effects of atorvastatin on FXR-induced target genes in mice (Fu *et al*., 2014), while Habeos *et al.* observed changes in the expression and DNA-binding activity of the receptor in the liver after treatment of syrian hamsters with simvastatin as well as in simvastatin-treated HepG2 cells (Habeos *et al*., 2005).

The FXR is a nuclear receptor targeted by bile acids like chenodeoxycholic acid (CDC), which is the most effective one (Makishima *et al*., 1999; Parks *et al*., 1999). It plays a role for regulation of lipid and bile acid metabolism, but also for glucose homeostasis (Fiorucci *et al*., 2009; Düfer *et al*., 2012a). FXR expression is high in liver, adrenal glands and intestine (Huber *et al*., 2002), however mRNA can also be found in other organs like the endocrine pancreas (Popescu *et al*., 2010). In our previous work we investigated the impact of an acute stimulation of the FXR by the bile acid taurochenodeoxycholic acid (TCDC) on insulin secretion. We detected an FXR-dependent insulinotropic effect of the bile acid, which includes inhibition of K ATP channels, membrane depolarization and increased Ca^{2+} influx (Düfer *et al*., 2012b). For this acute stimulatory effect on insulin secretion, cytosolic localization of FXR and bile acid-induced interaction with K_{ATP} channels are essential.

The reported impact of statins on FXR in liver and intestine, respectively (Habeos *et al*., 2005; Fu *et al*., 2014), raises the question of a comparable situation in the pancreas. The aim of our study was to gain insight into possible interactions between FXR and statins in pancreatic islets. Therefore, the influence of atorvastatin and its interaction with bile acid signaling was investigated in islets of wildtype and FXR knock-out (FXR-KO) mice by monitoring cytosolic Ca^{2+} concentration ($[Ca^{2+}]_c$), apoptosis and insulin release and content.

2. Materials and Methods

2.1. Cell and Islet Preparation

Experiments were performed with islets of Langerhans from adult male and female C57BL/6N mice (Charles River, Sulzfeld, Germany) or adult male and female FXR-deficient mice from a C57BL/6N background described earlier (Sinal *et al*., 2000). The principles of laboratory animal care were followed according to German laws. Mice were euthanized by CO_2. Islets were isolated by collagenase digestion. Dispersed cells or smaller cell clusters were obtained by trypsinization and used for $[Ca^{2+}]_c$ measurements and determination of apoptosis. Islets and cells were cultured in RPMI 1640 medium (11.1 mM glucose) supplemented with 10 % fetal calf serum, 100 U/ml penicillin, and 100h µg/ml streptomycin at 37 °C in 5 % CO_2 humidified atmosphere. After preparation islets or dispersed islet cells were kept overnight in standard culture medium. Next day, incubation started in the presence of atorvastatin or pravastatin for 24 h or 7 days. In case of pre-incubations with GW4064 atorvastatin was added one day later. Medium was changed every second or third day during the long-term incubation of 7 days.

2.2. Solution and Chemicals

Insulin secretion was performed in bath solution containing [mM]: 122 NaCl, 4.7 KCl, 1.1 $MgCl_2$, 2.5 $CaCl_2$, 10 HEPES (pH 7.4) and 0.5 % bovine serum albumin. $[Ca^{2+}]_c$ was measured in a solution which contained [mM]: 140 NaCl, 5 KCl, 1.2 $MgCl_2$, 2.5 $CaCl_2$, 10 HEPES (pH 7.4). Glucose was added as indicated.

Collagenase P was from Roche Diagnostics (Mannheim, Germany); annexin V reagent was from Essen BioScience (Michigan, USA); RPMI 1640, fetal calf serum,

and penicillin/streptomycin were obtained from Life Technologies (Darmstadt, Germany). Fura-2 AM and rat insulin were ordered from Biotrend (Köln, Germany). All other chemicals were from Sigma–Aldrich (Taufkirchen, Germany) or Diagonal (Münster, Germany).

2.3. Insulin Secretion and Content

Islets were moved to bath solution containing 5.6 mM glucose for 2 h after a culture period of 22 h or 7 days in the presence or absence of atorvastatin or pravastatin. During these 2 h the statin was still present. Following this, glucose was lowered to 3 mM for 1 h and bath solution did not contain atorvastatin or pravastatin anymore. Batches of five islets were incubated for 1 h at 37 °C with glucose concentrations and substances as described in the respective experiment. Thereafter, supernatant was removed for quantitative analysis and islets were lysed with acid ethanol in order to determine insulin content. Insulin was quantified by radioimmunoassay using rat insulin as standard.

2.4. Annexin V Assay

The live-cell analysis system IncuCyte® (Essen BioScience) was used for measurement of apoptosis. By means of this method cell viability could be monitored over a longer time period while cells were in stable conditions in an incubator.

After preparation, dispersed islet cells were cultured in a 96 well plate overnight. The following day, cells were incubated in the presence or absence of 15 µM atorvastatin. 50 µM H_2O_2 was used as a positive control. After adding annexin V green reagent to each well as instructed by the manufacturer, the measurement started for a time period of 44 h (37 °C, 5 % CO_2 humidified atmosphere). Changes in fluorescence of annexin V green reagent were monitored by excitation at 480 nm every 2 hours.

2.5. Determination of $[Ca^{2+}]_c$

Cells and cell clusters were loaded with the fluorescent dye fura-2-acetoxymethylester (fura-2 AM, 5 µM, 37 °C, 30 min). $[Ca^{2+}]_c$ was determined by

measuring fluorescence at 515 nm after alternate excitation with 340 and 380 nm, respectively. Cells were perifused with bath solution containing glucose and substances as indicated.

2.6. Data Evaluation and Statistical Analysis

All experiments were performed with islets or cells from at least three independent mouse preparations. $[Ca^{2+}]_c$ was determined by calculating the area under the curve (AUC) after baseline correction 10 min before changes in bath solution (Figure 3B) or by determining mean $[Ca^{2+}]_c$ over a period of 10 min (Figure 2). For quantification of apoptosis, the percentage of apoptotic area in relation to the whole cell area was determined. Values are presented as mean ± SEM. To compare two single groups, Student's t test was performed. For comparison among groups, statistical significance was assessed by analysis of variances (ANOVA) followed by Student-Newman-Keuls *post-hoc* test. Values of $p \leq 0.05$ were considered as statistically significant.

3. Results

3.1. Atorvastatin decreases glucose-stimulated insulin secretion

To investigate the effect of atorvastatin on insulin secretion, two incubation periods with different concentrations of the HMG-CoA reductase inhibitor were chosen.

Culturing islets in the presence of 15 µM atorvastatin for 24 h significantly decreased insulin release stimulated by 15 mM glucose. Islets exposed to 1.5 µM atorvastatin for 24 h only showed a tendency to reduced insulin secretion in response to stimulation with 15 mM glucose (Figure 1A). The culture period in medium supplemented with various concentrations of atorvastatin was extended to 7 days to investigate the influence of time. This prolonged treatment potentiated the detrimental effect of 15 µM atorvastatin on glucose-stimulated insulin secretion (24 h: 3.31 ± 0.28 ng/(islet*h), n = 10, *vs.* 7 d: 0.89 ± 0.19 ng/(islet*h), n = 7, $p \leq 0.001$). Moreover, already nanomolar concentrations of the statin (150 and 500 nM) showed a negative effect on insulin release after 7 days (Figure 1B). Since extension of the time period to 7 days led to stronger variations in secretion among

the individual preparations, absolute values were calculated as percentage of control (15 mM glucose) in this series of experiments.

3.2. Atorvastatin changes cytosolic Ca^{2+}, but has no effect on cell viability

Since the rise in $[Ca^{2+}]_c$ is crucial for insulin secretion, it was tested, whether the inhibitory effect of atorvastatin is caused by changes in $[Ca^{2+}]_c$. Incubating islet cells with 15 µM atorvastatin for 24 h slightly altered the Ca^{2+} response to a glucose stimulus: After exposure to atorvastatin, the first increase in $[Ca^{2+}]_c$ in response to 15 mM glucose was approximately half a minute delayed compared to standard conditions (Figure 2A). Apart from the effect on response time, pre-treatment with atorvastatin reduced the mean concentration of $[Ca^{2+}]_c$ (Figure 2B).

Insulin content was not affected even after incubating pancreatic islets in standard culture medium (10 mM glucose) supplemented with atorvastatin for the long-term period of 7 days (Figure 2C). Corresponding to these results there was no induction of apoptosis by the exposure of islet cells to 15 µM atorvastatin in standard culture medium for up to 44 h compared to the control (% apoptotic area after 24 h: control 8.0 ± 0.9 % *vs*. 15 µM atorvastatin, 24 h, 8.9 ± 1.5 %, n = 3, n. s.) (Figure 2D).

3.3. Atorvastatin abolishes the insulinotropic effect of the bile acid CDC

In order to evaluate if atorvastatin influences the FXR or its signaling pathway in pancreatic islets as described for the liver (Fu *et al*., 2014), the acute effect of the bile acid CDC on insulin secretion was tested after culturing islets under control conditions or in the presence of 15 µM atorvastatin and 200 µM pravastatin for 24 h, respectively.

The acute application of CDC in a concentration of 500 nM enhanced insulin secretion under standard conditions as described earlier (Düfer *et al*., 2012b). Interestingly, culturing islets with 15 µM atorvastatin for 24 h abolished the acute insulinotropic effect of CDC (Figure 3A). In this series of experiments CDC elevated insulin secretion from 3.55 ± 0.32 to 4.68 ± 0.47 ng/(islet*h), n = 13, p ≤

0.05. After culture with 15 µM atorvastatin for 24 h, glucose-stimulated insulin release (1 h) was 2.69 ± 0.32 ng/(islet*h) in the absence and 2.49 ± 0.31 ng/(islet*h) in the presence of CDC (500 nM) (n = 13, n. s.). This was also fact for the lower concentration of 1.5 µM atorvastatin (insulin release in response to 15 mM glucose after 24-h culture with 1.5 µM atorvastatin: 4.13 ± 0.93 ng/(islet*h) *vs*. same conditions + CDC 500 nM: 4.64 ± 1.38 ng/(islet*h), n = 6, n. s.)

The same experiment was performed with pravastatin, which is more hydrophilic than atorvastatin. 24-h culture with 200 µM pravastatin also inhibited the stimulatory effect of CDC (Figure 3B), pointing to a class effect of statins (insulin release in response to 15 mM glucose after 24-h culture with pravastatin: 3.55 ± 0.45 ng/(islet*h) *vs*. same conditions + CDC 500 nM: 3.07 ± 0.39 ng/(islet*h), n = 12, n. s.).

Since the effect of CDC on insulin secretion depends on a rise in $[Ca^{2+}]_c$, this parameter was measured in islet cells and cell clusters which were exposed to 15 µM atorvastatin prior to the experiment for 24 h. $[Ca^{2+}]_c$ was determined by calculating the area under the curve (AUC) after baseline correction. In agreement with the acute effect on insulin secretion described above, the acute application of 500 nM CDC provoked an increase in $[Ca^{2+}]_c$ under control conditions. This was significantly diminished after exposure of the cells to atorvastatin (Figure 3C), explaining the ineffectiveness of CDC on insulin secretion after treatment with the lipophilic statin.

3.4. Inhibitory effect of atorvastatin in FXR-deficient islets

We demonstrated in previous work that the increase in $[Ca^{2+}]_c$ in response to bile acids depends on FXR and is absent in beta cells of FXR-KO mice (Düfer *et al*., 2012b). Consequently, the results described above indicate an interaction between statins and the FXR leading to elimination of the insulinotropic effect of CDC. This interaction provoked the question whether there might also be an impact *vice versa*. Therefore, the experiments shown in figure 1A were repeated with pancreatic islets from FXR-deficient mice. After exposing FXR-KO islets to different concentrations of atorvastatin for 24 h, 15 µM atorvastatin caused a significant

decline in insulin secretion, while a concentration of 1.5 µM – similar to the effect in wildtype islets – only tended to reduce insulin release (Figure 4).

Comparison of the amounts of insulin, secreted in response to 15 mM glucose (1 h, expressed as percentage of control) after 24-h culture of the islets with 15 µM atorvastatin, revealed no difference between wildtype and FXR-deficient islets (insulin secretion after 24-h culture with atorvastatin (15 µM): wildtype 64.7 ± 5.6 % of control, n = 27, *vs*. FXR-KO 66.6 ± 10.5 % of control, n = 8, n. s.).

3.5. FXR modulates the damaging effect of atorvastatin

Although the experiments with FXR-deficient islets show the independency of the negative effect of atorvastatin on insulin secretion from the nuclear receptor *per se*, we made a remarkable observation after detailed analysis of the experiments with wildtype islets. Of 27 experiments with wildtype islets not every preparation responded to the acute application of 500 nM CDC with an increase in insulin secretion under control conditions. Some preparations were non-responsive to the bile acid, which means that the cytosolic K_{ATP}/Ca^{2+}-dependent signaling pathway of FXR is not operative. This might indicate a shift in the localization of FXR from the cytosol to the nucleus of the cell (Schittenhelm *et al*., 2015). To address this issue, the preparations were divided into two groups, CDC-responsive and CDC-non-responsive experiments, for subgroup analysis. Thereby, we detected a modulatory role of the FXR concerning the degree of damage caused by atorvastatin. Atorvastatin seems to be less harmful, when islets are CDC-responsive, while the inhibitory effect is aggravated, when islets are non-responsive to CDC under control conditions (Figure 5A): After 24-h treatment with 15 µM atorvastatin, glucose-stimulated insulin secretion was reduced to 77.0 ± 6.9 % of control in CDC-responsive preparations (n = 17). By contrast, 24-h treatment of CDC-non-responsive preparations with atorvastatin lowered glucose-stimulated insulin release to 43.8 ± 4.5% of control (n = 10). Noteworthy, we observed that the inhibitory effect of atorvastatin on insulin release of CDC-non-responsive wildtype preparations was higher than in FXR-KO islets (GSIS after 24-h treatment with atorvastatin (15 µM): CDC-non-responsive wildtype islets 43.8 ± 4.5 % of control, n = 10 *vs*. FXR-KO islets 66.6 ± 10.5 % of control, n = 8, $p \leq 0.05$). This points to a

more negative effect of statins when FXR is still present but lost its influence on the cytosolic pathway compared to complete absence of the receptor.

To confirm that FXR influences the damaging effect of atorvastatin, experiments were performed in which the FXR was forced into the nucleus of the cell. To achieve this, islet cells were exposed to the strong, synthetic FXR agonist GW4064 for an extended period. Previous work showed that the cytosolic, K_{ATP}-dependent signaling pathway of FXR is inactive after prolonged receptor activation by GW4064 (Schittenhelm *et al*., 2015). To be able to compare the degree of damage caused by atorvastatin in dependence of the ability of FXR to act as a cytosolic receptor, only preparations responding to 500 nM CDC under control conditions, but not after 48-h culture with GW4064 were included. Figure 5B shows that GW4064-treated islets, which have lost the cytosolic pathway of FXR (dark grey *vs.* light grey bar), were much more sensitive to the inhibitory influence of atorvastatin compared to control (black *vs.* white bar). As already described above, atorvastatin had only a small effect on islets of CDC-responsive preparations (~ 14 % inhibition in this series of experiments). After pre-incubation of the islets with GW4064 (500 nM) for 24 h and addition of the statin for another 24 h, insulin secretion induced by 15 mM glucose was diminished by 80 %. Of note, glucose-stimulated insulin release was ~ 2-fold higher after 48-h culture with GW4064 compared to control.

4. Discussion

In accordance with other publications (Zhao and Zhao, 2015; Urbano *et al*., 2017) incubation of pancreatic islets with atorvastatin reduced insulin secretion. Noteworthy, experiments varied among species and concentration of atorvastatin. We observed that the effect of atorvastatin is not only dose-dependent (Figure 1A), but also time-dependent: Besides the potentiation of the detrimental effect of 15 µM atorvastatin, a decrease in insulin release was already provoked by nanomolar concentrations (150 and 500 nM) of the statin after long-term treatment for 7 d (Figure 1B). The inhibitory effect of atorvastatin involves changes in Ca^{2+} influx (Figures 2A and B) which points to an interaction with the triggering pathway that regulates beta cell function. Even though the exact mechanism remains to be

elucidated, the diabetogenic effect of atorvastatin is unquestioned. Insulin content was not altered between control and any of the applied concentrations of atorvastatin even after 7 d (Figure 2C). In contrast to reports of others (Zhao and Zhao, 2015; Sadighara *et al*., 2017), we could not attribute the detrimental effect on insulin secretion to changes in cell viability. These discrepancies might result from different experimental approaches, as the effect of atorvastatin on cytochrome c release was monitored in isolated mitochondria (Sadighara *et al*., 2017) and cell survival was investigated by an MTT assay which does not give any information about apoptosis (Zhao and Zhao, 2015). In summary, an effect of atorvastatin on insulin biosynthesis or a dramatic loss of beta cell mass can be ruled out as explanations for the decrease in insulin release in our investigation.

Our data show for the first time that statins interfere with the insulinotropic effect of bile acids. In the postprandial state plasma levels of bile acids can rise up to 15 µM (Everson, 1987; Houten *et al*., 2006). This is not only necessary for the absorption of lipids, but also important for lowering blood sugar peaks by stimulation of insulin secretion. The stimulatory effect of the FXR-agonistic bile acid CDC, we already described in our previous investigations (Düfer *et al*., 2012b; Schittenhelm *et al*., 2015), was clearly seen under control conditions, but completely disappeared after 24-h culture with atorvastatin or pravastatin (Figure 3A and B). Corresponding to this loss of efficacy on glucose-stimulated insulin release, the CDC-mediated increase in $[Ca^{2+}]_c$ was reduced to less than 50 % (Figure 3C). For patients being treated with statins, this implies not only a decline in islet function induced by the statin *per se*, but also the loss of an important physiological regulatory function of bile acids for glucose homeostasis. In addition, a reduction of the postprandial plasma concentrations of bile acids was reported in obese (Glicksman *et al*., 2010) and pre-diabetic (Shaham *et al*., 2008) patients, actually patient groups with the common indication for cholesterol-lowering drugs such as statins.Taken together, the already reduced contribution of bile acids to the postprandial regulation of blood glucose concentration in those patients would be progressively more or, worst case, entirely abolished during long-term therapy with statins. The exact mechanism leading to inhibition of the effect of CDC needs to be further investigated. Since the link between FXR activation and K_{ATP} channel closure has not yet been clearly identified, it might be possible that incubation with atorvastatin

interferes with some target downstream to FXR, but upstream to the closure of KATP channels. Bearing in mind that statins impair the prenylation and thereby regulation of proteins by inhibiting the mevalonate pathway (Li *et al*., 1993), atorvastatin could disrupt some factor derived from this pathway linking FXR stimulation to KATP channel closure. Furthermore, our results demonstrate that the interference between atorvastatin and the FXR is not unilateral, but of a bidirectional character. The experiments with FXR- KO islets show that the impairing effect induced by atorvastatin is partly independent of FXR (Figure 4). But in addition, our data reveal that FXR plays a modulatory role with regard to the degree of damage caused by the statin (Figure 5A). The availability of the receptor in the cytosol seems to be crucial for this modulation. Apparently, a localization close to the plasma membrane that enables interaction of FXR with the cytosolic triggering pathway for insulin secretion via KATP channel closure and Ca^{2+} influx is protective and reduces the negative effect of atorvastatin on insulin release. Disruption of this pathway is associated with an increased inhibitory effect of statins on insulin release (Figure 5B).

Popescu *et al.* detected a translocation of the FXR into the nucleus in obese *ob/ob* mice, whereas the receptor is mainly located in the cytosol in wildtype beta cells (Popescu *et al*., 2010). With respect to the pathway described above, differences in receptor localization – and thereby in receptor function – between lean and obese organisms might be critical determinants for the statin-bile acid interaction. In line with the idea of fundamental differences in FXR function, dependent on body weight and/or lipid homeostasis, it was reported that ablation of FXR is associated with decreased insulin secretion and insulin content under control conditions as well as peripheral insulin resistance (Cariou *et al*., 2006; Popescu *et al*., 2010). However, these negative characteristics completely change in a glucolipotoxic environment. FXR-deficient islets were resistant to glucolipotoxicity, while wildtype islets kept in glucolipotoxic medium showed an impaired glucose-stimulated insulin release (Schittenhelm *et al*., 2015). Supporting the hypothesis, that – in beta cells – cytosolic localization of FXR is a prerequisite for its positive impact on cellular function, Schittenhelm *et al.* demonstrated that the potentiating effect of FXR agonists on insulin secretion is lost in islets derived from mice after high-fat diet (Schittenhelm *et al*., 2015). Taken together, these data suggest that certain

conditions (i. e. genetic or diet-induced obesity *in vivo*, glucolipotoxicity or prolonged receptor activation *in vitro*) disrupt the cytosolic interaction between FXR and KATP channels and might thereby aggravate the diabetogenic risk of statins. It is tempting to speculate that obese patients might be exceptionally sensitive to statin-induced beta cell damage as – similar to the genetic mouse model or to islets kept in a glucolipotoxic environment – their profile of FXR distribution and interaction may change during disease. Thereby, they not only lose the beneficial effect of bile acids on the endocrine pancreas, but also risk progression of beta cell failure by direct statin-induced impairment of glucose-stimulated insulin release.

Acknowledgments

We thank Melanie Arning for excellent technical assistance.

References

Cariou B, van Harmelen K, Duran-Sandoval D, van Dijk TH, Grefhorst A, Abdelkarim M, Caron S, Torpier G, Fruchart J-C, Gonzalez FJ, Kuipers F, and Staels B (2006) The farnesoid X receptor modulates adiposity and peripheral insulin sensitivity in mice. *J Biol Chem* **281:**11039–11049.

Düfer M, Hörth K, Krippeit-Drews P, and Drews G (2012a) The significance of the nuclear farnesoid X receptor (FXR) in beta cell function. *Islets* **4:**333–338.

Düfer M, Hörth K, Wagner R, Schittenhelm B, Prowald S, Wagner TFJ, Oberwinkler J, Lukowski R, Gonzalez FJ, Krippeit-Drews P, and Drews G (2012b) Bile acids acutely stimulate insulin secretion of mouse β-cells via farnesoid X receptor activation and K_{ATP} channel inhibition. *Diabetes* **61:**1479–1489.

Everson GT (1987) Steady-state kinetics of serum bile acids in healthy human subjects: single and dual isotope techniques using stable isotopes and mass spectrometry. *J Lipid Res* **28:**238–252.

Fiorucci S, Mencarelli A, Palladino G, and Cipriani S (2009) Bile-acid-activated receptors: targeting TGR5 and farnesoid-X-receptor in lipid and glucose disorders. *Trends Pharmacol Sci* **30:**570–580.

Fu ZD, Cui JY, and Klaassen CD (2014) Atorvastatin induces bile acid-synthetic enzyme Cyp7a1 by suppressing FXR signaling in both liver and intestine in mice. *J Lipid Res* **55:**2576–2586.

Glicksman C, Pournaras DJ, Wright M, Roberts R, Mahon D, Welbourn R, Sherwood R, Alaghband-Zadeh J, and Le Roux CW (2010) Postprandial plasma bile acid responses in normal weight and obese subjects. *Ann Clin Biochem* **47:**482–484.

Habeos I, Ziros PG, Psyrogiannis A, Vagenakis AG, and Papavassiliou AG (2005) Statins and transcriptional regulation: the FXR connection. *Biochem Biophys Res Commun* **334:**601–605.

Houten SM, Watanabe M, and Auwerx J (2006) Endocrine functions of bile acids. *EMBO J* **25:**1419–1425.

Huber RM, Murphy K, Miao B, Link JR, Cunningham MR, Rupar MJ, Gunyuzlu PL, Haws TF, Kassam A, Powell F, Hollis GF, Young PR, Mukherjee R, and Burn TC (2002) Generation of multiple farnesoid-X-receptor isoforms through the use of alternative promoters. *Gene* **290:**35–43.

Li G, Regazzi R, Roche E, and Wollheim CB (1993) Blockade of mevalonate production by lovastatin attenuates bombesin and vasopressin potentiation of nutrient-induced insulin secretion in HIT-T15 cells. Probable involvement of small GTP-binding proteins. *Biochem J* **289 (Pt 2):**379–385.

Makishima M, Okamoto AY, Repa JJ, Tu H, Learned RM, Luk A, Hull MV, Lustig KD, Mangelsdorf DJ, and Shan B (1999) Identification of a nuclear receptor for bile acids. *Science* **284:**1362–1365.

Parks DJ, Blanchard SG, Bledsoe RK, Chandra G, Consler TG, Kliewer SA, Stimmel JB, Willson TM, Zavacki AM, Moore DD, and Lehmann JM (1999) Bile acids: natural ligands for an orphan nuclear receptor. *Science* **284:**1365–1368.

Pedersen TR, Kjekshus J, Berg K, Haghfelt T, Faergeman O, Faergeman G, Pyörälä K, Miettinen T, Wilhelmsen L, Olsson AG, Wedel H, and Scandinavian Simvastatin Survival Study Group (1994) Randomised trial of cholesterol lowering in 4444 patients with coronary heart disease: the Scandinavian Simvastatin Survival Study (4S). *The Lancet* **344:**1383–1389.

Popescu IR, Helleboid-Chapman A, Lucas A, Vandewalle B, Dumont J, Bouchaert E, Derudas B, Kerr-Conte J, Caron S, Pattou F, and Staels B (2010) The nuclear receptor FXR is expressed in pancreatic beta-cells and protects human islets from lipotoxicity. *FEBS Lett* **584:**2845–2851.

Sadighara M, Amirsheardost Z, Minaiyan M, Hajhashemi V, Naserzadeh P, Salimi A, Seydi E, and Pourahmad J (2017) Toxicity of atorvastatin on pancreas mitochondria: a justification for increased risk of diabetes mellitus. *Basic Clin Pharmacol Toxicol* **120:**131–137.

Sattar N, Preiss D, Murray HM, Welsh P, Buckley BM, Craen AJM de, Seshasai SRK, McMurray JJ, Freeman DJ, Jukema JW, Macfarlane PW, Packard CJ, Stott DJ, Westendorp RG, Shepherd J, Davis BR, Pressel SL, Marchioli R, Marfisi RM, Maggioni AP, Tavazzi L, Tognoni G, Kjekshus J, Pedersen TR, Cook TJ, Gotto AM, Clearfield MB, Downs JR, Nakamura H, Ohashi Y, Mizuno K, Ray KK, and Ford I (2010) Statins and risk of incident diabetes: a collaborative meta-analysis of randomised statin trials. *The Lancet* **375:**735–742.

Schittenhelm B, Wagner R, Kähny V, Peter A, Krippeit-Drews P, Düfer M, and Drews G (2015) Role of FXR in β-cells of lean and obese mice. *Endocrinology* **156:**1263–1271.

Sever PS, Dahlöf B, Poulter NR, Wedel H, Beevers G, Caulfield M, Collins R, Kjeldsen SE, Kristinsson A, McInnes GT, Mehlsen J, Nieminen M, O'Brien E, and Östergren J (2003) Prevention of coronary and stroke events with atorvastatin in hypertensive patients who have average or lower-than-average cholesterol concentrations, in the Anglo-Scandinavian Cardiac Outcomes Trial—Lipid Lowering Arm (ASCOT-LLA): a multicentre randomised controlled trial. *The Lancet* **361:**1149–1158.

Shaham O, Wei R, Wang TJ, Ricciardi C, Lewis GD, Vasan RS, Carr SA, Thadhani R, Gerszten RE, and Mootha VK (2008) Metabolic profiling of the human response to a glucose challenge reveals distinct axes of insulin sensitivity. *Mol Syst Biol* **4:**214.

Sinal CJ, Tohkin M, Miyata M, Ward JM, Lambert G, and Gonzalez FJ (2000) Targeted disruption of the nuclear neceptor FXR/BAR impairs bile acid and lipid homeostasis. *Cell* **102:**731–744.

Thompson PD, Panza G, Zaleski A, and Taylor B (2016) Statin-associated side effects. *J Am Coll Cardiol* **67:**2395–2410.

Urbano F, Bugliani M, Filippello A, Scamporrino A, Di Mauro S, Di Pino A, Scicali R, Noto D, Rabuazzo AM, Averna M, Marchetti P, Purrello F, and Piro S (2017) Atorvastatin but not pravastatin impairs mitochondrial function in human pancreatic islets and rat β-cells. Direct effect of oxidative stress. *Sci Rep* **7:**11863.

Yada T, Nakata M, Shiraishi T, and Kakei M (1999) Inhibition by simvastatin, but not pravastatin, of glucose-induced cytosolic Ca^{2+} signalling and insulin secretion due to blockade of L-type Ca^{2+} channels in rat islet beta-cells. *Br J Pharmacol* **126:**1205–1213.

Yaluri N, Modi S, López Rodríguez M, Stančáková A, Kuusisto J, Kokkola T, and Laakso M (2015) Simvastatin impairs insulin secretion by multiple mechanisms in MIN6 cells. *PLoS ONE* **10:**e0142902.

Zhao W and Zhao S-P (2015) Different effects of statins on induction of diabetes mellitus: an experimental study. *Drug Des Devel Ther* **9:**6211–6223.

Footnotes

Parts of this work were supported by a project grant of the Deutsche Diabetes Gesellschaft to M. D.

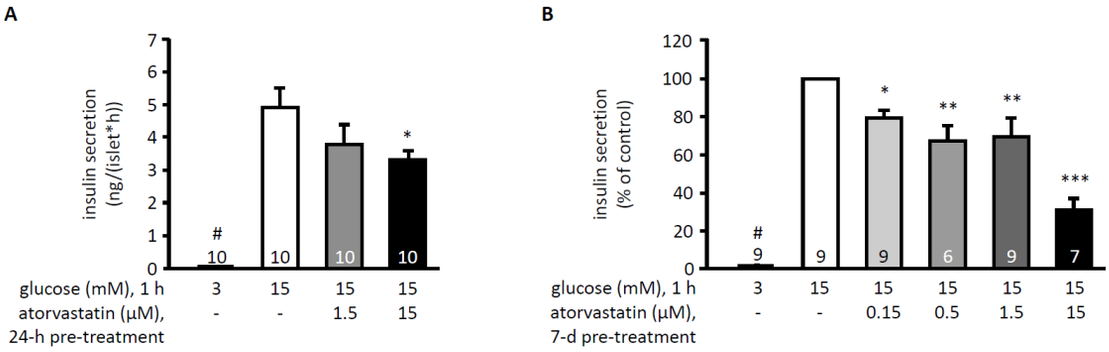

Figure 1

The influence of atorvastatin on insulin secretion depends on concentration and incubation time. A) Culturing islets of Langerhans for 24 h in standard medium supplemented with atorvastatin caused a decrease in glucose-stimulated insulin release (1 h steady-state incubation) in a concentration-dependent manner. B) Extending culture time to 7 d significantly increased the damaging effect of the statin. The number of independent preparations is given in the bars of each diagram. #, p ≤ 0.001 (A) and p ≤ 0.01 (B) *vs*. all other conditions; *, p ≤ 0.05; **, p ≤ 0.01; ***, p ≤ 0.001 *vs.* control (15 mM glucose).

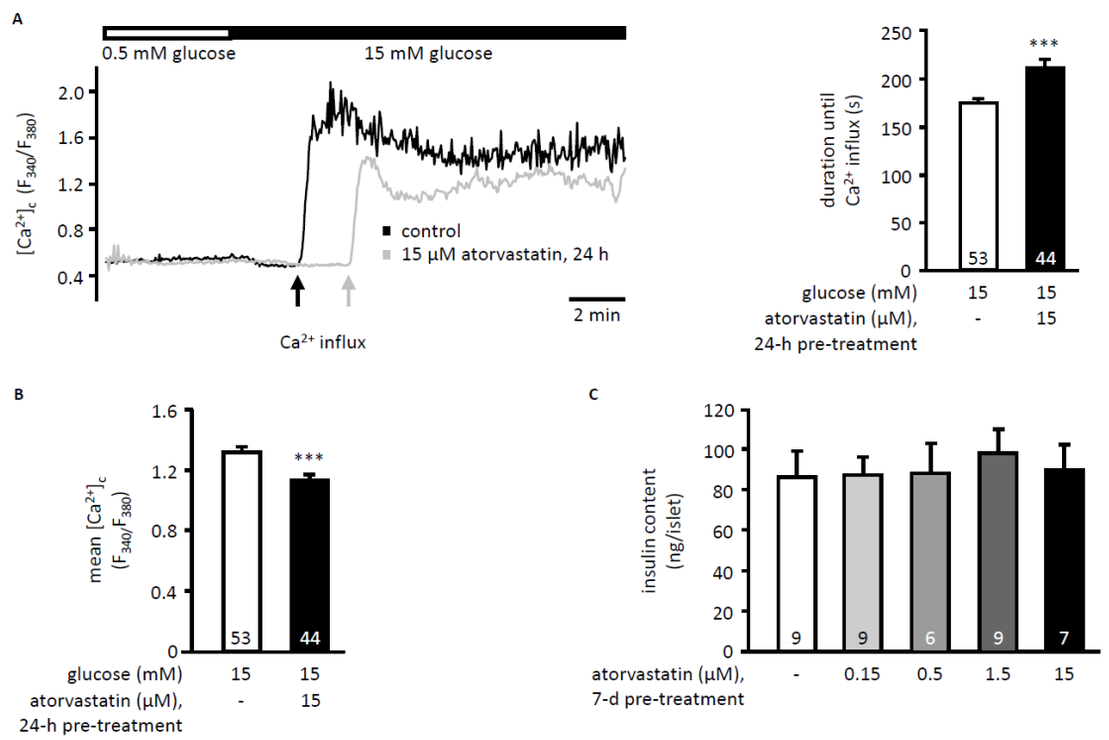

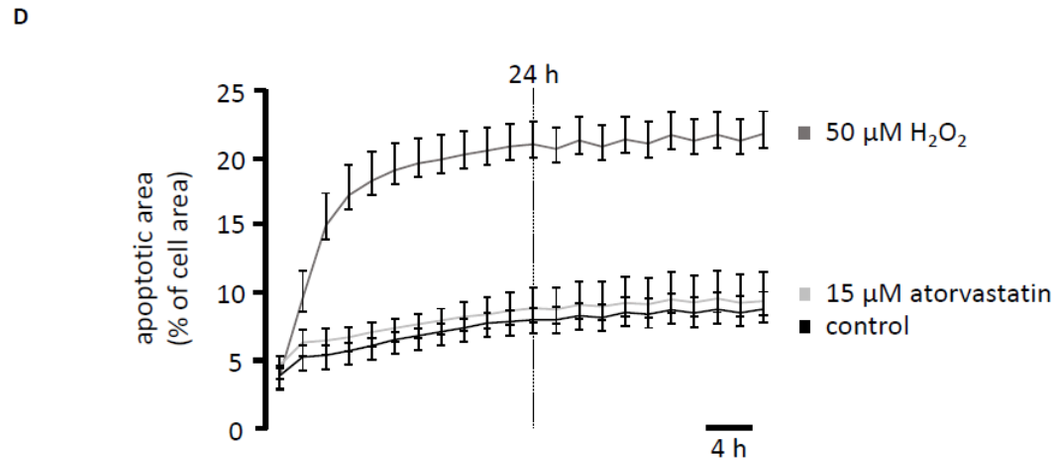

Figure 2

The detrimental impact of atorvastatin on insulin secretion is associated with altered $[Ca^{2+}]_c$, but not with changes in insulin content or apoptosis. A) After acutely stimulating islet cells with 15 mM glucose the initial increase in $[Ca^{2+}]_c$ was delayed in those cells that were exposed to atorvastatin before (15 µM, 24 h). B) The increase in $[Ca^{2+}]_c$ was reduced as well. C) No difference in insulin content was observed after culturing islets for 7 d in the presence or absence of atorvastatin (0.15 - 15 µM). D) Atorvastatin (15 µM) did not alter the fraction of apoptotic cell area *vs*. control. H_2O_2 (50 µM) was included as a positive control in each experiment. In (A) a representative recording is shown for each condition. The diagram in (B) summarizes the mean $[Ca^{2+}]_c$ determined in the first 10 minutes after the rise in $[Ca^{2+}]_c$ induced by changing bath solution from 0.5 to 15 mM glucose. The number of cells (A, B) or independent preparations (C) is given in the bars of each diagram. Data presented in (D) are obtained from 3 independent experiments; ***, $p \leq 0.001$ *vs.* control (15 mM glucose).

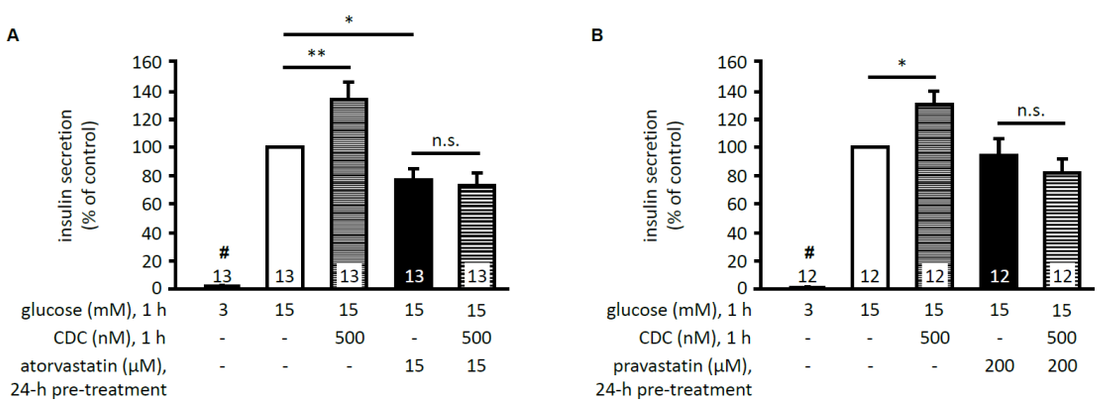

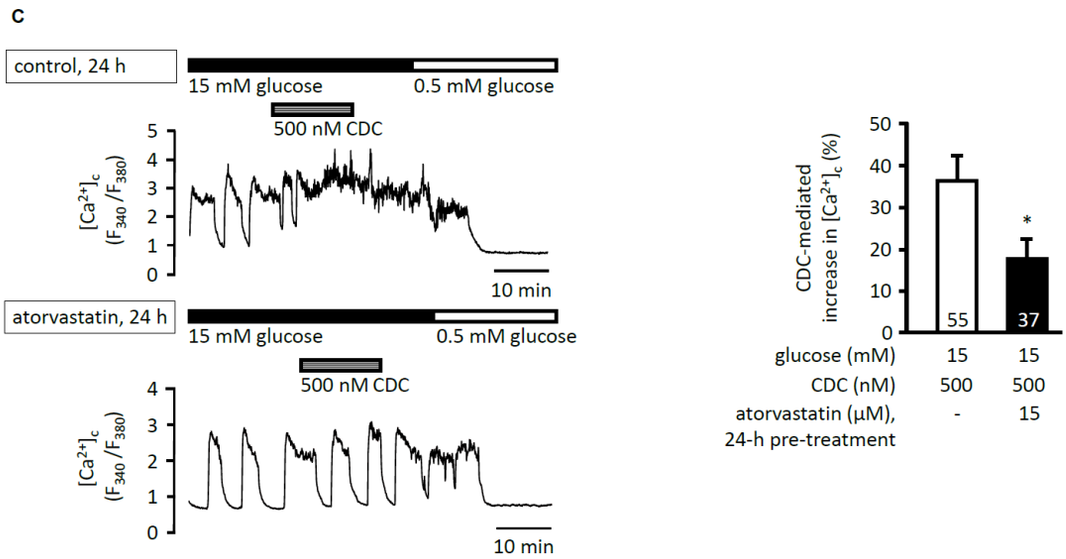

Figure 3

The insulinotropic effect of the bile acid CDC is abolished after exposure to atorvastatin or pravastatin. A, B) The acute application of 500 nM CDC increased insulin secretion under stimulatory conditions (15 mM glucose, 1 h). After exposure to atorvastatin (15 µM) or pravastatin (200 µM) for 24 h the stimulatory effect of CDC was abolished. C) Under stimulatory conditions (15 mM glucose) CDC caused a rise in $[Ca^{2+}]_c$. Pre-treatment with atorvastatin (15 µM) for 24 h significantly reduced the bile acid-mediated increase in $[Ca^{2+}]_c$. In (C) representative recordings for each condition are shown, the diagram summarizes the percentage increase in $[Ca^{2+}]_c$ after application of CDC. $[Ca^{2+}]_c$ was determined by calculating the area under the curve (AUC) after baseline correction. The number of independent preparations (A, B) or cells (C) is given in the bars of each diagram. #, $p \leq 0.001$ *vs*. all other conditions; *, $p \leq 0.05$, **, $p \leq 0.01$ *vs.* respective control, n. s.: not significant.

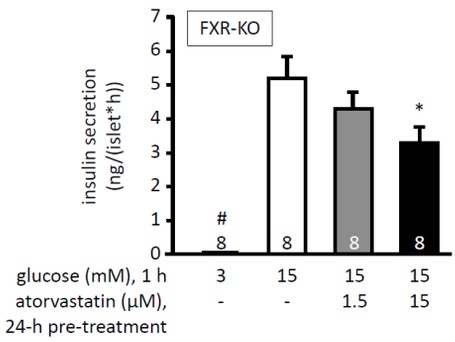

Figure 4

FXR is not essential for the inhibitory effect of atorvastatin on glucose stimulated insulin secretion. A) Culturing pancreatic islets of FXR-deficient mice for 24 h in standard medium supplemented with atorvastatin (15 µM) decreased glucose-induced insulin secretion in a concentration-dependent manner similar to wildtype islets. The number of independent preparations is given in the bars of the diagram. #, p ≤ 0.001 *vs*. all other conditions; *, p ≤ 0.05 *vs.* control (15 mM glucose).

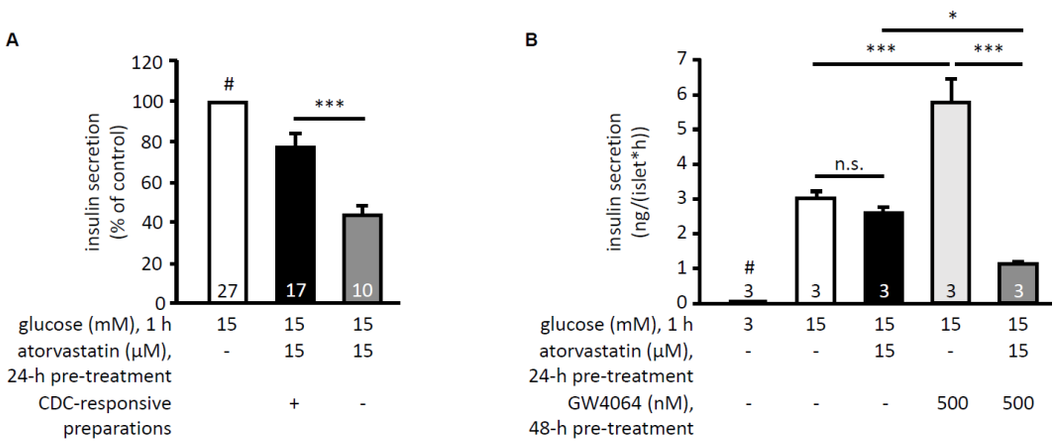

Figure 5

FXR modulates the negative effect of atorvastatin in dependence of the responsivity of the islets to CDC. A) The degree of inhibition caused by atorvastatin (15 µM) was more pronounced in preparations that were non-responsive to 500 nM CDC (grey bar) under standard conditions (i. e. 1-h-stimulation with 15 mM glucose) compared to those 17 out of 27 preparations that showed a potentiating effect in response to glucose (black bar). B) Islets were cultured with the synthetic FXR agonist GW4064 (500 nM) for 48 h. After 24 h, atorvastatin (15 µM) was added for 24 h. For evaluation only those preparations were included in which GW4064 abolished the acute stimulatory effect of CDC. In these preparations atorvastatin only tended to decrease insulin release in response to 15 mM glucose (black vs. white bar). In islets exposed to GW4064 before and during atorvastatin treatment (dark grey bar) the inhibitory effect was drastically increased compared to both, GW4064-treated and control islets. The number of independent preparations is given in the bars of each diagram. #, p ≤ 0.001 (A) and p ≤ 0.05 (B) *vs*. all other conditions; *, p ≤ 0.05; ***, p ≤ 0.001.